HYPERSPECTRAL AND GEOCHEMICAL SIGNATURES ON CORUNDUM BEARING ROCKS IN PART OF SOUTHERN KARNATAKA, INDIA.

THESIS SUBMITTED TO
THE UNIVERSITY OF MYSORE FOR THE AWARD OF
THE DEGREE OF

DOCTOR OF PHILOSOPHY
IN
EARTH SCIENCE

By

Mr. MARUTHI N.E

Under the Guidance of

Prof. H.T. BASAVARAJAPPA

DEPARTMENT OF STUDIES IN EARTH SCIENCE,
CENTRE FOR ADVANCED STUDIES IN PRECAMBRIAN GEOLOGY
MANASAGANGOTHRI, MYSURU – 570006

May 2019

DECLARATION

I do hereby declare that this Research work entitled **"HYPERSPECTRAL AND GEOCHEMICAL SIGNATURES ON CORUNDUM BEARING ROCKS IN PART OF SOUTHERN KARNATAKA, INDIA"** is completely carried out by me and submitted to the **University of Mysore, Mysuru** for the award of the Degree of ***DOCTOR OF PHILOSOPHY*** in **EARTH SCIENCE.** This is the original research work carried out in the Department of Studies in Earth Science, University of Mysore, Manasagangothri, Mysuru, under the research guidance of **Prof. H.T. Basavarajappa,** Earth Science. I further declare that the present work has not been submitted for the award of any degree in this University or any other University.

Date:

Place:

MARUTHI N.E

(Research Candidate)

Dr. H.T. BASAVARAJAPPA, M.Sc, Ph.D, FMSI, FISG, FISCA, FIAEME
Professor of Earth Science, Former Chairman & Head,
Co-ordinator: Centre for Advanced Studies (CAS)
Chairman: ISG-Mysore Chapter
President: Geology Alumni Association, MGM
Treasure: Mineralogical Society of India
Principal Investigator: UGC-MRP
Co-PI: ISRO/NRSC-MRP

DEPARTMENT OF STUDIES IN EARTH SCIENCE
CENTRE FOR ADVANCED STUDIES IN PRECAMBRIAN GEOLOGY
UNIVERSITY OF MYSORE
Manasagangothri, Mysore-570006, INDIA
Ph.No: (O) 0821 - 2419718/2419724
(Res) 0821-2412740,
Mobile-9448800520
basavarajappaht@gmail.com

MEMBER OF THE ACADEMIC COUNCIL, UNIVERSITY OF MYSORE

CERTIFICATE

I do hereby declare that the thesis entitled **" HYPERSPECTRAL AND GEOCHEMICAL SIGNATURES ON CORUNDUM BEARING ROCKS IN PART OF SOUTHERN KARNATAKA, INDIA"** submitted by **Mr. MARUTHI N.E,** for the award of the **Doctor of Philosophy in Earth Science**, Department of Studies in Earth Science, Centre for Advanced Studies in Precambrian Geology, University of Mysore, Manasagangothri, Mysuru - 570 006 was carried out in this Department under my Guidance and Supervision after fulfilling the basic requirements specified by the University of Mysore.

Place: Mysuru

Date:

RESEARCH SUPERVISOR

ACKNOWLEDGEMENTS

I get more pleasure to recall the inspiration, encouragement, moral support and overwhelming help rendered by teachers, friends, near and dear ones for the completion of this research and thesis work.

I express my sincere and heartful gratitude to ***Prof. H.T. BASAVARAJAPPA,*** *for his valuable guidance, help and encouragement that enabled me to sustain my efforts.*

Out of my heavy debt, my sincere thanks and gratitude to ***Prof. M.S. SETHUMADHAV,*** *Chairman, Department of Studies in Earth Science, Centre for Advanced Studies in Precambrian Geology, University of Mysore, Mysuru – 570 006.*

I would like to thank Board of Studies Chairman ***Prof. P. MADESH*** *and members of the doctoral committee* ***Prof. K.G. ASHAMANJARI and Prof. K.N. PRAKASH NARSIMHA*** *for their advice and valuable technical suggestion during the research work.*

I proudly announce my pleasure, to tender my thanks to ***Prof. A. BALASUBRAMANIAN; Prof. D. NAGARAJU and Prof. B.V. SURESH KUMAR,*** *Department of Studies in Earth Science, Centre for Advanced Studies in Precambrian Geology, University of Mysore, Manasagangothri, Mysuru – 570 006 and all the Non-teaching staffs for their timely help and source of inspiration during my research work.*

My grateful thanks to The ***Deputy Secretary, NFST - UGC, New Delhi*** *for providing the financial support with successful completion of the grades* ***Junior & Senior Research Fellowships*** *and my sincere thanks to the Deputy Registrar, SC/ST Special cell, University of Mysore, Mysuru for their kind service.*

With great pleasure, I submit my sincere thanks to Geological Survey of India, Bengaluru; Geological Survey of India Training Institute, Hyderabad; Chitradurga; NRSC-ISRO, Hyderabad and United State Geological Survey (USGS) website.

My expressions in sincerity, gratitude and special thanks from the bottom of my heart to my research colleagues, ***Dr. Manjunatha M.C; Dr. Jeevan L; Mr. Harshavardhana A.S; Mr. Siddaraju M.S; and Mr. Reza Ravanshad*** *and to my* ***Research seniors*** *for their cooperation and encouragement in the department.*

I indepthly thank ***Dr. M. Sundararajan,*** *Faculty;* ***Mr. R.G. Rejith;*** *Research Scholar Materials Science & Technology Division, National Institute for Interdisplinary Science and Technology (NIIST) Thiruvananthapuram, Kerala, India. for providing Geochemical analysis data of collected Samples from Southern Karnata and valuable discussions and suggestions.*

In this auspicious moment, my deep appreciation, commemoration and thankful remembrance to my ancestors.

I am particularly indebted to my beloved Father ***Mr. Eranna*** *and My mother* ***Smt. Varalakshmamma,*** *my Younger Sister* ***Smt. Shruthi N.E*** *my brother-in-law* ***Mr. C. Papanna;*** *and my Niece,* ***Indu Shree*** *and* ***Sindu Shree*** *and all the* ***family members*** *giving me their constructive encouragement and support for liberty to educate and initiate to sustain throughout this research work.*

MARUTHI N.E

ABSTRACT

Corundum-bearing rocks are associated with metamorphosed mafic rocks in a metamorphic terrain mainly of metasedimentary rocks including gneiss, schist, amphibolite, and minor iron formation. Un oriented corundum crystals surrounded by alkali feldspar halos formed by replacement of the gneiss with the addition of Al and K in Granulite facies metamorphism of an aluminous sediment produced biotite syenite gneiss. Corundum also occurs in cordierite sillimanite schist, gneisses round closepet granite, contact of ultramafics Pegmatite's, Aplite veins disseminated grains in anorthosite kyanite/ staurolite schist, high grade pelitic schist gravel beds and stream sediments as a placer. It's generally associated with spinel, garnet, kyanite, and high-calcium feldspars in plutonic pegmatite and metamorphic rocks. Some of its varieties are oriental amethyst, oriental emerald, oriental topaz, sapphire, ruby (gemstones) and emery (massive). Karnataka state, Dharwar Craton is composed of an active and dynamic geological setting with prospects of many different kinds of economic mineral deposits, including shear zones bearing valuable minerals and gemstones in Precambrian basement rocks. The study area Southern Karnataka covers 20 districts, Field observation using ground truth check , Geochemical analysis data and Hyperspectral data demarcated the Corundum bearing horizons in the Study area. Hyperspectral (350-2500nm) is a special type of multispectral imaging scanner which provides a high spectral resolution data to bring out diagnostic features on lithological contacts for better discrimination and rapid demarcated the Corundum bearing rocks across Southern Karnataka. The hyperspectral data on lithological contacts and themes like geomorphology, geology, structure, soil, rocks and minerals will be studied using high resolution satellite data such as Landsat 8 is a high multispectral imaging radiometer consists of three separate subsystems, Visible near InfraRed (VNIR-15m), Short Wave InfraRed (SWIR-30m) and Thermal InfraRed (TIR-90m) that have become potential tool for mapping of precious gemstones in between lithological contacts and mineralized zones.

The present study aims to integrate the advent hi-tech tools of hyperspectral Remote Sensing (RS), Geochemical analysis data, EDS analysis data and Geographical Information System (GIS) in demarcating, exploration, scientific surveying of corundum bearing litho units in Precambrian basement rocks of Southern Karnataka.

TABLE OF CONTENTS

CHAPTER – III

CHAPTER – IV

CHAPTER – V

CHAPTER – VI

CHAPTER – VII

LIST OF FIGURES

LIST OF TABLES

CHAPTER-I

1.1. INTRODUCTION

Precambrian basement rocks of Karnataka Dharwars are composed of the active and dynamic geological settings with enormous economic mineral deposits and variety of gemstones. These gemstones were noticed all along the lithological contacts of Green Schist Belts, younger granites, Granodiorites and granitoids of DharwarCraton. Minerals are important natural, finite and non-renewable resources essential for mankind. Minerals are the treasures of the state, therefore systematic, scientific and sustainable harnessing of minerals wealth should be the cornerstone of development objectives of the state. The utilization of these minerals has to be guided by long term goals and perspectives. All these goals and perspectives are dynamic and responsive to the economics in scenario, the Karnataka mineral policy has to evolve. (Karnataka mineral policy 2008) Gems can be defined as generally a fine-quality or superlative, rarity and durability specimen usable in gem industry to make jewels or ornaments. The chemical makeup of such specimens can be of inorganic or organic origin or a fashioned stone which possesses quality, beauty and durability for in jewelry, such as Diamond, Pearl, Ruby, etc. (Dictionary of Gemology 2004). Gem deposits including a gem bearing gravel or placer containing amounts of gem minerals that were formed from preexisting rocks found in river or lake beds associated with other minerals such as garnets, sapphires, rubies, etc. There is also host rocks which should be identified and mapped therefore there is a need for inclusive and accurate scientific mapping using new technologies to meet the goals

Corundum first named corinvindum in 1725 by John Woodward and derived from the Sanskrit, Kuruvinda (Ruby). Richard Kirwan used the current spelling corundum in 1794. Known by many names in ancient time's adamant, sapphire, ruby, hyacinthos, asteria. Corundum is a crystalline form of aluminium oxide (Al_2O_3) that is found in igneous, metamorphic, and sedimentary rocks. It is one of the naturally clear transparent material, but can have different colors such as, red, blue, white, grey, green, yellow, or brown-based on when impurities are present usually contains various impurities such as the oxides of iron and chromium and mica pinite and other silicates, It

occurs in hexagonal crystals usually in double ended pyramids the faces of which are often curved and give the crystals the shape of an elongated barrel (Basavarajappa et al., 2017). Transparent specimens are used as gems, called ruby if red and padparadscha if pink-orange. All other colors are called sapphire example green sapphire for a green specimen. The red color is caused by minor amounts of trivalent Cr replacing Al in the crystal structure, the mineral is widely known for its extreme hardness and for the fact that it is sometimes found as beautiful transparent crystals in many different colors. The extreme hardness makes corundum an excellent abrasive, and when that hardness found crystals is the perfect material for cutting gemstones (Maruthi et al., 2018). The ruby and sapphire are mineralogical mere colored crystals of corundum, whose mineral composition on chemical analysis is shown to consist of earth alumina in crystallized state nearly in pure condition, In addition to its hardness of up to 9 on Mohs scale, corundum's density of 4.02 g/cm3 is unusually high for a transparent mineral composed of low atomic mass elements, such as, aluminium and oxygen, the bulk of the corundum, thus collected is of abrasive (industrial) quality and a very small proportion of them form gem quality popularly known as ruby and sapphire (Basavarajappa and Maruthi., 2018).

Ruby, from ruber (latin for red) it is commonly known as Manak or Lal in Hindi and Manikya in Kannada. It is the transparent red-colored variety of corundum mineral. The word corundum is derived from the Sanskrit word Kuruvinda and in Sanskrit ruby stands for Ratnaraj which means something like king of the gemstones. Ruby is distinguished for its bright red color, being the most famed and fabled red gemstone. Besides, its bright color, it is a most desirable gem due to its magnificent color, excellent hardness and outstanding brilliance, durability, luster and rarity. Transparent rubies of large sizes are even rarer than diamonds and ruby is found in hexagonal prisms and blades forms (Basavarajappa et al., 2018). The ruby, which sprays out red rays in the sunlight and glow in darkness, is considered a superior quality gemstone. Ruby when rubbed on a stone and the stone shows signs of rubbing and also the ruby does not lose its weight, it is considered to be of a superior quality. The chemical formula for ruby is, Al_2O_3, sp. gr., 3.9-4.1 and its hardness is 9 (Basavarajappa and Maruthi, 2018).

Trace amounts of iron and titanium can produce a blue color in corundum. Blue corundum are known as "sapphires." The name "sapphire" is used for corundum that range from a very light blue to a very dark blue color. The blue can range from a greenish blue to violetish blue. Gems with a rich blue to violetish blue color are the most desirable. Gem-quality corundum occurs in a wide range of other colors, including pink, purple, orange, yellow, and green. These gems are known as "fancy sapphires." It is surprising that a single mineral can produce gemstones of so many different colors.

Sapphire in true sense is the blue, transparent, gem variety of corundum but in trade parlance all gem varieties other than red are called as sapphire. Natural sapphire has low dispersion and hence no fire. Some of them are characterized by the presence of fine parallel fibres as inclusions exhibiting the phenomenon of 'Silk'. With an abnormal amount of silk developed along the lines of crystallization and when the crystal is cut in en-cabochon fashion, it shows 'asterism' i.e. a white, six-rayed star seen on the surface when examined in light. The blue color of sapphire is considered to be due to the presence of titanium. Sapphire occurs as disseminated crystals formed by the 1. Magmatic segregation in basic/ultrabasicigneous rocks.2. Desilication of pegmatite dykes intruded intobasic igneous rocks.3. Metamorphism of highly aluminous rocks.It also occurs in alluvial placers. Though theresources of sapphire are confined only in Jammu &Kashmir, its occurrences are reported from AndhraPradesh, Karnataka, Kerala and Tamil Nadu also.Basis of Grade ClassificationSapphire is the prime gem varieties of corundum.This is the most fascinating gem stone after diamond.

1.2. NOMENCLATURE OF CORUNDUM

There are now recognized three varieties of corundum, depending on purity, degree of crystallization, and structure. These are: (a) Sapphire, including all the highly colored varieties of corundum which are transparent to translucent and are of value as gems; (b) Corundum, including all those varieties of dark and dull colors and also the massive lighter-colored varieties that are not transparent, as the blue to gray, brown, and white; and (c) emery, including the intimate mixture of very fine granular corundum with magnetite and sometimes with hematite, in appearance very similar to a fine-grained iron ore (Viswanatha., 1972). The varieties that are brought under this head are, with the

exception of emery, all those that cannot be used as gems. As a commercial product there are differences, such as texture, purity, etc., that have considerable influence upon its value, in the same way in which color and transparency affect the gem corundum. In 1805 Haiiyformally united these different varieties under the one species, corundum. Various names derived from its color, hardness, parting, structure, etc., have been applied to corundum. The following names have been used to designate the different varieties of this mineral (Joseph Hyde Pratt, 1906).

Names that have been applied to corundum, sapphire, and emery.

CORUNDUM	
Adamant (Kirwan).	Adamantine spar (Kirwan).
Adamas siderites (Pliny).	Alumina.
Anthrax.	Armenian stone (King).
Gorindon (Haiiy).	Corindon adamantine (Brougniart).
Corindonharmophane (Haiiy).	Corivindum.
Corivindum (Woodward).	Corundite.
Corundum (Greville).	Demantspath (Klaproth).
Diamond spar.	Gyrasole (Kirwan).
Hard spar.	Imperfect corundum (Greville-Bournon).
Karuud (Hind).	Korund (Werner).
Kurund (India).	Rhombohedral corundum (James).
Rhombohedrischercorund (Mobs).	Soimonite.
Spath adamantine (Delameth).	Thoneride.

SAPPHIRE	
Amethisteorientale.	Cat sapphire.
Anthrax (Theophrastus).	Chlor sapphire.
Apyrote.	Corindonhyalin .
Asterie.	Corindon perfect.
Asteria (Pliny).	Corindontelesle (Brongniart).

Asteriated sapphire.	Emerald.
Barklyite (Stephen).	Emeraude.
Bleu du rol.	Emeraudeorientale.
Blue sapphire.	Green sapphire.
Bronze corundum.	Hyacinth.
Carbunculus (Pliny).	Hyacinthos (Pliny).
Hyaline.	Jacut (Arabian).
Lichnis (Pliny).	Luchssaphir.
Luchs sapphire.	Lychnis (Pliny).
Lynx sapphire.	Occidental amethyst.
Opalescent sapphire.	Opaline.
Oriental aquamarine.	Oriental chrysolite.
Oriental emerald.	Oriental hyacinthe.
Oriental peridot.	Oriental ruby.
Oriental sapphire.	Oriental topaz.
Orieutaliskrubin (Wallerius).	Pink sapphire.
Pearl corundum .	Rubieetoile.
Rubin.	Rubis.
Rubis oriental (Werner).	Sagenite corundum.
Salamstein (Werner).	Salamstone.
Saphir (Werner).	Saphirasteria.
Saphirblanc.	Saphir de chat.
Saphiretoile.	Sapphire.
Sapphirus (Wallerius).	Spath adamantine (Delameth).
Star sapphire.	Star stone.
Telesia (Haiiy).	Telesie (Haiiy).
White sapphire.	Yellow sapphire.

EMERY	
Acone ex Armenia (Theophrastus).	Armenian stone.
Armenian whetstone.	Corindongranuleux (Haiiy).
Emeri.	Emeril (Haiiy).
Emerite (Shepard).	Emery.
Feroxydequartzifere (Haiiy).	Granular corundum.
Grinding spar.	Naxium (Pliny).
Naxium ex Armenia (Pliny).	Pyrites vivus (Pliny).
Schmergel.	Schmirgel.
Smergel (Wallerius).	Smirgel.
Smiris (Agricola).	Smirisferrea (Wallerius).
Smyris (Agricola and Dioscorides).	

The list has been compiled from Dana's System of Mineralogy, sixth edition; Dictionaryof the Names of Minerals, by Chester; Catalogue of Minerals and Synonyms, byEgleston, and from the names used by the lapidaries.

1.3. TYPES OF CORUNDUM

Althoughthe hardness of the pure corundum is practically the same that is, 9 the cutting qualities of corundum vary, has already been stated,according to the alteration that has taken place in the mineral andto the development of parting planes (Joseph Hyde Pratt, 1906). The usual colors of this ordinary corundum are gray to white, shades of blue, white mottled with blue, and also the darker colors, brown to black. According to its structure, corundum is divided into three groups, known as (1) Block corundum, (2) Crystal corundum, and (3) Sandcorundum.

(1) Block corundum includes the massive corundum, whether in small or large masses. In some of the deposits the Block corundum is often intermixed with feldspar, hornblende, muscovite, margarite, or chlorite, according to the characterof the rock in which it occurs, so that the separation of thecorundum from these foreign minerals is sometimes a rather difficultprocess. Where the corundum occurs in masses of

considerableweight, there is often great inconvenience in mining, as, on accountof its toughness and hardness, it is not always readily broken and itis almost impossible to drill through it. The Block corundum,.which shows but little development of the parting planes already referredto and no ingrowth of muscovite, margarite, or chlorite in cracksor seams, makes the best corundum ore, and the difficulty of cleaningis reduced to a minimum (Joseph Hyde Pratt, 1906).

(2) Crystal Corundum. Under this head are included all the crystal varieties of corundum. These are present in deposits of both Sand and Block corundum. Atmany of the localities the crystals show the hexagonal prism merginginto the pyramid, thus causing the crystal, as it tapers toward the end, to assume the form known as barrel corundum. At anumber of mines loose, tapering crystals of rather indefinite formare found, which are inclosed by compact margarite. At many of the veins the crystals occur in a mass of feldspar, at others in biotite or muscovite, and at still others in chlorite (Joseph Hyde Pratt, 1906).

(3) Sand Corundum consists of very small to minute crystals and small irregular grains, such as are found in the chlorites and vermiculites. developed in the ore bodies occurring between the peridotite and other rocks, such as gneisses and schists (Smeeth, and SampathIyengar 1916).

1.4. PHYSICAL PROPERTIES OF CORUNDUM

Chemical Classification	Oxide
Chemical Composition	$Al_2 O_3$
Color	Typically gray to brown. Colorless when pure, but trace amounts of various metals produce almost any color. Chromium produces reed (ruby) and combinations of iron and titanium produce blue (sapphire).
Streak	Colorless (harder than the streak plate)

Luster	Admantine to vitreous
Diaphanety	Transparent to translucent
Cleavage	None. Corundum does display parting perpendicular to the c-axis.
Mohs Hardness	9
Specific Gravity	3.9 to 4.1 (very high for a nonmetallic mineral)
Diagonostic Properties	Hardness, high specific gravity, hexagonal crystals sometimes tapering to a pyramid, parting luster, conchoidal fracture
Crystal System	Hexagonal
Geological application	Used in abrasives, jewelries, pigments, electrical items and medical purpas

1.5. OPTICAL PROPERTIES OF CORUNDUM

The luster of corundum is adamantine to vitreous, while that of emery is metallic to sub metallic. On the basal surface of corundumthe luster is sometimes pearly. Pleochroism in ordinary light is very strongly marked in the deeplycolored varieties, especially the sapphires and rubies, the ruby showinga deep red color when viewed in the direction of the verticalaxis, and a much lighter color to nearly colorless in some instanceswhen viewed at right angles to this axis. The sapphire exhibits adeep blue color when viewed in the direction of the vertical axis, and agreenish to greenish white or bluish whitewhen viewed at right angles.By means of this pleochroism exhibited by corundum, the stones arereadily distinguished from spinel, garnet, and other gem minerals,which resemble some of the corundum gems.The action of the Roentgen rays or X rays upon corundum gems isanother means of distinguishing the ruby and the sapphire from otherminerals which resemble them, and from artificial or imitation stones.Corundum allows these rays to pass through it freely, being exceededin this respect only by the diamond, which allows the passage of tenlimes as much light. According to their resistance to the passage ofthe X rays, Doctor Doelter has arranged the minerals into the followinggroups, the diamond allowing the most light to pass through it: Corundum is normally uniaxial with

negative double refraction.The mean index of refraction is high, being' about 1.765. The double refraction of corundum is0.008 to 0.009, or about the same as quartz. Some varieties of corundumhave been observed that are abnormally biaxial (Joseph Hyde Pratt, 1906).

1.6. CHEMICAL COMPOSITION OF CORUNDUM

Theoretically pure corundum contains only alumina, Al_2O_3 butwith few exceptions, all the specimens that have been examined showthe presence to a greater or less degree of other chemical compounds,the principal ones being silica (SiO2), water (H_2O), and ferric oxide(Fe_2O_3). Water is almost always present in amounts from a traceto 2 percent or more. The silica and ferric oxide also vary fromnothing in some corundum to as much as 5 percent in others. Ofcourse this does not apply to emery, which is a mechanical mixture ofcorundum and magnetite; but it does apply to the corundum whenseparated from the mixture, and the impurity in this corundum isusually ferric oxide. The purest known form of corundum is thetransparent crystallized variety, or what might be called the sapphireor gem variety (Joseph Hyde Pratt, 1906).

1.7. INTERNAL STRUCTURE OF CORUNDUM

Corundum is the crystalline form of aluminum oxide. Its hardness is next to diamond andfor this reason it is used in manufacturing abrasive materials and also as a precious stone.Corundum in purest form is colourless having tetragonal structure. The oxygen atoms lieon planes in nearly hexagonal closed packed configuration with their cations betweenthese planes in octahedral coordination (Hughes, 1991), For every three octahedral, two distortedcations are occupied by an aluminum atom in an orderly arrangement; thus eachaluminum atom is surrounded by six oxygen atoms. The polyhedron model of corundumis shown in (Fig. 1). The internal structure of corundum is having three oxygen atoms above the aluminum are closer to each other than the three oxygen atoms below, and the aluminum atom is a little lower than halfway down.

Half of the aluminum atoms have this arrangement, and the other half have an inverted arrangement. If this arrangement is viewed in terms of ionic bonds, then the positive aluminum ion is surrounded by six negative charges (oxygen ions). Each aluminum atom donates three electrons to become Al^{3+} and has no unoccupied energy levels, while each oxygen atom receives two electrons, ensuring that it has no unoccupied energy levels. Therefore, two aluminum atoms donate a total of six electrons, and three oxygen atoms receive a total of six electrons, to produce Al_2O_3.In pure corundum, all electrons are paired and there is no absorption of light. Once one out of every hundred aluminum atoms is replaced by chromium atoms, negatively charged oxygen ions surround the aluminum ion (which has donated 3 electrons), so a chromium atom must donate three electrons to become Cr^{3+} , replacing Al^{3+}, in order for the charge to remain the same. In Al^{3+} there are no partially filled energy levels or orbitals. However, in Cr^{3+} there are partially filled energy levels or orbital's. It is these electrons that can be excited and that cause absorption of certain wavelengths of light, resulting in color (Joseph Hyde Pratt, 1906).

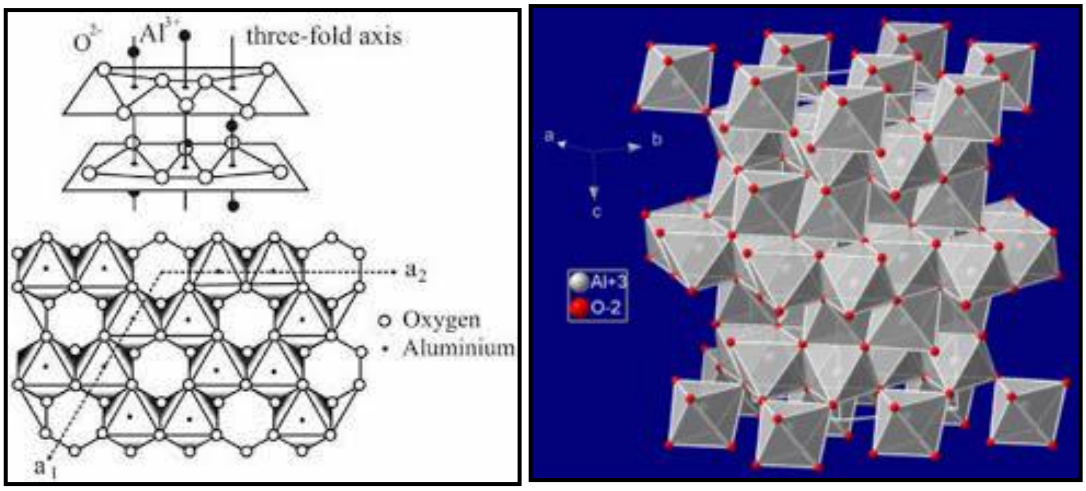

Fig.1.1. Polyhedral model of Corundum (Hughes, 1990)

The same corundum structure is also seen in Cr_2O_3, V_2O_3, Ti_2O_3, Fe_20_3etc; some ofthese when found along with Al_2O_3 in the earth's crust during the formation ofcorundum, the position of A1 atom in the lattice is replaced by Cr^{3+}, V^{3+}, Ti^{3+}, Fe^{3+} ions.When A1 atom is replaced by Cr atom in the lattice structure, red colour ruby are obtained(Hughes, 1991). Transition metal causes colour because of their unpaired electrons and

variablevalence. These impurities when present even in traces greatly influence the appearance of gems (Hughes, 1991). Transparent gem varieties of corundum are known as Ruby and Sapphire. Gemcorundum other than red in colouris generally called sapphire (Hughes, 1991).The known methods for identification of gemstones utilize the knowledge of RefractiveIndex (RI), Specific Gravity (SG), Double Refraction (DR), hardness, color, luster, spark andappearance(Peter, 1983).

Corundum belongs to the hematite group (X_2O_3) of rhombohedral oxides comprising hematite (Fe_2O_3), corundum (Al_2O_3), eskolaite (Cr_2O_3), karelianite (V_2O_3), and tistarite (Ti_2O_3). There are no solid solutions between any of the five species but they have the same type of structure. Hematite group mineral structures are based upon hexagonal closest packing of O atoms, with cat ions in octahedral coordination (Cesbron et al., 2002). Euhedral crystals can present different faces (Fig.1.2) that correspond to seven crystalline forms (Cesbron et al. 2002) the pinacoid {00.1}, the first order hexagonal prism {10.1} and second order {11.0}, the hexagonal prism {kk.0}, the hexagonal dipyramid {hh.l}, the ditrigonal scalenohedron {hk.l} and the rhombohedron {h0.l}. The first five crystalline general forms are also present in the classes that belong to the hexagonal system. Corundum can also crystallize in a particular texture called trapiche (Sunagawa et al., 1999, Garnier et al., 2002).

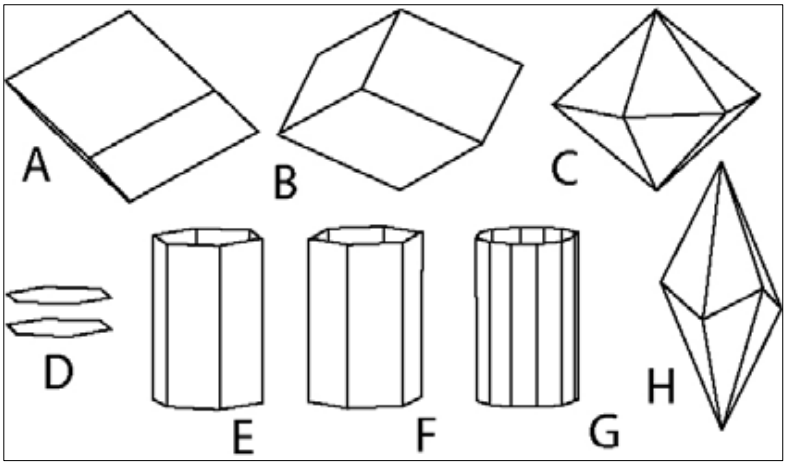

Fig.1.2. Crystalline forms of the 3 2/m class of the rhombohedral system (after Cesbron *et al.* 2002). A, positive rhombohedron {10.1}; B, negative rhombohedron {01.1}; C, hexagonal dipyramid {hh.l}; D, pinacoid {00.1}; E, hexagonal prism of first order {10.1}; F, hexagonal prism of second order {11.0}; G, dihexagonal prism {hk.0}; H, ditrigonal scalenohedron{hk.l}.

1.8. GEOLOGICAL OCCURRENCE OF CORUNDUM

Corundum is found as a primary mineral in Igneous rocks such as syenite, nephelinesyenite, and pegmatite. Some of the world's most important ruby and sapphire deposits are found where the gems have weathered from basalt flows and are now found in the downslope soils and sediments. Corundum is also found in Metamorphic rocks in locations where aluminous shales or bauxites have been exposed to contact metamorphism. Schist, gneiss, and marble produced by regional metamorphism will sometimes contain corundum. Some of the sapphires and rubies of highest quality, color, and clarity are formed in marble along the edges of subsurface magma bodies. Corundum's toughness, high hardness, and chemical resistance enable it to persist in sediments long after other minerals have been destroyed. This is why it is often found concentrated in alluvial deposits. These deposits are the most important source of rubies and sapphires in several parts of the world. Traditional sources of alluvial rubies and sapphires include Burma, Cambodia, Sri Lanka, India, Afghanistan, Montana, and other areas. In the past few decades, several parts of Africa, including Madagascar, Kenya, Tanzania, Nigeria, and Malawi(Joseph Hyde Pratt, 1906).Corundum mines In the USA, from Chester, Hampden Co., Massachusetts; the Cortland district, Westchester Co., New York; at Franklin, Sussex Co., New Jersey; large crystals from Hogback Mountain, Jackson Co., and Buck Creek, Clay Co., North Carolina; and from the Laurel Creek mine, Rabun Co., Georgia. At Bancroft and Haliburton, Ontario, Canada.On Naxos and Samos Islands, Greece.Large crystals from around the Soutpansberg, Transvaal, South Africa. Red gems from: the Mogok district, Myanmar (Burma). In the Ratnapura district, Sri Lanka.Around Mysore Dharwarcraton Karnataka, India.In the Jegdalek marble, near Sorobi, Laghman Province, Afghanistan.At Merkestein, near Longido, and the Morogoro district, Tanzania.From Ampanihy, Madagascar. Blue, green, and yellow gems from: Chanthaburi and Trat, Thailand. Around Bottambang and Pailin, Cambodia.In the Umba Valley, Tanzania.From around Andranondambo and Antsiermene, Madagascar.At Anakie, Queensland, Australia. From Yogo Gulch, 25 km southwest of Utica, Fergus Co., Montana, USA, have become important producers of ruby and sapphire.

1.8.1. Corundum Resources in India

India is considered as a country with big potential for gemstones. Many kinds ofgemstones have been found and mined in different areas of the country. Among thesegemstones, diamonds, rubies and sapphire are of most importance. Corundum is found inmetamorphosed shale and unsaturated igneous rocks (Karanth, 2000). It is found in association withkyanite and sillimanite in Assam, Meghalaya and Maharashtra. Ruby and Sapphirefound From the Zanskar district, Kashmir, India. It occurs in syenites andultrabasic rocks in Andhra Pradesh (Karanth, 2000). Pegmatites containing corundum occur in Bastardistrict, Chhattisgarh and Morena district of Madhya Pradesh. In Chhattisgarh corundum occurs in Bhopalpatnam and Sukma areas of Dantewara district, minor occurrences are also reported from Deobog area of Raipur district and small areas Kuchnoor, Ulloor, Dampaya area, Dhangal, Chikudapalli, Yapla and SonakukanarSukma area. Occurrences of sapphirehave been reported from Katamalkailakat-Baberi-Amera, Bhujipadar and Ghumur-Sargigunda belts in Kalahandi district of Orissa. Occurrence of Ruby has been reportedfrom Jillingdhar in Kalahandi district of Orissa. Precious and semi-preciousvarieties of corundum have also been reported from Tamil Nadu in Kangeyam beltstretching over Karur and Kulithalai Tehsils in Tiruchirapalli district, and Vedachandurtehsil in Dindigul district of Tamil Nadu (Karanth, 2000).

1.8.2. Corundum Deposits of Karnataka

Corundum occurrences in karnataka Bellary, Chitradurga, Shivamogga, Bangaluru, Tumahur, Chikballapura, Chikmagalur, Kodagu, Hassan, Dakshina Kannada, Mysuru, Mandya, Ramanagara, Chamarajanagara and Kolar districts.

1.8.3. Corundum Resources in Study area

Corundum occurrences are alsoreported from study area of Bangalore, Chickmagalur, Hassan, Mysore, Corundum occurs in peliticschists and gravel derived Kupya, Varuna, Bannur,H.D.Kote and Sargur Reddish Corundum crystalsoccur in a north-south trending linear tract of 210 km length extending from Kupya of Narsipur taluka of Mysore district to Mandya, In different area of Mysore, bright red ruby crystals embedded in a thinlayer of white surrounding rocks have also been reported (Karanth, 2000) Corundum is widely

distributed in the district mining appears to have been attempted on a large scale in Heggadadevankote Mysuru and Hunsurtaluks large sized barrel shaped crystals are embedded in a tough kayanite matrix at Pilhalli,Heggadadevankotetaluk at Singamaranhalli, Nadapanhalli and Voddarahosahalli in Hunsurtaluk, corundum occurs in soft grey talcose schist Manikpur, Yarekalmonti, Gollabidu, Gumsihalli, Chattanhalli and Kyatanhalli are villages in Mysore taluk where corundum is reported to occur in abundance of Mysuru district. At Budipadaga, corundum occurs in Pilitic granulites of B.R hills high grade granulites of regional metamorphic terrain (Basavarajappa et al., 2008) (Basavarajappa and Maruthi., 2018). Important deposits are reported from Satanur near Mandya, Erehalli, Kirangur and Ramanahalli areas. There are several reported occurences of corundum in this district specially near Bellundigere, 6km NE of Mandya Nelimakanhalli and Gurudevarahalli in Malavalli taluk Arsinkere, Basaralu, Satnuru, Yerehalli, Tarasanhalli and Kirlgandur. Corundum gems occurring at the contact of ultramafic rocks and pegmatite in Kollur, Maddur tract and Malavalli Doddi tract of Mandya district. Another tract with corundum deposits extends about 60 km. from near Ramanagaram to Malavalli (Karanth, 2000). Occurrence of corundum in nepheline syenite has been reprted from Kanakapura of Bangalore district. Good ruby corundum along with kayanite is seen in tremolite schist near Kadaneru in Sringeritaluk, ruby corundum is also found at Melkoppa in the Koppataluk of Chikmagalur district. Corundum occurs in the Challakere taluk, Loose barrel shaped crystals of pink corundum are reported to be scattered in the soil cap in the Ullavarti – kaval east of Challakere, so for these have not been commercially exploited on a large scale this type of Corundum seen in the Ullavartikaval of Challakere taluk of Chitradurga district. Corundum has been reported from several places in the Uppinangadi taluk as at Pachera, Pilenki and at Keladka in Puttur taluk of Dakshin Kannada district. Important occurrences are near the village of Kalyadi and Undiganhal to the south and southwest of Arsikere. There is a good show of corundiferous rock and also a number of old working in the hill to the west of Kalyadi grey corundum in the form of radiating bunches occurs in a kaolinized pegmatite cutting amphibolite. Dark sapphire blue granular corundum in pegmatite is seen near Adihalli about 3km ENE of Bageshpura other occurences are near Doddenhalli, Arasikeretaluk near Basavanpura and Agrahara in the Channarayapatna taluk, near

Hardur, granular pink corundum occurs together with circular radiating patches of kayanite weathered schist is washed near Kikkeri for the recovery of red ruby corundum of Hassan district. Workable deposits of corundum are found at Dodderi 3km NNW of Kamasamudra and at Doddenur and Yelesandra in the Bangarpet taluk from the size of excavations, it is evident considerable quantities of pink granular corundum appear to have been recovered several abandoned shafts are also seen corundum is found as an ingredient of cordierite sillimanite gneiss, corundum is also reported to be available in large quantities near Marahalli near Thondebhavi stray crystals of corundum are reported from several parts of Sidlaghatta and Chintamani taluk of Kolar district. A number of shallow working for corundum are seen at Baichapura and Alpenhalli in Kortageretaluk there are many reported occurrences especially in the region bordering the closepet granites in parts of Sira, Madhugiri and Pavagada taluks, corundum gem occurring at the contact of ultramafic rocks and pegmatite Honmachanahalli, Bandihalli and tract of Tumkur-Pavagada and Baichapurr-Madhugiri of Tumkur district. Gems occurring at the granulites in Budipadaga of Chamarajnagar district.

1.9. HYPERSPECTRAL STUDY

Hyperspectral (350-2500nm) is a special type of multispectral imaging scanner which provides a high spectral resolution data to bring out diagnostic features on lithological contacts for better discrimination and rapid mapping across the Study area. The hyperspectral data on Mineral targeting, lithological contacts and themes like geomorphology, geology/ mineral mapping, structure, soil, drainage, lineament, slope, landuse/land cover will be studied using high resolution satellite data such as Landsat 8 OLI, SPOT resolution the area coverage that have become potential tool for mapping of precious gemstones in between lithological contacts and mineralized zones.

Hyperspectral imaging has been an area of active research and development, and hyperspectral images have been available only to researchers. With the recent appearance of commercial airborne hyperspectral imaging systems, hyperspectral imaging is poised to enter the mainstream of remote sensing.Hyperspectral images will find many applications in resource management, agriculture, mineral exploration, and environmental monitoring. But effective use of hyperspectral images requires an

understanding of the nature and limitations of the data and of various strategies for processing and interpreting it.Hyperspectral images are produced by instruments called imaging spectrometers. Spectroradiometers are instruments designed to measure the spectral power distributions of illuminants. They operate almost like spectrophotometers in the visible region. They are commonly used to evaluate and categorize lighting for sales by the manufacturer, or for the customers to confirm the lamp they decided to purchase is within their specifications.Spectroradiometers are frequently used to calibrate LCD and CRT displays such as on laptops and HDTVs. CIE color values are measured and compared to predefined values, to ensure that the color displayed is correct, thus removing color variance between multiple displays.

Spectral signature measures all types of wavelengths that reflect, absorb, transmit and emit electromagnetic energy from the objects of the earth surface (Ali M. Qaid et al., 2009). Specral Evolution (SR-3500) Spectro-radiometer instrument has the ability to measure the spectral signatures of different rocks/ minerals. The SR-3500 operate in the wavelength range of 350–2500 nm with three detector elements: a 512-element Si PDA (Photodiode Array) covering the visible range and part of the near infrared (up to 1000nm) and two 256-element InGaAs arrays extending detection to 2500nm.The spectral signatures of the representative samples were compared with mineral spectra of USGS spectral library in DARWin SP.V.1.3.0 (Hunt et al., 1971). Absorption spectral values obtained from the DARWin software lab Spectra is the one character helps in the study of major and minor mineral constituents.

1.10. REMOTE SENSING AND GIS TECHNIQUES

Remote Sensing is based on the measurement of Electromagnetic (EM) energy. EM energy can take several different forms. The most obvious form of EM energy that is experienced is light. All forms of electromagnetic radiation, including light, behave both as waves and as particles (Dury: 1987, AL-Daghastani: 2003). EM energy travels at the speed of light (3×10^8 m/sec). It is commonly treated as a wave with both electric and magnetic fields, which are perpendicular to the propagation direction (Hunt: 1980, Harris and Bertolucci: 1989).

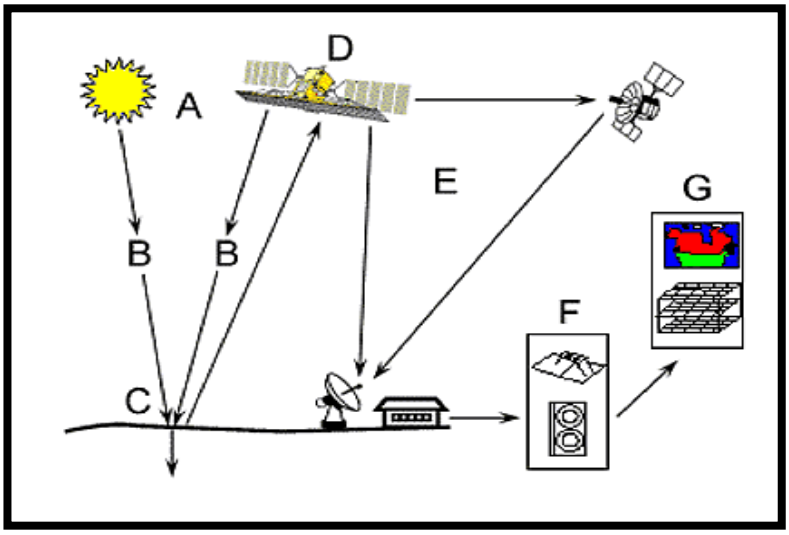

Fig.1.3. Remote Sensing Process

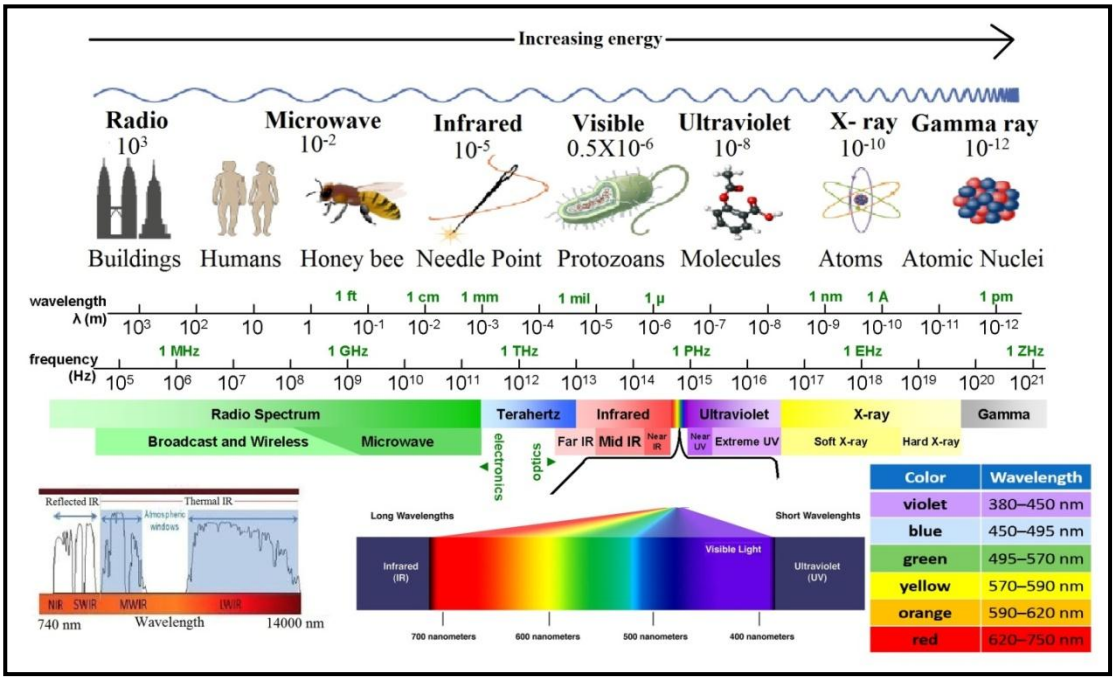

Fig.1.4. Electromagnetic Spectrum Wavelength Regions.

This study deals only with the visible, near-infrared, short wave infrared and thermal regions. Enhancement Thematic Mapper Plus (ETM+) measures reflected radiation in 6 bands between 0.45 and 2.35 $\boldsymbol{\mu}$ **m** (VNIR and SWIR), and emits radiation in one band in the 10.40-12.50 $\boldsymbol{\mu}$ **m** range (Ali et al-2008, 2009).

Our eyes are sensitive to just a small portion of the electromagnetic spectrum.The sun, normal incandescent bulbs, and most fluorescent bulbs produce nearly whitelight by mixing all the frequencies (colours) together. White light can be separatedinto its component colours, called a spectrum, by passing the light through a prism ora diffraction grating. If a light source produces all the visible frequencies (such as thesun), the spectrum is called a Continuous Emission Spectrum (CES). If the sourcesproduce only certain frequency (such as a gas at low pressure, neon sign for example,the resulting spectrum is called a Bright Line Emission Spectrum (BLES). If atransparent substance (such as stained glass) absorbs or removes certain frequenciesfrom white light, the spectrum produced is called an Absorption Spectrum (AS).

Fig.1.4. explains the EMS wavelength regions and region of EMS which isutilized in the application of Remote Sensing technology. Visible and Infrared regionsare most usable radiation in the field of remote sensing. Atmospheric window is therange of wavelengths at which radiation is slightly absorbed by the water vapor andcloud.Electromagnetic waves can be described in terms of velocity, wavelength andfrequency:

- Velocity: The speed of light, **c = 3×108 m/sec**).
- Wavelength (**l**): the distance from any position in a cycle to the same position inthe next cycle, measured in the standard metric system (Fig.1.6). Two units areusually used: the micrometer (**mm, 10-6 m**) and the nanometer (**nm, 10-9 m**).
- Frequency (**n**): the number of wave crests passing a given point in specific unit oftime, with one hertz being the unit for a frequency of one cycle per second.

Wavelength and frequency are related by the following formula:**c = l × n**

Electro-Magnetic radiation consists of an electrical field (E) which varies inmagnitude in a direction perpendicular to the direction in which the radiation istraveling, and a magnetic field (M) oriented at right angles to the electrical field (Fig.1.5). Both these fields travel at the speed of light (c).

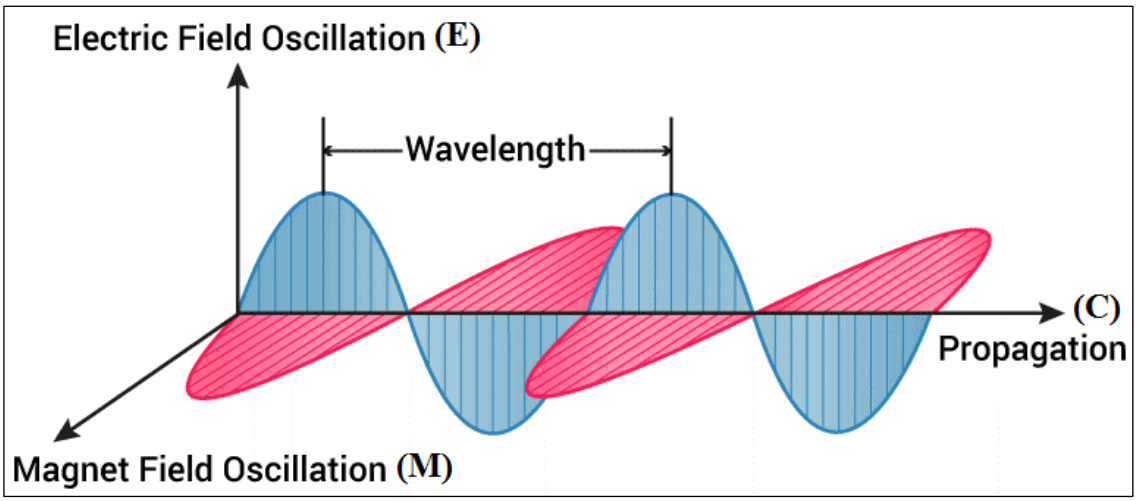

Fig.1.5. Electromagnetic radiation.

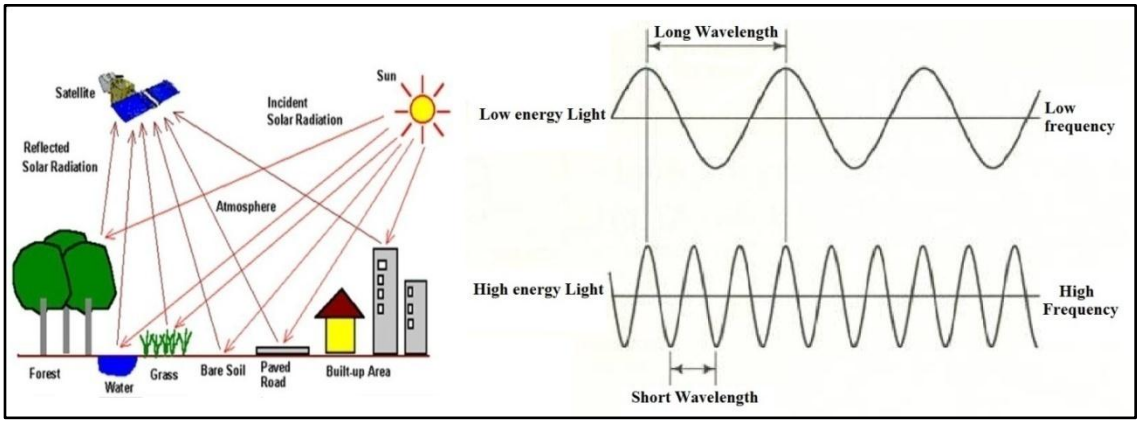

Fig.1.6. Wavelength and frequency.

1.10.1. ENERGY INTERACTION MECHANISMS WITH THE MATTER

Number of interactions is possible when Electromagnetic energy encounters matter irrespective of it physical nature like, solid, liquid and/or gas. The interactions that take place at the surface of a substance are called surface phenomena. Penetration of Electromagnetic radiation beneath the surface of a substance results in interactions called volume phenomena.

The surface and volume interactions with matter can produce a number of changes in the incident Electromagnetic radiation; primarily changes of magnitude, direction, wavelength, polarization and phase. The science of Remote Sensing detects and records

of these changes. The resulting images and data are interpreted according to the changes recorded remotely to identify the characteristics of the matter that areproduced through Electromagnetic radiation.

The common interactions occurred in the surface is given below:

Radiation may be transmitted, that is, passed through the substance. The velocity of Electromagnetic radiation changes as it is transmitted from air, or a vacuum into other substances. A substance can absorb the radiation by give up its energy largely to heatingthe substance. Radiation may be emitted by a substance as a function of its chemical structure and temperature interaction. At absolute temperature all the matters interacts with light energy will emit some source of energy above to the absolute zero degree kelvin (0° K), emitted energy can be detectable in the advance techniques of Remote Sensing.

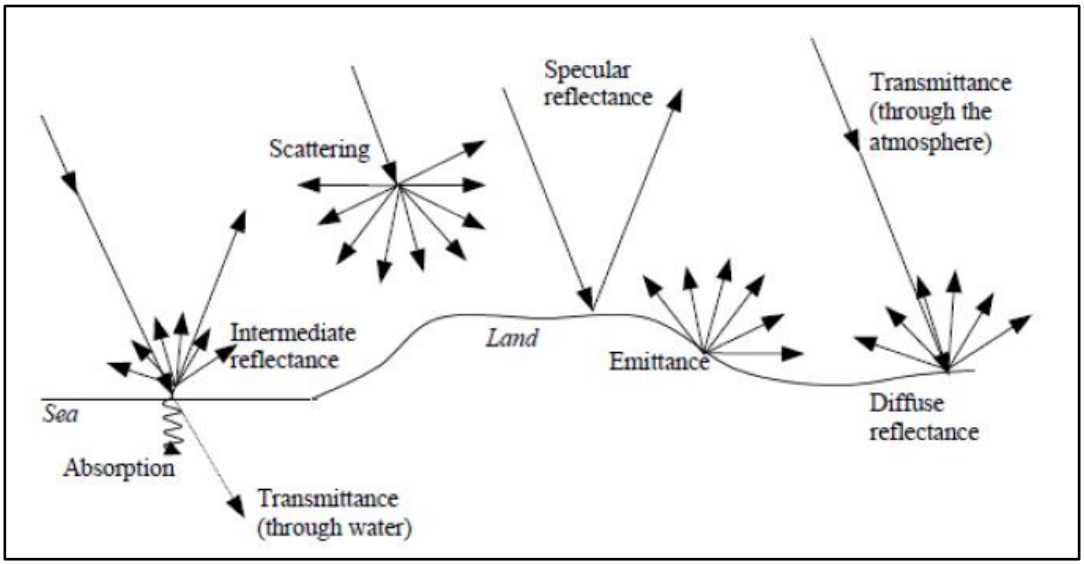

Fig.1.7. Electromagnetic radiation interactions with different surface features.

Radiation may be scattered i.e deflected in all directions and lost ultimately to absorption or further scattering (as light is scattered in the atmosphere).

Radiation may be reflected. If it is returned unchanged from the surface of a substance with the angle equal and opposite to the angle of incidence, it is termed specular reflectance (as in a mirror). If radiation is reflected equally in all directions, it is termed

as diffuse. The EMR interaction with different surficial feature is given in the Fig.1.7 explains the direction of propagation of reflected light.

The interactions with any particular form of matter are selective with regard tothe Electromagnetic radiation and to the specific matters, depending primarily upon surface properties, chemical constituents, atomic and molecular structure of the matter.

The Electromagnetic radiation is divided by specific wavelength region and according to the application and interaction of the radiation, the radiation division name, wavelength range, interesting facts and related uses are listed in the table 1.

Reflected IR radiation is commonly used in remote sensing application, divide in to following regions:

- Near Infra-Red (NIR) between 0.7 to 1.1 μm.
- Middle Infra-Red (MIR) between 1.3 to 1.6 μm
- Short Wave Infra-Red (SWIR) between 2 to 2.5 μm.

Remote Sensing and GIS have been more widely used as an important tool for analysis in the areas of mineral exploration. They have become important tools for locating mineral deposits, in their own right, when the primary and secondary processes of mineralization result in the formation of spectral anomalies. Additionally, some factors can be mitigated with ground support during over flights and field validation to improve statistical mapping methods. High resolution data are available, which can help in detecting small objects.The introduction of GIS to the geological sciences has provided powerful tools to help geologists to manage and analyze geological data much more efficiently than ever before. Several examples exist of GIS applications in the geosciences where multiple data sets are integrated to provide new information to users. Some of these studies used GIS for prospecting areas of mineral potential (Bonham-carter et al., 1988; Rencz et al., 1994) and land-use planning and management (Madigan et al., 1988).

Table.1. Specific Electromagnetic Radiations Wavelength Range (nm) and uses

RADIATIONS	WAVELENGTH RANGE	INTERESTING FACTS	APPLICATIONS / RELATED CAREERS
RADAR	0.3 to 300 cm	Object detection system mainly uses radio waves. Active mode of microwave Remote Sensing.	Determines direction, or speed, altitude, range, of both moving and fixed objects examples like aircraft, ships, spacecraft, guided missiles, motor vehicles, and weather formations.
MICROWAVE	0.3 to 300 cm	These longer wavelengths can penetrate clouds and fog. Imagerymay be acquired in the active or passive mode.	cooking; long distance TV and phone; Microwave Remote sensing
THERMAL IR	3 to 5 mm 8 to 14 mm	These are the principal atmospheric windows in the ThermalRegion. Imagery at these wavelengths is acquired through the useof optical-mechanical scanners, not by film.	Track active Volcanoes, Forest Fires, and Quantitative information of Forest Canopy structure, age and Biomass.
REFLECTED IR	0.7 µm to 3 mm	This is primarily reflected solar radiation and contains noinformation about thermal properties of materials.	NIR,SWIR and Long wave IR **Mainly used in Satellite remote sensing for mineral exploration.**
INFRARED(IR)	0.7 µm to 300 mm	Interaction with matter varies with wavelength. AtmosphericTransmission windows are separated by absorption bands.	heating & drying; "night vision" cameras; TV & garage door remotes;
VISIBLE	0.4 to 0.7 µm	Detected with film and photodetectors. Includes earth reflectance peak at about 0.5 mm.	what the eye and typicalfilm can “see”; optometrist
PHOTOGRAPHIC UV	0.3 to 0.4 µm	Transmitted through the atmosphere. Detectable with film and Photodetectors, but atmospheric scattering is severe.	Detection of skin disorder, and it reveals many artifacts
ULTRAVIOLET(UV)	3 nm to 0.4 µm	Incoming UV radiation atmosphere wavelengths 0.3 mm isCompletely absorbed by ozone in the upper atmosphere.	Germicidal, photochemical,Photo-electriceffects; hardening casts inMedicine.
X-RAY	0.03 to 0.3 µm	Incoming radiation is completely absorbed by atmosphere. NotEmployed in Remote Sensing.	Medicine; crystallography;astrophysicist
GAMMA	<0.03 nm	Incoming radiation from the sun is completely absorbed by the Upper atmosphere, and is not available for Remote Sensing. Gamma radiation from radioactive minerals is detected by low flying. Aircraft as a prospecting method.	Research into structure ofnucleus; geophysics;mineral exploration

GIS offers as a potential tool for accomplishing the acquiring, managing, analyzing, integrating and visualizing of the large volumes of geosciences data collected from a variety of sources (Harris et al., 2001).

GIS can be regarded as a set of tools to analyze spatial data- meaning the space around us, where there is live and function. Specifically, a GIS is an automated system that can capture store, retrieve, analyze and display spatial data from actual surrounding for a particular objective (Burrough and McDonnell, 1988). GIS is often described as integration of data, hardware and software designed for management, processing, analysis and visualization of georeferenced data (Neteler and Mitasove, 2007). Remote Sensing played a part in the development of GIS, as a source of technology as well as a source of data (Paul et al., 2005). GIS is widely used to manage data that have a special component. A digital GIS offers more viewing flexibility than a simple paper map, and also has tools to enable data analysis. Remotely sensed data from the earth observation satellites are particularly well suited for use in GIS since satellite imagery is already in a digital form.

In this work, the GIS software system such as Arc GIS 10.3 provide anexcellent graphic user interface for visualizing spatial data, the complexity ofgeospatial data and some specific application such as visualization of sub pixelmineral abundance images, nevertheless call for new visualization technique. Themost of the work done in this thesis is carried by the Digital Image Processingmethods and spectral radiometer with spectral signatures.

1.11. PETRO – CHEMICAL CHARECTISTICS

Petrography is a branch of petrology that focuses on detailed descriptions of rocks. The mineral content and the textural relationships within the rock are described in detail. Petrographic descriptions start with the field notes at the outcrop and include megascopic description of hand specimens. However, the most important tool for the Petrographer is the petrographic microscope. The detailed analysis of minerals by optical mineralogy in thinsection and the micro-texture and structure are critical to understanding the origin of the rock.

Geochemistry: Geochemistry in the study of composition, structure, processes, and other physical aspects of the Earth and its parts (Crust, Mantle and Core). To understand and examine the distribution of chemical elements in rocks and minerals, as well as the movement of these elements into soil and water systems.There is a wealth of information buried in the liquids, gases, and mineral deposits of rocks soil and water. The geochemistry is deals with understanding this information and make informed decisions on a range of extensive industrial and scientific research applications. Understanding the chemical composition of rocks of earth crust Geochemistry is the science that uses the tools and principles of chemistry to explain the mechanisms behind major geological systems such as the Earth's crust and oceans floares. The realm of geochemistry extends beyond the Earth, encompassing the entire Solar System and has made important contributions to the understanding of a number of processes including mantle convection, the formation of planets and the origins and composition of hole earth like crust, mantle and the core.

1.12. OBJECTIVES

1) To demarcate the corundum bearing horizons the study area.

2) To identify the spectral characteristics and different types of corundum bearing associated rocks.
3) To understand the geochemical signatures.

4) To Integrate and Correlate Geochemistry.

1.13. METHODOLOGY

Collection of base line information and preparation of base/location maps of the study area and to study the existed literatures on the application of hyperspectral remote sensing spectral signatures. To Study the Field Geological and Petrological work on Corundum bearing rocks of the study area. Interpretation of spectral reflectance characteristics of Corundum bearing rocks and associated lithological mineralization on hyperspectral satellite data for the understanding of their distribution, association, etc. by

visual interpretation, image processing, GIS, geo-spatial techniques.Interpretation of corundum associated mineralization zones and lithological contacts using Hyperspectral Instrument (SR-3500).Measurement of field hyperspectral signatures using Spectroradiometer and collection of GPS based geo-referenced samples for Ground Truth check. Analysis using Arc-GIS on spectral matching techniques, sub-pixel immixing retrieval techniques and identification of end member spectra etc then Discrimination of corundum mineral associated litho units and to validate the hyperspectral signatures data.

Study the physical, optical and chemical characters of samples using sophisticated analytical instruments and comparison and characterizing of their hyperspectral signatures obtained by spetroradiometr.

FinalyIntegration of all results Geological, Petrological, Geochemical and Hyperspectral Signatures on corundum bearing litho-units of the study area, detailed understanding of their distribution, association, etc. by visual interpretation, image processing (ERDAS 2014), GIS (Arc map10.3), Hyperspectral (ENVI 4.6) and GPS geo-spatial techniques has done.

OUTCOME OF THE RESEARCH

The Research Study Aims to carry out on corundum bearing horizons and their detail Mapping through hyperspectral and with the mineralization, its characterization is particular the types of corundum is precious and semi-precious to utilization in Gem Industry, which is having gemology and Gemstone in Industrial Applications of the state and Indian region.

10.14. GEOGRAPHICAL LOCATION OF THE STUDY AREA

The Karnataka is located within 11°30' to 18°30' North latitudes and 74° to 78°30' East longitude is southern part of Indian sub-continent. The state covers an area of 191,976 square kilometres (74,122 sq mi), or 5.83 per cent of the total geographical area of India. It is situated on a tableland where the Western Ghats ranges converge into the Nilgiri hill complex, in the western part of the Deccan Peninsular region of India. The State is bounded by Maharashtra and Goa States in the north and northwest; by the Arabian Sea

in the west; by Kerala and Tamil Nadu States in the south and by the States of Andhra Pradesh in the east. Karnataka extends to about 750 km from north to south and about 400 km from east to west.

The study area particularly in Southern Karnataka located between11°30' to 15°00' North latitudes and 74° 00′ to 78°30' East longitude, covering 20 districts with an aerial extent of 95,988sq km (Fig.1.8).

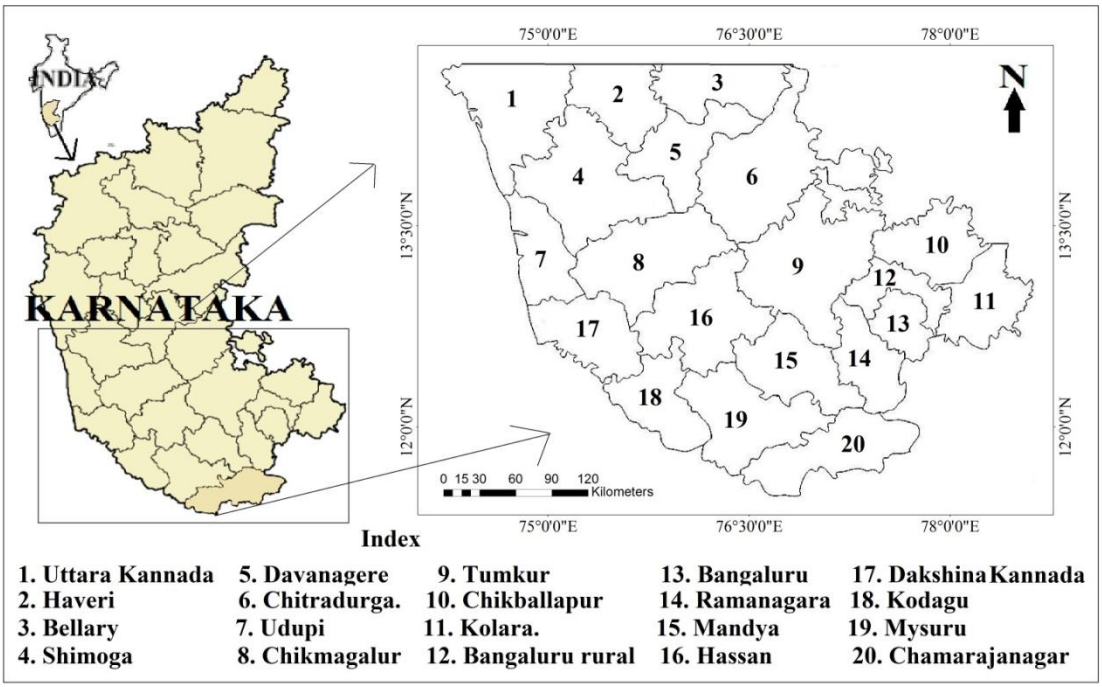

Fig.1.8: Location Map of the Study area

1. 15. LITERATURE REVIEW

Literature Review is a consideration of reports of information found related to selected area of study to constrain a theoretical framework for a present research topic. It provides an up to date understanding of a subject and significance of different techniques at present condition; Identifies the method used by previous researchers ona topic and provides a comparisons for own research findings. This literature review understanding of the research topic and it helps to identify the potentiality of the methods adopted in the Remote Sensing (RS) for mapping and advancement in the mapping of geological features and finally it gives information of a study area and similar work done so far within the area. A detailed review on the study sites, mineral exploration and mapping,

image processing, multispectral and hyperspectral Remote Sensing for mineral mapping and ground truth spectroradiometry has been carried out to furnish the upcoming chapters.

Zen, (1981) the mineral assemblages from metamorphosed slightly calcic Pelitic rocks of the Taconic Range in southwestern Massachusetts and adjacent areas of Connecticut and New York were studied petrographically and chemically. These rocks vary in metamorphic grade from those below the chloritoid zone through the chloritoid and garnet zones into the kyanite-staurolitezone.Microprobe data on the ferromagnesian minerals show that the sequence of increasing Fe/ (Fe+Mg) value is, from the lowest, chlorite, biotite, hornblende, chloritoid, staurolite, garnet. Hornblende, epidote, garnet, and plagioclase are the most common minerals that carry significant calcium. Muscovite contains small though persistent amounts of iron and magnesium in octahedral positions but has a variable K/Na ratio, which is potentially useful as a geothermometer**.**

Kruse F.A, (1988) done Classical geologic mapping and mineral exploration utilizingthe physical characteristics of rocks and soils such as mineralogy, weatheringcharacteristics, geochemical signatures, and landforms to determine the nature anddistribution of geologic units and to determine exploration targets for metals andindustrial minerals. Subtle mineralogical differences, often important for makingdistinctions between rock formations, or for defining barren ground versus potentialeconomic ore, are often difficult to map in the field. Hyperspectral Remote Sensing,the measurement of the Earth's surface in up to hundreds of spectral images and fieldinvestigated spectral signatures, provides a unique means of Remotely MappingMineralogy (RMM). A wide variety of hyperspectral data are now available, alongwith operational methods for quantitatively analyzing the data and producing mineralmaps. This review paper serves to illustrate the potential of these data and how theycan be used as a tool to aid detailed geologic mapping and exploration.

Alvaro P Crosta et al., (1998) used hyperspectral remote sensing for mineralmapping at Alto paraiso DE Goias area at Central Brazil. Here the authors examinethe capability of hyperspectral data acquired by AVIRIS airborne instrument over anarea comprises

Proterozoic metasediments with little mineralogical variations andalthough it does not represent an ideal side for the use of hyperspectral data, someinteresting results were found in terms of mineral identification in portions of theimage where enough ground exposure existed. Mineral deposits always holds themixture of primary and secondary minerals, related to later weathering process wereidentified in the imagery based on spectral signatures of pure pixels this mixturecomprised mainly hematite, goethite, halloysite, kaolinite and Na montmorillonite.AVIRIS data and the efficiency of the methods employed for mineral targetingincludes digital image processing (DIP) and the results are confirmed by laboratoryreflectance measurement and Scanning Electron Microscope (SEM) analysis of soilsamples.

Tomoaki Morishita and Shoji Arai (2001) corundum bearing mafic rocks study in the Horoman complex, they studied type II mafic rocks based on their chemical composition and structures show their cumulus origin with primary minerals assemblage controlled by crystallization of olivine plagioclase and clinopyroxene indicative of a low pressure origin.

Parikh et al., (2002) they are studied the Cr–K-edge XANES and EXAFS in natural Indian rubies from two sources and a synthetic ruby at ESRF. Weight % of various constituents in them is determined using EDAX measurements.Taking the results from the three techniques together we are able to demonstrate their feasibility in quantitative study of precious stones. They are made EDAX, XANES and EXAFS measurements (Cr–K-edge) on three ruby crystals from different sources, two natural and one synthetic. The results from three measurements show very good agreement and taking all of them together we are able to successfully demonstrate how these techniques can be used in study of the precious stones.

Peter Bajcsy et al., (2004) done methodology for hyperspectral band selection. Whilehyperspectral data are very rich in information, processing the hyperspectral dataposes several challenges regarding computational requirements, informationredundancy removal, relevant information identification, and modeling accuracy. Inthis paper the authors present a new methodology for combining

unsupervised andsupervised methods under classification accuracy and computational requirementconstraints that is designed to perform hyperspectral band (wavelength range) selection and statistical modeling method selection. The band and method selectionsare utilized for prediction of continuous ground variables using airborne hyperspectralmeasurements. The novelty of the proposed work is in combining strengths ofunsupervised and supervised band selection methods to build a computationallyefficient and accurate band selection system. The outcomes of the analysis led to aconclusion that the optimum number of bands in this domain is the top 4 to 8 bandsobtained by the entropy unsupervised method followed by the regression treesupervised method evaluation. Although the proposed band selection approach in thispaper is demonstrated with a data set from the precision agriculture domain, it appliesin other hyperspectral application domains.

Tomoaki Morishita et al., (2004) Coronitic textures around corundum in the sample suggest that corundum was not stable in mafic rock compositions during the late-stage *P*–*T* conditions recorded in the complex. Based on the experimental results, corundum is stable in aluminous mafic compositions at pressures of 2–3 GPa under dry conditions suggesting that the corundum-bearing mineral assemblages developed under upper-mantle conditions, probably within the surrounding peridotite Variations in the trace-element compositions of the corundum-bearing mafic rock and related rocks can be controlled by modal variations of plagioclase, clinopyroxene and olivine, suggesting that they formed as gabbroic rocks at low-pressure conditions They show no evidence for partial melting after their formation as low-pressure cumulates. TheHoroman complex is an example of a large peridotite body containing possible remnants of subducted oceanic lithosphere still retaining their origin geochemical signatures without chemical modification during Subduction and exhumation.

Fernando et al., (2005) Sri Lanka has long been renowned for its wide variety of gemstones dominated by varieties of corundum, chrysoberyl, garnet, spinel, tourmaline, zircon etc. Most of the gem deposits occur in stream valleys as placer deposits.A peculiar kind of corundum-spinel-scheelite-taafeite occurrence has been found associated with marble at Bakamuna within the central granulite belt of Sri Lanka Althoughscheelite and

taaffeite are found in Sri Lankan alluvial plains, this is the first reported in-situ occurreces of scheelite and taaffeite (Fernando &Hofmeister, 2000). Corundum deposits localized in marbles are widely known in history as a source of precious stones in many countries including Burma, Kashmir, Afghanistan, Tanzania and as well as the Urals and the Pamirs deposits

Prakash et al., (2013). They report a new occurrence of sapphirine-spinel-corundum bearing granulite's enclosed in granitic gneisses near Jagtiyal in the Eastern DharwarCraton (EDC). These granulite's are very important in deciphering the prehistory of the thermal peak of metamorphism due to the presence of refractory phasesThe P–T evolution of these sapphirinegranulite's has been constrained through the use of thermocalcprogram.Temperature of formation of sapphirine-spinel assemblages is high, around 800 °C, and pressure ranges from 5-7 kbars, suggesting that sapphirine formation took place during decompression stage.

Ali Mohammad Qaid and Basavarajappa (2008) studied the VNIR, SWIR and TIRbands of Multispectral Remote Sensing Satellite images such as ASTER and Landsat-7 ETM+ to reveal their capabilities in mapping hydrothermal alterations and otherPrecambrian rocks in North East of Hajjah, Yemen. The results of the chemicalanalyses revealed high anomalies of potentially economic minerals like Au, Ni, Cuand Zn. Empirical Line Method on ASTER and ETM+ showed high satisfactoryresults. PCA, band ratio, lineaments analyses and laboratory spectral reflectanceyielded a good correlation with the marked areas in presence of hydrothermallyaltered zones. In the band ratios 5/7 and 3/1 of ETM+ and their equivalent 4/6 and 2/1of ASTER data altered clays and iron oxide were mapped successfully.

Tangestani and Hosseinjani (2008) used Spectral Angle Mapping (SAM) and LinearSpectral Unmixing (LSU) algorithms to map alteration minerals using the imagespectra and the spectra selected from USGS library. Spectra of the image wereextracted using the "spectral end-member selection" procedures, including MinimumNoise Fraction (MNF), Pixel Purity Index (PPI) and n-dimensional visualization.Linear Spectral Unmixing (LSU) using the image spectra obtained

reasonable resultsand successfully discriminated pixels with highest proportions of alteration minerals, around copper deposits; while the abundance values of endmembers selected from theUSGS spectral library were not satisfied for output pixels. The study concluded thatoutputs obtained from the SAM and LSU algorithms were more reliable when usingthe ASTER image spectra in comparison to using spectra from the USGS library.Furthermore, LSU and SAM algorithms discriminated similar regions for eachalteration zone when using the image spectra.

Ian Graham et al., (2008). Recent discoveries over the last decade of new gemfields, exploitation of new and existing deposits, and application of relatively new techniques have greatly increased our knowledge of the basalt-derived gem sapphire–ruby–zircon deposits in West Pacific continental margins. they also critically review existing data on the gem corundum deposits, in order to further refine a model for their origin Some fields only produce a simple eruptive and zircon/corundum crystallization event while others contained multiple eruptive events, but only one or two zircon crystallization events.

Ali et al., (2009) use the spectral reflectance of 18 samples fromthe Precambrian basement for mapping the mineral resources in the north east ofHajjah, here the authors tried to map the altered system using VNIR-SWIR regions ofelectromagnetic spectrum and said reflectance is a physical property of materials thatdescribes how light in a continuous electromagnetic spectrum interacts with thematerial.

Raja et al., (2010) The spectral absorption characters of magnetite iron ore of study area are studied by the collection of spectral signatures using portable field based Ground Truth ASD(Analytical Spectral Device) Spectroradiometer working in the wavelength range of 350-2500nm with 10 nm band widths.The results of analyses in the Hyperspectral of Magnetite Iron ore is strong absorption in 0.91.0μm , (VNIR) wavelength regions and compared with the spectral library like this USGS, JPL(Jet Propulsion Laboratory), and JHU(Johns Hopkins Library). The result of analysis for magnetite iron ore is best matched between laboratory hyperspectral signature and library hyperspectral signature

Narayana and Pavanaguru, (2013) Khammam Schist Belt in Andhra Pradesh is considered as a northern extension of the Nellore Schist Belt (NSB). Both KSB and NSB are referred to a single unit of 600 km long westvergent Nellore-Khammam Schist Belt (NKSB) occurring as a paleo - proterozoic/late archaean greenstone belt on the basis of similar geological and structural setup in the Precambrian terrain of South India The Nellore Khammam Schist Belt (NKSB) is considered to be the equivalent of Sargur Schist Belt (3.3 Ga,).The pelitic meta-sediments such as sillimanite-kyaniteschists, sillimanite-cordierite orthopyroxene- corundum bearing rocks, pegmatites and banded iron formations (quart-magnetites).The KSB is endowed with economically viable corundum (ruby variety) and podiform chromite occurrences; however, they are significantly controlled by both lithology and structure.

Basavarajappa et al., (2015) used Landsat 7 ETM+ for discriminationof Banded Magnetite Quartzite and associated Precambrian Rock around Chkkanayakanahalli area in the southern part Chitradurga Schist Belt. Here theauthors implemented different image processing method like PCA, Mineral Composite and Band Ratio to delineate Manganese, Iron and Limestone deposits ofthe study area.

Basavarajappa et al., (2017) analyzed the spectral sensitivity of Visible to SWIR region of electromagnetic spectrum for Komatiite samples from the Kummanagattaarea, Gattihosahalli Schist Belt Chitradurga using ASD spectral radiometer. Here theauthors given application of spectral signature obtained in the SWIR region andabsorption in the wavelength region 1500 nm to 2500nm.

Basavarajappa et al., (2017) recently carried out the spectral studies for the Corundum bearing lithounits of the Arisikere area using ASD spectral radiometer and laterally did the Petrographic studies to identify the corundum presence in the Amphibolite schist rock.

Manjunatha and Basavarajappa (2017) they carried out hyperspectral charectrization and mapping of iron ore deposits in Chitradurga district. ASD spectral radiometer and laterally did the Petrographic studies to identify the iron presence and deposited in the parts of chitradurga district.

Jeevan and Basavarajappa (2018) recently carried out the spectral studies for the hydrothermal alteration zone of southern part of Chitradurga schist belt. ASD spectral radiometer data and Hyperspectral Remote Sensing data in field and laboratory environ ment and did the image processing it is helps to identify the hydrothermal alteration zones.

Chris Yakymchuk and Kristoffer Szilas (2018). Corundum is known to have formed in situ within Archean metamorphic rocks at several localities in the North Atlantic Craton of Greenland they studied two types of corundum bearing horizons one is Maniitsoq region, where kyanite paragneiss hosts ruby corundum, and second is Nuuk region, where sillimanite gneiss hosts ruby corundum. The bulk-rock geochemistry of the ruby-bearing rocks is consistent with significant depletion of SiO2 in combination with addition of Al2O3, MgO, K2O, Th and Sr relative to an assumed aluminous precursor metapelite.

1.15.1. EARLIER WORKS PERTAINING ON STUDY AREA

Foote, (1886) first gave the name 'Dharwar' to the highly altered crystalline schists of Archaean age and grouped them in to separate system, younger than the associated granitoid gneisses, having been laid over the eroded edges of the gneisses unconformably.

Smeeth, (1916) classified the Dharwar Succession in to two broad division- an older hornblendic and a younger chloritic division. This proved convenient for mapping and for representing the two distinct associations – one largely volcanic occupying stratigraphically lower position and other mainly sedimentary, made up of argillite, phyllite, limestone and greywacke, forming a younger less metamorphosed, and andchloritic group occupying the upper part of Dharwar Craton.

Fermor, (1909) grouped the Archaean provinces of India in to Charnockitic and noncharnockitic regions based on the charnockitisation occurred in the southern India.

Ram Rao (1940) and Pichumuthu (1946) based on the presence of the unconformities and Conglomerate within the succession classified Dharwar system in to three groups- Lower, Middle and Upper.

Radhakrishna, (1967) mentioned that Dharwar itself undergone more than one orogenic cycle hence he disagreed the classification made by using the prefixes upper, middle and lower. Based on lithostratigraphy and classification of Dharwar in to five series he treated the basement for the dharwar is peninsular gneisses.

The Precambrian terrains in worldwide occurrences and compared to southern India made in to two broad categories namely low greenstone and high grade granulite terrain **(Radhakrishna and Vasudev 1977). Later Chadwick et al., (1981)** considered the above mentioned terminology cumbersome prefer to describe the terrains as composed of gneiss and supracrustal rocks.

In the recent year a new classification has been proposed based on the rock type and the order of superposition following the internationally accepted code of stratigraphic nomenclature, the entire Dharwar succession is divided in to two main groups- the Bababudan group occupying a basal position and the Chitradurga group an upper position.

Schistose rocks were first separated from the granitic gneiss; all the schists are stretched linearly grouped under the Dharwar system. The first attempt in the past years divide the supracrustal of the craton into the Dharwar type of the western block and Keewatian type of eastern block these blocks are separated geologically the linear Closepet granite **(Anhaeusser et al., 1969; Ramkrishnan et al., 1976; Swami Nath et al., 1976).Viswanatha and Ramakrishnan (1976)** distinguished a third unit called it as Sargur group of rocks.

The occurrence of large volume of clastic sediments from shallow water shelf horizon and conglomerate distinguishes the Dharwar Supercrustals from the greenstone belts of other shield area. Therefore these are named as Dharwar type greenstone **(Shackleton 1976, Goodwin 1974);** younger greenstones **(Radhkrishna1976, Radhakrishna and Vasudev 1977)**; secondary greenstones **(Glikson, 1976)** and Geosynclinals piles **(Naqvi, 1978). Ramakrishnan et al., 1976** dissociate these belts from the greenstone concept and designated Proterozoic basins and geosynclines together as Dharwar Super group.

Peninsular Gneiss are controversial and many workers tried to establish therelative age of the gneiss and schists since the two rock types occur together. **Smeeth(1916), SampathIyengar(1920), Fermor (1936), Ram Rao (1936), Pichamuthu(1947) and Srinivasan and Sreenivas (1968)** found numerous instance of gneissic intrusion into the schists and therefore they considered the schistose formation to be older.

According to **Foote (1886, 1900), Radhakrishna (1967, 1976, 1977), Nautiyal (1966) and Iyengar and Jayaram (1970)** the basement nature Peninsular Gneiss Complex overlain by the greenstone rocks is the oldest. Further there is evidence of post dharwar mobilization of older granite gneiss producing local intrusive contacts with the overlying Dharwar rocks. A gradual withdrawal from the above extreme position is evident and it has been suggested that gneisses while intruding the high-grade schist form the basement of the younger schist **(Radhakrishna 1977, Swami Nath et al., 1976, Ramakrishnan et al., 1978). Picharnuthu (1951), Naganna (1975), Radhakrishna (1967), Srinivasan and Sreenivas (1968)** have been worked for studying the Stratigraphy, Structure and Mineral deposits of the study area: **Devaraju and Anantamurthy (1977, 1984)** have studied and done the mapping of manganese and iron ores and carbonates of the southern part of Chitradurga schist belt. **Mukhopadhyay and Baral (1974)** explained the structural and intra-tectonic history of the study area.

1.16. OUTLINE OF THE THESIS

The present work of "Hyperspectral and Geochemical Signatures on Corundum Bearing Rocks in part of Southern Karnataka, India" involves the evaluation of various fields/high-tech tools and technologies. These various techniques of the work undertaken in the present studyare presented in 7 chapters. The relevant tables and figures in different chapters have been prepared using appropriate software's and hardware's.

There are 7 chapters, which consolidate the thesis and help in achieving theaim and objectives of this research. Brief descriptions of these chapters are presented as follows:

Chapter 1 Introduction deals with the research problem, Basics of mineral Corundum, nomenclature, internal structure, petro- chemical charectistics and types of Corundum. Basic software's used in RemoteSensing, Hyperspectral Radiometer. The Objectives and

Methodology of thepresent study are listed and given the brief detail on the location of the study area. Detailed collection of base line information, previous literature undertaken byvarious authors and scientists on Hyperspectral Remote Sensing spectral signatures has beendiscussed in this chapter.

Chapter 2 Deals with the detail explain geology of the study area, explains thelitho-units in detail, Geological settings & regional traverses and the corundum bearing lithology and contacts with physiographic setting, origin and occurances of corundum minerals, geomorphologies tectonic setting of the study area and detail location map of the study area.

Chapter 3 Deals with information on field investigations, sample collections and field photos, Petrography for the selected rock samples collected during the fieldinvestigation. Ground truth chek using GPS and base maps of the study area.

Chapter 4 Deals with the concentrates on geochemical signatures and charectistics of corundum bearing litho units of the study area. Geochemistry XRF analysis using PANalytical Epsilon3 Omnian software's helps to find out a whole rock geochemistry data. Origin pro 8.5 and TRIDRAW saftwares give the results bring Chemical characteristics, genisis and discrimination of corundum bearing rocks. This Result shows purity of the corundum mineral present in the Precambrian basement rocks of the Southern Karnataka.

Chapter 5 Deals with the Spectral signature measures all types of wavelengths that reflect, absorb, transmit and emit electromagnetic energy from the objects of the earth surface. Hyperspectral signatures analyses for all samples were carried out using Lab Spectro-radiometer instrument (Spectral Evolution SR-3500). Spectro-radiometer instrument has the ability to measure the spectral signatures of different rocks/ minerals. The SR-3500 operate in the wavelength range of 350–2500 nm andDARWin SP.V.1.3.0 software is well utilized in analyzing each spectral curves obtained from the collected samples (average of 4 spectral curves from each samples) and well correlated with the standard curves of USGS, JPL and JHU.

Chapter 6 gives overall the result and discussion and correlate the geochemistry data and hyperspectral signature data correlated with help of software's.

Chapter 7 highlights the overall summary, conclusions on the results and recommendations of the proposed research study.

CHAPTER-II

CORUNDUM LOCATIONS AND GEOLOGICAL SETTING OF THE STUDY AREA

2.1. GEOLOGY OF INDIA

The Geological History of India began with the geographical transformation of other parts of the earth, to be precise, 4.57 Ga (billion years back). India is famous for its varied geological features. Various parts of India are made up of rocks of all categories of several geologic periods (Ramakrishnan and Vaidyanadhan., 2010). A few of the rocks are poorly malformed and metamorphosed. At the same time, other types of rocks are newly silted alluvial soils that are still to go through chemical and physical changes (Radhakrishna and Naqvi., 1986). Source of minerals of significant diversity is seen in the subcontinent area in substantial amount. Even the fossil evidences are remarkable that contain invertebrates, stromatolites, and plant and vertebrates fossils.

To begin with, the Deccan Trap encompasses nearly the whole area of Maharashtra and parts of Karnataka, Gujarat, Andhra Pradesh, and Madhya Pradesh to some extent. It is assumed that the Deccan Trap was created as a consequence of sub aerial volcanic operations related to the tectonic shift in this portion of the earth in the Mesozoic period (Ramakrishnan and Vaidyanadhan., 2010). This is the reason why rocks seen in this area are usually of igneous category. At the time of its passage to the north following its separation from the remainder of Gondwana, the Indian tectonic plate went above a geologic hotspot, which is known as the Reunion hotspot (Radhakrishna and Naqvi., 1986). This resulted in widespread melting below the Indian craton. The melted materials penetrated the shell of the craton in a huge flood basalt occurrence, forming what is named as the Deccan Trap. It is also believed that Reunion Hotspot resulted in the partition of India and Madagascar. The Vindhyan and Gondwana contain within its crease areas of Chhattisgarh, Madhya Pradesh, Bihar, Orissa, Andhra Pradesh, West Bengal, Jammu and Kashmir, Maharashtra , Himachal Pradesh, Punjab, Uttaranchal, and Rajasthan. The GondwanaSupergroup creates an exclusive series of fluviatile stones deposited in Permo-Carboniferous period. Rajmahal hills and Sone and Damodar river

basins in the eastern India are reservoirs of the Gondwana rocks (Swaminath and Ramakrishnan, 1981).

The oldest stage of tectonic evolution was identified by the chilling and hardening of the outermost layer of the shell of the earth in the Archaean period (earlier than 2.5 billion years), which is characterized by the presence of granites and gneisses, particularly on the peninsular area (Basavarajappa., 1992; Rama Rao, 1945; Ravindrakumar, 1982; Srikantappa and Hensen., 1992). These rocks create the center of the Indian craton. The Aravalli Mountain Range is the remains of a prehistoric Proterozoic geological formation, known as the Aravalli-Delhi geologic formation, which coupled the two earlier parts that comprise the Indian craton (Ramakrishnan and Vaidyanadhan., 2010). It stretches for about 311 miles or 500 km from its northernmost tip to remote hills and stony crests into Haryana, culminating close to Delhi (Radhakrishna and Naqvi., 1986).

2.1.1. PRECAMBRIAN SUPER-EON

A substantial territory of peninsular India, which is also known as the Indian Shield, comprises schists and Archean gneisses and these are the earliest forms of rocks seen in India. The Precambrian rocks of India are categorized into two systems and they are as follows. The Archean System the Dharwar System the stones of the Dharwar System are mostly sedimentary rocks. They are typically found in Mysore and Bellary in Karnataka and Aravalli Mountain Range, Rajputana, Rajasthan. These rocks serve as sources of minerals like iron ore and manganese. Gold is found in the Kolar gold mines in Kolar, Karnataka (Ramakrishnan and Vaidyanadhan., 2010) (Basavarajappa., 1992; Rama Rao, 1945; Ravindrakumar, 1982; Srikantappa and Hensen., 1992). The Vaikrita System, located to the west and north of India, which exists in Kumaon, Hundes, and Spiti territories, the Shillong sequence in Assam and the Dailing sequence in Sikkim, are assumed to be of the equal age as the Dharwarsystem.The gneisses or metamorphic stones can be further categorized into the Bundelkhand gneiss, the Bengal gneiss, and the Nilgiri gneiss. The Niligiri system is made up of Charnockites varying from granites to granular intrusive rocks (Swaminath and Ramakrishnan, 1981).

2.1.2. PHANEROZOIC

Lower Paleozoic – Stones of the oldest Cambrian era are seen in Spiti in the central Himalayan ranges and the Salt range in Punjab. These areas comprise a dense series of fossilized layers. The Pseudomorph Area in the Salt Range is made up of sandstones and dolomites (Radhakrishna and Naqvi., 1986). The sediments in Spiti are named as Haimanta system and they are made up of dolomitic limestones, micaceous quartzite, and slates. The Ordovician stones consist of limestones, flexible shales, quartzites, red quartzites, puddingstones, and sandstones. Silurian stones which include distinctive Siluria fauna are also seen in the Vihi district in Kashmir (Ramakrishnan and Vaidyanadhan., 2010).

Upper Paleozoic: Corals and Devonian fossils are seen in black-colored calciferous limestone in the Chitral region and grey-colored calciferous sedimentary rocks in the Central Himalayan Mountain Ranges. The Carboniferous consists of two separate series and they are - lower Carboniferous Lipak and upper Carboniferous (Swaminath and Ramakrishnan, 1981). Trilobites and brachiopods fossils are seen in the calcareous and arenaceous stones of the Lipak sequence. In Kashmir, the Syringothyris limestone also is a part of the Lipak. The genus of limestones is broadly denoted as productus limestone. This limestone has its source in the ocean and can be categorized into the Late Permian Chideru (with high ammonite content), the Middle Permian Amb division, and the Late Middle PermainVirgal (Ramakrishnan and Vaidyanadhan. 2010).

2.1.3. MESOZOIC

During the Triassic periods, the Ceratitestonebeds were formed, which derived their name from the ammonite ceratite. They comprise marls, calcareous sandstones, and sandy limestones. The Jurassic comprises two separate divisions – the upper Jurassic and the middle Jurassic. The Upper Jurassic is characterized by the black shales in Spiti and expanses from Sikkim to the Karakoram. Cretaceous stones encompass a huge territory in India.In South India, the sedimentary rocks are categorized into four types; the Ariyalur, the Niniyur, the Utatur, and the Trichinopoly phases (Ramakrishnan and Vaidyanadhan., 2010).

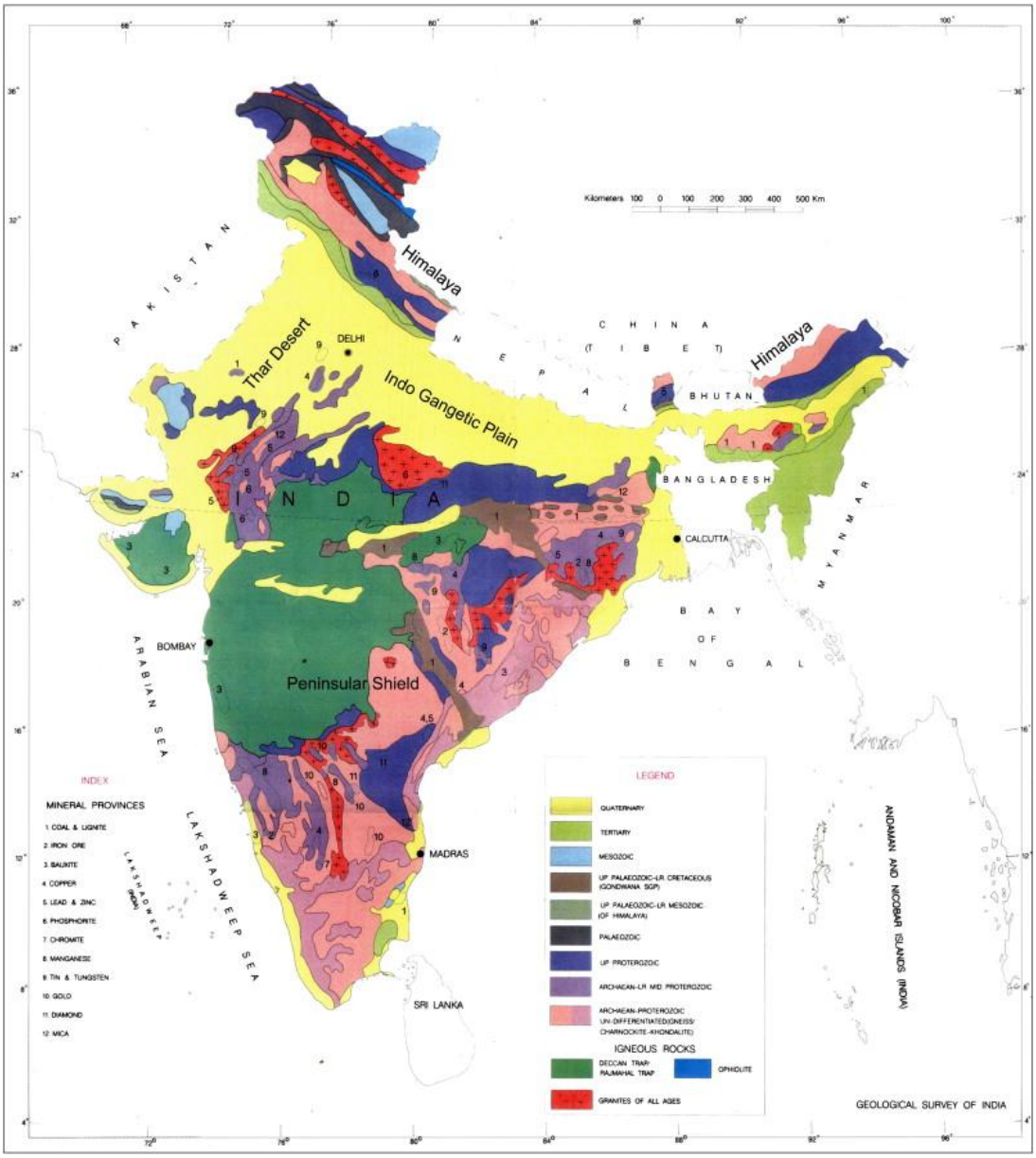

Fig.2.1.Geological map of India (after Geological Survey of India, 1993).

2.1.4. CENOZOIC

Tertiary period – This is the era when the Himalayan geological process started and the volcanic activities related to the Deccan Traps gone on. The rocks of this period have priceless deposits of coal and petroleum. Granites or sandstones are seen in Punjab. In Shimla, three types of stones are found – the Sabathu Series (Grey and red shales), the Kasauli Series (sandstones), and the DagshaiSeries (bright red clays). You will see Nummulitic limestone in the Khasi hills to the east of Assam. Beside the foothills of the

Himalayas, there are puddingstones, sandstones, and shales, collectively known as the Siwalik Molasse (Ramakrishnan and Vaidyanadhan., 2010).

Quaternary Period – The alluvial soil seen in the Indo-Gangetic basin is of this period. The alluvial deposits are categorized into older alluvium and newer alluvium. The newer alluvial soil is known as Khaddar and the older alluvial soil is known as Bhangar. This soil is worn down from the Himalayas and is one of the productive soils in the country (Ramakrishnan and Vaidyanadhan., 2010).

2.2. GEOLOGY OF SOUTHERN INDIA

The high-grade metamorphic rocks of the Precambrian terrain of south India is predominately composed of orthopyroxene bearing, greenish grey to brownish grey coloured, greasy looking rocks, generally termed as Charnockites (Holland 1900). Based on petrographic and mineralogical studies, these rocks have been classified as chamockitic, chamo-enderbitic and enderbitic granulites which show major and trace element composition of granitic, tonalitic to trondhjemitic composition. Associated with these rocks are numerous basic granulites (two pyroxene-plagioclase ± garnet granulites) and ultramafic rocks. Quartz-plagioclase-sillimanite/ kyanite-k-feldspar-gamet (khondalites); quartzplagioclase- k-feldspar -garnet bearing gneisses (leptynites) and other metasedimentary like banded magnetite quartzite, marbles and quartzite occur associated with chamockites charnoeuderbites. The southern Indian Peninsular shield has been divided into the Dharwar Cratonic nuclei, surroimded by mobile belts of varying ages (Radhakrishna and Naqvi, 1986). The granulite facies rocks in southern India is divided into two distinct crustal blocks viz. Northern Granulite Terrain (NGT) and Southem Granulite Terrain (SGT), separated by a major E-W trending Palghat Cauvery Shear System (PCSS) (Fig.2.1). The Archaean Dharwarcraton (DC) is essentially composed of granite-greenstone belts within the peninsular gneissic complex in the central part with granulite facies rocks occurring all along the western and southern margins of the craton. These granulites are distinctly of Archaean age and considered to be post-accretional type granulites (protoliths age of 3.400.m.y) and metamorphosed around 2500.m.y. (Peucat et al., 1989). These granulites are variously termed as Biligiri

Rangan Granulites (BRG) Basavarajappa and Srikantappa., 2014, Satnur-Halagur Granulites (SHG), Male Mahadeshwara Granulites (MMG), including the Mercara Granulites (MG). In addition to these, the late Archaeansyn-accretional type of granulites (accreted and metamorphosed around 2500 m.y. ago), termed as the Nilgiri Granulite (NG) and Salem- Madras Granulites (SMG) occur within the NGT. The Moyar-Bhavani shear zone (MBSZ), which separates the early-Archaean DC with the late Archaean NG is considered as a major terrane boundary in southem India (Srikantappa et al., 1986; Raith et al., 1990; 1999).The southern granulite terrain (SGT), also termed as Pandiyan mobile belt, (PMB;Ramakrishnan, 1993 and 1998) include chamockites, both banded/gneissic and massivetypes, two pyroxene granulites interlayered with high grade homblende-biotite gneisses.Pre-deformational, pre-metamorphic intrusives of" peridotite-pyroxenite gabbroanorthosite complexes are significant. Post-deformational, post-metamorphic intrusives gabbro-anorthosite plutons to alkali carbonatite complexes and granite plutons as wellas dolerite dyke (Gopalakrishnan, 1994). Within the SGT, different granulite blocks like Madurai Granulite block, Kodaikanal Granulite Block (KGB) bounded by Palghat Cauvery Shear Zone (PCSZ) in the north and Achankovil Shear Zone (ACSZ) in the south occur. The Kerala Khondalite belt (KKB), south of the ACSZ upto Kannyakumari is composed of two granuliteblock viz., Trivandrum Granulite Block (TGB) and Nagercoil Granulite Block (NGB) (Srikantappa et al.,1985; Yoshida and Santosh, 1996). The southern granulite terrain (SGT) comprises ancrustal domains of contrasting composition and tectonothermal evolution (Buhl, 1987;Peucat et al., 1989; Choudary et al., 1992; Harris et al., 1994; Raith et al., 1999).Two types of chamo-enderbiticgranulites have been recorded in the Precambrian terrane of south India viz..Massive Banded Chamockite (MBC) and Incipient Chamockite (IC). Patchy charnockites of Kabbaldurga and Kerala. Charnoenerbites, Basavarajappa., 1992; and Prekash Narasimha., 1992; sheared controlled incipient charnockites of Kollegala Shear Zone (KSZ) in Northern Granulite terrain of Biligirirangan Hill ranges Basavarajappa et al., 1992; Basavarajappa., 2015.

"Massive/Banded" Chamockite (MBC): The medium to coarse grained, Massive Banded Charnockite (MBC), which are generally massive (look homogeneous in outcrop occur asmappable units) covering large areas and generally occupy upland regions (could be

upliftedmasses during neotectonism). Numerous basic enclaves occur as boundins or layers parallelto foliation planes imparting banded structures in the field. These rocks show evidence of atleast two periods of deformation as seen in BiligjriRangan granulite and Nilgiri granulite inthe northern granulite terrain (NGT). Typical examples of Massive to Banded Chamockites (MBC) occur in the Biligiri Rangan Granulite (BRG), Nilgiri Granulites (NG), Mercaragranulites (MEG) and Kerala Khondalitebeh (KKB)."Incipient" Chamockite (IC) are orthopyroxene bearing acid granulites which have beendeveloped locally as veins, patches or lenses within the predominately amphibolite faciesgneisses. IC are considered to represent an arrested stage of transformation of an amphibolite facies gneiss to granulite. Two typical examples of IC formation documented inthe Precambrian terrane of southem India viz. The protoliths for the Kabbai type incipientchamockite veining is an ortho-gneiss (Pichamutu, 1960; Janardhan et al., 1979; Stable etal., 1987), whereas in the Ponmudi type, it is a para-gneiss (Srikantappa et al., 1985; Ravindra Kumar et al., 1985; Hansen et al., 1987; Santosh et al., 1991).

South Indian Precambrian crystalline complex consists of schistose and gneissose type rocks form the hypogene series by Newbold in 1846. Bruse Foot (1886) separated the crystalline schistose rock from the association of gneisses and named it as ‘Dharwar System’ to include all the schistose rocks. The ‘Great Eparchaean Unconformity’ underling in the gneisses and schistose makes the Dharwar schist group same as crystalline gneisses of Archaean age (Holland 1900). Fermor (1909) while endorsing the thought of Holland modified the term Dharwar to embrace all meta-sedimentary schists lying below the unconformity. Later with respect to lithological forms Smeeth (1916) divided the Dharwars in to two groups- a lower hornblendic group and an upper chloritic group. Smith’s classification is totally agreed by Jayaram (1920). An Archean province of Indian is divided as Charnokite and Non- charnokite region by Fermor (1936). RamoRao (1940) identified different group of schist belt and he made this schistose in to five groups and presented three fold classification of the Dharwar system. Nautiyal (1966) divided the Dharwars in to Upper, Middle and Lower with respect to lithology, tectonic cycle and metamorphism. Radhakrishna (1967) after field studies recognized the number of orogenic cycle within in the Dharwar region itself hence he said it is improper

method to give the term upper, middle and lower. Further while classifying he considered the Peninsular Gneisses as the basement for the Dharwar group.

In 1946 Pichamuthu investigated a geosynclinals development in the Dharwar group and given the detail about two cycle of sedimentation with attendant magmatism. Srinivasan and Sreenivas in 1968 recorded a geosynclinals history in Chitradurga Schist Belt starting with a pre-geosynclinal shelf facies, followed by a flysh-geosynclinals facies and finally ending with the apogeosynclinalmolasse-faceis. In 1972 based on the atmospheric evolution and tectono-magmatic activity they divided Dharwar in to four divisions.

Radhakrishna and Vasudev (1977) compared the Precambrian terrain of south India to the similar ones in the rest of the world and they come across the two main categories called granite-greenstone of low grade rock and granulite terrains of high grade rock. Chadwick et al 1981considered this terminologies and oriented to describe the terrains as composed of gneisses and supracrustal rocks.Anhaeusser et al (1969), Ramakrishnan, Swaminath (1976) following the green belt concepts, made these schistose rocks in to two groups of supracrustal unit named as Dharwar type of Western Block and Keewatian type of Eastern Block and these blocks are separated by linear closepet granite. The Sargur group of supracrustal rocks with their distinct high grade metamorphic characteristics and Ramakrishna et al. 1976 and Swaminath et al. 1976 were compared these rocks in to high grade metamorphites of other cratontaken the name sargursupracrustal rocks, but Naqvi in 1978 treats this high grades also as a true greenstones, to resolve this conflicts Ramakrishna and Swaminath (1981) suggested to treat these rocks as ancient supracrustal (Bridgwater et al.1974). In the later part Glikson (1976) also suggested not to consider the oldest supracrustal occurring as an enclaves and xenoliths within the peninsular gneiss in to the primary greenstone belt.

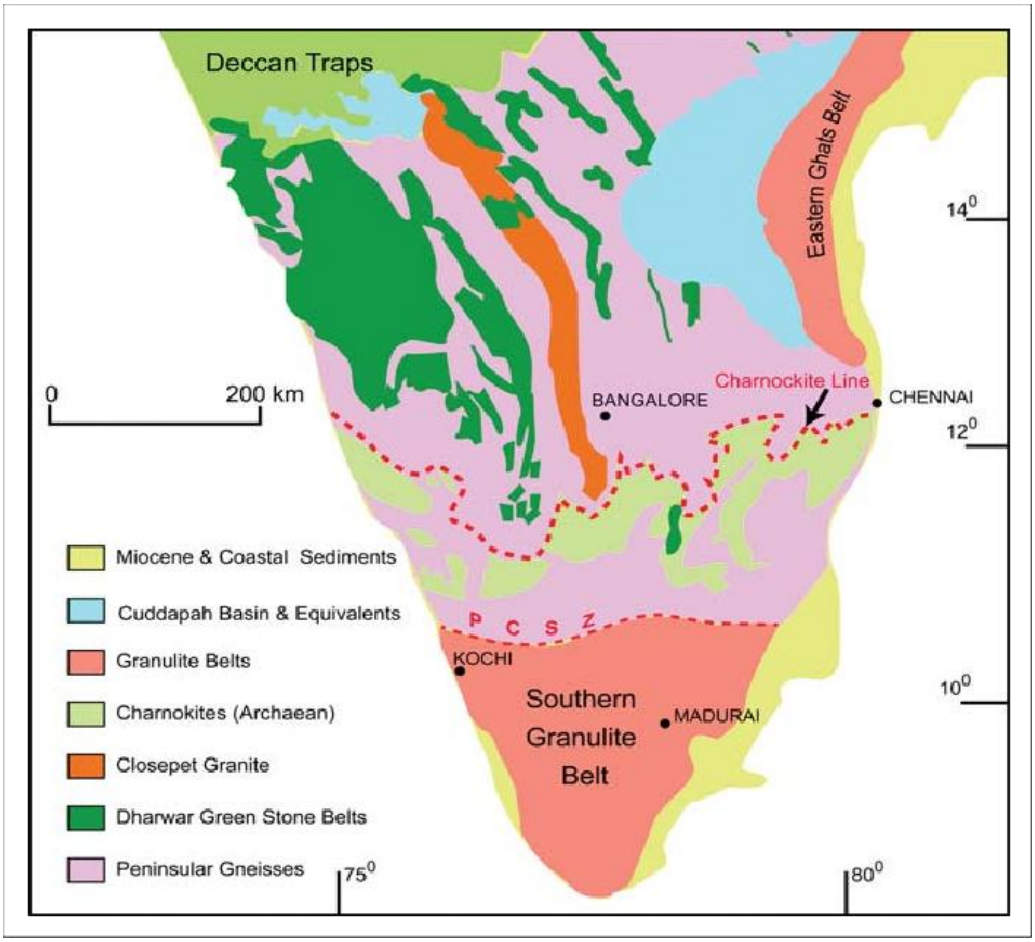

Fig.2.2. Geological map of Southern India (after Chardon et al., 2008).

2.3. DHARWAR CRATON

The Dharwar Cratonis bounded in the N 12º 00' to 17º 00' latitude and E 74º 00' to 79º 00' longitude and geographically it covers an area of~4,00,000 km2. Spatially we can see the Proterozoic sediments and Deccan traps in the northern end, Cuddapah basin and Easter Ghats Mobile Belt (EGMB) towards the eastern margin, the fault planes dipping steeply covered by the Arabian sea is occurred in the western side and Southern Granulite is mostly covers over the southern end of the peninsula demarcates the Dharwar super group with well noticed boundaries. Dharwar Craton made of greenstone belts, supracrustal and granitic gneiss basements are well exposed and most of the green stone belts are mineralized by gold and copper sulfide deposits. Radhakrishna*et al*. (1967); Narayanaswamy*et al*. (1970);Swaminath and Ramakrishnan, 1981; Naqviet al.

1974explained the two different green schist rocks one with preserving the oldest rocks that made up the early continental crust and another with the younger greenstone belts divided the main Dharwar Craton into two blocks named as, eastern and western blocks (Figure 2.3) considered that these two blocks were separated byelongated K-rich plutonic bodies known as "Closepet Granites" of an age 2500 Ma old. Closepet Granites were emplaced along a network of vertical shear zones representing boundary between two blocks (Moyenet al. 2003).

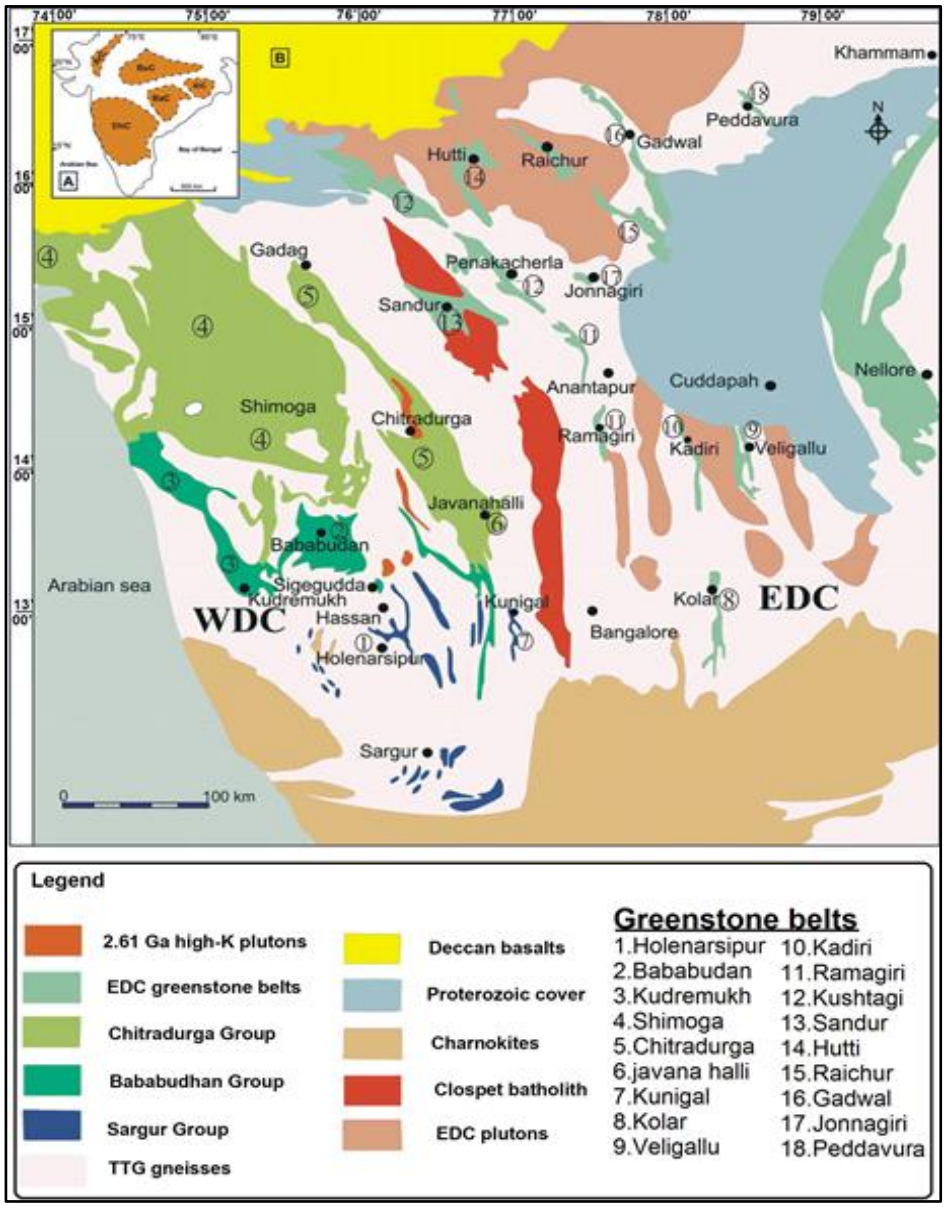

Fig.2.3. Geological map of Dharwar Craton (after Srinivasan., 1991).

2.4. GEOLOGY OF KARNATAKA

Karnataka state is located in the wedge shaped Indian peninsular as per the geological map prepared by Geological Survey of India (1981) and extents the area of 2,10,000 Km^2 representing the major parts of Dharwar Craton (Karnataka Craton) (Swaminath and Ramakrishnan, 1981). Geologically, it consists of linear to curvilinear subparallel series of schist belts within the peninsular gneiss. These schist belts are bounded by (i) Sedimentary basins of Kaladgi and Badami group and Deccan volcanics in the north (ii) to the west by phanerozoic sediments along the coast and (iii) by the Charnockite Biligiri-Ranganahill ranges in the south and north-eastern parts of Koorg hill ranges and parts of Mysore (Basavarajappa., 1992; Rama Rao, 1945; Ravindrakumar, 1982; Srikantappa and Hensen., 1992).

The geological history of Karnataka is mainly confined to the two major oldest eras namely the Archaean and Proterozoic. Minor sediments of recent age are also exposed along the western coastal margin according to the regional changes lithological variations differences in volcano-sedimentary environments and grades of metamorphism, the Karnataka Craton can be divided into the two blocks as i) the western block, characterized by a larger (Dharwar type) schist belts, showing evidences of having accumulated in distinct sedimentary basins and, ii) An Eastern block, characterized by reworked and mobilized gneisses with remnants and slivers of schist belt (Kolar type) which are auriferous and developed in an oceanic environment. The N-S trending Closepet granite demarcates the boundary between the two blocks (Fig.2.4) (Jayananda et al., 1995).

The early Precambrian rocks preserved in the Karnataka Craton encompassing cycles of magmatism, volcanism, sedimentation, metamorphism and deformation. The Dharwar Craton is described as a compact elliptical region bordered by a string of K-rich granites (Radhakrishna and Naqvi., 1986). The present work is concerned with the application of Hyperspectral Remote Sensing and GIS on major rock/ mineral/ ore types in Chitradurga district, Dharwar Craton. The granite-greenstone belts which constitute the Dharwar nuclei have been well studied and it can be stated based on the earlier workers

that the Dharwar Craton can be divided into two groups: the older Sargur group and the younger Dharwar super group (Swaminath and Ramakrishna, 1981).

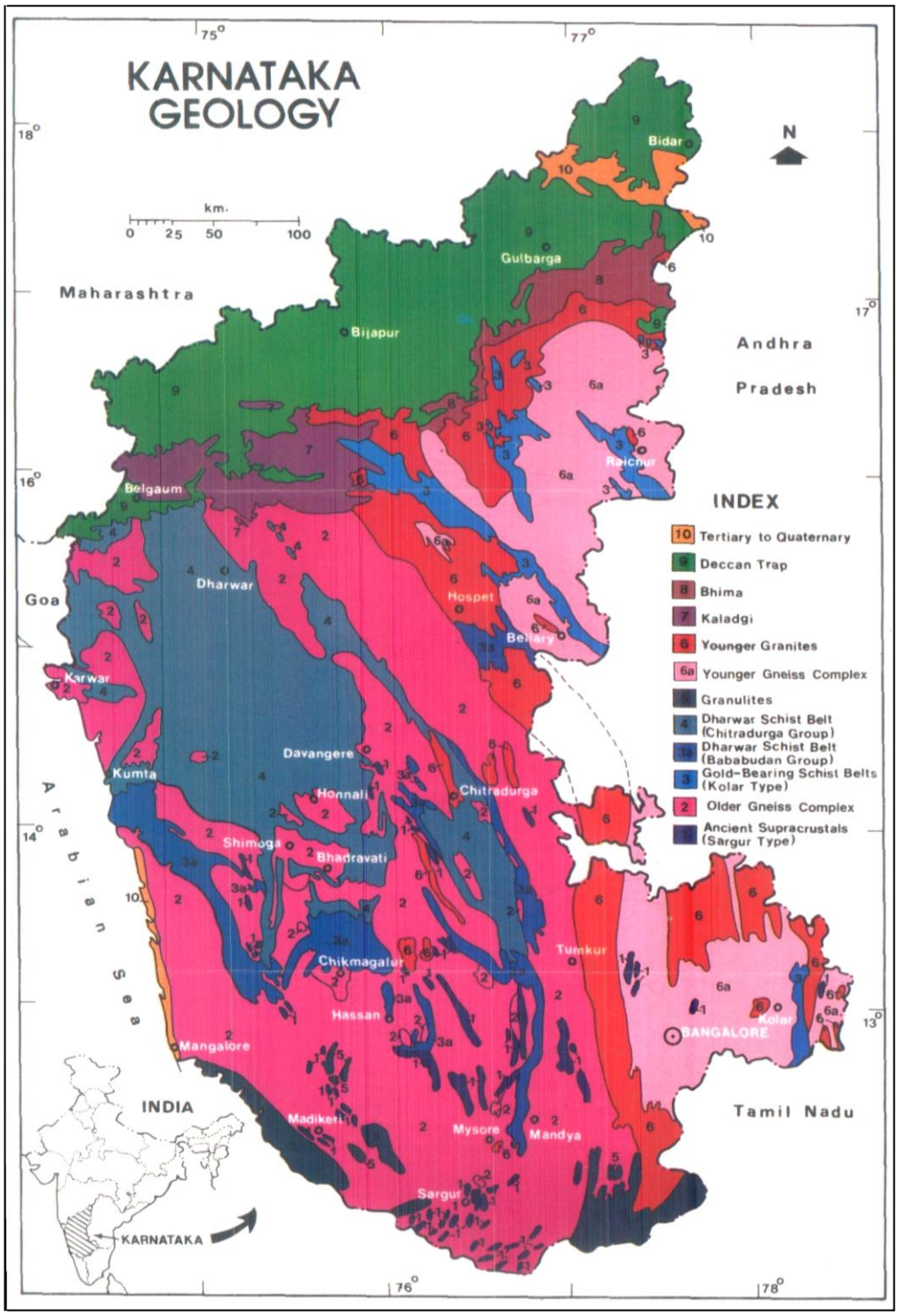

Fig.2.4. Geological map of Karnataka (after Radhakrishna et al., 1994)

The age of Sargur Supracustal sequence ranges between 3450 and 3100m.y (Nutman et al., 1992) and consists of volcano sedimentary rocks intruded by ultramafic, mafic complex, peninsular gneisses of 2950-3000m.y separate the older Sargur Supracrustals from the younger Dharwar greenstone belts. The age of Dharwar super group is 2900 m.y and consist volcano sedimentary sequence formed in an intra-continental rift basin setting. The top most sequence of this group gives an age of 2650 m.y (Crawford., 1969). Younger granites intrude these sequences of rocks at 2600 m.y, which constraints the upper age limit of Dharwars.

Three major categories of Archaean Supracustal sequence of Karnataka are (a) The ancient Supracustal enclaves (b) The Auriferous Schist belts of Karnataka (c) The Dharwar type Schist belts of Western Karnataka sequence. The important feature of the Archaean sequence is their actual N-S trends with convexity towards east. The schist belts are wider in the north, tapering down towards the south younger and younger sequences get exposed towards north, one of the explanations offered is that the peninsula as a whole has got tilted to the north, with the result deeper and deeper sections are exposed to the south (Radhakrishna and Vaidyanathan., 1997) (Fig.2.4).

2.4.1. CHITRADURGA GROUP

The study area is represented by Chitradurga group which unconformably overlies the Bababuddan group and PGC. This group comprises of in ascending order Vanivilas, Ingaldhal and Hiriyur formations (Swaminath and Ramakrishnan., 1981). The Vanivilas formation exposed along the western margin of the belt includes the Talya conglomerate, chlorite schist, quartzite limestone, dolomite and banded Mn-Fe chert (Rama Rao., 1962). These litho-units are well exposed around the Sirankatte gneissic dome. The Ingaldhal formation comprising basic to acidic lavas, pyroclastics, Banded Iron Formation (BIF) and fine grained clasts (argillite) is exposed mainly in the south and eastern parts of Chitradurga (Ramakrishnan and Vaidyanadhan., 2010). The Hiriyur formation is represented by the greywacke-argillite suite, interspersed with BIF, metabasalt and polymictic conglomerate. A persistent polymictic conglomerate zone at Kuruba-Maradikere popularly known as K.M.Kere conglomerate forms the lower unit of this formation. It is succeeded by the volcanic of Maradihalli, Narenahalu and Bellara areas.

The greywacke suite well exposed around Aimangala and Hosakere is characterized by the presence of polymictic (GSI Memoir., 1981).

2.4.2. SARGUR GROUP

Sargur Group is represented in the Chitradurga belt by a varied assemblage of lithologies in the sub-belts of Ghattihasahalli, Nagamangala, Mayasandra, Neralakere, Sasivala, Honakere, Sunkiapur, Javanahalli and Yadiyur-Karighatta which occupy the flanks and extensions of the main schist belt (GSI Memoir., 1981). These rocks are isoclinally folded, highly metamorphosed and are devoid of clues as to top and bottom direction, thus preventing the establishment of their stratigraphic order of superposition (Ramakrishnan and Vaidyanadhan., 2010).

2.4.3. PENINSULAR GNEISS

Peninsular gneiss was termed to emphasize its extensive distribution throughout the Indian Peninsula (Smeeth W.F., 1916). This name is widely used to represent the complex of gneisses and associated granitoids with their own set of pegmatites and aplites giving evidences of successive injections extending over a long and protracted period of plutonic activity (Ramakrishnan and Vaidyanadhan., 2010). The Peninsular Gneiss flanks the schist belt to the east and west and also occurs as diapiric domes within the belt (GSI Memoir., 1981). In its typical form, the Peninsular Gneiss is a migmatite consisting of bands of melanosomes and leucosomes. Various degree of mobilization of the neosomes in the migmatite has given rise to assorted structures such as stromatic, surreitic, folded, ptygmatic, ophthalmic, schlieric, and nebulitic (Mehnert., 1973). The gneissic complex encloses several lenticular bodies of ultramafite adjoining and parallel to the schist belt as near Chikkanayakanahalli. These were considered related to the geosynclinals episode of the main schist belt (Jayaram B.N., 1965).

2.4.4. DHARWAR SUPERGROUP

Chitradurga schist belt is the only belt in the lower part of the Bababuddan Group, characterized by rhythmic metabasalt-quartzite suite is well represented. The Chitradurga Group overlies the Bababuddan Group and Peninsular Gneisses with

Table.2.1. Generalized Geological succession of the study area

(After Seshadri et al., in Swaminathan and Ramakrishnan., 1981)

DHARWAR SUPER GROUP	**CHITRADURGA GROUP**	Basic dyke gabbro and dolerite Younger granites (Chitradurga, Hosadurga and Jampalnaikankote)	
		Hiriyur Formation	Basic Dykes (Gabbro and Dolerite) Younger granite (Chitradurga, Hosadurga and J.N.Kote) Greywacke – argillite suit + Basic to intermediate volcanic Banded ferruginous chert and Polymict Conglomerates (Aimangala and Holelkere) K.M Kere and G.R. Halli conglomerates ----------Disconformity----------
		Ingaldhal Formation	Basic, intermediate/ acid lavas/ pyritiferouschert argillite Chloriticphyllite Banded ferrugionouschert Limestone and dolomite
		Vanivilas Formation	Chlorite- biotite + garnet Phyllite/ Quartizite and quartz schist Talya conglomerate ----------Unconformity----------
	BABABUDAN GROUP	AmygdularMetabasalt closely interbeded with cross bedded and ripple marked quartzite ultramafite (Talc-tremolite chlorite and serpentinite) and thin beds of iron stones oligomictic conglomerate (Neralakatte) ----------Unconformity----------	
PGC		Peninsular Gnessic Complex	
SARGUR 3300 M.a		Gattihosahalli belt Fuchsite quartzite with barites Aluminous quartz schist Meta-ultramafite Amphibolite	

Chlorite- biotite + garnet

Phyllite/ Quartzite and quartz schist

Talya conglomerate

----------Unconformity----------

a prominent unconformity and constitutes the major part of the DharwarSupergroup (Ramakrishnan and Vaidyanadhan., 2010). The Chitradurga Group extends as a continuous chain of hills/ bandsfrom Dodguni village in the south to Chitradurga village in the north and further northward, these band were wraps around the Chitradurga plutonicgranite forming the U-curve of Chitradurga area. The western arm extends for a short distance up to Mayakondavillage and the eastern arm continues up to Gadagtalukin the north.

2.4.5. BABABUDAN GROUP

Bababudan group of rocks occupy an area of 2,650 sq.km spread in parts of Hassan, Shimoga, Dharwar, Chikmagalur, and north districts of Karnataka and neighbor state Goa. The litho units of Bababudan group commences with basal conglomerate and quartz phenoclasts resting unconformly on gneissic basement. The Bababudan group is exposed in the sub-belts of Kibbanahalli, Madadkere-Mayakonda, Halekal and Yadiyur-Karighatta (GSI Memoir., 1981).

2.5. GEOLOGY OF THE STUDY AREA

South Karnataka is occupied by vast areas of Peninsular Gneiss along with two prominent superbelts of Bababuddan- Western Ghats-Shimoga and Chitradurga-Gadag belonging to the Dharwar Super group. In the southern part, there is a group of narrow, linear schist belts belonging to the older Sargur Group, like Hole Narsipur, Nuggihalli, Krishnarajpet, Mayasandra, Nagamangala and Melikote, Karighatta as well as innumerable medium to high-grade schistose enclaves within Peninsular Gneiss, as at Sargur, Mercara and their extentions in Kerala (Ramakrishnan and Vaidyanadhan., 2010). Geologically constituted of Southern Karnataka comprises of greenstone-granite belts, Gneisses and granulites (Swaminath and Ramakrishnan., 1981). Greenstone belts essentially consist of meta-volcano sedimentary Sequences surrounded and dissected by Peninsular Gneiss (GSI Memoir., 1981). At the southern end of the craton these give way to granulite suite of rocks. The craton preserves a billion year orogenic history from 3400 m.a. to 2400 m.a, Younger granites (~2600 Ma) like Chitradurga, Hosadurga, Arsikere and Banavara occur as isolated plutons in the gneissic country. An undated layered basic

intrusion (Konkanahundi or Thagaduru) and a syenite ring intrusion (KunduruBetta) are also seen. Proterozoic basic dykes are also abundant. Rarely, Neoproterozoic granite (Chamundi granite) and associated alkaline dykes are seen near Mysore and Harohalli. Pan-African syenite-carbonatite complexes (e.g., Dharmapuri) (Radhakrishna and Naqvi., 1986). The oldest Gneiss in Western DharwarCraton is a site of trondhjemitic gneiss with associated tonolites and granodiorites called as Gorur Gneiss. The gneiss yields whole rock Rb-Sr and Pb-Pb isochrones at 3300-3600Ma. Still older SHRIMP U-Pb zircon and other isotopes model ages of 3500 to 3600Ma in Western DharwarCraton do not srelate to any known rocks, but are suggestive of earlier events (Ramakrishnan and Vaidyanadhan., 2010).

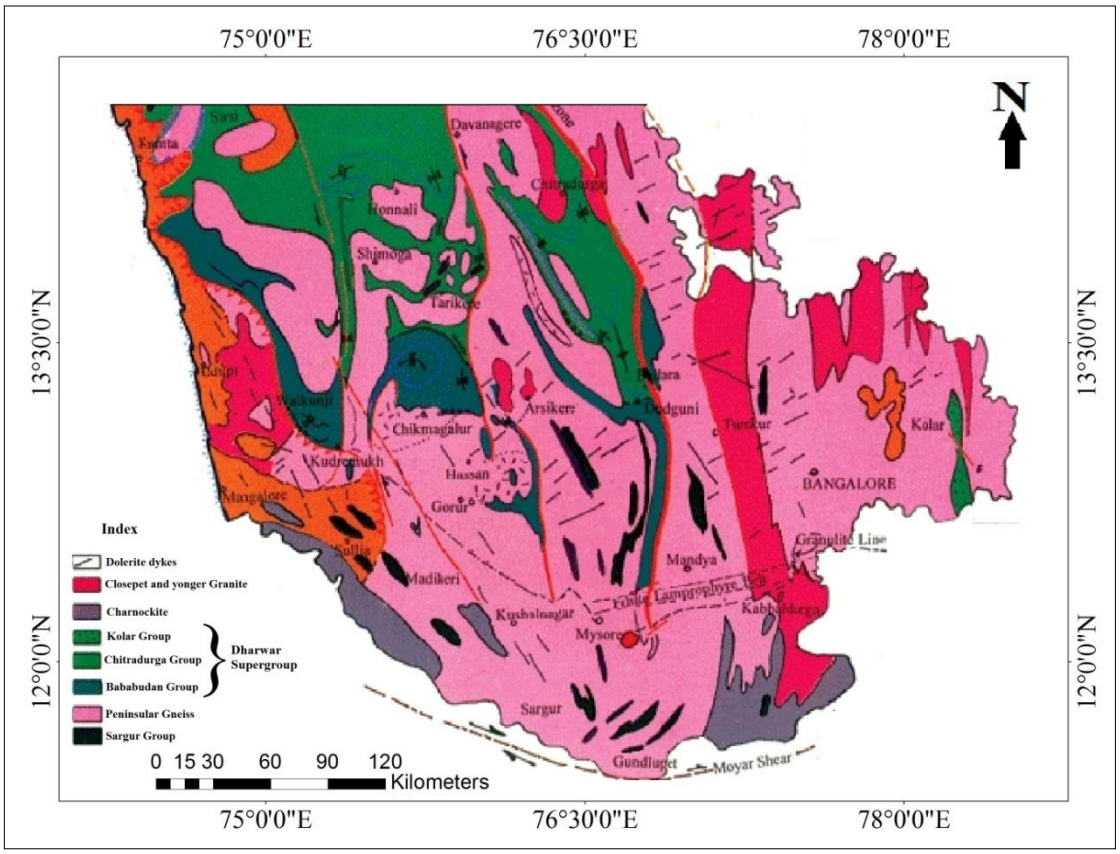

Fig.2.5. Geological map of the Study area (after Swami Nath et al., 1981).

2.6. ORIGIN OF CORUNDUM DEPOSITS

Corundum (sapphire and ruby) is a crystalline form of the aluminum oxide, that can be found in three main geological environments (Aydogan and Moazzen, 2012): (1) magmatic, mainly in syenites, monzonites, and lamprophyres; as xenocrysts and in xenoliths in alkali basalts; but rarely in granites (2) metamorphic, mainly in marbles, skarns, granulites, cordieritites, gneisses, migmatites, mafic-ultramafic metamorphites, and metabauxites; and (3) secondary alluvial, colluvial and eluvial deposits. Corundum crystals are usually closely associated with Tertiary alkaline basalt, basanite, nephelinit, which occurs as flows, plugs, and pyroclasts (Sutherland, 1998a). They have been found as corroded megacrysts in these basaltic rocks, along, with numerous xenoliths; including metasediments, granulite, granite, anorthosite, pyroxenite or lherzolite. Corundum crystal has been found as inclusion in clinopyroxenocrystal in Nong Bon alkali basalts in eastern Thailand and in diamond (Kepezhinskas, 2011). Corundum, as a mineral, is encountered in a range of rocks. It is relatively common in many metamorphic rocks of varied lithologies and its P–T stability domain is vast. For example, this mineral appears during forest fires on bauxite soils, and is observed as a high pressure phase in diamonds and eclogites. Non-gem corundum may also be a hydrothermal alteration product, for example of andalusite. Because of its chemical composition, it is present in alumina rich, silica-poor rocks. Corundum–quartz bearing assemblages are rare and these minerals are usually not in contact. Exceptions, in which quartz and corundum form a stable or metastable assemblage, are known in high pressure and high temperature granulites and in hydrothermally altered quartziferous porphyry.

Magmatic deposits Corundum in magmatic deposits is found in plutonic and volcanic rocks. In plutonic rocks, corundum is associated with rocks deficient in silica and their pegmatites, especially syenite and nepheline syenite. Corundum is formed by direct crystallization from the magmatic melt as an accessory mineral phase. The classical examples are the syenite pluton from Haliburton and Bancroft (Moyd., 1949), and the Kangayansyenite (Coimbatore district, Madras, India, Hughes 1997). In addition, aluminous rocks carried as xenoliths by plutonic rocks can lead to the formation of corundum, as in the xenoliths of biotite schist carried by a monzonite at San Jacinto, in

Southern California (Murdoch and Webb 1942). Corundum is found also as an accessory mineral in porphyry Cu deposits (Botril 1998).

In volcanic rocks, sapphire and less commonly ruby are found in continental alkali basalt extrusions (Sutherland et al. 1998a). Corundum is found as xenocrysts in lava flows and plugs of subalkaline olivine basalt, high alumina alkali basalt, and basanite. The sapphire is blue-green-yellow (BGY) and the deposits only have economic importance because advanced weathering in tropical regions concentrates sapphire in eluvial and especially large alluvial placers. Sapphire also occurs in alkaline basic lamprophyre (Brownlow and Komorowski 1988) as mafic dikes of biotitemonchiquite (lamprophyre characterized by the abundance of phlogopite and brown amphibole, olivine, clinopyroxene, analcime), ouachitite and diamond-bearing kimberlite.

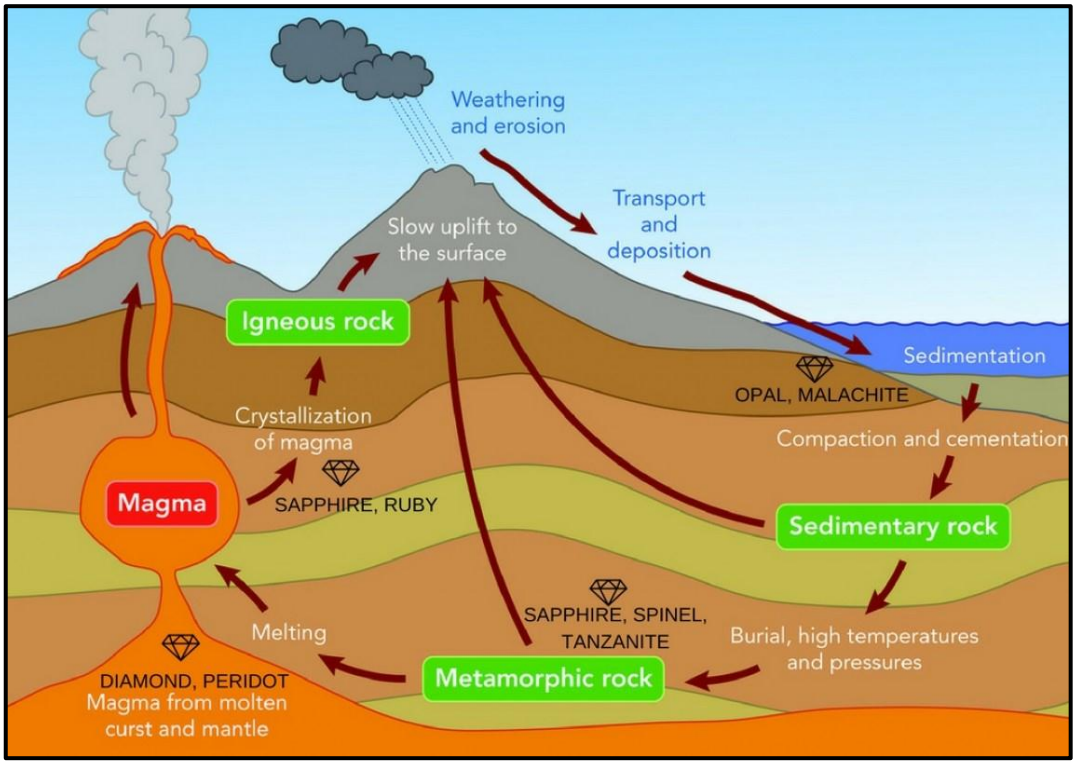

Fig.2.6. Corundum Deposition and Process (Giuliani et al., 2014).

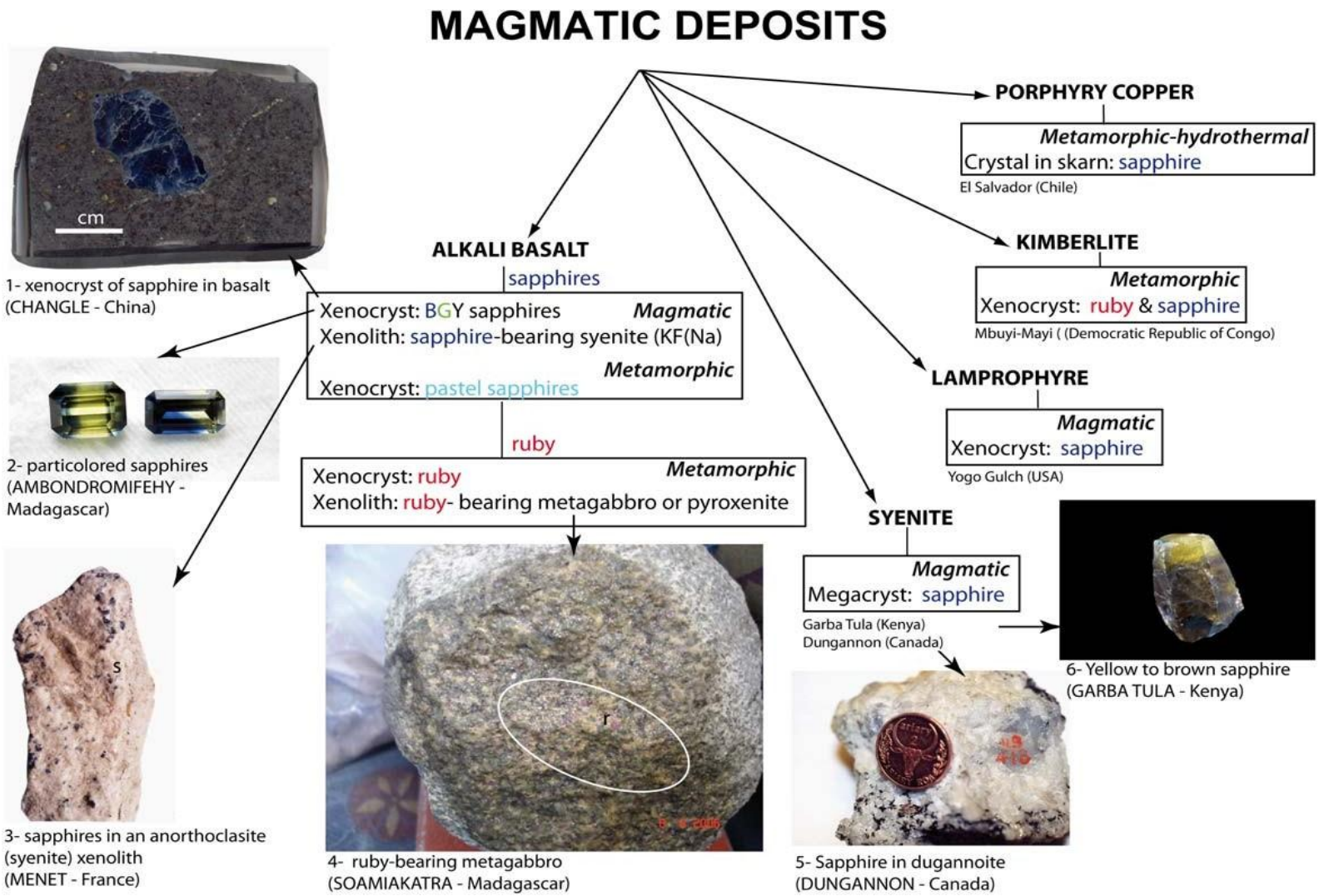

FIG. 2.7.Classification of Primary Corundum Deposits based on the lithology of the corundum-host rocks.A, The magmatic deposits with their main types. For each type the origin of ruby and/or sapphire is precised: magmatic *versus* metamorphic. Photographs respectively 1 courtesy of F. Fontan, 2 and 6 of L.-D. Bayle, 3 and 5 G. Giuliani, and 4 of S. Rakotosamizanani.

2.6.1. CLASSIFICATION OF CORUNDUM DEPOSITS

An attempt to classify gem corundum deposits must consider primary and secondary deposits. In primary deposits, the host rock crystallized the corundum. In secondary deposits, corundum is present as an inherited mineral, whether a clast or a xenocryst, for which its primary origin can sometimes be determined. Thus in sedimentary deposits, corundum is a clast of detrital origin, and in basaltic deposits, corundum is a xenocryst in the lava (Coenraads, 1992). Keeping this distinction in mind, the classification here follows the usual classification of rocks into sedimentary, metamorphic and igneous types. Among metamorphic rocks, a subdivision emphasizes the role of metasomatism in the formation of some corundum deposits. Within each category, deposits are grouped according to shared petrographic and genetic features. The proposed classification is shown in (Fig.2.8).

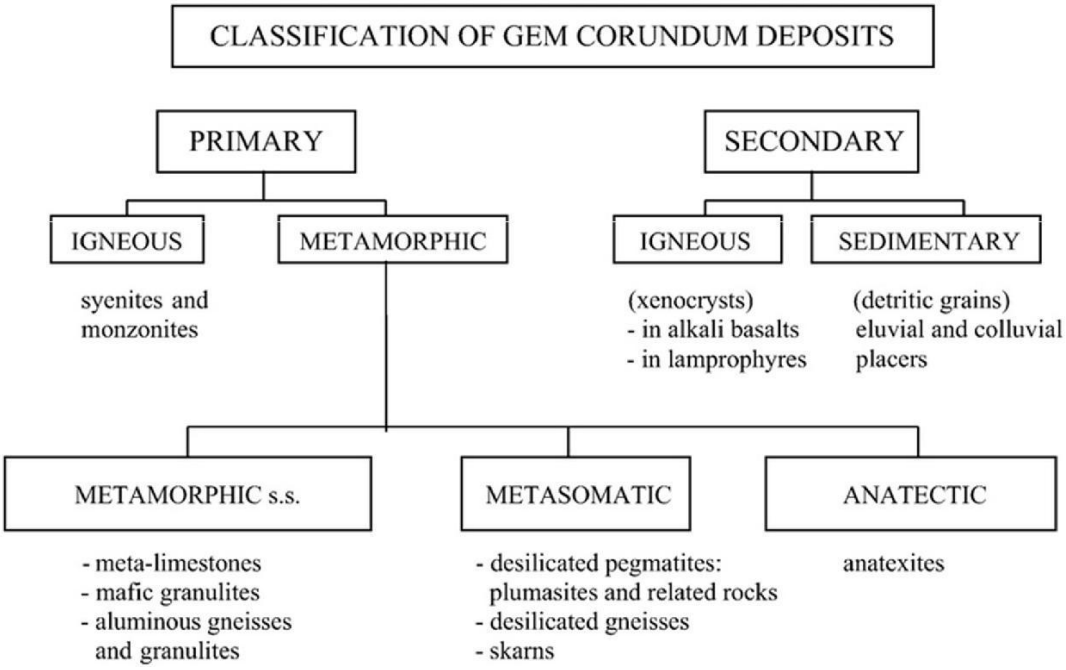

Fig. 2.8. Classification scheme for Gem Corundum Deposits (Simonet et al., 2008).

2.6.2. IGNEOUS DEPOSITS

Corundum, gem or non-gem, is often quoted in mineralogy hand books as a mineral originating from syenites. In fact, this kind of occurrence is relatively rare and only a few in-situ igneous corundum deposits are described. The documented primary gem

corundum deposits include the alkaline igneous rock of the Garba Tula deposit in Central Kenya (Simonet et al., 2008). Originally believed to be a monzonite, it is now realized that the rock is a syenite. There, sapphires are mined from a vertical dike emplaced in a series of biotite and hornblende-bearing gneisses of the Mozambique Belt. Sapphires display colors from a dark ink blue to a golden yellow, through various shades of blue and green. Crystals appear as barrels or as truncated bipyramids, and may reach more than 100mm in length. They contain about 1 wt.% FeO and traces of TiO_2 and Ga_2O_3. Corundum-bearing magmatic xenoliths have sometimes been noticed in various types of lava. Brousse and Varet (1966) described sub-gem blue sapphire barrels in anorthoclasite xenoliths from a trachyte dome in Cantal, and considered these enclaves and the host trachyte as homogenetic. Robertson and Sutherland (1992) described sapphire–anorthoclasite xenoliths from a basalt plug in central Queensland, Australia. Upton et al. (1999) described rare corundum-bearing anorthoclasite xenoliths in alkali basalt sills and dikes from Scotland. Corundum, of barrel-shaped habit, is dark blue andshows some characteristics similar to sapphires from basaltic (secondary) deposits. Upton et al. (1999) considered that these xenoliths have crystallized from a trachytic liquid of mantle origin.

2.6.3. METAMORPHIC DEPOSITS

Metamorphic rocks are a major source of high-quality gem corundum. As a mineral, corundum is relatively common in these rocks and appears in a wide range of pressure and temperature conditions. Generally speaking, factors that will allow or prevent the appearance of corundum are P, T, the protolith mineralogy and chemistry, the presence or absence of fluids, and their chemical characteristics. This last point emphasizes the role of metasomatism. The omnipresence of fluids in the Earth's crust means that metamorphism rarely occurs in a closed system, and metasomatism is critical to the genesis of many gem corundum deposits. Three sub-categories of metamorphic deposits are considered here in: metamorphic sandstone, metasomatic and anatectic. In metamorphic deposits sandstone corundum crystallized as a result of isochemical metamorphic reactions in silica-poor or alumina-rich rocks. This happened mainly in closed systems, although in some cases large-scale chemical exchanges may have assisted crystallization of corundum. However, such chemical exchanges are often

difficult to identify and quantify when samples of non-metasomatized protolith are not available. The geometry of such deposits follows that of the protolith and their size can be hundreds of m to km in scale. Gem corundum-bearing aluminous gneisses and granulites are an important source of sapphire, ruby, and other gemstones, and are the source of major sedimentary deposits, leading to large corundum provinces. The best known example is that of southern Sri Lanka, where numerous authors recognized the importance of granulites and charnockites of the Highlands Group as the main source for this country's alluvial and eluvial deposits. The rare in-situ deposits are corundum-bearing gneisses containing aluminous minerals such as garnet, spinel, sapphirine, cordierite and sillimanite. They have been subjected to high temperatures and moderate pressures (amphibolite facies to low pressure granulite facies). Generally, the existence of these aluminous minerals is ascribed to the existence of locally Al-enriched layers in the metasediments, but some authors consider possible a wide-scale desilication owed to mafic granulites. The Highlands Group, and most of Sri Lanka's Precambrian rocks, are now largely considered as an eastern extension of the Mozambique Belt. It is therefore not surprising that the rest of the Mozambique Belt is also known for its granulite-hosted gem corundum deposits. Ruby and/or sapphire-bearing gneisses are particularly frequent in southern Kenya (Simonet et al., 2008) and are also the main source of corundum in the alluvial deposits of Tunduru-Songea (Southern Tanzania) and Ilakaka (Madagascar). Gem corundum from such granulites is dipyramidal, and more rarely prismatic or tabular. It is often blue or yellow although virtually all colors may be found. Rubies occurring in marbles are of high repute for their superior quality, for example the “pigeon blood” color. The chemical composition of rubies from marbles is characterized by a high Cr_2O_3 content (up to 2.5 wt. %) and a low FeO content (typically less than 0.04wt.%) which is considered to be responsible for the quality and purity of their red color. Vanadium traces are also often present. Ruby is sometimes associated with mauve, pink, and more rarely blue sapphire, and in most cases has rhombohedral or tabular habit, sometimes prismatic or truncated dipyramidal. Associated minerals include red or blue gem spinel, and various Al-, Mg or Ca-silicates, as well as sulfides and oxides. This type of deposit must not be confused with corundum-bearing skarns, which also occur in a marble environment. Ruby and/or sapphire-bearing marbles occur in Myanmar, Afghanistan (Hughes, 1997),

Pakistan, Tajikistan, Nepal, Urals, Tanzania (Morogoro deposits) and Vietnam. The origin of this type of deposit remains problematic, the main question being that of the origin of aluminum and chromium. Several authors proposed that non carbonate minerals in marbles come from mineral impurities in the pre-metamorphic limestone. However, Kissin (1994) notes that the marble's alumina content is not a critical factor for the presence of corundum, but that magnesium activity strongly influences the stability of spinel with regard to corundum. Since it is difficult to explain the presence of detrital chromian minerals in the pre-metamorphic carbonated sediment, that has been seldom documented, it is likely that chromium in the marble is of exogenetic origin, which implies that ruby-bearing marbles are at least partially the result of metasomatism. Although chromium is usually considered as an immobile element in such conditions, the mobility of this element can in some cases be high, especially if anions such as F or Cl are present in the fluid phase. Some authors such as Terekhov et al. (1999) and Koltsov (2001) advocate a metasomatic origin for this type of deposit. P–T formation conditions of these deposits are often not precisely known. Koltsov (2001) gives conditions of amphibolite facies for the formation of ruby in marbles from Kashmir and Afghanistan. In most cases, the marbles and their host rocks underwent amphibolite to granulite facies metamorphism. Ruby-bearing mafic granulites are mostly known for their ornamental qualities, under such names as the “anyolite” from Longido, Tanzania, or the “rubysmaragdite” from North Carolina. Ruby-bearing mafic granulites have also been described from Chantel in France by (Lasnier, 1977). Faceting-quality rubies are rarely encountered in this type of deposit, which explains why they are often overlooked as a ruby source, except in the Losongonoi deposit (Tanzania) which yielded significant quantities of gemqualityruby (Simonet et al., 2008) and the Chimwadzulu Hills area of Malawi. Also, the non-transparent star rubies from the Mysore area, Karnataka, India, are found in an amphibolite. These granulites are generally vivid green rocks because of the high Cr content of the rock-forming aluminosilicates (pargasitic amphibole, zoisite). Corundum is pink to dark red and has a typical tabular habit (blades). It is rich in Cr_2O_3 (up to 1.7 wt.%) and FeO (up to 0.8 wt.%). In most deposits, it is associated with pargasite, gedrite, calcic plagioclase and spinel. When present, sapphirine is regarded as a higher-grade mineral than corundum. These rocks result from the hydration of

plagioclase-rich rocks (anorthosites, troctolites and norites) under granulite facies conditions. They are systematically associated with mafic–ultramafic complexes, either layered intrusions or ophiolitic remnants. Metasomatic deposits result from the introduction of reactive fluids along a tectonic structure (channelized metasomatism), or from the accidental contact between two chemically different rocks (contact metasomatism). In both cases the mineralization is essentially planar and of relatively small size, with typically a m-scale thickness and a 10 m scale lateral extension. Sharp mineral zonations with limits parallel to the mineralization plane characterize these types of deposits. Small-scale metasomatic events responsible for the formation of gem corundum deposits are usually desilication phenomena. They involve a silica-deficient rock and a silica- and alumina-rich rock or fluid (silica-aluminous component). The silica-deficient component can be an ultramafic rock (serpentinite or sagvandite), a mafic rock, a metacarbonate, or a fluid equilibrated with ultramafic rocks. The silica-aluminous component can be an intrusive granitic or syenitic pegmatite, gneiss, or a fluid equilibrated with silicic rocks (meta-pelite, granite, etc...). In most cases, the silica aluminous component undergoes a desilication, the silica being "pumped out" by the silica-deficient unit. Alumina, which is less mobile, remains in the protolith and recrystallizes as Corundum, spinel, kyanite and other alumina-rich silicates. The most common geological settings are summarized below (Fig.2.10). Plumasites and related rocks.Plumasite originally described by (Lawson, 1903) is an example of Corundum bearing metasomatic rock. A plumasitesensustricto consists of greyor bluish Corundum, oligoclase and biotite, but the term has been widened to include rocks with alkali feldspars and other minerals. Corundum is usually not of gemquality, except in some deposits such as the Kinyiki sapphire deposit in southern Kenya. Such rocks result from the desilication of pegmatites that have intruded ultramafic rocks. Desilication causes quartz to react out and aids the crystallization of Corundum in the pegmatite. Concomitant silication of the host ultrabasite causes the development of anthophyllite and phlogopite "blackwalls" along the pegmatite. Gem corundum-bearing metasomatized pegmatites closely related to plumasites include Kashmir sapphire deposits (Peretti et al., 1990) and Umba fancy sapphire deposits in Tanzania. The host rocks in Kashmir and Umba differ from proper plumasites by different mineral assemblages, the presence of

gem quality Corundum, and its colors. Ruby deposits of the Mangare area (Simonet et al., 2008) originate from more complex desilicationphenomena involving pegmatites and ultrabasites. Characteristics of the crystals vary from one deposit to the other.

Kinyiki sapphires appear as truncated dipyramids and Kashmir sapphire asdipyramids. These sapphires contain small amounts of iron (typically <0.5 wt. %FeO) and their blue color is mostly due to charge transfers between Fe^{2+} and Ti^{4+}. Umba sapphires often have a prismatic habit, and their color as well as their chemical composition varies from one vein to the other. Rubies from the Mangare area are typically dipyramids and contain up to 0.4 wt. % Cr_2O_3 and less than 0.05 wt. % FeO. Metasomatic alteration, including desilication, can also affect felsic rocks such as gneisses or other quartzofeldspathic rocks that have been tectonically put in contact with ultramafites. Examples of such rocks include the Kangerdluarssuk ruby deposit (Greenland), the "Goodletite" of New Zealand, and some ruby and sapphire deposits of southern Kenya (Simonetet al., 2008).Corundum-bearing skarns form from reactions between pegmatites, or metapelite-equilibrated fluids, with metalimestones. The desilication reaction is initiated by the silica-deficient host rock, which is in this case a meta-carbonate instead of an ultramafic rock. The geometry of the mineralization, with phyllosilicate "blackwalls", is strikingly similar to that of plumasitic deposits. Sapphire-bearing skarns have been described from Sri Lanka and East Africa (Simonet et al., 2008). The south-eastern Madagascar sapphire deposits near Andranondambo have been described as due to desilicatedpegmatites, but were reinterpreted as skarns (Peretti and Hahn., 2013). Crystals typically have a dipyramidal habit. This type of deposit should not be confused with ruby-bearing meta-limestones, although both types of deposits can co-exist.

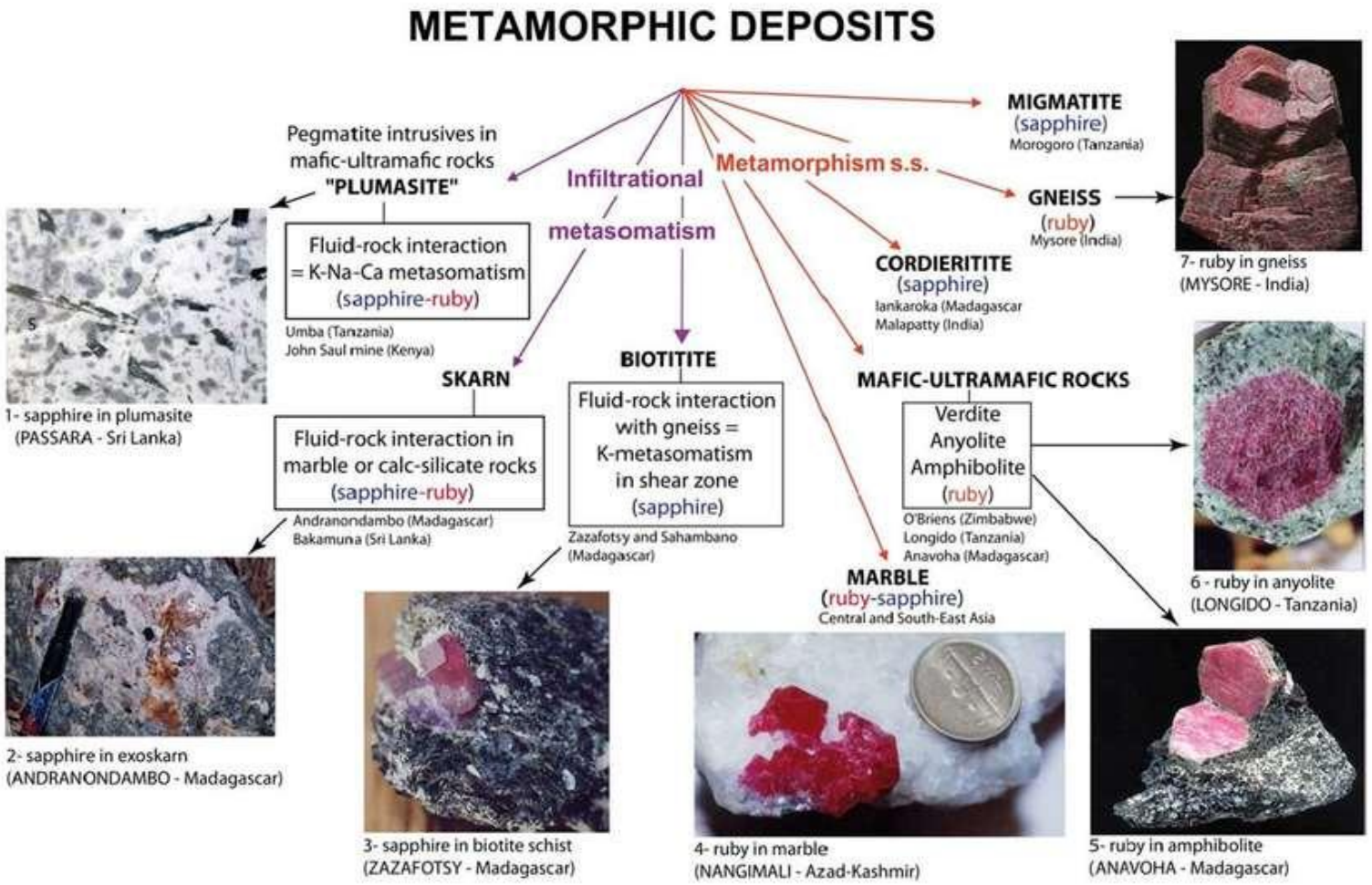

FIG.2.9. Classification of Primary Corundum Deposits based on the lithology of the corundum-host rocks. **B**, The metamorphic deposits with their main types.Photographs respectively 1 to 4, and 6 courtesy of G. Giuliani, 5 and 6 of L.-D. Bayle.

2.6.4. SEDIMENTARY DEPOSITS

To the best of our knowledge, there are no examples of authigenic (primary) gem corundum in sedimentary rocks. Gem corundum sedimentary deposits are eluvial or colluvial accumulations, alluvial and marine placers. They may or may not be consolidated depending on their age. Corundum crystals are present as clasts inherited from other types of deposits. These deposits are a major source of gem corundum (Garnier et al., 2004a), especially in Sri Lanka, eastern Australia, east Africa. The formation of gem corundum alluvial deposits obeys the same depositional rules as for other heavy mineral deposits. Concentration of gem-quality corundum in such deposits is higher than in primary deposits, due to a filtering process during erosion and transport, the most included and fractured stones being more rapidly destroyed. (Garnier et al., 2004a). The formation of gem corundum alluvial deposits obeys the same depositional rules as for other heavy mineral deposits. Concentration of gem-quality corundum in such deposits is higher than in primary deposits, due to a filtering process during erosion and transport, the most included and fractured stones being more rapidly destroyed.

Sutherland et al. (1998a) proposed a genetic model in four stages for the formation of 'magmatic' sapphire from eastern Australia. The lithosphere is displaced above a mantle plume. A low rate of initial fusion generated felsic magma enriched in volatile elements in zones where the lithosphere is rich in amphibole, allowing the crystallization of corundum and zircon. This magma can also be derived from a mantle enriched inamphibole and mica, or from a mantle enriched in felsic components, at between 45 and 90 km depth. When the lithosphere is located above the plume, a high rate of partial fusion produces alkali basaltic magma that extracts and carries assemblages with corundum as xenocrysts and in xenoliths. When the lithosphere moves away from the plume, the rates of fusion decrease and lead again to the crystallization of corundum and zircon. This model explains the enrichment of Hf, Nb, and Ta, generally observed in minerals cogenetic with corundum, and in amphibole veins found in the peridotite xenoliths (Sutherland et al. 1998b).

The presence of a mantle plume under the lithosphere is a main geodynamic feature for thegenesis of such "magmatic corundum", but the mechanism of generation of the Al-rich

magma is not yet constrained.Pin et al. (2006). Pin et al. (2006) observed that the Si—Al—Na-dominated bulk composition is similar to that of certain glass inclusions included in peridotitic xenoliths in alkali basalt. In addition, the extreme enrichment of incompatible elements in the albitite implies premelting metasomatism by a fluid or a melt. These rocks are interpreted to be products of very low degree of partial melting of a harzburgite source previously enriched by carbonatite-related metasomatism. The presence of volatile phases such as H_2O and CO_2 may account for the variation of the solubility of SiO_2 and Al_2O_3 in mantle fluids and the consequent precipitation of corundum in some batches of felsic magma.

2.7. CORUNDUM LOCATIONS OF THE STUDY AREA

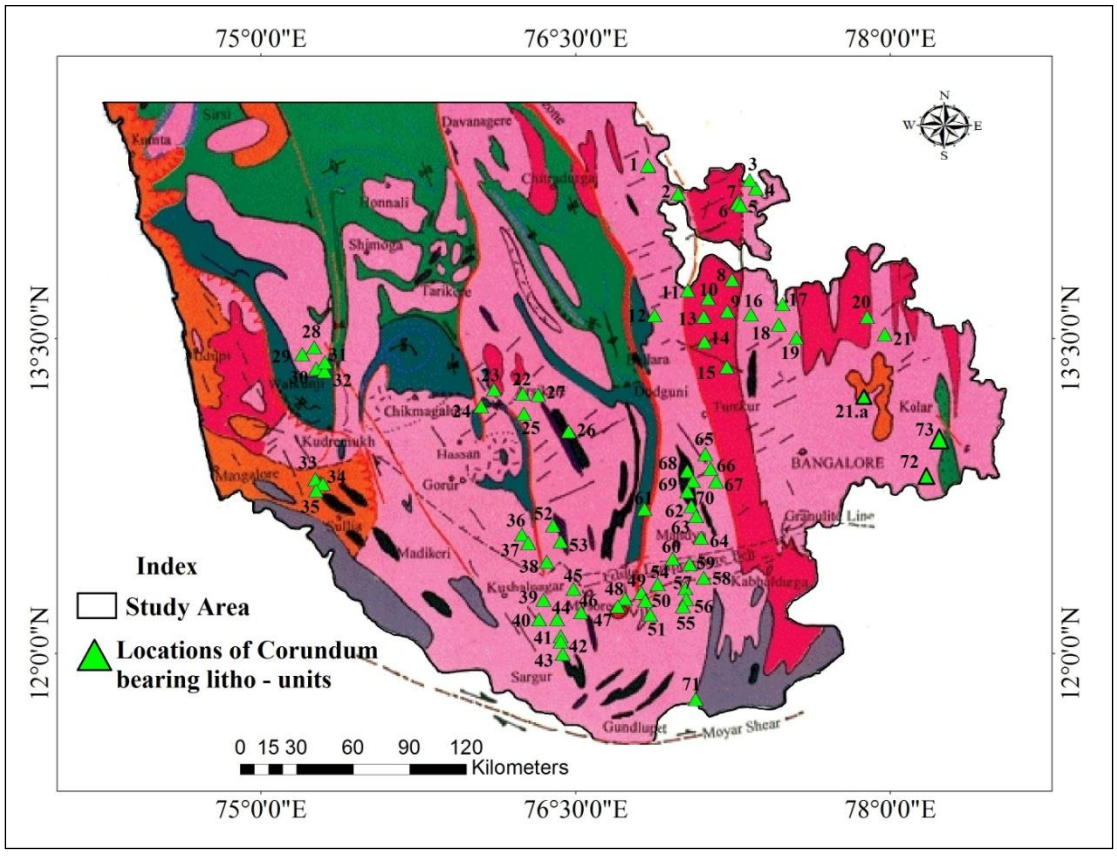

Fig.2.10. Corundum bearing litho-unit locations of the study area.

Table.2.2. Samples collected and it's GPS Location

CHITRADURGA				
Sl No	**Samples Name**	**Villages name**	**Latitude**	**Longitude**
01	Corundum	Ullarti kaval	$14^0$22.360'	76^0 43.206'
02	Corundum	Kyadigunte	$14^0$11.492'	76^0 59.261'
2.A	Corundum bearing Amphibolite schist	Kyadigunte	$14^0$11.650'	76^0 59.762'

TUMAKUR DISTRICT				
Sl No	**Samples Name**	**Villages name**	**Latitude**	**Longitude**
03	Corundum	Bettadakelaginahalli	$14^0$15.176'	77^0 19.767'
04	Corundum	Kyathaganakere	$14^0$13.074'	77^0 21.440'
05	Corundum bearing closepet granite	Thimmapura	$14^0$08.230'	77^0 17.436'
06	Corundum	Veerammanahalli	$14^0$08.470'	77^0 16.414'
07	Corundum	Kanikalabande	$14^0$09.237'	77^0 14.814'
08	Corundum	Channamallanahalli	$13^0$46.799'	77^0 16.204'
09	Corundum bearing closepet granite	ChinakaVajra	$13^0$37.913'	77^0 13.286'
10	Corundum	Bittanakurke	$13^0$41.709'	77^0 07.682'
11	Corundum	Basmangikaval	$13^0$43.944'	77^0 02.036'
12	Corundum	Molanahalli	$13^0$36.693'	77^0 52.604'
13	Corundum	Chickthimmanahalli	$13^0$35.987'	77^0 06.838'
14	Corundum	Devalapura	$13^0$29.156'	77^0 06.860'
15	Corundum	Devarayanadurga	$13^0$22.012'	77^0 13.318'

CHIKBALLAPURA				
Sl No	**Samples Name**	**Villages name**	**Latitude**	**Longitude**
16	Corundum	Hunasavadi	$13^0$37.207’	77^0 20.451’
17	Corundum	Malenahalli	$13^0$39.764’	77^0 29.199’
18	Corundum	Kachamachanahalli	$13^0$34.033’	77^0 28.429’
19	Corundum	Kadiridevarahalli	$13^0$30.321’	77^0 33.176’
20	Corundum bearing closepet granite	Neralemaradalli	$13^0$36.321’	77^0 53.419’
21	Corundum	Poolakuntahalli	$13^0$31.424’	77^0 58.476’
21.a	Corundum bearing closepet granite	Sidlaghatta	$13^0$24.122’	77^0 50.791’

HASSAN DISTRICT				
Sl No	**Samples Name**	**Villages name**	**Latitude**	**Longitude**
22	Corundum	Makanahalli	$13^0$13.893’	76^0 14.807’
23	Corundum	Undiganalu	$13^0$15.555’	76^0 06.574’
24	Corundum bearing Amphibolite schist	Dasagodanahalli	$13^0$10.802’	76^0 02.980’
25	Corundum bearing chlorite schist	Nandihalli	$13^0$08.551’	76^0 15.237’
26	Corundum	Dyavalapura	$13^0$03.508’	76^0 27.968’
27	Corundum	Belagumba	$13^0$13.843’	77^0 19.390’

CHIKMAGALUR DISTRICT				
Sl No	**Samples Name**	**Villages name**	**Latitude**	**Longitude**
28	Corundum	Melukoppa	$13^0$27.310’	75^0 15.201’
29	Corundum	Kogodu	$13^0$25.751’	75^0 11.931’
30	Corundum	Malanadu	$13^0$21.283’	75^0 15.719’
31	Corundum bearing	Kunchebylu	$13^0$23.135’	75^0 18.207’

	Amphibolite schist			
32	Corundum bearing Amphibolite schist	Heggaru	$13^0$20.798’	75^0 17.929’

DAKSHINA KANNADA DISRICT				
Sl No	**Samples Name**	**Villages name**	**Latitude**	**Longitude**
33	Corundum	Uppinangadi	$12^0$49.886’	75^0 15.502’
34	Corundum	Koila	$12^0$48.563’	75^0 17.700’
35	Corundum bearing Amphibolite schist	Shanthigodu	$12^0$46.687’	75^0 15.750’

MYSURU DISTRICT				
Sl No	**Samples Name**	**Villages name**	**Latitude**	**Longitude**
36	Corundum	Honnenahalli	$12^0$34.065’	76^0 14.663’
37	Corundum	Bylapura	$12^0$31.650’	76^0 16.545’
38	Corundum bearing Amphibolite schist	Krishnarajanagara	$12^0$26.364’	76^0 21.714’
39	Corundum	Uddukaval	$12^0$15.405’	76^0 20.843’
40	Corundum	Padukotekaval	$12^0$09.888’	76^0 19.571’
41	Corundum	Adahalli	$12^0$40.770’	76^0 25.783’
42	Corundum	Katur	$12^0$30.651’	76^0 25.385’
43	Corundum bearing Amphibolite schist	Halasur	$12^0$00.272’	76^0 25.907’
44	Corundum	Hanumanthapura	$12^0$18.898’	76^0 24.731’
45	Corundum	Handanahalli	$12^0$12.326’	76^0 29.440’
46	Corundum	Mavinahalli	$12^0$12.077’	76^0 31.274’
47	Corundum bearing Amphibolite schist	Someshwarapura	$12^0$13.264’	76^0 42.049’
48	Corundum	Varuna	$12^0$15.712’	76^0 44.168’

49	Corundum	Kuppya	$12^0$17.487’	76^0 48.778’
50	Corundum	Bommanayakanahalli	$12^0$15.242’	76^0 50.014’
51	Corundum	Eswaragowdanahalli	$12^0$11.234’	76^0 51.309’

MANDYA DISTRICT				
Sl No	**Samples Name**	**Villages name**	**Latitude**	**Longitude**
52	Corundum	Machaholalu	$12^0$36.712’	76^0 23.531’
53	Corundum bearing Amphibolite schist	Adaguru	$12^0$32.063’	76^0 25.722’
54	Corundum	Bannur	$12^0$20.025’	76^0 53.430’
55	Corundum	Hemmige	$12^0$13.631’	77^0 00.720’
56	Corundum	Ballegere	$12^0$15.670’	77^0 01.594’
57	Corundum	Doddaboovalli	$12^0$18.729’	77^0 01.371’
58	Corundum	Malavalli	$11^0$21.666’	77^0 06.582’
59	Corundum	Nelamakanahalli	$12^0$25.686’	77^0 02.731’
60	Corundum	Ahasale	$12^0$27.243’	76^0 57.716’
61	Corundum bearing Amphibolite schist	Tharanagere	$12^0$41.376’	76^0 49.747’
62	Corundum	Kesthur	$11^0$41.929’	77^0 03.292’
63	Corundum	Hanumanthapura	$12^0$39.377’	77^0 04.437’
64	Corundum	Maddur	$12^0$32.920’	77^0 06.651’

RAMANAGARA DISTRICT				
Sl No	**Samples Name**	**Villages name**	**Latitude**	**Longitude**
65	Corundum	Huthridurga	$12^0$56.764’	77^0 07.143’
66	Corundum	Varthehalli	$12^0$53.311’	77^0 08.403’
67	Corundum	Akkur	$12^0$49.398’	77^0 09.966’
68	Corundum	Hosahalli	$12^0$52.658’	77^0 02.182’
69	Corundum bearing	Lakkashettypura	$12^0$49.402’	77^0 03.596’

	Amphibolite schist			
70	Corundum bearing Amphibolite schist	Byranaikanahalli	$12^0$46.710’	77^0 02.061’

CHAMARAJANAGAR DISTRICT				
Sl No	**Samples Name**	**Villages name**	**Latitude**	**Longitude**
71	Corundum bearing Pelitic rock	Budipadaga	$11^0$47.122’	77^0 04.375’
71.a	Fe, Garnet rich Corundum rock	B.R.Hills	$11^0$47.583’	77^0 03.076’

KOLAR				
Sl No	**Samples Name**	**Villages name**	**Latitude**	**Longitude**
72	Corundum	Yelesandra	$12^0$53.160’	78^0 10.276’
73	Corundum	Kammasandra	$13^0$00.660’	78^0 10.276’

CHAPTER-III

3.1. FIELD GEOLOGY AND PETROGRAPHY

When rocks and rock materials are investigated in their natural environment and in their natural relations to one another, the study is called field geology. Field geology seeks to describe and explain the surface features and underground structure of the lithosphere. Physiography and structural geology are equally important in the science of field geology. Subsurface geology, likewise very important, pertains to the study of rock relationships by the use of data obtained underground, as in mines or from drilled wells. It is in contrast to surface geology, which is the-collection and study of superficial evidences (Frederich., 1941).

3.2. OBSERVATION AND INFERENCE

Necessarily Field geology founded upon observation and inference. Only features that' are superficial can be observed; all else must be inferred. We may study the surface of an outcrop, of a valley, or of a corundum origin, but in attempting to explain the internal structure of the outcrop, or what underlies the valley, or how the corundum grain was fashioned, we are forming inferences by interpreting certain visible facts.

The ability to infer and to infer correctly is the goal of training in field geology, for one's proficiency as a geologist is measured by one's skill in drawing safe and reasonable conclusions from observed phenomena. Southern Karnataka mainly formed high granulitic terrain and composition of green stone belts, in this terrain most of the amphibolite schist contact and associated with corundum mineral, some places without hosting rock corundum occur and pelitic rock also hosting corundum we seen in the study area.

3.3. FIELD EQUIPMENTS

3.3.1. Base Maps: Before starting any field work it is important to be clear about the aim of the investigation for this decision will guide the choice of map scale and control the nature of the techniques which are needed to cover the area in the detail necessary to

resolve the problem. For most kinds of geologic field work, some sort of a preliminary map of the region is of great advantage. a good topographic contour map, or an aerial photographic map, which has been previously prepared and on which the geologist can ploting data in the field, is termed a base map or a working map. Study area contain 17 Quadrangle Geology maps (48j, 48k, 48l, 48m, 48n, 48o, 48p, 57b, 57c, 57d, 57f, 57g, 57h, 57k, 57l, 58a and 58e) of 1:2,50,000 scale is used and helps to better understanding corundum bearing litho-units in field and demarcation of corundum presence in the map.

3.3.2. Global Positioning Systems (GPS)

Global Positioning Systems (GPS) use ultra high - frequency radio wave signals from satellites to trigonometrically derive your position to within a few metres laterally. Global Positioning Systems units do not work in deep ravines and on some coastal sections; they are also not particularly accurate for altitude. The GPS can be set up for the particular grid system that you are working with or for a global reference that is based on latitude and longitude. The global reference World Geodetic System 1984 (WGS84) is the most commonly used. The unit may take some time to locate the satellites if the GPS has been moved hundreds of kilometers. We used GPS together with hard copy maps on our main location device in the field and accurately plot the position. In this study used Garmin- 72 GPS model this GPS is a burgeoning technology, which provides unequalled accuracy and flexibility of positioning for navigation, surveying and GIS data capture. Garmin GPS Navigation Satellite Timing and Ranging Global Positioning System (NAVSTAR) is a satellite-based navigation, timing and positioning system. This GPS provides continuous three-dimensional positioning 24 hrs a day throughout the world. The technology seems to be beneficiary to the GPS user community in terms of obtaining accurate data up to about 100m for navigation, meter-level for mapping, and down to millimeter level for geodetic positioning. This GPS technology has tremendous applications if GIS data collection, surveying and mapping.

Fig.3.1. GPS Garmin-72

3.3.3. Brunton Compass

Fig.3.2. Brunton Compass

The Brunton compass is used by more geologists for field mapping of geological objects. The Brunton compass was originally designed by a Canadian geologist named D.W. Brunton, and built by William Ainsworth Company in Denver, Colorado. Despite its tough design, its delicate mirror and glass components are vulnerable to shock and Moisture requiring care and periodic maintenance for proper application. See Compton, 1985 for maintaining the compass. Since 1972, genuine Bruntons are manufactured by the Brunton Company in Riverton, Wyoming, which was acquired by Silva Production, AB of Sweden in 1996 (Babaie., 2001) . In this study brunton compass used for identification dip and strike direction of rock body and Detailed measurement of geological objects, such as fold hingeline, axial trace, and axial plane, and geological mapping. Mainly its helps to determining the magnetic declination then attitude of linear and planar geological objects and measuring vertical angles height and distance.

3.3.4. Additional Equipment:

In addition to the instruments which may be used, the geologist will need various equipments. The hand lens is an essential piece of equipment for the detailed observation of all rock Types and we used a good hand lens with a moderate magnification (x10) is absolutely essential for the examination of a fresh rock surface to determine such features as mineral content grain shape and micro structures in a rock. We used hammer this is also very needful equipment in the field. Hammer is a critical tool for obtaining rock specimens for laboratory work and for chipping away weathered rock surface. Field note book information that cannot be recorded on the geological map is written in the note book and we used black pencils to record orientation data and colored pencils are used to record rock litho-logy on the field map. Finally the work necessitates the collection of rock specimens, we carried our self hammer, a collecting bag, small paper bags or newspapers in which the specimens can be collected. The last but not the list Camera is

almost an essential part of a geologist's field equipment. There is considerable divergence of opinion as to which is the most satisfactory kind to use for field photos.

3.4. FIELD INVISTIGATIONS

Corundum is of common occurrence in Karnataka but transparent gem quality corundum colored blue, green, yellow and violet is rare. The name ruby is reserved for the red transparent variety and sapphire for the blue transparent red ruby corundum was explored near Budipadaga in Chamarajanagar district. Red colored corundum not quite transparent but opaque when polished in to cabochons displays asterism such varieties are called star ruby or star corundum many corundum crystals collected in Mysuru, Mandya, and Tumkur districts displays this character, gem quality ruby corundum is occasionally found at Kadamane, corundum is associated with gem quality kyanite. The mineral occurs in decomposed granite gneiss in the form of loose crystals up to half an inch in length, pink to amethyst colored corundum from weathered pegmatite near Kamasamudra, Kolar district. Corundum from near Kalyadi in Hassan district is blue in color and shows well developed basal sections with pronounced asterism, corundum crystals from near Undiganhalu close to Kalyadi are blood red in color.

Numerous occurrences of ruby corundum lie within a tract nearly 250km long and having a width of 30 – 40km restricted to the eastern and western margins of the N-S trending closepet granite, LANDSAT color composites have revealed numerous dark toned areas which represent exposures of basic schist not delineated in the geological map, these enclaves are the host rocks for ruby corundum.

Two types of occurrences noticed are (1) in-situ corundum related to intrusive pegmatites laying within metamorphic rocks mainly amphibolites and meta-gabbro, talc-chlorite schists and calc-silicate rocks and (2) placer corundum within gravels of older alluvium.

Nine tracts have been identified with potential for the occurrence of gem quality corundum and other precious stones

Table.3.1. Corundum deposit tract of the study area

Sl. No	Tract	Extent in km^2
1	Kunigal – T-Narsipura	1905
2	Madhugiri – Dodballapura	392
3	Madhugiri – Doddaladbetta	400
4	Pavagada	252
5	Hosahudya and surroundings	26
6	Bangarpet – Kamasamudra	66
7	Arsikere – Heggadadevanakote	2072
8	Gundlupete – Chamarajanagar & surroundings	121
9	Sringeri	18
	Total	**5252 km^2**

Among these tracts, the occurrences noticed at Tarur, Kuntegowdanahalli and Irabommanhalli in Sira taluk. Chikunda in Hunsur taluk, Jakkanahalli and Jagankote in Heggadadevanakote taluk have been studied and the corundum tested for its gemological properties and it is stated that there is good potential for star variety as well as light colored translucent variety the Chikunda occurrence was reported favorably with possibility of finding transparent good quality red ruby corundum.

3.5. CORUNDUM BEARING LITHO-UNITS OF THE STUDY AREA

3.5.1. Field traverse in Chitradurga District

Chitradurga Geologicaly famous in Chitradurga District of Chitradurga schist belt its start from Gadag to Srirangapatna. Chitradurga mainly consist of fractured granitic-gneisses, gneisses and hornblende-schists rocks form, another major iron ore deposited and Soil types of the district comprise deep and shallow black soil, mixed red and black soil, red loamy and sandy soil. Physiographically the district comprises of undulating plains, interspersed with sporadic ranges and isolated low ranges of rocky hills. Corundum occurs in the Challakere taluk, Loose barrel shaped crystals of pink corundum scattered in the soil cap in the Ullavarti – Kaval east of Challakere, so for these have not

been commercially exploited on a large scale (fig.3.3). Kyadigunte it is also village of Challakere taluk and it is near to Closepet zone in field investigation ruby occurs with hornblend schist this the geologicaly contact zone of Closepet granite and Chitradurga schist along this belt mafic magma activity helps to corundum reaches to surface the contact zone and wall rock alteration, migmatization and pegmatite veins also helps corundum reaches to the surface this deposition we seen the 2km away from south west direction of the village and adjacent to the this deposition dolerite dyke travel along with corundum bearing hornblende schist (fig.3.3).

Fig.3.3. Photographs of corundum Ullarthi area and corundum bearing Amphibolite schist Kyadigunte around Chitradurga district, Sl no 1 – 2.a.

3.5.2. Field traverse in Tumakur District

Tumkur District exposes mainly rock types belonging to the Peninsular Gneissic Complex (PGC), schistose rocks of Sargur group and Dharwar super group, younger intrusives (Closepet Granite and basic dykes) and thin patches of quaternary gravels, Corundum bearing cordierite-sillimanite schist/gneiss occur on either side of Closepet Granite as enclaves in Peninsular Gneisses and eastern border of Closepet Granite in which Corundum is sporadically distributed in a stretch of 60 km extending from Koratagere to Pavagada. These schists are intensely altered and new minerals like diopside, hypersthene varieties of garnets, cordierite, sillimanite and corundum have developed giving rise to several interesting rock types. All these rock types are considered to be highly metamorphosed phases of impure argillitic sediments preserved

here and there as remnants of the original schists in the gneissic complex (Swaminath and Ramakrishnan, 1981). Field observation a number of shallow working for corundum are seen at Baichapura and Alpenhalli in Kortagere taluk occurrences especially in the region bordering the Closepet Granites in parts of Sira, Madhugiri and Pavagada taluks, corundum gem occurring at the contact of ultramafic rocks and pegmatite Honmachanahalli, Bandihalli and tract of Tumkur-Pavagada and Baichapurr-Madhugiri, other field investigation observed corundum bearing Closepet Granite deposited Thimmapura, ChinakaVajra and Devalapura area and corundum occurs Bittanakurke, Bettadakelaginahalli, Kyathaganakere, Veerammanahalli, Kanikalabande, Channamallanahalli, Basmangikaval, Molanahalli, Chickthimmanahalli and Devarayanadurga area (fig.3.4).

Fig.3.4. Photographs of corundum samples around Tumkur District Sl no 3 – 15.

3.5.3. Field traverse in Chikaballapur District:

Chikballapur district is the eastern gateway to Karnataka. It formed by bifurcating old Kolar district in to Chikballapur and Kolar districts. It is land locked district and hard rock terrain of Karnataka in the Maiden (plain) region and covers an area of 4207 sq.km. The general elevation varies from 250 to 909 m above mean sea leve. The district lies almost in the central part of Peninsular India, which has immensely bearing on its geoclimatic conditions. This district experiences tropical climate throughout the year. The soils of Chickballapur district occur on different landforms such as hills, ridges, pediments, plains and valleys. The types of soils distributed range from red loamy soil to

red sandy soil and lateritic soil. Field observation of this district exposes mainly rock types of Granites, gneisses, schists; laterites and alluvium underlie the district. Basic dykes intrude the above formations at places. Granites and gneisses occupy major portion of the district. Schists are mostly confined to the northwestern part of Gauribidanur taluk. Laterites occupy small portions in Chickballapur, and Sidlaghatta taluks. Alluvium is confined to river courses. Corundum bearing Closepet Granite occurs Neralemaradalli area and corundum occurs Hunasavadi, Malenahalli, Kachamachanahalli, Kadiridevarahalli and Poolakuntahalli area. Fractures or lineaments occupy well defined structural valleys and majority of them trend NE-SW (fig.3.5).

Fig.3.5. Photographs of Gorundum samples around Chikballapur District, Sl no 16 – 21.a.

3.5.4. Field traverse in Hassan District

Hassan district is located on the border of the Western Ghats, in the southern part of Karnataka state. It is located between 12° 30’ and 13° 35’ North latitude and 75° 15’ and 76° 40’ East longitude. The major part of the district is in Cauvery main basin drained by Cauvery, Hemavathy and Yagachi rivers, which flow towards east to join the Bay of Bengal. The district is divided into three distinct geomorphic units i.e. the Western and North-Eastern hilly terrains constituting part of the Western Ghats, the Central Transition Zone and the Eastern Maidan (plain) region. The soils of the district display a wide diversity and are quite fertile. The main soil types are Red soil, Red sandy soil, Mixed soil and Silty clay soil. The soils in the western taluks are derived from granites, laterites and schists. These soils are shallow to medium in depth and the color changes with depth

from red at the surface and red and yellow mottles at depth. In the eastern taluks, the soils are red sandy type, which are derived from granite, gneisses and schists. Field observation the district exposes mainly composition of Holenarasipura and Nuggihalli schist belts and this area belongs to Sargur group of rocks which comprises corundum bearing rocks were principally made up of interspersed by lands tremolite schist, hornblende gneiss, amphibolites schist along with intrusive dykes of dolerite and reefs of quartzite. Corundum occurs Makanahalli, Undiganalu, Dyavalapura and Belagumba area. Corundum bearing Amphibolite schist occurs Dasagodanahalli area and Corundum bearing chlorite schist occurs Nandihalli area (fig.3.6).

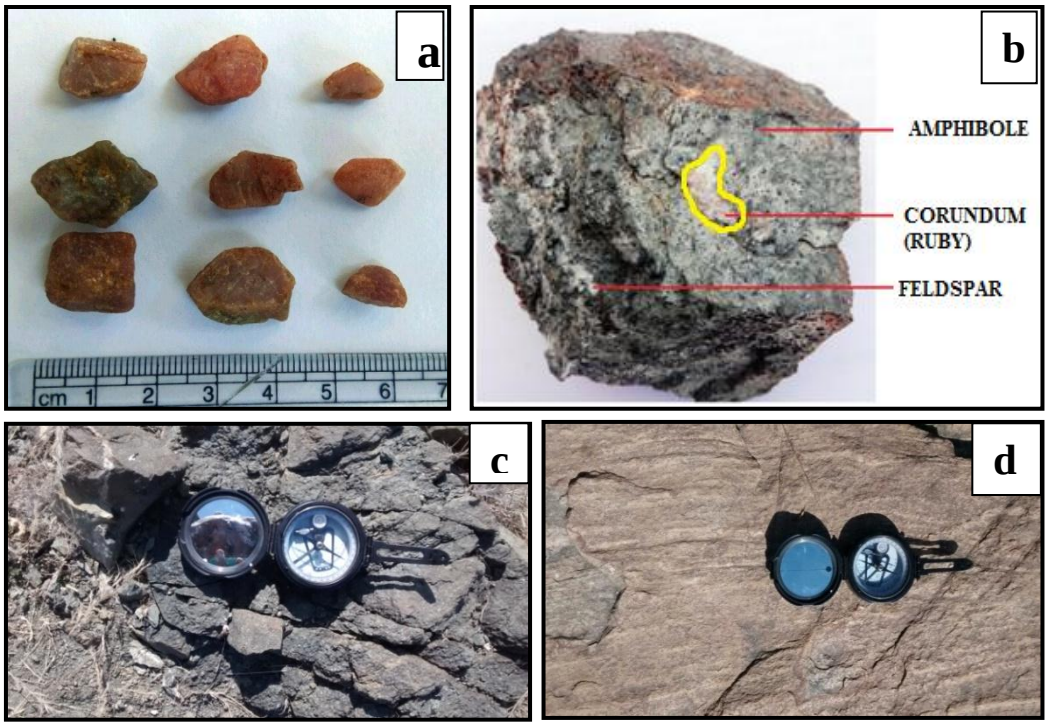

Fig.3.6. Photographs of (a) corundum (b) Corundum bearing Amphibolite schist (c) Corundum bearing Chlorite schist (d) Gneiss around Hassan District, Sl no 22 –27.

3.5.5. Field traverse in Chikmagalur District

Geologically the Chikmagalur area made up of Archean Schists and basement Gneissic rocks. The Dharwar schists occupy 50% of the area of the district and occur as three distinct belts, The Kudremukh Gangamwla belt, the koppa belt and Baba budan belt (Manjunatha and Harry., 1994). The district encompasses rich economic minerals such as iron ore, kaolin, kyanite, asbestos, bauxite, chromite, clay, copper, corundum, garnet,

graphite, limestone, manganese, mica. Among these minerals, iron ore is being exploited on a large scale. Nearly 70% of the area in Sringeri taluk is covered by gneiss and rest of the area is occupied by schist formation. Weathered, fractured and jointed gneiss and schist rocks (Ramakrishnan and Vaidyanadhan., 2008). And further these rocks have specks of Corundum bearing units.

Fig.3.7. Photographs of corundum and corundum bearing amphibolites schist around Chikmagalur District, Sl no 28 - 32.

In field investigation district has six kinds of litho units with economically viable minerals including gemstones varieties particularly in contact zones of ultramafics, Banded Iron Formation, amphibolite schist with gneiss and metabasalt & amphibolite - metagabbro. Random samples were collected such as amphibolite, gneiss and corundum within basement crystalline rocks through GTC (Ground Truth Check) corundum occurs Melukoppa, Kogodu and Malanadu area. Corundum bearing amphibolites schist occurs Kunchebylu and Heggaru area (fig.3.7).

3.5.6. Field traverse in Dakshina Kannada District

The district exposes mainly rock types migmatites and granodioritic to tonalitic Gneiss, schistose rocks, younger granite, kyanite sillimanite schist. The coastal stretch and the adjacent Western Ghats are composed of Precambrian (Archeaen) rocks and the Phanerozoic formations. Sargur group is composed of high grade metamorphic rocks of upper amphibolitic to lower granulitic facies, occurring within gneisses and granites (Swaminath and Ramakrishnan, 1981). Awasthi and Krishnamurthy, (1979) and Ravindra

and Janardhan, (1981), in their study reported the presence of rock type equivalent to Sargur group in the southern most part of coastal Karnataka such as Puttur, Sullia and Dharmasthala.

Fig.3.8. Photographs of Corundum and Corundum bearing Amphibolite schist around Dakshina Kannada District, Sl no 33 – 35.

The greater part of the Sullia taluk is laterite covered. Beneath this cover, major rock types encountered are gneisses and granulites containing enclaves of kyanite-sillimanite ± corundum schist; kyanite-sillimanite-garnet-graphite schist; quartz-chlorite-biotite schist; quartzite; chlorite-tale-actinolite schist and amphibolites (Ravindra and Janardhan, 1981). Field observation carried out corundum occurs Uppinangadi and Koila area. Corundum bearing amphibolites schist occurs Shanthigodu and Sullia area (fig.3.8).

3.5.7. Field traverse in Mysuru District

The district is mainly composed of igneous and metamorphic rocks of Precambrian age either exposed at the surface or covered with a thin mantle of residual and transported soils (Ramakrishnan and Vaidyanadhan., 2008). And its has a vast expanse of Magnetite gneisses. This high-grade schist is considered as oldest group of supracrustal rocks. These high-grade schists are noticed as rafts within the gneissic complex in the southern parts of the districts and form the type which belongs to Sargur group (Chandrashekhar, H. and Nazeer Ahmed, 1994). Chamundi hill and Varuna area is essentially a flat lying basement gneisses, ultramafic and amphibolite schist, These rocks are of great economic importance because of the presence of corundum and garnets. Sargur area also mainly occupying the rock type's Gneiss, ultramafics, metapelites and amphibolites schistose

rocks, these rocks are of great economic importance because of the presence of graphite, corundum and garnets in them. They extend from Bilikere region up to the southern border of the district in the south-southwest direction for nearly 50 km (Swaminath and Ramakrishnan, 1981). In field investigation Mavinalli area belongs to Sargur group of rocks, main rock types in contact zones of ultramafics, fuchsite quartzite with kayanite, Amphiolite and hornblende schist with crystaline limestone, Banded iron formation with high grade metapelites and grey migmatite granodiorite tonalitic banded gneiss.These rocks are of great economic importance because of the presence of corundum and garnets. Overall district field observation and collected samples corundum occurs Honnenahalli, Bylapura, Uddukaval, Padukotekaval, Adahalli, Katur, Hanumanthapura, Handanahalli, Mavinahalli, Varuna, Kuppya, Bommanayakanahalli and Eswaragowdanahalli area. Corundum bearing amphibolites schist occurs Krishnarajanagara, Halasur and Someshwarapura area (fig.3.9).

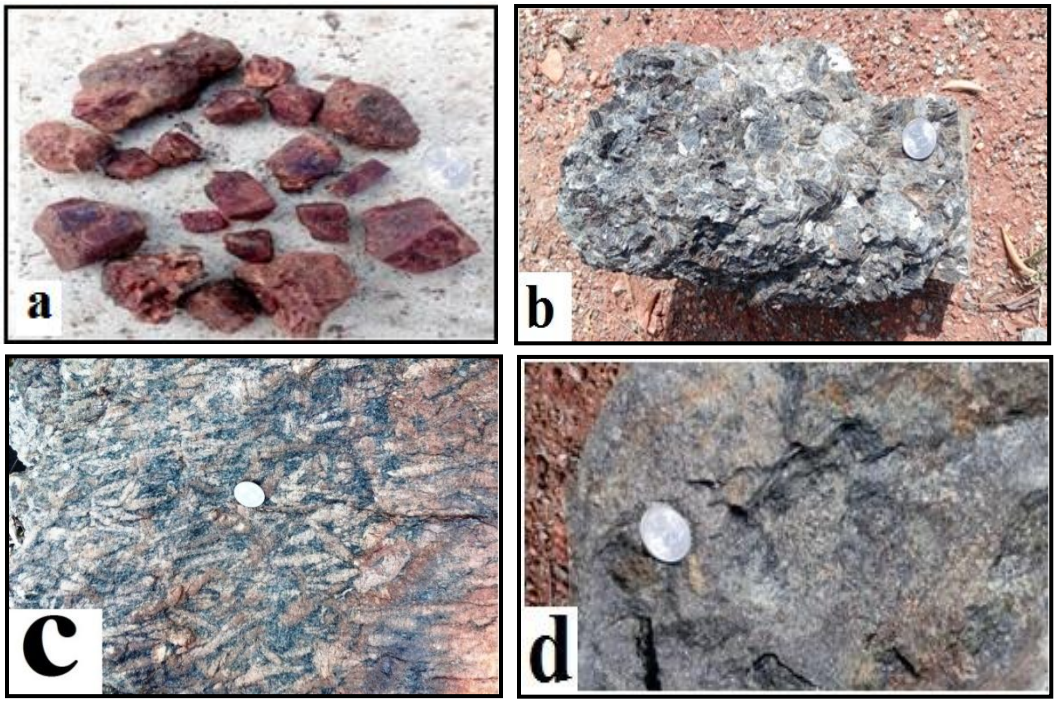

Fig.3.9. Photographs of (a) Corundum (b) Actinolite Schist (c) Pyroxene Granulate (d) Amphibolite Schist collected samples around Mysuru district, Sl no 36 – 51.

3.5.8. Field traverse in Mandya District

The district belongs to Archaean era. They have been subjected to deformation and have undergone metamorphism. They have varied chemical compositions and are most complex and aptly designated as Archaean complex and consist of a wide variety of granite, gneisses and schist with associated quartzite and limestone (Ramakrishnan and Vaidyanadhan., 2008). Maddur area mainly occupying the rock type's graniitoid gneiss, ultramafics, Banded Magnetite Quartzite (BMQ) and basic dyke, these rocks are of great economic importance because of the presence of corundum. Important deposits are reported from Satanur near Mandya, Erehalli, Kirangur and Ramanahalli areas (Ramakrishnan and Vaidyanadhan., 2008). In field observation in the district most part, is made up of gneisses which are generally gray in colour with well developed gneissosity. Corundum occurs Machaholalu, Bannur, Hemmige, Ballegere, Doddaboovalli, Malavalli, Nelamakanahalli, Ahasale, Kesthur, Hanumanthapura and Maddur area. Corundum bearing amphibolites schist occurs Adaguru and Tharanagere area (fig.3.10).

Fig.3.10. Photographs of Corundum and Corundum bearing Amphibolites schist around Mandya District, Sl no 52 – 64.

3.5.9. Field traverse in Ramanagara District

The district mainly comprise rocks belong to Sargur group, granulite group, Peninsular Gneissic Complex (PGC), Closepet granite, and basic and younger intrusives of the Precambrian era (Ramakrishnan and Vaidyanadhan., 2008). Granulite and migmatites, Sargur group comprises ultramafic rocks, amphibolites, banded magnetite quartzites,

occurring as small bands, and lenses within the migmatite and gneisses (Radhakrishna and Naqvi, 1986). Field observation Ramanagara district, it has three kinds of litho units with economically viable minerals including gemstones varieties particularly in contact zones of ultramafics, amphibolite schist with gneiss and younger granites, samples were collected such as gneiss, and corundum bearing amphibolite schist through GTC (Ground Truth Check). Corundum occurs Huthridurga, Varthehalli, Akkur and Hosahalli area. Corundum bearing amphibolites schist occurs Lakkashettypura and Byranaikanahalli area.

Fig.3.11. Photographs of Corundum and Corundum bearing Amphibolites schist around Ramanagara District, Sl no 65 – 70.

3.5.10. Field traverse in Chamarajanagara District

Geologically the district is mainly self-possessed of igneous and metamorphic rocks of Precambrian age either exposed at the surface or covered with a thin mantle of residual and transported soil (Basavarajappa., 1992). The rock formation of the district falls into mainly three groups (a) Amphibolite Facies Gneissic equalent to Sargur group. (b) Amphibolite gneiss mixed with incipient and retrograde charnockite equalent to high grade shear zone (c) high grade massive and banded charnockitic granulites equalant to Archean type NGT (Northern Granulite Terrain) charnockite series and granite gneiss or genesis granite (Basavarajappa and Srikantappa., 1998,1999). A fairly wide area of the district consists of Chamockites series of rocks particularly along the southeastern border of Yalandur taluk and Biligirirangana Hills (Basavarajappa et al., 2004). Field

observation the area occupying the corundum bearing pelitic rocks vary in thickness from few cms to meters well exposed around Budipadaga, generally they trend in NS direction, pelites consists of qtz+plag+k.felds+bio+corun+stau+gt (Basavarajappa et al., 2004). Corundum bearing pelitic rock occurs Budipadaga area. Fe, Garnet rich corundum bearing rock and Corundum, Garnet bearing Mylonite occurs Biligirirangana Hills. (fig.3.12).

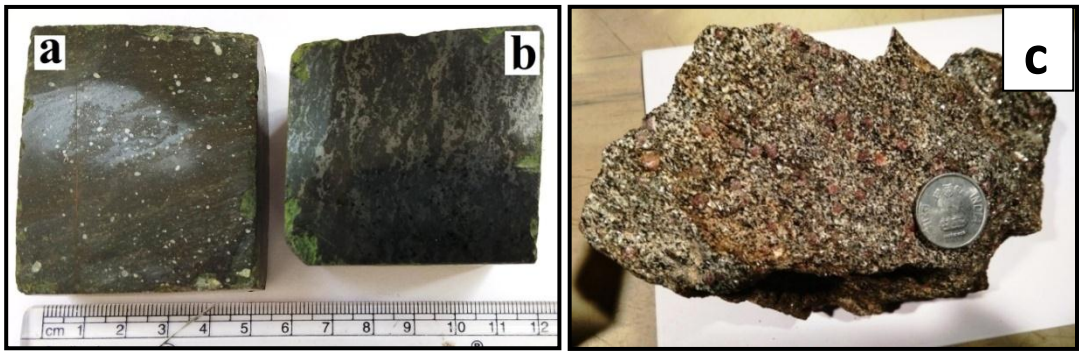

Fig.3.12. Photographs of (a) Corundum Garnet bearing mylonite (b) Fe, Garnet rich Corundum rock and (c) Corundum bearing pelitic rock around Chamarajanagara districts, Sl no 71 – 71.a.

3.5.10. Field traverse in Kolar District

Kolar belongs to the Maidan (plains) group of districts as distinct from the western portions of the State called ma1nad and it is the eastern most district of Karnataka State. Granites, gneisses, schists, laterites and alluvium underlie the district. Basic dykes intrude the above formations at places. Granites and gneisses occupy major portion of the district. Schists are mostly confined to two places - around Kolar Gold Fields and in the northwestern part of Gauribidanur taluk. Laterites occupy small portions in Kolar, Srinivaspura and Sidlaghatta taluks. Alluvium is confined to river courses. Fractures or lineaments occupy welldefined structural valleys and majority of them trend NE-SW. Field observation the topography of the district is undulating to plain. The central and eastern parts of the district forming the valley of Palar Basin, are well cultivated. The soils of Kolar district occur on different landforms such as hills, ridges, pediments, plains and valleys. Workable deposits of corundum are found at Dodderi 3km NNW of Kamasamudra and at Doddenur and Yelesandra in the Bangarpet taluk from the size of excavations, it is evident considerable quantities of pink granular corundum appear to

have been recovered several abandoned shafts are also seen corundum is found as an ingredient of cordierite sillimanite gneiss, corundum is also reported to be available in large quantities near Marahalli near Thondebhavi. Corundum occurs Yelesandra and Kammasandra area. Corundum bearing Amphibolite schist occurs near Kammasandra area (fig.3.13).

Fig.3.13. Photographs of Corundum and Corundum bearing Amphibolites Schist around Kolara district, Sl no 72 – 73.a.

3.6. PETROGRAPHIC STUDY

In this study corundum bearing litho - units carried carefully to the research Petrographic Laboratory at Department of Studies in Earth Science, University of Mysore, Mysuru, to make thin section for petrographic work. A thin section of rock is cut from the sample with a diamond saw & ground optically flat and mounted on a glass slide. Then the ground parts of the samples were made smooth using progressively finer abrasive grit until the sample is only 30 μm thick. Petrographic characters of all the section were carried out using Leitz XPL-2 petro-microscope Lawrence and Mayo (Fig.3.14).

Fig.3.14. Research Microscope

3.6.1. Corundum bearing Samples around Chitradurga District

The corundum optical properties show Color: colorless, blue, pink to light red colored The red color is caused by the mineral chromium and shows brownish tone due to the presence of iron. Relief shows high to very high. Prismatic, tabular or skeletal crystals and Rhombohedral parting/ cleavages are common. pleochroism is very strong in ordinary light and shows deep red color when viewed in the direction of vertical axis and a much lighter color to nearly colorless in view at right angles to this axis. Birefringence weak, Uniaxial negative. but often up to low II order due to extra thickness of ultra-hard corundum. Parallel extinction. In hornfelses, high grade pelites and syenitic gneisses, environment contact and regionally metamorphosed rocks (Fig.3.15).

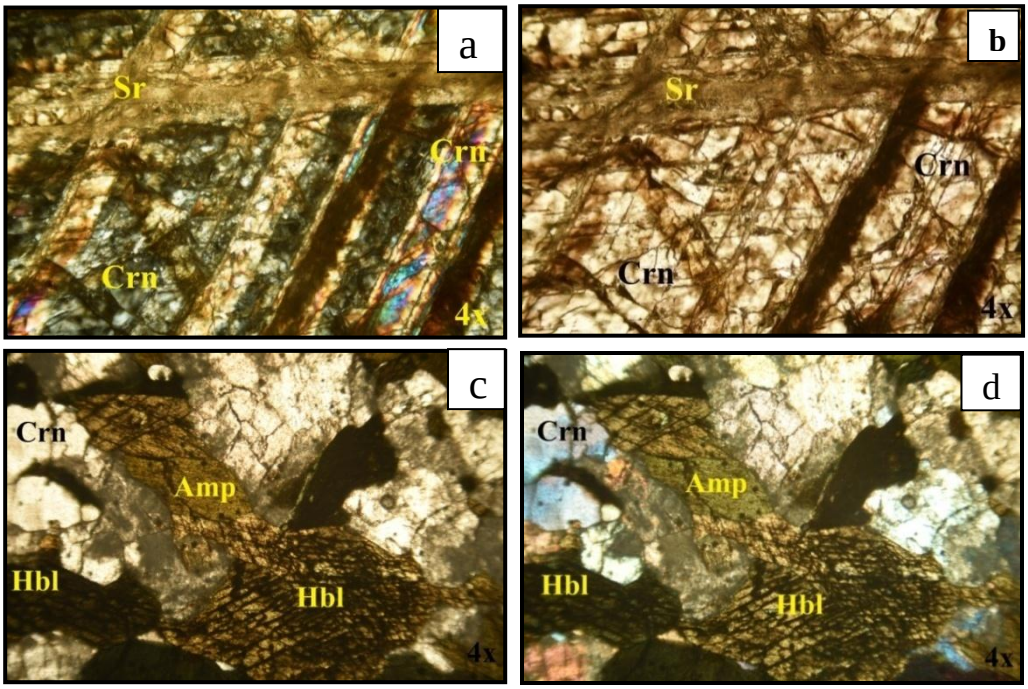

Fig.3.15. Photomicrographs of a and b Corundum samples (xpl and ppl) c and d Corundum Bearing Amphibolites Schist around Chitradurga district, Sl no 1 – 2.a.

Sericite optical properties shows Color: Brown or turbid pale greyish, Monoclinic system, anisotropic, Pleochrosim – nil Relief weak, Cleavage very good in one direction in basal sections have no cleavage, Biaxial high birefringence sericite also fills the micro fractures in plagioclase, but it does it in elongated crystals, unlike the rather equant hematite crystals. Sericite is a fine-grained variety of muscovite, with the same

composition $KAl_2(AlSi_3O_{10})(OH)_2$. It usually forms by hydrothermal alteration of K-feldspars, which provide the necessary potassium. It grows in pre-existing microfractures where the fluids can penetrate, or in fractures created by the fluid pressure., sericite fills cracks around and across plagioclase crystals, sericite that probably has replaced feldspar (Fig.3.15).

Amphibole is usually strongly green in colour, yellow-blue, blue-green and brown. It shows strong pleochroic, moderate relief, high cleavage, birefringence biaxial and pleochroic appears in various shades of green and brown. In plane polarized light, the mineral colour of amphibole ranges from yellowish green to dark green in Colour. The central part is associated corundum which shows pale blue color; uniaxial; low birefringence and surface relief is high (Fig.3.15). Various shades of yellowish green and reddish brown to dark brown are observed in hornblende gneiss showing Slender prismatic to bladed crystals, with 4 or 6 sided cross section which exhibit amphibole cleavage also has anhedral irregular grains which shows moderate to high positive relief. Hornblende cleavages on intersection at fragment shape is controlled by cleavage; birefringence; interference colors usually has higher first or lower second order. The mineral shows simple and lamellar twinning; biaxial and shows alteration to biotite & chlorite or other Fe-Mg silicates. Corundum shows pale yellow colour; uniaxial; low birefringence, surface relief is high (Fig.3.15). The corner edge part is associated corundum which shows pale blue color; uniaxial; low birefringence and surface relief is high (Fig.3.15).

3.6.2. Corundum bearing Samples around Tumkur District

The corundum optical properties show Color: colorless, pink to blood-red colored. Relief shows high to very high. Prismatic, tabular or skeletal crystals and Rhombohedral parting/ cleavages are common. pleochroism is very strong in ordinary light and shows deep red color when viewed in the direction of vertical axis and a much lighter color to nearly colorless in view at right angles to this axis. Birefringence weak, Uniaxial negative. but often up to low II order due to extra thickness of ultra-hard corundum. Parallel extinction. In hornfelses, high grade pelites and syenitic gneisses, environment contact and regionally metamorphosed rocks (Fig.3.16). Sericite optical properties shows

Color: Brown or turbid pale greyish, Monoclinic system, anisotropic, Pleochrosim – nill Relief weeak, Cleavage very good in one direction in basal sections have no cleavage, Biaxial high birefringence sericite also fills the micro fractures in plagioclase, but it does it in elongated crystals, unlike the rather equant hematite crystals (Fig.3.16).

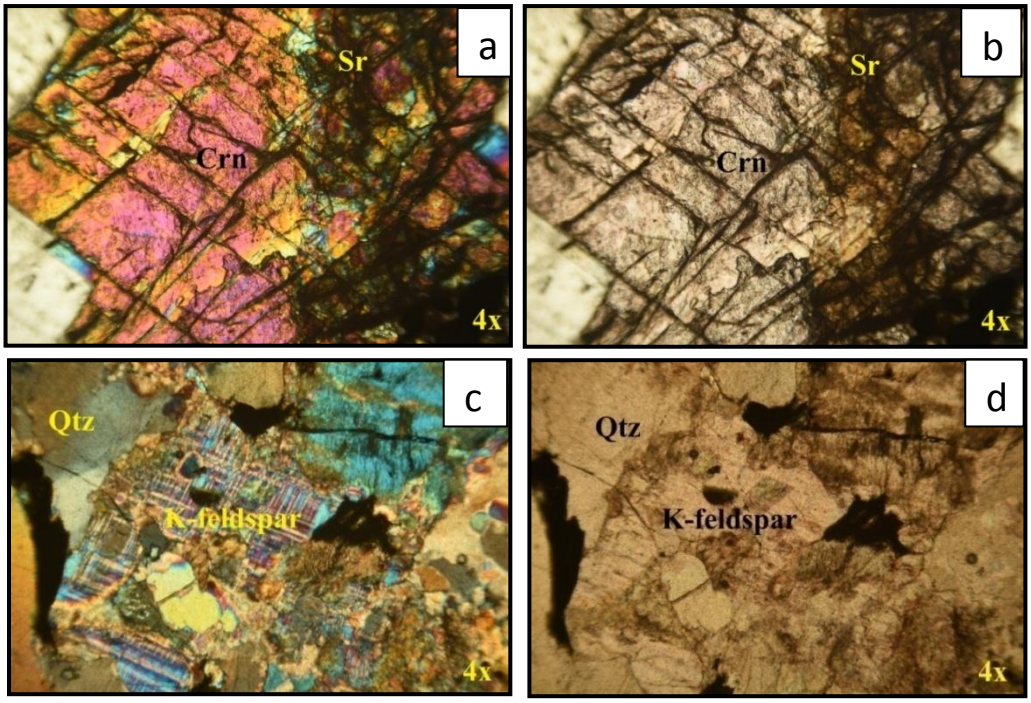

Fig.3.16. Photomicrographs of a and b Corundum samples (xpl and ppl) c and d Corundum Bearing Closepet Granite around Tumakur district, Sl no 3 – 15.

Granite composed of Qurtz + K- Felspar + Biotite mica. Quartz shows Colorless, transparent and unaltered. Cleavage absent, Relief low positive, so that the outlines of the grains are not well marked with smooth surface. Birefringence weak, uniaxial positive. Feldspar shows central part of micro section (Fig.3.16), colorless, but often cloudy due to alteration. Cleavage is visible as thin lines in two directions nearly 90^0 other grains will show no cleavage or one direction only and Relief low negative. Birefringence weak, simple twinning, mineral distinguished from quartz by its cloudy appearance due to alteration, shows low negative relief, presence of cleavage and by simple twinning. Biotite is Silicate of magnesium, iron, aluminium and potassium with hydroxyl fluorine. Colour brown, yellowish brown, reddish brown, dark brown, green or dark green. Cleavage perfect in one direction basal sections do not show any cleavage. Birefringence strong, parallel extinction (Fig.3.16).

3.6.3. Corundum bearing Samples around Chikballapura District

The corundum optical properties show Color: colorless, pink to light pink colored Relief shows high to very high. Prismatic, tabular or skeletal crystals and Rhombohedral parting cleavages are common. pleochroism is very strong in ordinary light and shows deep pink color when viewed in the direction of vertical axis and a much lighter color to nearly colorless in view at right angles to this axis. Birefringence weak, Uniaxial negative. but often up to low II order due to extra thickness of ultra-hard corundum. Parallel extinction. (Fig.3.17).

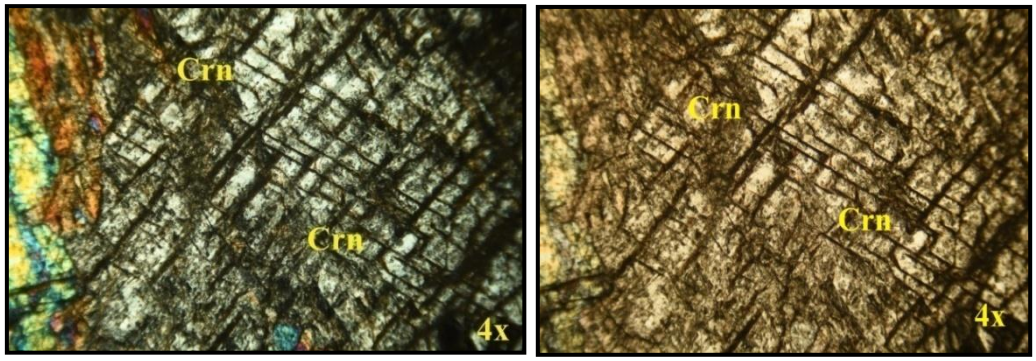

Fig.3.17. Photomicrographs of Corundum (XPL and PPL) around Chikballapura district, Sl no 16 – 21.a.

3.6.4. Corundum bearing Samples around Hassan District

Corundum: The corundum shows similar color appearance in both plane and crossed polarized lights. Corundum is depicted by pink to blood-red colored and can vary within each gem variety of the mineral Corundum. The red color is caused by the mineral chromium and shows brownish tone due to the presence of iron. It shows uniaxial, birefringence & pleochroism is very strong in ordinary light and shows deep red color when viewed in the direction of vertical axis and a much lighter color to nearly colorless in view at right angles to this axis (Fig.3.18 a and b)

Corundum bearing Chlorite Schist: The mineral chlorite is a hydrous silicate of aluminium, iron and magnesium optical properties shows colourless or pale green to deep green faintly to moderately pleochroic in shades of green and yellow. Prominent cleavage traces parallel to the length; birefringence is weak; extinction parallel to the cleavage trace are observed in most of the chlorite minerals and crystal system is monoclinic.

Tremolite is a mineral that is typically associated with secondary alteration processes in igneous rocks as well as in metamorphic rocks in the form of typical mineral facies of green schists. It occurs as a result of alteration of micas, although it is commonly found as alteration of amphiboles and pyroxenes. The pleochroic property shows light green to colorless; while medium relief interference color shows berlin blue color. The second order interference color is depicted by the mineral mica. The central part is associated corundum which shows pale blue color; uniaxial; low birefringence and surface relief is high (Fig.3.18 c and d)

Corundum bearing Hornblende gneiss: Various shades of yellowish green and reddish brown to dark brown are observed in hornblende gneiss showing Slender prismatic to bladed crystals, with 4 or 6 sided cross section which exhibit amphibole cleavage also has anhedral irregular grains which shows moderate to high positive relief. Hornblende cleavages on intersection at fragment shape is controlled by cleavage; birefringence; interference colors usually has higher first or lower second order. The mineral shows simple and lamellar twinning; biaxial and shows alteration to biotite & chlorite or other Fe-Mg silicates. Corundum shows pale yellow colour; uniaxial; low birefringence, surface relief is high (Fig.3.18 e and f).

Amphibolite schist with sphane: Hornblende is the commonest amphibole found in igneous rocks and is most abundant in acid and intermediate rocks. It is less common in ultrabasic and basic rocks where other amphiboles are more commonly found. Most of the minerals show abundant in high grade regional metamorphic rocks such as schist, gneiss and granulite. It can also be found within immature sediments as clastic grains. Hornblende often alters to an intergrowth of tremolite and actinolite sometimes with epidote, giving a blue-green appearance in hand specimen. Amphibole is usually strongly green in coloure, yellow-blue, blue-green and brown. It shows strong pleochroic, moderate relief, high cleavage, birefringence biaxial and pleochroic appears in various shades of green and brown. In plane polarized light, the mineral colour of amphibole ranges from yellowish green to dark green in Colour (Fig.3.18 g and h).

Sphene mineral appears as slightly brownish color with extremely high relief and high interference colors. Euhedral forms having acute rhombic (elongated diamond-

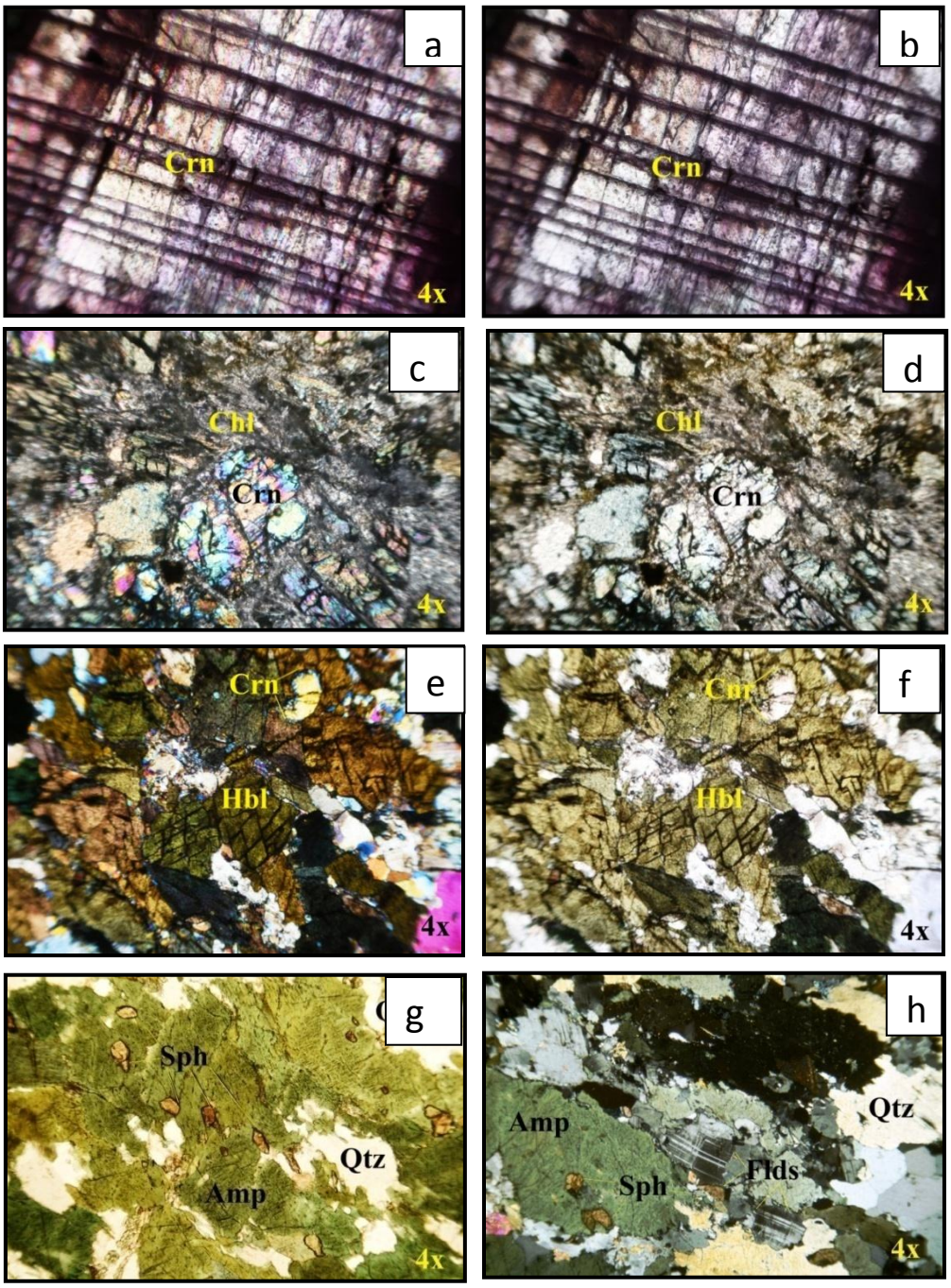

Fig.3.18. Photomicrographs of a and b Corundum (xpl and ppl) c and d Corundum bearing Chlorite schist, e and f Corundum bearing Hornblende schist and g and h Amphibolite schist with sphene around Hassan district, Sl no 22 – 27.

shaped) cross sections. Birefringence very strong high order white interference colours but are usually masked by the strong body colour or destroyed by total reflection, biaxial positive. Rhombic sections have symmetrical extinction. It does not extinguish

completely on rotation of stage does not show complete darkness in extinction positions due to strong dispersion. It shows acute rhombic cross sections with extremely high relief (Fig.3.18 g and h).

3.6.5. Corundum bearing Samples around Chikmagalur District

Corundum: The corundum optical properties show Color: pink to blood-red colored (some time spotted in red – Ruby or blue-Sapphire) The red color is caused by the mineral chromium and shows brownish tone due to the presence of iron. Relief shows high to very high. Prismatic, tabular or skeletal crystals and Rhombohedral parting/ cleavages are common. pleochroism is very strong in ordinary light and shows deep red color when viewed in the direction of vertical axis and a much lighter color to nearly colorless in view at right angles to this axis. Birefringence weak, Uniaxial negative. but often up to low II order due to extra thickness of ultra-hard corundum (Fig.3.19 a and b).

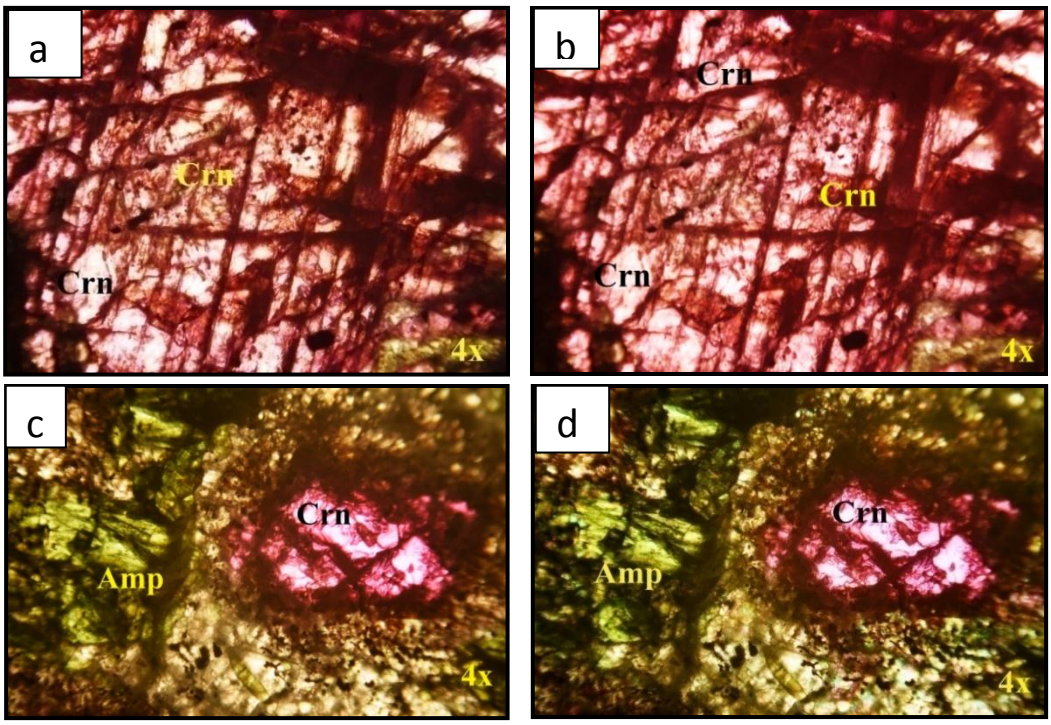

Fig.3.19. Photomicrographs of a and b Corundum samples (xpl and ppl) c and d Corundum bearing Amphibolite schist around Chikmagalur district, Sl no 28 – 32.

The central part is associated corundum which pink to blood-red colored; uniaxial; low birefringence and surface relief is high. Amphibole is usually strongly green in coloure,

yellow-blue, blue-green and brown. It shows strong pleochroic, moderate relief, high cleavage, birefringence biaxial and pleochroic appears in various shades of green and brown. In plane polarized light, the mineral colour of amphibole ranges from yellowish green to dark green in Colour (Fig.3.19 b and c).

3.6.6. Corundum bearing Samples around Dakshina Kannada District

Corundum: The corundum optical properties show Color: colorless, pink to blood-red colored the red color is caused by the mineral chromium and shows brownish tone due to the presence of iron. Relief shows high to very high. Prismatic, tabular or skeletal crystals and Rhombohedral parting/ cleavages are common. pleochroism is very strong in ordinary light and shows deep red color when viewed in the direction of vertical axis and a much lighter color to nearly colorless in view at right angles to this axis. Birefringence weak, Uniaxial negative, but often up to low II order due to extra thickness of ultra-hard corundum, Parallel extinction. In hornfelses, high grade pelites and syenitic gneisses and regionally metamorphosed rocks (Fig.3.20 a and b).

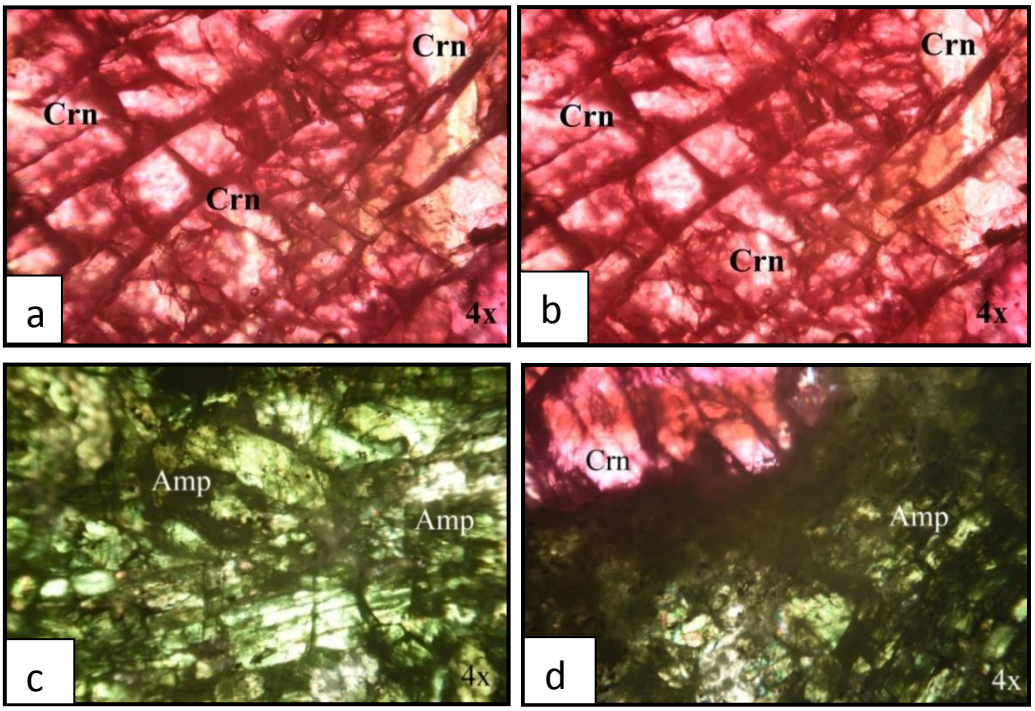

Fig.3.20. Photomicrographs of a and b Corundum samples (xpl and ppl) c and d Corundum bearing Amphibolite schist around Dakshina Kannada district, Sl no 33 – 35.

Corundum bearing Amphibolite schist: Amphibole is usually strongly green in coloure, yellow-blue, blue-green, dark greenish and brown. It shows strong pleochroic, moderate relief, high cleavage, birefringence biaxial and pleochroic appears in various shades of green and brown. In plane polarized light, the mineral colour of amphibole ranges from yellowish green to dark green in Colour. The corner part is associated corundum which shows pinkish red color; uniaxial; low birefringence and surface relief is high (Fig.3.20 c and d). Amphibolite hosted Corundum shows various shades of yellowish green and reddish brown to dark brown are observed in hornblende showing Slender prismatic to bladed crystals, with 4 or 6 sided cross section which exhibit amphibole cleavage also has anhedral irregular grains which shows moderate to high positive relief. Hornblende cleavages on intersection at fragment shape is controlled by cleavage; birefringence; interference colors usually has higher first or lower second order. The mineral shows simple and lamellar twinning; biaxial and shows alteration to biotite & chlorite or other Fe-Mg silicates. Corundum shows pale yellow colour; uniaxial; low birefringence, surface relief is high (Fig.3.20 c and d).

3.6.7. Corundum bearing Samples around Mysuru District

The corundum optical properties show Color: pink to blood-red colored. Relief shows high to very high. Prismatic, tabular or skeletal crystals and rhombohedral parting/ cleavages are common. Pleochroism is very strong in ordinary light and shows deep red color when viewed in the direction of vertical axis and a much lighter color to nearly colorless in view at right angles to this axis. Birefringence weak, uniaxial negative but often up to low II order due to extra thickness of ultra-hard corundum (Fig.3.21 a and b).

Amphibole is usually strongly green in coloure, yellow-blue, blue-green and brown. In plane polarized light, the mineral colour of amphibole ranges from yellowish green to dark green in Colour. The central part is associated corundum which shows pale blue color; uniaxial; low birefringence and surface relief is high (Fig.3.21 c and d).

The Central par Corundum shows red, pale blue and pale yellow colour; uniaxial; low birefringence, surface relief is high. Hypersthene is an iron magnesium silicate with more than 15% $FeSio_3$, (Mg, Fe) Sio_3 Color: body colour more marked than in enstatite,

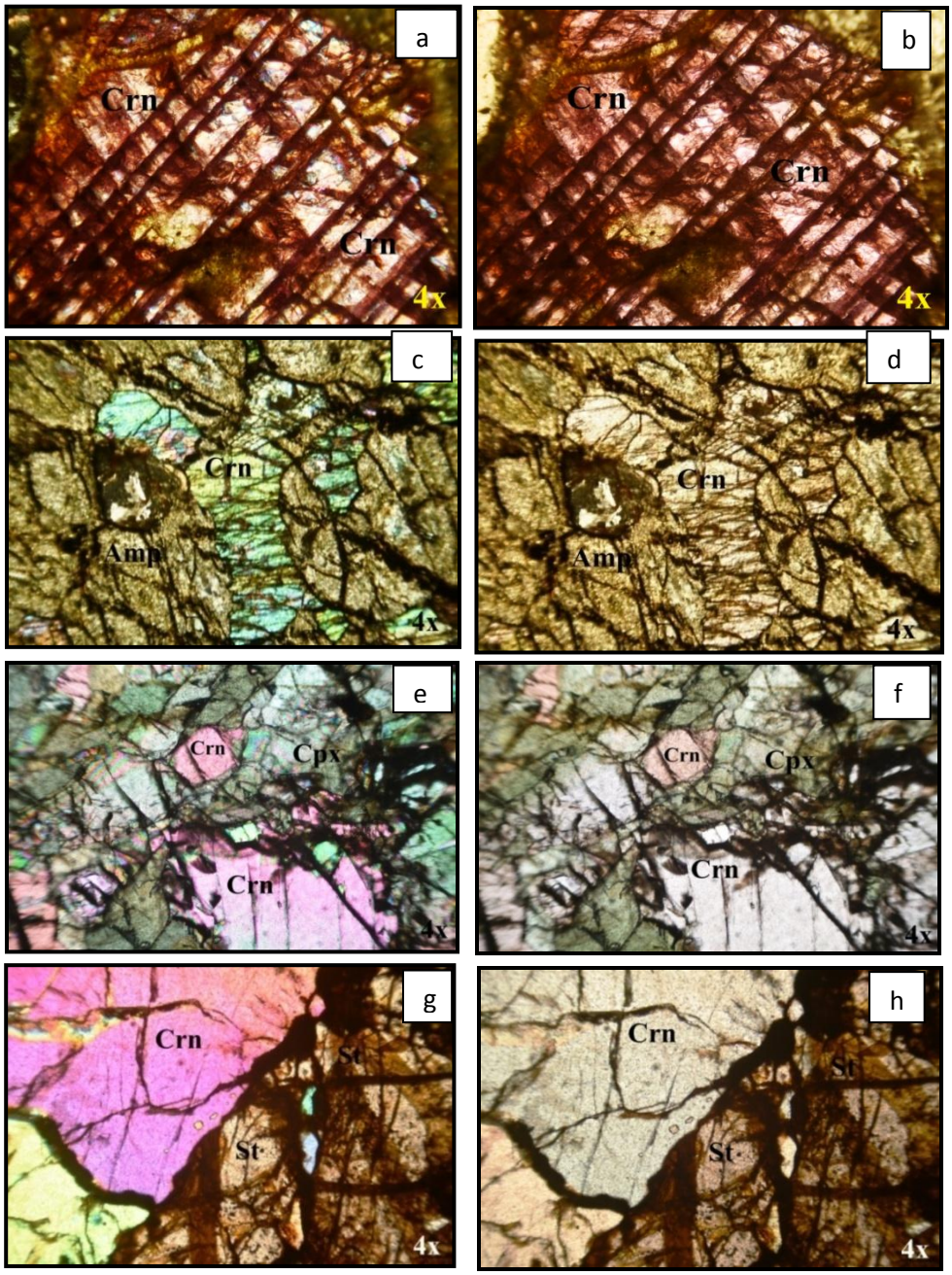

Fig.3.21. Photomicrographs of a and b Corundum samples (xpl and ppl) c and d Corundum bearing Amphibolite schist, e and f Corundum Bearing Pyroxene Granulate and g and h Corundum with Staurolite around Mysuru district, Sl no 36 – 51.

colorless to pale green or pale red. Form usually as prismatic grains the cross sections are nearly square. Well developed one set of cleavage traces in prismatic grains and two sets of cleavage traces at right angles to each other in (cross section) grains having nearly square shape. Relief high. Birefringence weak (slightly stronger than in enstatite) yellow

to red of the I order interference colors positive elongation, biaxial negative. Extinction parallel in most sections. (fig 3.21 e and f).

Staurolite shows Porphyroblast and Staurolite grain at extinction, where the diamond shape is clearly visible. Color pale honey yellow or brown, pleochroism weak to moderate in honey yellow, relief high and cleavage weak, its shows anisotropic and biaxial Twinning not obvious in thin section, Distinguishing Features Staurolite's yellow color, pleochroism, relief and habit make it distinguishing. It is vitreous and has a grey streak. Staurolite's hand sample has characteristic penetration twinning and unique crystal habit. The crystals are brown, red or yellow in color. May resemble tourmaline in thin section, but tourmaline is uniaxial. Occurrence Staurolite is found in medium-grade pelitic metamorphic rock, and is used as an index mineral in metamorphic zoning. Staurolite may be found with garnet, cordierite, kyanite, muscovite, biotite and quartz. It is in the lower to middle amphibolite facies. (Fig3.21 g and h).

The corundum shows Pinkish red color appearance in plane polarized light. Corundum is depicted by pink to blood-red colored and can vary within each gem variety of the mineral Corundum. It shows uniaxial, birefringence & pleochroism is very strong in ordinary light and shows deep red color when viewed in the direction of vertical axis and a much lighter color to nearly colorless in view at right angles to this axis (Fig.3.21 g and h)

3.6.8. Corundum bearing Samples around Mandya District

Corundum: The corundum optical properties show Color: colorless, pink to blood-red colored The red color is caused by the mineral chromium and shows brownish tone due to the presence of iron. Relief shows high to very high. Prismatic, tabular or skeletal crystals and Rhombohedral parting cleavages are common. pleochroism is very strong in ordinary light and shows deep red color when viewed in the direction of vertical axis and a much lighter color to nearly colorless in view at right angles to this axis. Birefringence weak, Uniaxial negative. but often up to low II order due to extra thickness of ultra-hard corundum. Parallel extinction. (Fig.3.22 a and b).

Sericite optical properties shows Color: Brown or turbid pale greyish, Monoclinic system, anisotropic, Pleochrosim – nill Relief weeak, Cleavage very good in one direction in basal sections have no cleavage, Biaxial high birefringence sericite also fills the micro fractures in plagioclase, but it does it in elongated crystals, unlike the rather equant hematite crystals. Sericite is a fine-grained variety of muscovite, with the same composition $KAl_2(AlSi_3O_{10})(OH)_2$. It usually forms by hydrothermal alteration of K-feldspars, which provide the necessary potassium (Basavarajappa and Maruthi., 2018). It grows in pre-existing microfractures where the fluids can penetrate, or in fractures created by the fluid pressure., sericite fills cracks around and across plagioclase crystals, sericite that probably has replaced feldspar (Maruthi et al., 2018) (Fig.3.22 a and b).

Amphibole is usually strongly green in coloure, yellow-blue, blue-green and brown. It shows strong pleochroic, moderate relief, high cleavage, birefringence biaxial and pleochroic appears in various shades of green and brown. In plane polarized light, the mineral colour of amphibole ranges from yellowish green to dark green in Colour. The central part is associated corundum which pink to blood-red colored; uniaxial; low birefringence and surface relief is high (Fig.3.22 c and d).

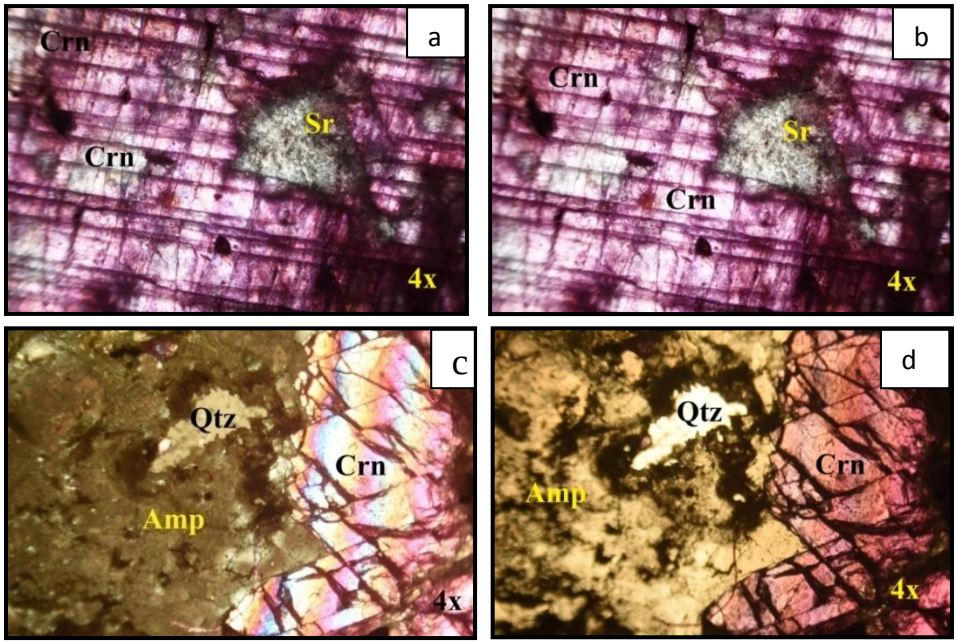

Fig.3.22. Photomicrographs of a and b Corundum samples (xpl and ppl) c and d Corundum bearing Amphibolite schist around Mandya district, Sl no 52 – 64.

3.6.9. Corundum bearing Samples around Ramanagara District

Corundum: The corundum optical properties show Color: pink to blood-red colored (some time spotted in red – Ruby or blue-Sapphire) The red color is caused by the mineral chromium and shows brownish tone due to the presence of iron. Relief shows high to very high. Prismatic, tabular or skeletal crystals and Rhombohedral parting/ cleavages are common. pleochroism is very strong in ordinary light and shows deep red color when viewed in the direction of vertical axis and a much lighter color to nearly colorless in view at right angles to this axis. Birefringence weak, Uniaxial negative. but often up to low II order due to extra thickness of ultra-hard corundum (Fig.3.23 a and b).

The central part is associated corundum which pink to blood-red colored; uniaxial; low birefringence and surface relief is high. Amphibole is usually strongly green in coloure, yellow-blue, blue-green and brown. It shows strong pleochroic, moderate relief, high cleavage, birefringence biaxial and pleochroic appears in various shades of green and brown. In plane polarized light, the mineral colour of amphibole ranges from yellowish green to dark green in Colour (Fig.3.23 c and d).

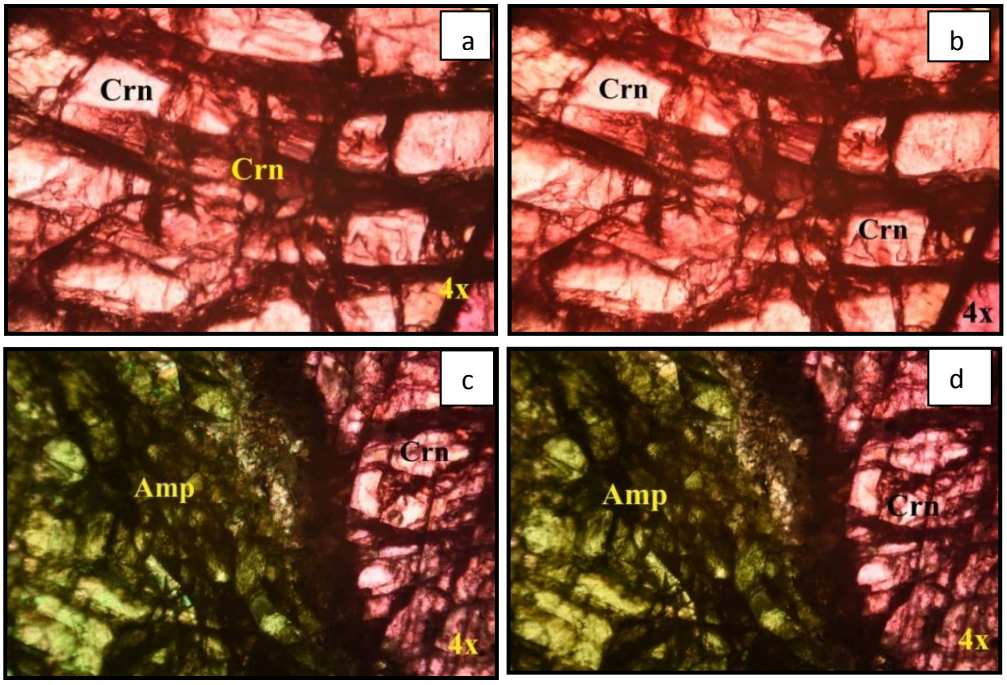

Fig.3.23. Photomicrographs of a and b Corundum samples (xpl and ppl) c and d Corundum bearing Amphibolite schist around Ramanagara district, Sl no 65 – 70.

3.6.10. Corundum bearing Samples around Chamarajanagara District

Corundum bearing Pelitic gneiss: The corundum optical properties show Color: colorless, to gray colored Relief shows high to very high. Prismatic, tabular or skeletal crystals and rhombohedral parting/ cleavages are common. Pleochroism is very strong in ordinary light and shows gray color when viewed in the direction of vertical axis and a much lighter color to nearly colorless in view at right angles to this axis. Birefringence

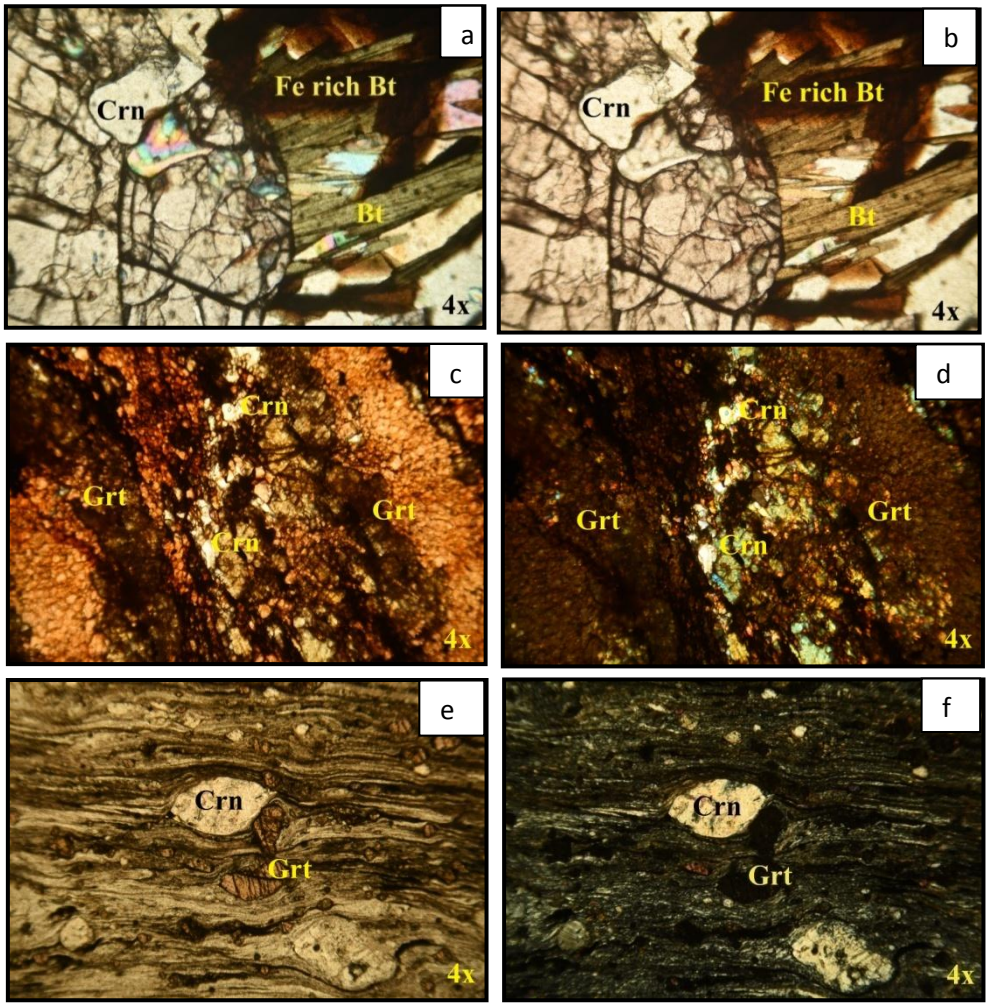

Fig.3.24. Photomicrographs of a and b Corundum bearing Pelitic rock (xpl and ppl) c and d Fe Garnet rich Corundum rock and e and f Corundum Garnet bearing Mylonite around Chamarajanagara district, Sl no 71 – 71.a.

weak, Uniaxial negative, but often up to low II order due to extra thickness of ultra-hard corundum, Parallel extinction. In hornfelses, high grade pelites and syenitic gneisses and regionally metamorphosed rocks (Maruthi et al., 2018) (Fig.3.24 a and b). primary quartz

occure as bigger grains and are stretched and elongated. Plagioclase and K.feldspar occur as alternate bands within the schistose fabric in the pelites, tabular crystals of biotite occure with serrated margins and exibit bent lamellae, biotite are pleochroic from brown to dark brown color, porphyroblast garnets occur with inclusions of corundum, quartz, plagioclase and biotite (Basavarajappa et al., 2004) (Fig.3.24 a and b).

Iron rich Garnet shows rounded brown color shape, under microscope it's a silicate of various divalent metals (Aluminium,ferrous iron, and chromium) and trivalent metals (calcium, magnesium. Ferric iron and manganese) brown color with pitted appearance and inclusions of other minerals. Form as rounded polygonal section. Traversed by cracks. Cleavage nill. Very high relief and birefringence nill, istropic, its form very high relief and isotropism are characteristic. It is distinguished from olivine by its forms absence of alteration in to serpentine and isotropism (Fig.3.24 c and d).

Ultra mylonite also high defers and highly sheared the corundum shows color: colorless, Relief shows high to very high. Birefringence weak, Uniaxial negative, but often up to low II order due to extra thickness of ultra-hard corundum. Garnet shows rounded brown color shape, under microscope, Very high relief and birefringence nill, istropic, its form very high relief and isotropism are characteristic (Fig.3.24 e and f).

3.6.11. Corundum bearing Samples around Kolara District

Corundum: The corundum optical properties show Color: colorless, pink to blood-red colored (some time spotted in red – Ruby or blue-Sapphire) the red color is caused by the mineral chromium and shows brownish tone due to the presence of iron. Relief shows high to very high. Prismatic, tabular or skeletal crystals and rhombohedral parting/ cleavages are common. Pleochroism is very strong in ordinary light and shows deep red color when viewed in the direction of vertical axis and a much lighter color to nearly colorless in view at right angles to this axis. Birefringence weak, Uniaxial negative. but often up to low II order due to extra thickness of ultra-hard corundum. Parallel extinction. In hornfelses, high grade pelites and syenitic gneisses, environment contact and regionally metamorphosed rocks (Fig.3.25 a and b).

Sericite optical properties shows Color: colorless or turbid pale greyish, Monoclinic system, anisotropic, Pleochrosim – nill Relief weeak, Cleavage very good in one direction in basal sections have no cleavage, Biaxial high birefringence sericite also fills the micro fractures in plagioclase, but it does it in elongated crystals, unlike the rather equant hematite crystals. Sericite is a fine-grained variety of muscovite, with the same composition $KAl_2(AlSi_3O_{10})(OH)_2$. It usually forms by hydrothermal alteration of K-feldspars, which provide the necessary potassium. It grows in pre-existing microfractures where the fluids can penetrate, or in fractures created by the fluid pressure., sericite fills cracks around and across plagioclase crystals, sericite that probably has replaced feldspar (Fig.3.25 a and b).

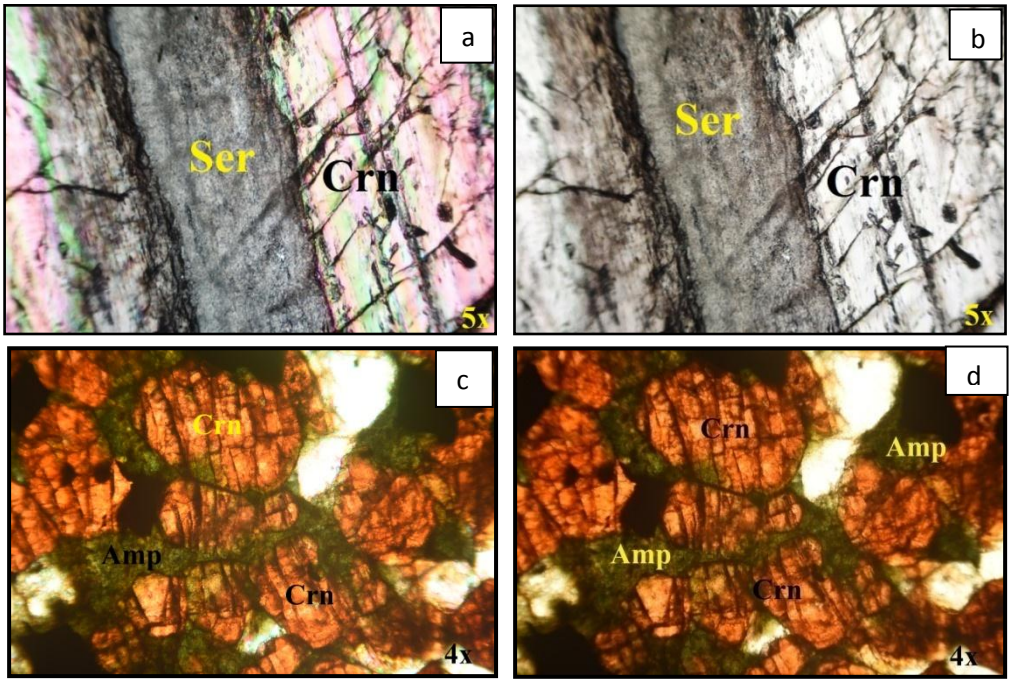

Fig.3.25. Photomicrographs of a and b Corundum samples (xpl and ppl) b and c Corundum bearing Amphibolite schist around Kolara districts, Sl no 72 – 73.a.

corundum shows color: red to blood red, Relief shows high to very high. Birefringence weak, Uniaxial negative. Amphibole is usually strongly green in coloure, yellow-blue, blue-green and brown. It shows strong pleochroic, moderate relief, high cleavage, birefringence biaxial and pleochroic appears in various shades of green and brown. In plane polarized light, the mineral colour of amphibole ranges from yellowish green to dark green in Colour (Fig.3.25 c and d).

CHAPTER-IV

4.1. GEOCHEMISTRY

Geochemistry is the branch of Earth Science that applies chemical principles to deepen an understanding of the Earth system and systems of other planets. Geochemistry is the science that uses the tools and principles of chemistry to explain the mechanisms behind major geological systems such as the Earth's crust and its oceans (Albarede Francis., 2007). The realm of geochemistry extends beyond the Earth, encompassing the entire Solar System (McSween et al., 2010) and has made important contributions to the understanding of a number of processes including mantle convection, the formation of planets and the origins of granite and basalt (Albarede Francis., 2007). The term geochemistry was first used by the Swiss-German chemist Christian Friedrich Schonbein in 1838 a comparative geochemistry ought to be launched, before geochemistry can become geology, and before the mystery of the genesis of our planets and their inorganic matter may be revealed (Kragh, Helge., 2008) However, for the rest of the century the more common term was "chemical geology", and there was little contact between geologists and chemists (Kragh, Helge., 2008).

Corundum (sapphire and ruby) is a crystalline form of the aluminum oxide. When aluminum oxides are pure, the mineral is colorless, but the presence of trivalent cations (as Ti3+, V3+, Cr3+, Fe3+) or conveniently compensated, divalent (such as Fe2+) or tetravalent (Mn4+) ions substituting Al3+ in its lattice site gives the typical colors (including blue, red, violet, pink, green, yellow, orange, gray, white or black) of gemstones varieties (Khin Zaw et al., 2014). They are called ruby if red, while, all other colors are called sapphire. Chromium oxide is the coloring matter for ruby (Harlow and Bender, 2013). The color of blue sapphire results from the combination of titanium and iron oxides, when Fe2+ and Ti4+ substitute the Al3+ or when a Fe3+ and Ti4+ substitutes the Al3+. With the decreasing of titanium contents the color tends towards green and yellow (Harlow and Bender, 2013).

The obtained geochemical data allow the characterization of the corundum and consequently help to determine genetic parameters. The geochemical features of the

studied corundum grains are discussed. Since these depend on the availability of elements in the crystallization environment (Peucat et al., 2007) this suggests that the corundum crystallized in an environment associated with: alkali and alkaline earth metals, transitional metals, other metals and metalloids (Harlow and Bender, 2013).

4.2. ANALYTICAL METHOD

First randomly collected samples respective study area and purpose of know chemical composition of rock samples we taken help of XRF instrument , before going to instrument first prepare the rock sample convert to powder in department of Earth Science University of Mysore using auget matter prepared sample is equal to talcum powder. Elemental analysis with XRF is already the key to quality and production control in industries analyzing a wide range of oxide materials. Finding enough standards to setup reliable calibrations can be difficult and costly. That is why Malvern Panalytical has developed a set of 19 synthetic, multi-element wide-range oxide (WROXI) standards.

4.2.1. The PANalytical Epsilon 3

The PANalytical Epsilon 3 is an X-ray Fluorescence Spectroscopy system that utilizes an energy dispersive spectrometry (EDXRF) that has surpassed a technological barrier with an elemental analysis for measuring elements ranging from Carbon (C) to Americium (Am). Samples can be analyzed in various forms including powder, liquid, pressed pellet, and fusion pellet. This instrument is equipped with an automated sample changer that holds up to 10 samples and since each sample is isolated in an individual sample container, there is almost no chance for cross contamination.

Fig.4.1. XRF Instrument CSIR lab Thiruvananthapuram Kerala

Working in PANalytical Epsilon 3 X-ray Fluorescence Spectroscopy lab at Materials Science & Technology Division NIIST Thiruvananthapuram, Kerala. This instrument Combining the latest excitation and detection technology and smart design, the analytical performance of Epsilon 3 approaches that of more powerful and floor-standing spectrometers. Selective excitation and careful matching of the X-ray tube output to the capabilities of the detection system underlie the system's outstanding performance.

PANalytical Epsilon 3 is fast measurements are achieved by using the latest silicon drift detector technology that produces significant higher intensities. Unique detector electronics enable a linear count rate capacity to over 1,500,000 cps (at 50% deadtime) and a count rate independent resolution typically better than 135 eV for better separation of analytical lines in the spectrum. XRF is an ideal means of determining the chemical composition of all kinds of materials. Measurements in Epsilon 3 are carried out directly on the solid material (or liquid) with little to no sample preparation. There is no need for any dilution or digestion and therefore no disposal of chemical waste. Epsilon 3 spectrometers can handle a large variety of sample types weighing from a few milligrams to larger bulk samples. Samples can be measured as: Solids, Pressed powders, Loose powders, Liquids, Fused beads, Slurries, Granules, Filters, Films and coatings.

PANalytical Epsilon 3 X-ray Fluorescence Spectroscopy instrument using powerful Omnian software is ideal when there is no conventional calibration established for materials that require analysis. When faced with non-routine samples or materials for which there are no certified reference materials, Omnian provides excellent insight into the elemental composition. Designed to provide fast and reliable quantification, Omnian's advanced fundamental parameters (FP) algorithm automatically deals with the analytical challenges posed by samples of widely differing types.

4.3. WHOLE ROCK GEOCHEMICAL ANALYSIS OF CORUNDUM BEARING ROCKS AROUND CHITRADURGA DISTRICT

Bulk-rock major and trace element data for the samples from the Chitradurga region, corundum and corundum bearing amphibolites schist geochemical data carried out from lab Materials Science & Technology Division NIIST Thiruvananthapuram, Kerala (Table. 4.1).

Table: 4.1. Bulk-rock geochemical Analysis Data of Corundum bearing samples around Chitradurga area.

Major elements are in wt. %											
Sl no	SiO_2	Al_2O_3	Fe_2O_3	CaO	MgO	K_2O	Cr_2O_3	TiO_2	MnO	P_2O_5	Total
1	25.65	62.34	4.56	1.231	0	0.943	1.547	2.131	0.159	0.982	99.543
2	9.72	83.35	2.508	1.103	0	0.231	0.273	1.808	0.08	0.757	99.837
2.A	40.21	32.86	5.98	8.43	10.12	0.426	0.002	0.67	0.0322	0.595	99.3252

Minor and trace elements in ppm											
Sl no	CuO	ZnO	Ga_2O_3	Rb_2O	SrO	ZrO_2	NiO	Eu_2O_3	V_2O_5	Yb_2O_3	ThO_2
1	21.1	91.34	162	0	38.19	328.24	24.9	231.4	0	6.2	12.32
2	23.1	84.3	192	0	21.6	237.32	21.4	211.9	0	3.5	9.23
2.A	96.8	18	29.3	16.7	243.6	11	0.17	334.3	905.4	0	0

Whole – rock major element chemical compositions of the corundum bearing rocks, deal with ternary diagrams using Origin pro 8.5 (a) and (b) Tridraw softwares. (CaO+MgO) vs Al_2O_3 vs (Fe_2O_3 + TiO_2) its shows alumina rich and Mg rich minerals. Blue and red color symbols showas alumina rich rocks and green color symbol shows Mg and Ca rich metamorphic rock. Metamorphic corundum deposits and associated metamorphic/magmatic processes are closer to a transpersonal tectonic regime.

Chitradurga region ia near to closepet granite of transmission zone its effect on mantle anomaly mark as asthenospheric mantle flows related to reworking and contact zone corundum form and associated with metamorphic rocks, Al and Cr enriched metamorphic corundum suit Ullarti kaval sample no 1 corundum Al, Si, Fe, Cr and Ti rich and Mg, Ca and Mn poor in mineral assemblage. Kyadigunte sample no 2 corundum Al, Si, Ca, Fe and Ti rich and Mg poor, and 2.a corundum bearing amphibolites schist Mg, Ca and Al rich in mineral assemblages (Coenraada., 1992) (Fig.4.2) (Table.4.1).

The new geochemical data for the corundum bearing rocks are presented in Table 4.1 and Fig.4.3 shows selected binary plots with trends towards the corundum bearing amphibolites schist. Generally ultramafic rocks are Mg-rich and very depleted, although it should be noted that several samples, which are rich in amphibole (tremolite) also have

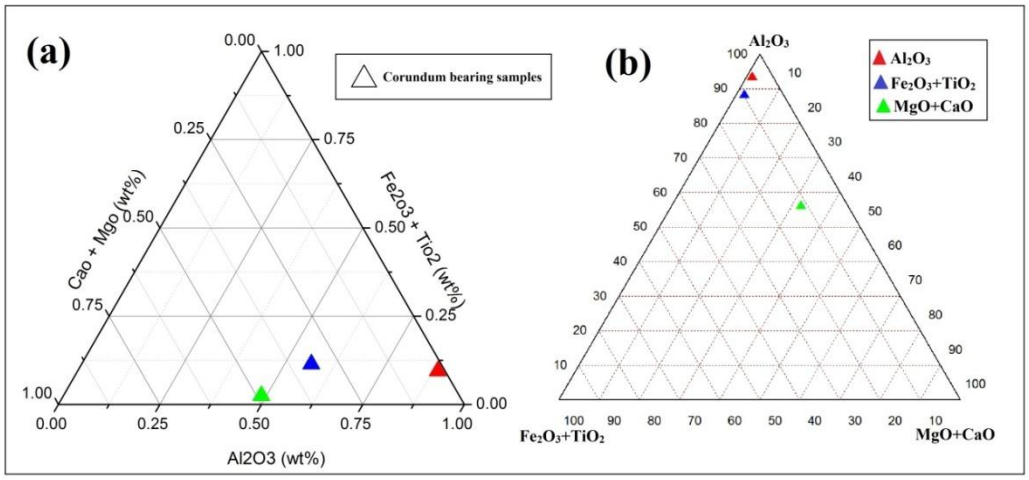

Fig.4.2. (a) and (b) Ternary diagrams showing rock involved in the corundum formation at Chitradurga District.

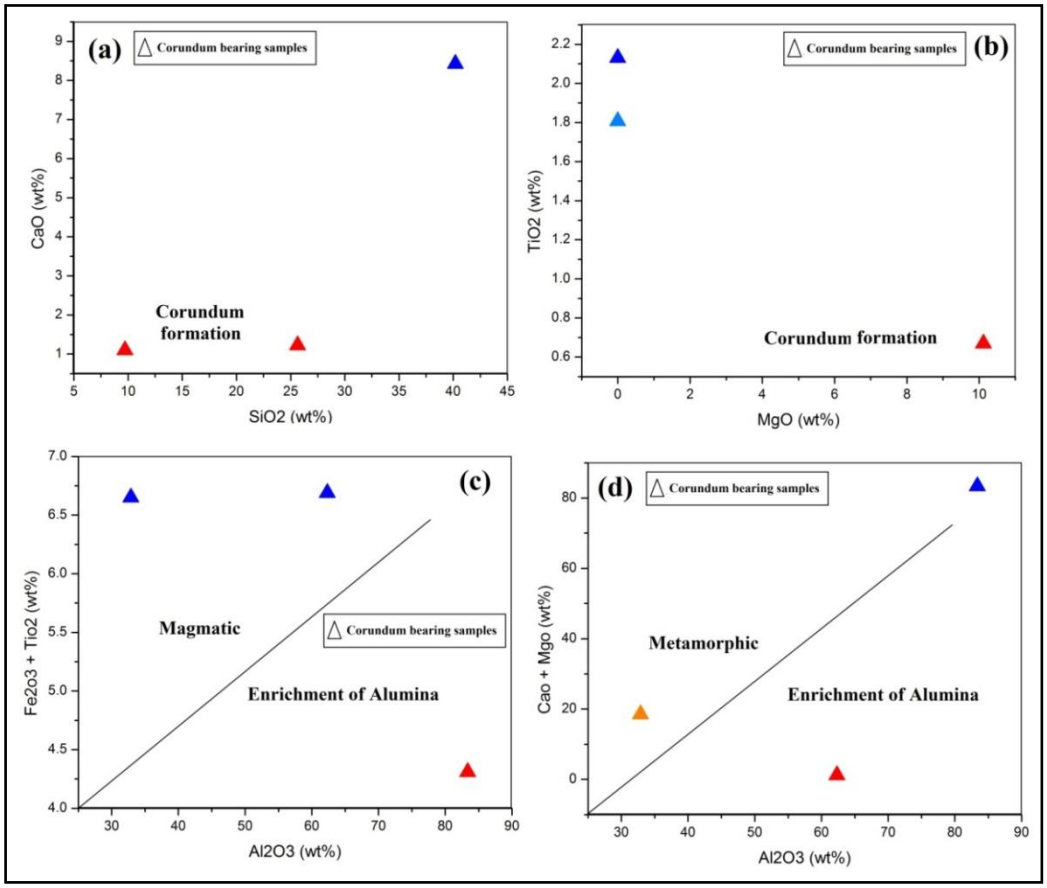

Fig.4.3. (a), (b), (c) and (d) Bulk rock geochemical analysis and binary plots of Chitradurga district samples.

distinctly elevated SiO2 of up to 40 wt.%. The Amphibolite schist rich in SiO_2 and Al_2O_3 with 40 wt.% and 32 wt.%, respectively. Corundum are characterized by having unusually high Al_2O_3 of up to 83 wt. % in combination with very low SiO2 of down to 9 wt. %. There is also strong enrichment in components such as K_2O, Sr and Th for the corundum-bearing rocks Coenraads et al., 1990; Sutherland et al., 2002a.

Bulk-rock geochemical diagrams shows Oxides are in wt. %. (a) CaO vs. SiO_2 showing a significant drop in silica content from the supracrustal rocks to the corundum-bearing rocks. (b) TiO2 vs. MgO showing a slight increase in MgO during the corundum formation. (c) (Fe_2O_3 + TiO_2) vs Al_2O_3 showing a strong enrichment in alumina for the corundum-bearing rocks. (d) (CaO+MgO) vs Al_2O_3 showing a strong enrichment in Mg for the corundum bearing amphibolite schist (Sutherland., 1996) (Fig.4.3).

4.4. WHOLE ROCK GEOCHEMICAL ANALYSIS OF CORUNDUM BEARING ROCKS AROUND TUMKUR DISTRICT

Corundum bearing rock samples were collected and 13 samples were carried out geochemical analysis of around Tumkur District. Chemical composition almost 78 wt% of alumina rich corundum sample occurs in the study area (table.4.2). Sapphire genesis related to melting of amphibole-bearing mantle source rocks at depths of 35 to 40 km, near the crust mantle boundary, forming Si and Al-rich magmas with up to 5 wt.% corundum either from basalt fractionation or directly (Sutherland et al., 1998a). Chemical compositions of the corundum bearing rocks, deal with ternary diagrams. (CaO+MgO) vs Al_2O_3 vs (Fe_2O_3 + TiO_2) its shows alumina rich and Mg rich minerals. Blue and red color symbols showas alumina rich rocks and green color symbol shows Mg and Ca rich metamorphic rock (Fig.4.4).

Bulk-rock geochemical diagrams shows Oxides are in wt. %. (a) CaO vs. SiO_2 showing a significant drop in silica content from the corundum-bearing rocks. (b) TiO2 vs. MgO showing a slight increase in MgO during the corundum formation in contact zone of closepet granite. (c) (Fe_2O_3 + TiO_2) vs Al_2O_3 showing a strong enrichment in alumina for the corundum-bearing rocks in Bittanakurke, Bettadakelaginahalli, Kyathaganakere, Veerammanahalli, Kanikalabande, Channamallanahalli Basmangikaval, Molanahalli,

Chickthimmanahalli and Devarayanadurga area of Tumkur district (d) (CaO+MgO) vs Al_2O_3 showing a strong enrichment in Mg for the corundum bearing closepet granite deposited Thimmapura, ChinakaVajra and Devalapura area of Tumkur district (fig.4.5).

Table: 4.2. Bulk-rock geochemical analysis data of Corundum bearing samples around Tumakur area.

Major elements are in wt. %											
Sl no	**SiO_2**	**Al_2O_3**	**Fe_2O_3**	**CaO**	**MgO**	**K_2O**	**Cr_2O_3**	**TiO_2**	**MnO**	**P_2O_5**	**Total**
3	**10.72**	**81.35**	**2.873**	**1.152**	**0**	**0.246**	**0.39**	**1.91**	**0.07**	**0.651**	**99.362**
4	**16.98**	**76.298**	**3.878**	**0.872**	**0**	**0.343**	**0.1**	**1.245**	**0.03**	**0.233**	**99.979**
5	**61.38**	**24.78**	**3.399**	**1.381**	**0.259**	**7.479**	**0**	**0.276**	**0.026**	**0.773**	**99.753**
6	**9.723**	**83.354**	**2.508**	**1.103**	**0**	**0.231**	**0.273**	**1.808**	**0.08**	**0.757**	**99.837**
7	**11**	**80.123**	**4.132**	**1.243**	**0**	**0.678**	**0.321**	**1.783**	**0.04**	**0.583**	**99.903**
8	**13.11**	**79.92**	**2.061**	**1.987**	**0**	**0.192**	**0.453**	**1.685**	**0.032**	**0.432**	**99.872**
9	**65.12**	**19.2**	**4.916**	**2.521**	**0.665**	**5.615**	**0**	**0.433**	**0.52**	**0.992**	**99.982**
10	**16.212**	**78.21**	**2.321**	**1.234**	**0**	**0.123**	**0.321**	**1**	**0.029**	**0.395**	**99.846**
11	**8.23**	**84.23**	**2.698**	**1.128**	**0**	**0.243**	**0.272**	**1.794**	**0.03**	**0.679**	**99.304**
12	**9.223**	**83.12**	**2.124**	**1.137**	**0**	**0.213**	**0.269**	**1.782**	**0.05**	**0.721**	**98.639**
13	**10.876**	**81.93**	**2.432**	**1.187**	**0**	**0.219**	**0.281**	**1.802**	**0.07**	**0.723**	**99.52**
14	**61.321**	**26.987**	**2.294**	**1.763**	**0.137**	**6.332**	**0**	**0.174**	**0.014**	**0.773**	**99.795**
15	**8.21**	**85.21**	**2.29**	**1**	**0**	**0.214**	**0.283**	**1.803**	**0.03**	**0.743**	**99.885**
Minor and trace elements in ppm											
Sl no	**CuO**	**ZnO**	**Ga_2O_3**	**SrO**	**Y_2O_3**	**ZrO_2**	**NiO**	**Eu_2O_3**	**Yb_2O_3**	**Rb_2O**	**ThO_2**
3	**21.2**	**92.34**	**160**	**39.19**	**0**	**318.24**	**25.9**	**232.9**	**6.3**	**0**	**12.65**
4	**18.5**	**87.1**	**156**	**35.98**	**0**	**293.43**	**19.87**	**219.12**	**5.9**	**0**	**11.4**
5	**14.6**	**62**	**28.1**	**178.8**	**19**	**367.9**	**12.8**	**141.4**	**0**	**201**	**85.1**
6	**29.1**	**99.9**	**172**	**42.7**	**20.7**	**333.3**	**27.6**	**245.7**	**7.5**	**0**	**13.9**
7	**21.23**	**92.3**	**165**	**38.54**	**21.3**	**345.1**	**31.2**	**239.4**	**7.2**	**0**	**12.3**
8	**22.5**	**87.2**	**139**	**32.38**	**23.43**	**323.7**	**32.6**	**242.8**	**6.8**	**0**	**11.2**
9	**53.4**	**101.7**	**37.4**	**433.4**	**23.9**	**384.4**	**20.7**	**196.5**	**0**	**216.8**	**33**
10	**21.32**	**17**	**21.93**	**29.78**	**22.98**	**312.3**	**26.2**	**235.2**	**6.9**	**0**	**10.23**
11	**28.12**	**98.1**	**171**	**39.2**	**20.5**	**332.4**	**25.5**	**241.1**	**7.5**	**0**	**13.2**
12	**29.21**	**98.5**	**169**	**40.3**	**20.2**	**329.1**	**24.2**	**244.2**	**6.9**	**0**	**12.4**
13	**27.9**	**99.3**	**167**	**41.6**	**19.2**	**330.2**	**23.1**	**243.1**	**7.2**	**0**	**13.8**
14	**22.9**	**25.7**	**25.6**	**564.8**	**1.8**	**194.1**	**10.6**	**109.3**	**0**	**134**	**23.7**
15	**26.3**	**97.3**	**162**	**42.3**	**19.1**	**331.8**	**22.1**	**232.9**	**7.4**	**0**	**12.3**

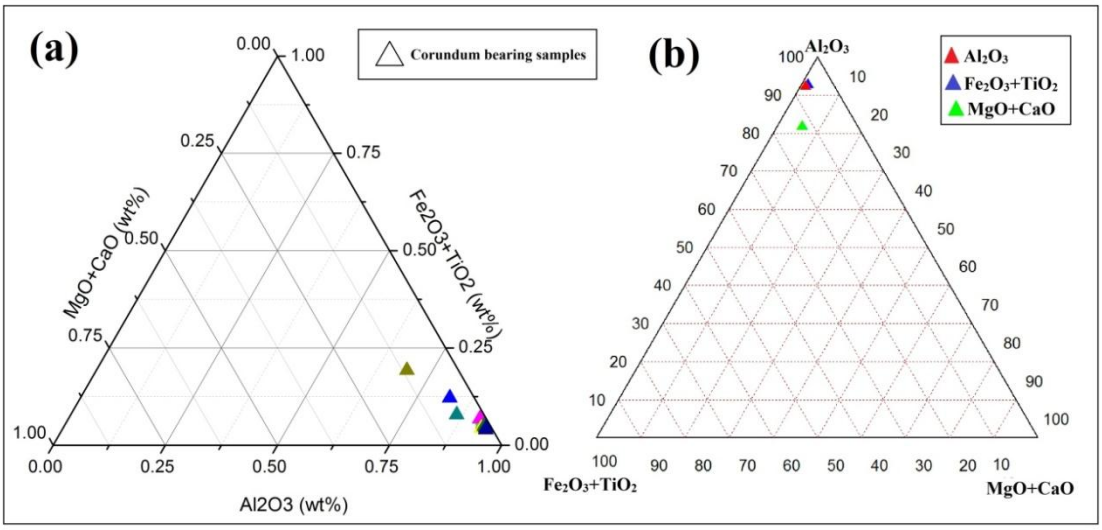

Fig.4.4. (a) and (b) Ternary diagrams showing rock involved in the corundum formation at Tumkur District.

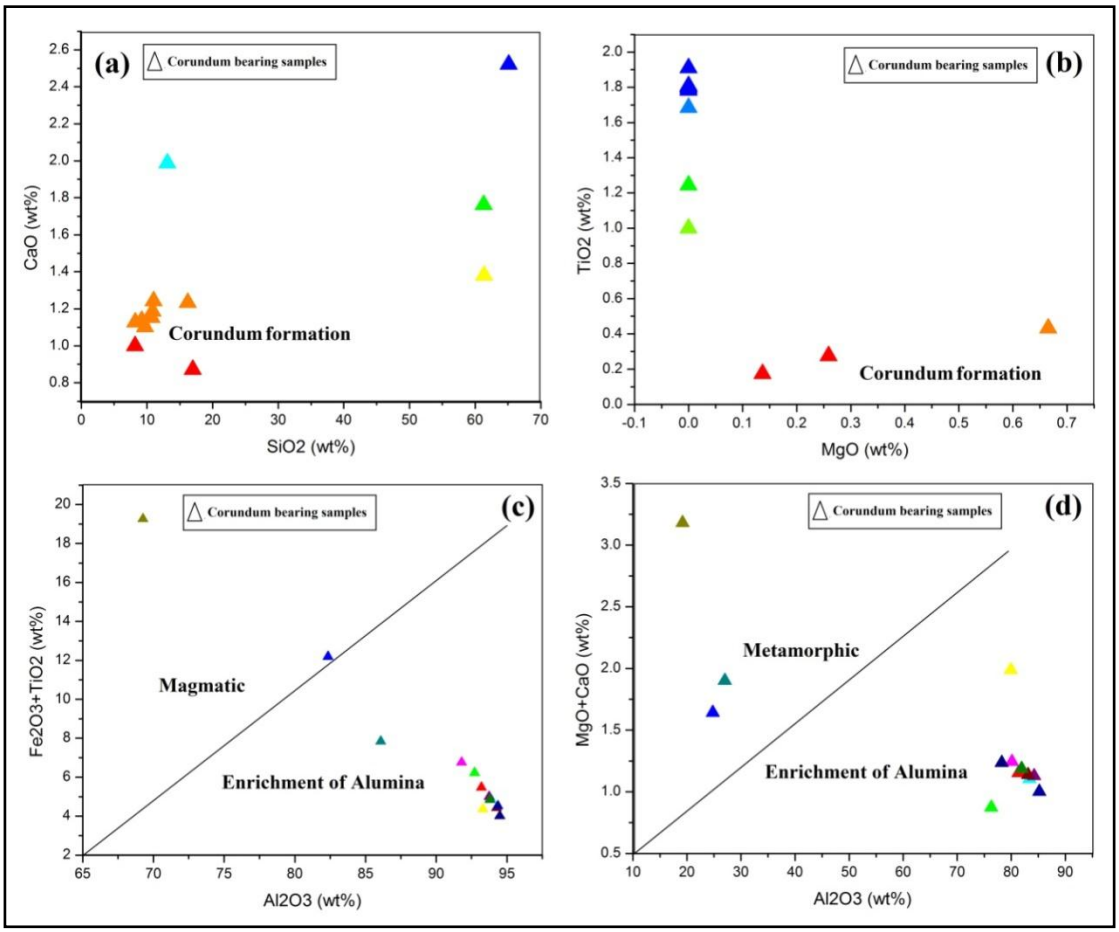

Fig.4.5. (a), (b), (c) and (d) Bulk rock geochemical analysis and binary plots of Tumkur district samples.

4.5. WHOLE ROCK GEOCHEMICAL ANALYSIS OF CORUNDUM BEARING ROCKS AROUND CHIKBALLAPURA DISTRICT

Chikballapura area around 6 corundum bearing samples collected and Geochemical data carried out through laboratory environment (Table.4.3). This area enriched alumina samples average Al 72 wt% of present in chikballapura area

Table: 4.3. Bulk-rock geochemical data of Corundum bearing samples around Chikballapura area.

Major elements are in wt. %											
Sl no	**SiO_2**	**Al_2O_3**	**Fe_2O_3**	**CaO**	**MgO**	**K_2O**	**Cr_2O_3**	**TiO_2**	**MnO**	**P_2O_5**	**Total**
16	**11.987**	**80.35**	**2.773**	**1.122**	**0**	**0.241**	**0.34**	**1.81**	**0.06**	**0.691**	**99.374**
17	**14.98**	**78.298**	**3.678**	**0.862**	**0**	**0.243**	**0.12**	**1.345**	**0.04**	**0.213**	**99.779**
18	**8.12**	**85.32**	**2.23**	**1.021**	**0**	**0.217**	**0.267**	**1.781**	**0.03**	**0.772**	**99.758**
19	**9.723**	**83.154**	**2.408**	**1.113**	**0**	**0.201**	**0.223**	**1.801**	**0.07**	**0.747**	**99.44**
20	**62.38**	**23.78**	**3.343**	**1.281**	**0.255**	**7.419**	**0**	**0.256**	**0.029**	**0.723**	**99.466**
21	**10.1**	**81.123**	**4.112**	**1.213**	**0**	**0.278**	**0.311**	**1.784**	**0.04**	**0.542**	**99.503**
Minor and trace elements in ppm											
Sl no	**CuO**	**ZnO**	**Ga_2O_3**	**Rb_2O**	**SrO**	**Y_2O_3**	**ZrO_2**	**NiO**	**Eu_2O_3**	**Yb_2O_3**	**ThO_2**
16	**20.2**	**91.34**	**162**	**0**	**39.29**	**0**	**328.24**	**24.9**	**242.9**	**6.1**	**12.12**
17	**19.5**	**88.1**	**123**	**0**	**36.98**	**0**	**283.43**	**18.87**	**239.1**	**6.9**	**11.9**
18	**27.7**	**91.1**	**155**	**0**	**41.1**	**18.4**	**323.2**	**24.2**	**211.2**	**7.8**	**12.4**
19	**29.2**	**98.9**	**172**	**0**	**42.2**	**21.7**	**323.1**	**26.5**	**235.7**	**7.4**	**14.9**
20	**13.6**	**61**	**27.1**	**202**	**168.8**	**18**	**357.9**	**13.8**	**131.4**	**0**	**75.1**
21	**20.29**	**92.3**	**162**	**0**	**37.54**	**21.6**	**355.2**	**32.2**	**229.4**	**7.5**	**12.4**

Geochemical compositions of the corundum bearing rocks, deal with ternary diagrams. (CaO+MgO) vs Al_2O_3 vs (Fe_2O_3 + TiO_2) its shows alumina rich and Mg rich minerals. Blue and red color symbols showas alumina rich rocks and green color symbol shows Mg and Ca rich rock this ternary diagram shows Fe, Al and Cr rich mineral assemblages in Chikballapura area (fig.4.6). Bulk-rock geochemical diagrams shows Oxides are in wt. %. (a) CaO vs. SiO_2 showing a significant drop in silica content from the corundum-bearing rocks. (b) TiO2 vs. MgO showing a slight increase in MgO during the corundum formation in contact zone of closepet granite. (c) (Fe_2O_3 + TiO_2) vs Al_2O_3 showing a strong enrichment in alumina for the corundum-bearing rocks in Hunasavadi, Malenahalli, Kachamachanahalli, Kadiridevarahalli and Poolakuntahalli area of Chikballapura distric. (d) (CaO+MgO) vs Al_2O_3 showing a strong enrichment in Mg for

the corundum bearing closepet granite deposited in Neralemaradalli area of Chikballapura distric (fig.4.7).

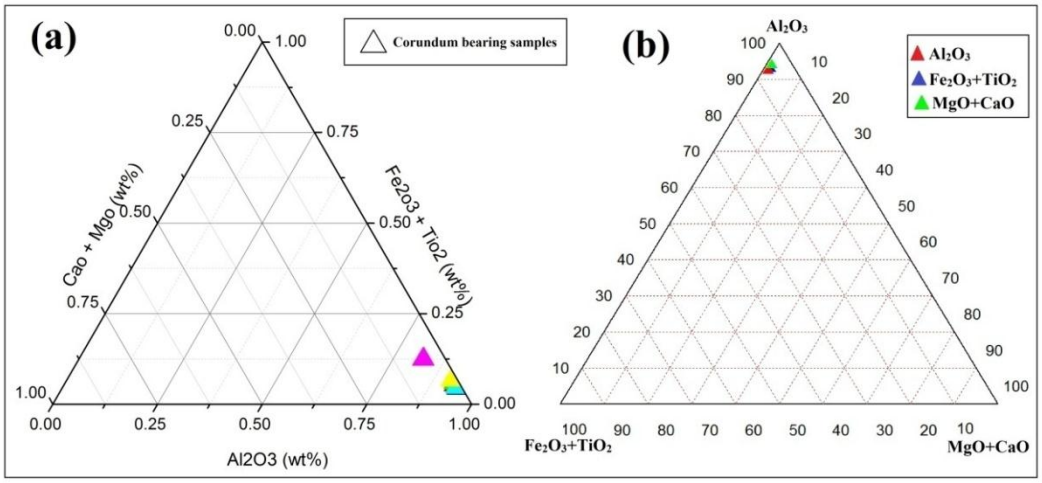

Fig.4.6. (a) and (b) Ternary diagrams showing rock involved in the corundum formation at Chikballapura District.

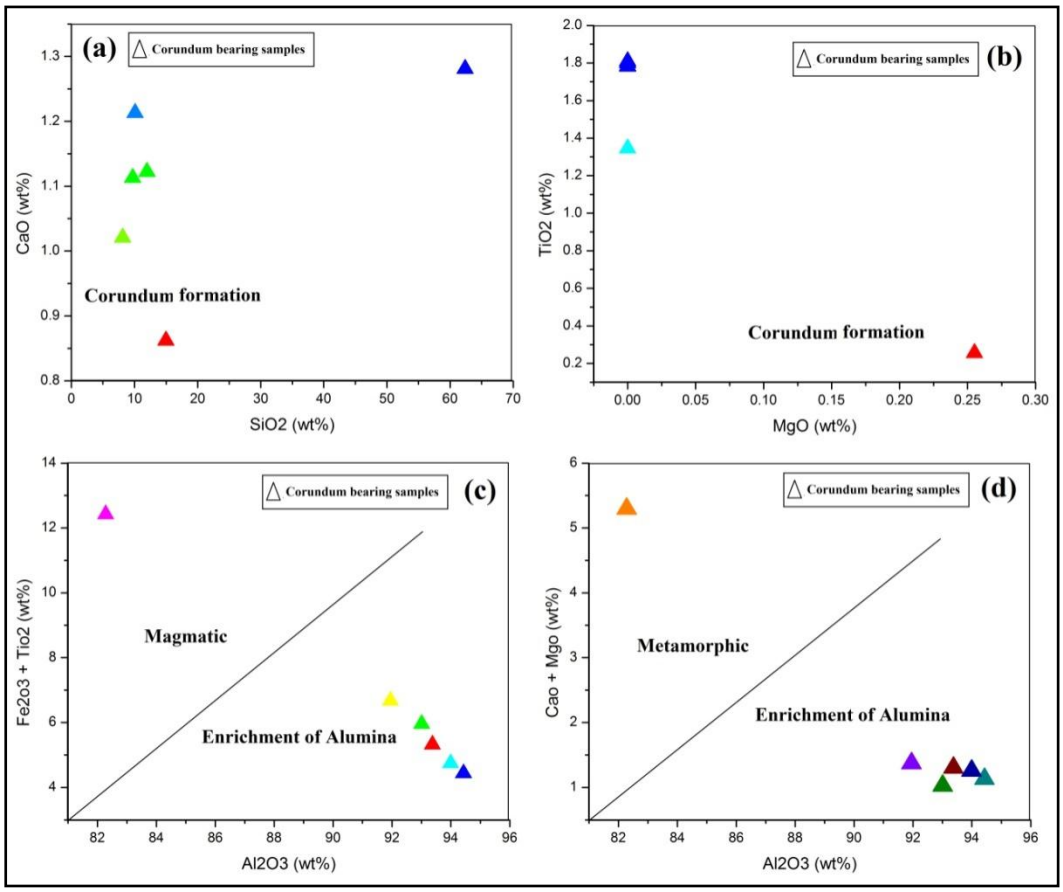

Fig.4.7. (a), (b), (c) and (d) Bulk rock geochemical analysis and binary plots of Chikballapura district samples.

4.6. WHOLE ROCK GEOCHEMICAL ANALYSIS OF CORUNDUM BEARING ROCKS AROUND HASSAN DISTRICT

Bulk-rock major and trace element data for the samples from the Hassan region, corundum and corundum bearing amphibolites schist geochemical data carried out from laboratory environment (Table. 4.4). Hassan district mainly covered Holenarasipura and Nuggihalli schist belts and this area belongs to Sargur group of rocks which comprises corundum bearing rocks were principally made up of interspersed by lands tremolite schist, hornblende gneiss, amphibolites schist along with intrusive dykes of dolerite and reefs of quartzite. Chemical compositions of the corundum bearing rocks, deal with ternary diagrams using Origin pro 8.5 (a) and (b) Tridraw softwares. (CaO+MgO) vs Al_2O_3 vs (Fe_2O_3 + TiO_2) its shows alumina rich and Mg rich minerals. Blue and red color symbols showas alumina rich rocks and green color symbol shows Mg and Ca rich metamorphic rock. Alumina enriched corundum in Makanahalli, Undiganalu, Dyavalapura and Belagumba area sample no 22, 23, 26 and 27 Al, Si, Fe, Cr and Ti rich and Mg, Ca and

Table: 4.4. Bulk-rock geochemical analysis data of Corundum bearing samples around Hassan area.

Major elements are in wt. %											
Sl no	**SiO_2**	**Al_2O_3**	**Fe_2O_3**	**CaO**	**MgO**	**K_2O**	**Cr_2O_3**	**TiO_2**	**MnO**	**P_2O_5**	**Total**
22	**21.82**	**70.29**	**0.637**	**6.72**	**0**	**0.028**	**0.143**	**0.015**	**0.003**	**0.236**	**99.904**
23	**18.43**	**74.32**	**1.231**	**5.21**	**0**	**0.019**	**0.124**	**0.043**	**0.002**	**0.263**	**99.65**
24	**29**	**30.2**	**10.61**	**14.31**	**14.06**	**0.425**	**0.166**	**0.099**	**0.2**	**0.645**	**99.726**
25	**34.13**	**28.12**	**10.54**	**5.91**	**19.23**	**0.085**	**0.244**	**0.062**	**0.131**	**0.718**	**99.181**
26	**15.12**	**78.43**	**1.24**	**4.12**	**0**	**0.121**	**0.162**	**0.032**	**0.001**	**0.197**	**99.43**
27	**7.12**	**86.32**	**2.13**	**1.02**	**0**	**0.207**	**0.271**	**1.791**	**0.04**	**0.712**	**99.614**

Minor and trace elements in ppm											
Sl no	**CuO**	**ZnO**	**Ga_2O_3**	**Rb_2O**	**SrO**	**ZrO_2**	**BaO**	**NiO**	**Eu_2O_3**	**IrO_2**	**V_2O_5**
22	**1.48**	**12.5**	**29.5**	**0**	**104.7**	**4.5**	**38.8**	**28.5**	**211.4**	**1.5**	**68.2**
23	**21.3**	**12.1**	**28.1**	**0**	**102.7**	**3.9**	**32.9**	**27.8**	**134.2**	**1.4**	**66.9**
24	**36.9**	**242.2**	**14.1**	**24.1**	**28.8**	**0.1**	**0.3**	**472.1**	**607.7**	**0**	**114.1**
25	**19.9**	**75**	**10.3**	**0**	**21.5**	**0.3**	**0.9**	**545.6**	**505.7**	**0**	**159.5**
26	**12.3**	**12.4**	**28.6**	**0**	**104.3**	**4,2**	**37.2**	**28.4**	**192.4**	**1.2**	**67.3**
27	**27.8**	**92.1**	**158**	**0**	**42.1**	**333.2**	**21.5**	**23.2**	**231.2**	**0**	**23.8**

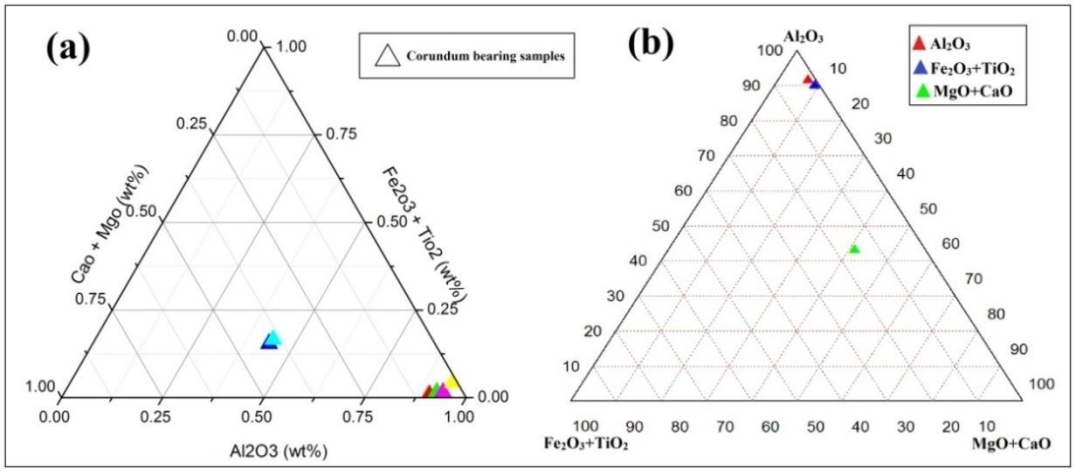

Fig.4.8. (a) and (b) Ternary diagrams showing rock involved in the corundum formation at Hassan District.

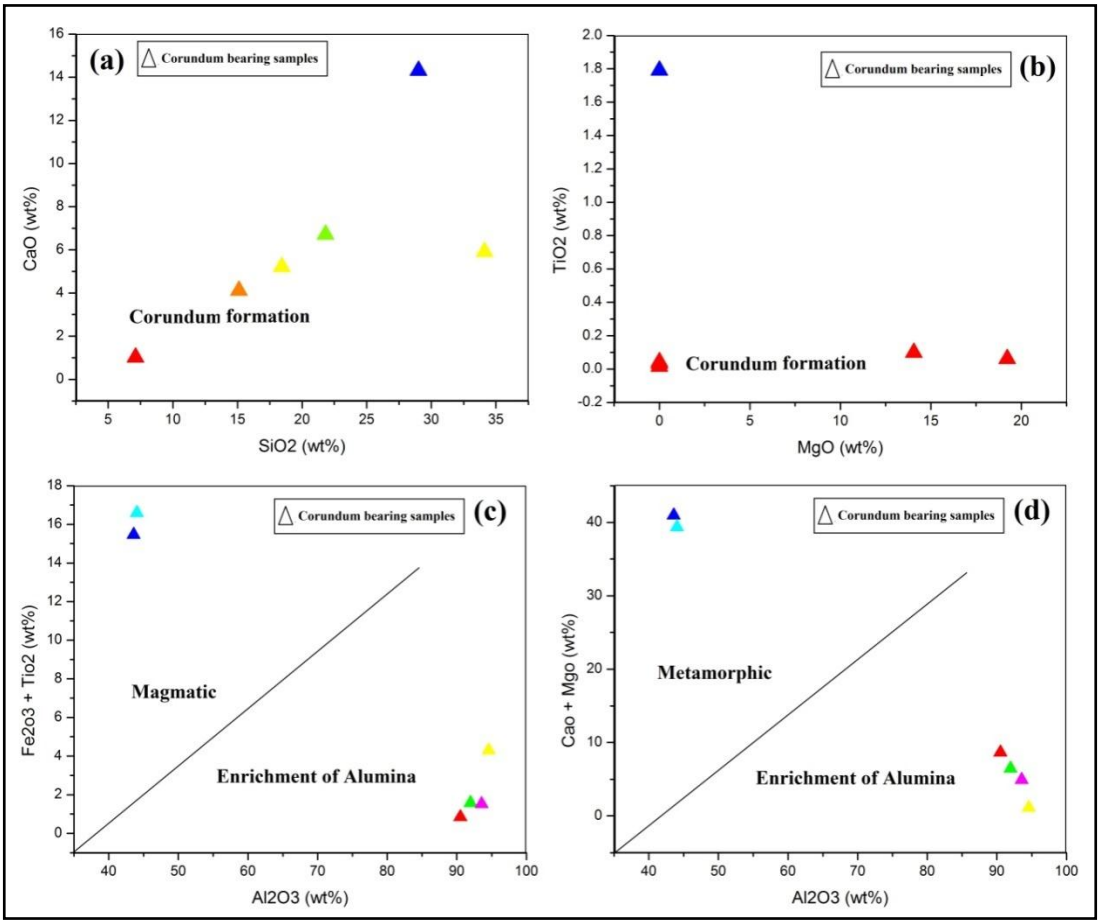

Fig.4.9. (a), (b), (c) and (d) Bulk rock geochemical analysis and binary plots of Hassan district samples.

Mn poor in mineral assemblage. Alumina enriched metamorphic corundum suit Dasagodanahalli area and Corundum bearing chlorite schist occurs Nandihalli area sample no 24 and 25 Mg, Ca and Al rich in mineral assemblages of Hassan district (Fig.4.8) (Table.4.1).

Bulk-rock geochemical data diagrams shows Oxides are in wt. %. (a) CaO vs. SiO_2 showing a significant drop in silica content from the corundum-bearing rocks. (b) TiO2 vs. MgO showing a slight increase in MgO during the corundum formation. (c) (Fe_2O_3 + TiO_2) vs Al_2O_3 showing a strong enrichment in alumina for the corundum-bearing rocks. (d) (CaO+MgO) vs Al_2O_3 showing a strong enrichment in Mg for the corundum bearing amphibolite schist (Fig.4.9).

4.7. WHOLE ROCK GEOCHEMICAL ANALYSIS OF CORUNDUM BEARING ROCKS AROUND CHIKMAGALUR DISTRICT

Chikmagalur area around 5 corundum bearing samples collected and Geochemical data carried out through laboratory environment (Table.4.5). This area enriched alumina content average Al 60 wt% of present in Chikmagalur area samples.

Table: 4.5. Bulk-rock geochemical data of Corundum bearing samples around Chikmagalur area.

Major elements are in wt. %											
Sl no	**SiO_2**	**Al_2O_3**	**Fe_2O_3**	**CaO**	**MgO**	**K_2O**	**Cr_2O_3**	**TiO_2**	**MnO**	**P_2O_5**	**Total**
28	**13**	***81.2***	**1.4**	**1.2**	**0**	**0.19**	**0.37**	**1.5**	**0.076**	**0.85**	**99.78**
29	**14.29**	***79.35***	**1.56**	**1.7**	**0**	**0.15**	**0.55**	**1.18**	**0.03**	**0.62**	**99.43**
30	**15**	***78.95***	**1.35**	**1.4**	**0**	**0.21**	**0.76**	**1.35**	**0.021**	**0.43**	**99.47**
31	**31**	***28.75***	**10.21**	**10.22**	**9.56**	**0.13**	**8.77**	**0.31**	**0.16**	**0.32**	**99.43**
32	**35**	***30.96***	**8.98**	**7.32**	**10.78**	**0.14**	**4.95**	**0.76**	**0.17**	**0.56**	**99.62**
Minor and trace elements in ppm											
Sl no	**CuO**	**ZnO**	**Ga_2O_3**	**Rb_2O**	**SrO**	**$Y2O_3$**	**ZrO_2**	**NiO**	**Eu_2O_3**	**Yb_2O_3**	**ThO_2**
28	**29.1**	**99.9**	**172**	**0.3**	**42.7**	**20.7**	**333.3**	**27.6**	**245.7**	**7.5**	**13.9**
29	**28.2**	**96.32**	**167**	**0.1**	**41.9**	**19.1**	**329.8**	**26.2**	**243.5**	**7.2**	**13.5**
30	**29.1**	**91.23**	**170**	**13.2**	**39.21**	**20.2**	**321.4**	**27.4**	**231.8**	**7.1**	**12.7**
31	**36.9**	**242.2**	**14.1**	**24.1**	**28.8**	**2.1**	**0.01**	**13.8**	**607.7**	**0**	**0**
32	**32.32**	**232.1**	**13.2**	**24.2**	**27.29**	**1.4**	**1.32**	**21.2**	**586.3**	**0**	**0**

Geochemical compositions of the corundum bearing rocks, deal with ternary diagrams. (CaO+MgO) vs Al_2O_3 vs (Fe_2O_3 + TiO_2) its shows corundum formation of the study area.

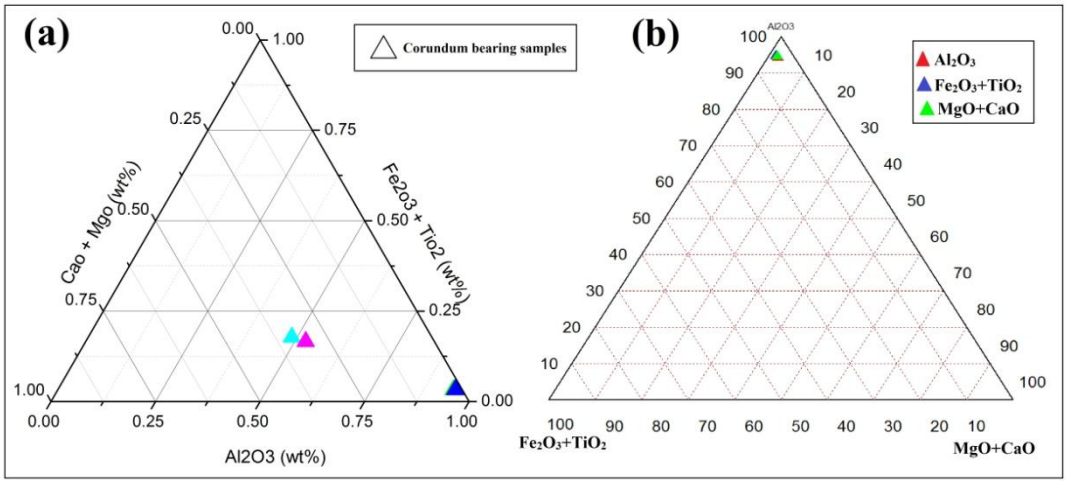

Fig.4.10. (a) and (b) Ternary diagrams showing rock involved in the corundum formation at Chikmagalur District.

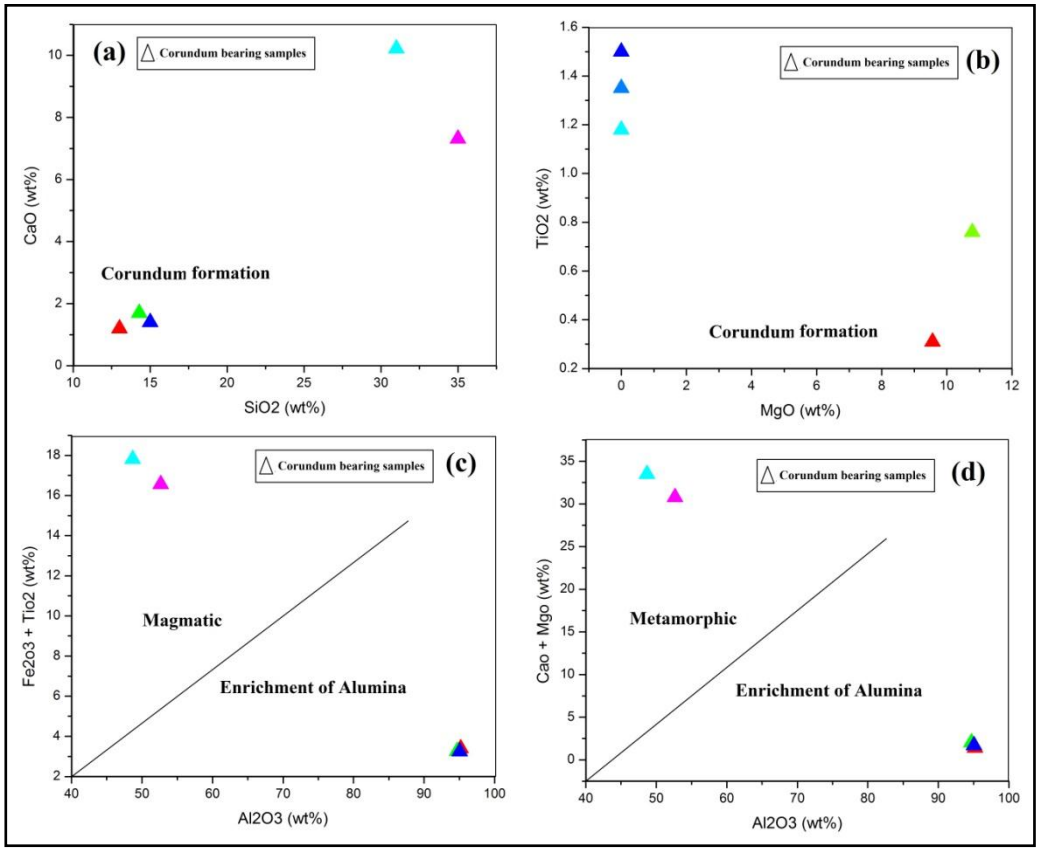

Fig.4.11. (a), (b), (c) and (d) Bulk rock geochemical analysis and binary plots of Chikmagalur district samples.

Blue and red color symbols showas alumina rich rocks and green color symbol shows Mg and Ca rich rock (Fig.4.10). Bulk-rock geochemical diagrams shows Oxides are in wt. %. (a) CaO vs. SiO_2 showing a significant drop in silica content from the corundum-bearing rocks. (b) TiO2 vs. MgO showing a slight increase in MgO during the corundum formation. (c) (Fe_2O_3 + TiO_2) vs Al_2O_3 showing a strong enrichment in alumina for the corundum-bearing rocks in Melukoppa, Kogodu and Malanadu area. (d) (CaO+MgO) vs Al_2O_3 showing a strong enrichment in Mg for the Corundum bearing amphibolites schist deposited Kunchebylu and Heggaru area of Chikmagalur district (Fig.4.11).

4.8. WHOLE ROCK GEOCHEMICAL ANALYSIS OF CORUNDUM BEARING ROCKS AROUND DAKSHINA KANNADA DISTRICT

Dakshina Kannada area around 3 corundum bearing samples collected and Geochemical data carried out through laboratory environment (Table.4.6). This area enriched alumina content average Al 60 wt% of present in Dakshina Kannada district area samples.

Table: 4.6. Bulk-rock geochemical analysis data of Corundum bearing samples around Dakshina Kannada area.

Major elements are in wt. %											
Sl no	**SiO_2**	**Al_2O_3**	**Fe_2O_3**	**CaO**	**MgO**	**K2O**	**Cr_2O_3**	**TiO_2**	**MnO**	**P_2O_5**	**Total**
33	**18.14**	***73.68***	**0.63**	**5.42**	**0**	**0.28**	**0.14**	**0.15**	**0.36**	**0.23**	**99.03**
34	**14.21**	**77.96**	**1**	**4.23**	**0**	**0.32**	**0.18**	**0.45**	**0.32**	**0.21**	**99.31**
35	**18.12**	**38.21**	**12.12**	**10.56**	**10.47**	**0.147**	**8.55**	**0.38**	**0.17**	**0.56**	**99.31**
Minor and trace elements in ppm											
Sl no	**CuO**	**ZnO**	**Ga_2O_3**	**SrO**	**Y_2O_3**	**ZrO2**	**NiO**	**Eu_2O_3**	**IrO_2**	**Yb_2O_3**	**ThO_2**
33	**28.1**	**98.1**	**169**	**41.9**	**20.4**	**328**	**27.2**	**243.1**	**0.1**	**7.4**	**13.2**
34	**28.9**	**97.2**	**171**	**42.4**	**20.6**	**319**	**27.4**	**239.2**	**0.02**	**7.2**	**13.7**
35	**1.3**	**362.2**	**29.3**	**42.5**	**12.5**	**213**	**0.17**	**123**	**3.5**	**1.4**	**1.9**

Chemical compositions of the corundum bearing rocks, deal with ternary diagrams. (CaO+MgO) vs Al_2O_3 vs (Fe_2O_3 + TiO_2), its shows corundum formation of the study area. Blue and red color symbols showas alumina rich rocks and green color symbol shows Mg and Ca rich rock (Fig.4.12). Bulk-rock geochemical diagrams shows Oxides are in wt. %. (a) CaO vs. SiO_2 showing a significant drop in silica content from the corundum-bearing rocks. (b) TiO2 vs. MgO showing a slight increase in MgO during the corundum formation. (c) (Fe_2O_3 + TiO_2) vs Al_2O_3 showing a strong enrichment in alumina for the corundum-bearing rocks in Melukoppa, Kogodu and Malanadu area. (d) (CaO+MgO) vs Al_2O_3 showing a strong enrichment in Mg for the Corundum bearing

amphibolites schist deposited Kunchebylu and Heggaru area of Chikmagalur district (Fig.4.13).

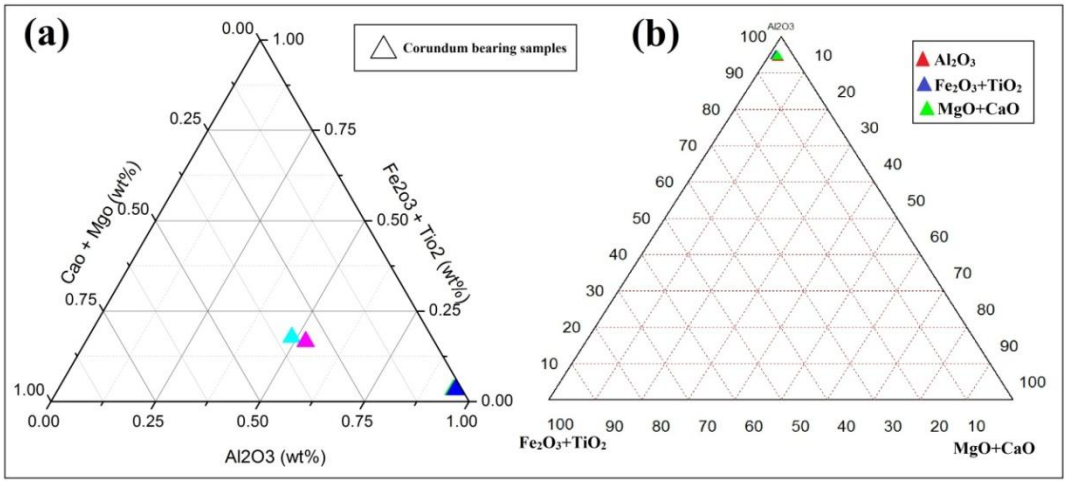

Fig.4.12. (a) and (b) Ternary diagrams showing rock involved in the corundum formation at Dakshina Kannada District.

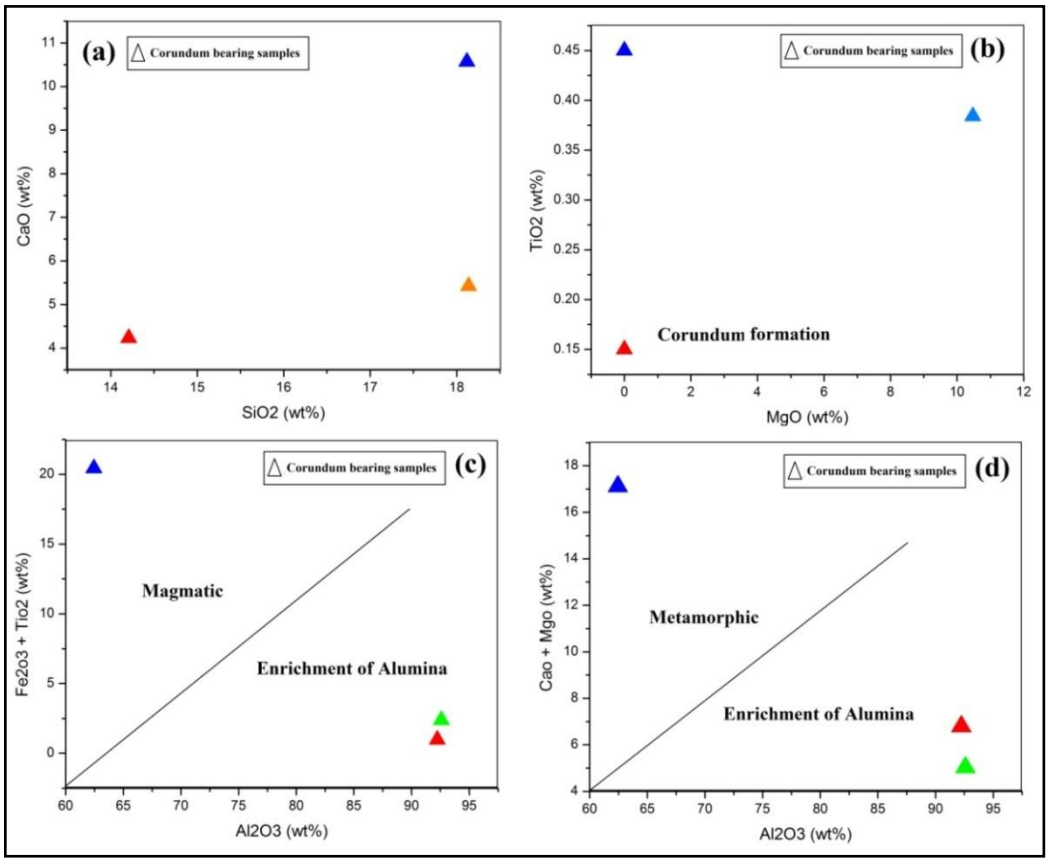

Fig.4.13. (a), (b), (c) and (d) Bulk rock geochemical analysis and binary plots of Dakshina Kannada district samples.

4.9. WHOLE ROCK GEOCHEMICAL ANALYSIS OF CORUNDUM BEARING ROCKS AROUND MYSURU DISTRICT

Table: 4.7. Bulk-rock geochemical analysis data of Corundum bearing samples around Mysuru area.

Major elements are in wt. %											
Sl no	**SiO_2**	**Al_2O_3**	**Fe_2O_3**	**CaO**	**MgO**	**K_2O**	**Cr_2O_3**	**TiO_2**	**MnO**	**P_2O_5**	**Total**
36	**4.246**	**93.25**	**0.31**	**1.12**	**0**	**0.11**	**0.34**	**0.231**	**0.13**	**0.21**	**99.947**
37	**3.94**	**92.82**	**0.53**	**0.24**	**0**	**0.13**	**1.15**	**0.606**	**0.045**	**0.04**	**99.501**
38	**24.13**	**41.21**	**11.121**	**9.526**	**10.21**	**0.137**	**1.459**	**0.484**	**0.19**	**0.552**	**99.019**
39	**3.17**	**94.82**	**0.33**	**0.16**	**0**	**0.12**	**0.83**	**0.071**	**0.03**	**0.01**	**99.541**
40	**4.81**	**93.42**	**0.612**	**0.15**	**0**	**0.113**	**0.061**	**0.191**	**0.12**	**0.02**	**99.497**
41	**4.31**	**83.55**	**2.61**	**2.1**	**0**	**0.14**	**4.31**	**1.87**	**0.21**	**0.05**	**99.15**
42	**1.66**	**95.27**	**0.41**	**0.12**	**0**	**0.23**	**1.23**	**0.074**	**0.02**	**0.03**	**99.044**
43	**25.12**	**39.21**	**10.12**	**10.43**	**10.58**	**0.137**	**2.559**	**0.284**	**0.18**	**0.572**	**99.188**
44	**8.21**	**84.92**	**1.01**	**1.93**	**0**	**0.231**	**1.54**	**1.21**	**0.04**	**0.432**	**99.523**
45	**24.82**	**29.18**	**34.67**	**1.474**	**7.96**	**0.01**	**0.126**	**0**	**0.787**	**0.701**	**99.731**
46	**13.32**	**80.91**	**1.32**	**1.24**	**0**	**0.231**	**1.03**	**1.12**	**0.32**	**0.321**	**99.812**
47	**25.32**	**40.22**	**10.42**	**10.12**	**10.48**	**0.137**	**1.559**	**0.374**	**0.18**	**0.552**	**99.358**
48	**12.89**	**81.072**	**1.934**	**1.45**	**0**	**0.237**	**0.412**	**1.138**	**0.024**	**0.725**	**99.882**
49	**15.12**	**79.92**	**1.23**	**1.21**	**0**	**0.236**	**0.321**	**1.02**	**0.021**	**0.724**	**99.802**
50	**9.1**	**85.32**	**1.92**	**1.12**	**0**	**0.132**	**0.411**	**1.136**	**0.019**	**0.583**	**99.741**
51	**7.9**	**87.12**	**1.32**	**1.01**	**0**	**0.324**	**0.392**	**1.121**	**0.022**	**0.721**	**99.93**
Minor and trace elements in ppm											
Sl no	**CuO**	**ZnO**	**Ga_2O_3**	**Rb_2O**	**SrO**	**$Y2O_3$**	**ZrO_2**	**NiO**	**V_2O_5**	**Yb_2O_3**	**Re**
36	**17.3**	**121.5**	**146**	**7.2**	**361.8**	**12**	**170.8**	**61.3**	**186.4**	**0.2**	**0.6**
37	**16.9**	**120.2**	**143**	**7.1**	**357.2**	**13**	**164.3**	**57.2**	**179.2**	**0.1**	**0.5**
38	**0**	**322.1**	**28.3**	**0**	**41.5**	**0**	**0**	**0.16**	**0**	**0**	**0**
39	**17.2**	**119.6**	**142**	**6.9**	**361.7**	**12**	**168.1**	**59.2**	**185.8**	**0.3**	**0.6**
40	**17.1**	**121.4**	**139**	**7.2**	**361.2**	**11**	**170.5**	**60.6**	**186.3**	**0.1**	**0.2**
41	**16.2**	**120.9**	**145**	**6.7**	**159.4**	**14**	**170.5**	**61.2**	**181.9**	**0.2**	**0.3**
42	**16.4**	**119.8**	**147**	**6.8**	**362.1**	**9**	**169.2**	**52.8**	**182.4**	**0.2**	**0.4**
43	**0**	**322.2**	**27.3**	**0**	**32.5**	**0**	**0**	**0.15**	**0**	**0**	**0**
44	**18.2**	**131.2**	**164**	**7.2**	**358.9**	**12**	**180.2**	**51.9**	**196.3**	**0.1**	**0.8**
45	**0**	**158.3**	**0**	**26.9**	**0**	**440.9**	**0**	**98.2**	**125.6**	**59.5**	**9**
46	**17.9**	**132.2**	**163**	**7.1**	**158.2**	**11**	**174.6**	**60.2**	**186.2**	**0.3**	**0.7**
47	**0**	**362.2**	**29.3**	**0**	**42.5**	**0**	**0**	**0.17**	**0**	**0**	**0**
48	**18.3**	**131.5**	**166**	**7.6**	**371.8**	**18**	**180.8**	**61.4**	**196.4**	**0.3**	**0.8**
49	**17.2**	**130.9**	**152**	**7.3**	**370.1**	**15**	**172.9**	**61.1**	**194.2**	**0.3**	**0.6**
50	**18.1**	**131.4**	**162**	**7.4**	**371.6**	**13**	**179.3**	**61.2**	**195.8**	**0.2**	**0.7**
51	**18.2**	**131.2**	**165**	**7.1**	**371.2**	**17**	**180.4**	**60.8**	**196.2**	**0.1**	**0.8**

Bulk-rock major and trace element data for the samples from the Mysuru region, corundum and corundum bearing amphibolites schist geochemical data carried out from laboratory environment at Trivendrum, Kerala (Table. 4.7).

Chemical compositions of the corundum bearing rocks, deal with ternary diagrams using Origin pro 8.5 (a) and (b) Tridraw softwares. (CaO+MgO) vs Al_2O_3 vs (Fe_2O_3 + TiO_2) its shows alumina rich and Mg rich minerals. Blue and red color symbols showas alumina rich rocks and green color symbol shows Mg and Ca rich metamorphic rock. Alumina enriched corundum in occurs Honnenahalli, Bylapura, Uddukaval, Padukotekaval, Adahalli, Katur, Hanumanthapura, Handanahalli, Mavinahalli, Varuna, Kuppya, Bommanayakanahalli and Eswaragowdanahalli area, sample no 36, 37, and 39 to 42 and 44 to 46 and 48 to 51 Al, Si, Fe, Cr and Ti rich and Mg, Ca and Mn poor in mineral assemblage. Alumina enriched metamorphic corundum suit Corundum bearing amphibolites occurs in Krishnarajanagara, Halasur and Someshwarapura area sample no 38, 43, 45 and 47 Mg, Ca and Al rich in mineral assemblages of Mysuru district area (Fig.4.14) (Table.4.7).

Bulk-rock geochemical data diagrams shows Oxides are in wt. %. (a) CaO vs. SiO_2 showing a significant drop in silica content from the corundum-bearing rocks. (b) TiO2 vs. MgO showing a slight increase in MgO magmatic deposition during the corundum formation. (c) (Fe_2O_3 + TiO_2) vs Al_2O_3 showing a strong enrichment in alumina for the corundum-bearing rocks. (d) (CaO+MgO) vs Al_2O_3 showing a strong enrichment in Mg for the metamorphic deposits of corundum bearing amphibolite schist (Fig.4.15).

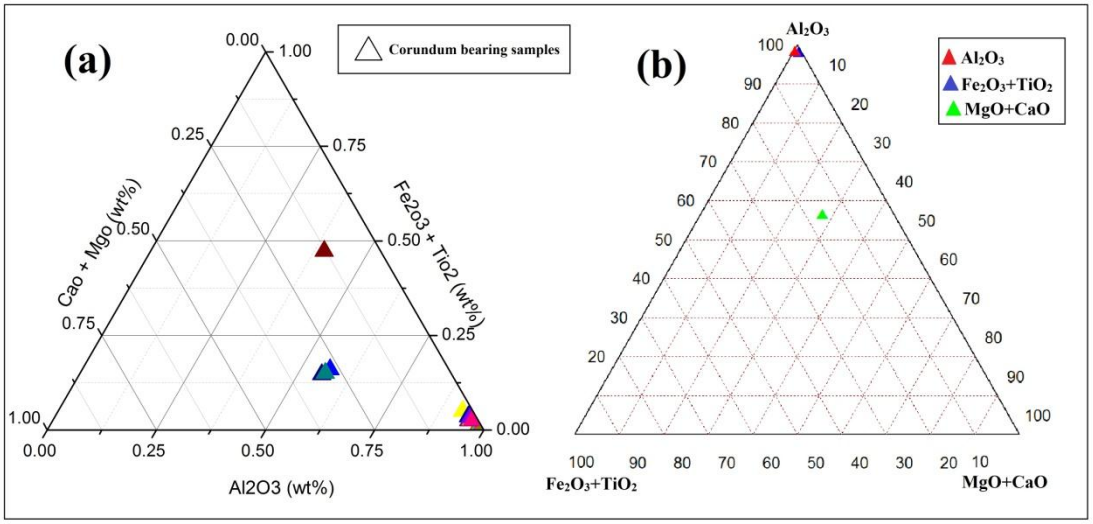

Fig.4.14. (a) and (b) Ternary diagrams showing rock involved in the corundum formation at Mysuru District.

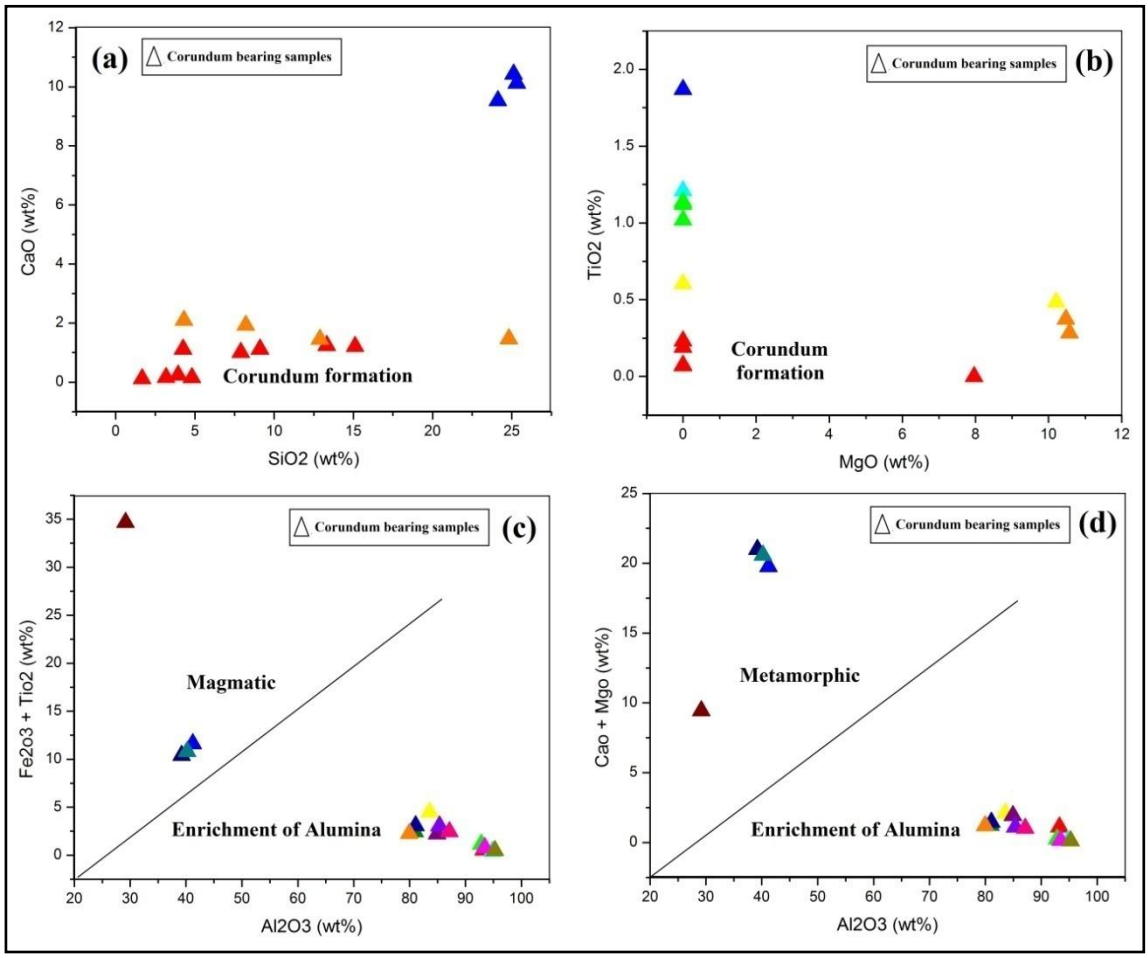

Fig.4.15. (a), (b), (c) and (d) Bulk rock geochemical analysis and binary plots of Mysuru district samples.

4.10. WHOLE ROCK GEOCHEMICAL ANALYSIS OF CORUNDUM BEARING ROCKS AROUND MANDYA DISTRICT

Mandya area around 13 corundum bearing samples collected and geochemical data carried out through laboratory environment (Table.4.6). This area enriched alumina content average Al 76 wt% of present in Mandya district area samples.

Table: 4.8. Bulk-rock geochemical analysis data of Corundum bearing samples around Mandya area.

Major elements are in wt. %											
sl no	**SiO_2**	**Al_2O_3**	**Fe_2O_3**	**CaO**	**MgO**	**K_2O**	**Cr_2O_3**	**TiO_2**	**MnO**	**P_2O_5**	**Total**
52	**10.72**	**83.21**	**2.20**	**1.003**	**0**	**0.221**	**0.253**	**1.408**	**0.07**	**0.747**	**99.84**
53	**38.21**	**34.86**	**5.91**	**8.45**	**10.14**	**0.416**	**0.003**	**0.69**	**0.032**	**0.515**	**99.22**
54	**16.24**	**78.32**	**1.93**	**1.01**	**0**	**0.222**	**0.245**	**1.094**	**0.05**	**0.739**	**99.85**
55	**13.1**	**81.23**	**1.43**	**1.002**	**0**	**0.19**	**0.249**	**1.092**	**0.06**	**0.741**	**99.09**
56	**12.86**	**80.93**	**2.11**	**1.003**	**0**	**0.22**	**0.252**	**1.023**	**0.07**	**0.742**	**99.21**
57	**11.32**	**84.21**	**1.13**	**1.012**	**0**	**0.211**	**0.239**	**1.123**	**0.04**	**0.694**	**99.97**
58	**9.1**	**86.12**	**1.01**	**1.023**	**0**	**0.218**	**0.231**	**1.432**	**0.03**	**0.632**	**99.79**
59	**15.14**	**79.28**	**2.12**	**1.019**	**0**	**0.215**	**0.252**	**1.393**	**0.07**	**0.232**	**99.72**
60	**12.21**	**82.34**	**1.02**	**1.002**	**0**	**0.212**	**0.25**	**1.342**	**0.04**	**0.742**	**99.15**
61	**35.21**	**39.86**	**5.12**	**7.43**	**10.21**	**0.413**	**0.002**	**0.68**	**0.031**	**0.495**	**99.45**
62	**10.1**	***84.1***	**1.57**	**1.09**	**0**	**0.19**	**0.23**	**1.01**	**0.032**	**0.75**	**99.09**
63	**10.2**	***83.9***	**1.23**	**1.27**	**0**	**0.21**	**0.2**	**1.7**	**0.083**	**0.71**	**99.52**
64	**8.56**	***85.6***	**1.08**	**1.4**	**0**	**0.22**	**0.27**	**1.6**	**0.084**	**0.74**	**99.58**
Minor and trace elements in ppm											
sl no	**CuO**	**ZnO**	**Ga_2O_3**	**SrO**	**Y2O3**	**ZrO_2**	**NiO**	**Nd_2O_3**	**Eu_2O_3**	**V_2O_5**	**Yb_2O_3**
52	**23.1**	**89.9**	**171**	**42.6**	**20.1**	**313.3**	**25.6**	**123.2**	**215.7**	**2.3**	**7.4**
53	**91.8**	**17**	**28.3**	**223.6**	**0**	**12**	**0.16**	**12.34**	**324.3**	**901.4**	**0**
54	**19.8**	**89.1**	**170**	**42.3**	**18.3**	**333.1**	**18.2**	**43.11**	**214.9**	**53.1**	**7.1**
55	**20.1**	**89.6**	**167**	**41.8**	**19.2**	**331.7**	**21.4**	**211.2**	**214.8**	**2.4**	**7.2**
56	**22.9**	**88.1**	**162**	**42.5**	**19.9**	**331.4**	**24.9**	**123.1**	**215.3**	**1.2**	**6.9**
57	**23.2**	**85.3**	**164**	**42.6**	**20.1**	**326.4**	**25.5**	**143.6**	**215.6**	**5.3**	**7.01**
58	**23.1**	**81.8**	**169**	**41.4**	**18.2**	**320.2**	**24.5**	**224.2**	**212.4**	**4.9**	**7.3**
59	**20.4**	**80.3**	**170**	**40.9**	**17.9**	**318.9**	**23.5**	**64.2**	**210.3**	**2.6**	**7.4**
60	**20.3**	**78.3**	**171**	**42.1**	**20.2**	**316.2**	**25.1**	**81.3**	**215.2**	**3.1**	**7.5**
61	**95.8**	**18**	**27.3**	**213.6**	**0**	**11**	**0.15**	**26.1**	**333.1**	**903.1**	**0**
62	**28.1**	**98.1**	**169**	**42.1**	**20.7**	**332.1**	**26.2**	**245.2**	**214.1**	**6.8**	**13.1**
63	**29.1**	**97.9**	**161**	**41.2**	**21.1**	**329.9**	**26.9**	**243.7**	**209.2**	**7.2**	**12.8**
64	**27.3**	**97.4**	**159**	**41.8**	**19.9**	**331.2**	**27.6**	**241.9**	**87.2**	**7.5**	**13**

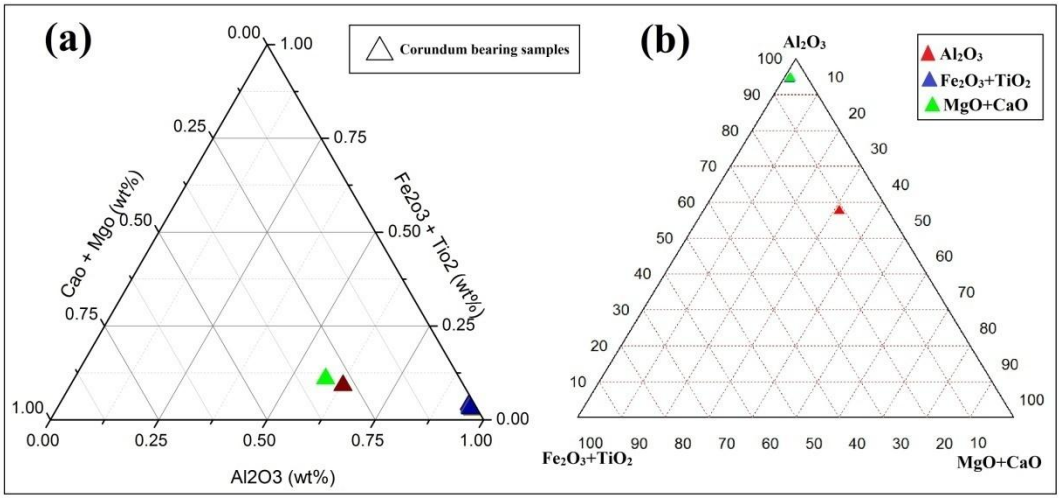

Fig.4.16. (a) and (b) Ternary diagrams showing rock involved in the corundum formation at Mandya District.

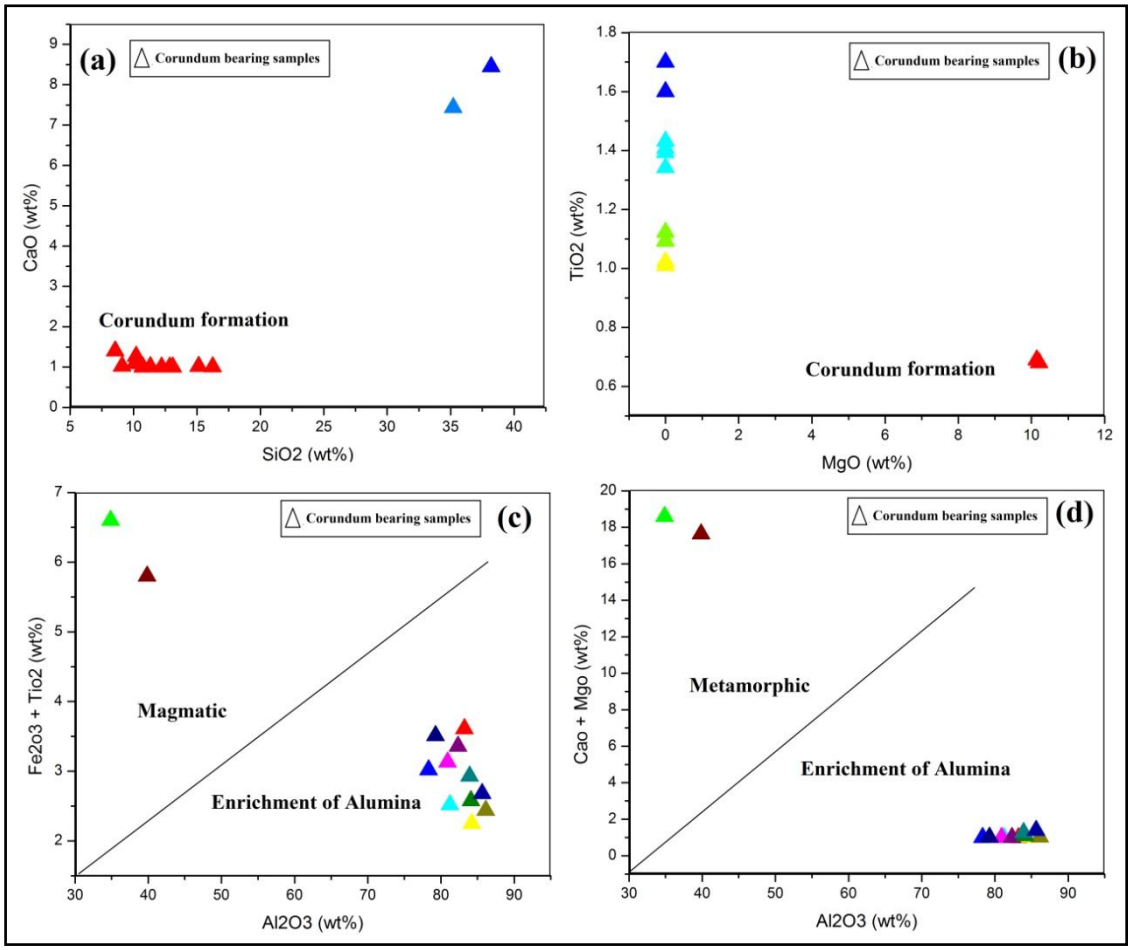

Fig.4.17. (a), (b), (c) and (d) Bulk rock geochemical analysis and binary plots of Mandya district samples.

Chemical compositions of the corundum bearing rocks, deal with ternary diagrams. (CaO+MgO) vs Al_2O_3 vs (Fe_2O_3 + TiO_2), its shows corundum formation of the study area. Blue and red color symbols showas alumina rich granulate rocks and green color symbol shows Mg and Ca rich rock (Fig.4.16).

Geochemical data diagrams shows Oxides are in wt. %. (a) CaO vs. SiO_2 showing a significant drop in silica content from the corundum-bearing rocks. (b) TiO2 vs. MgO showing a slight increase in MgO during the corundum formation. (c) (Fe_2O_3 + TiO_2) vs Al_2O_3 showing a strong enrichment in alumina for magmatic deposition of the corundum-bearing rocks in Machaholalu, Bannur, Hemmige, Ballegere, Doddaboovalli, Malavalli, Nelamakanahalli, Ahasale, Kesthur, Hanumanthapura and Maddur area. (d) (CaO+MgO) vs Al_2O_3 showing a strong enrichment in Mg for the Corundum bearing amphibolites schist deposited Adaguru and Tharanagere area of Mandya district (Fig.4.17).

4.11. WHOLE ROCK GEOCHEMICAL ANALYSIS OF CORUNDUM BEARING ROCKS AROUND RAMANAGARA DISTRICT

Bulk-rock major and trace element data for the samples from the Ramanagara region, corundum and corundum bearing amphibolites schist geochemical data carried out lab at Thiruvananthapuram, Kerala (Table. 4.9).

Whole – rock major element chemical compositions of the corundum bearing rocks, deal with ternary diagrams using softwares. (CaO+MgO) vs Al_2O_3 vs (Fe_2O_3 + TiO_2) its shows alumina rich and Mg rich minerals. Blue and red color symbols showas alumina rich rocks and green color symbol shows Mg and Ca rich metamorphic rocks. Metamorphic corundum deposits and associated metamorphic/magmatic processes are closer to a transpersonal tectonic regime. Ramanagara area is near to closepet granite of transmission zone its effect on mantle anomaly mark as asthenospheric mantle flows related to reworking and contact zone corundum form and associated with metamorphic rocks, Al and Cr enriched metamorphic corundum suit. sample no 65 to 68 corundum Al, Si, Fe, Cr and Ti rich and Mg, Ca and Mn poor in mineral assemblage. sample no 69 and 70 corundum bearing amphibolites schist Mg, Ca and Al rich in mineral assemblages (Fig.4.18) (Table.4.9).

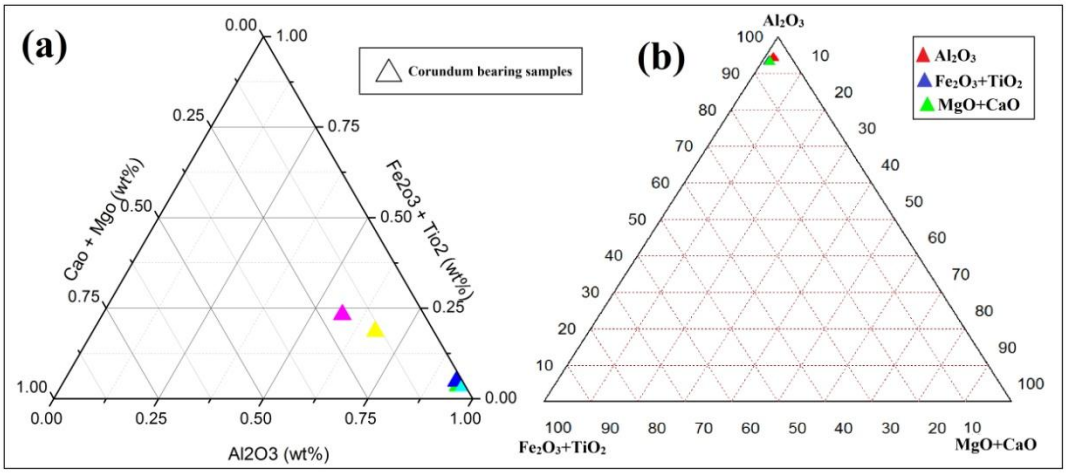

Fig.4.18. (a) and (b) Ternary diagrams showing rock involved in the corundum formation at Ramanagara District.

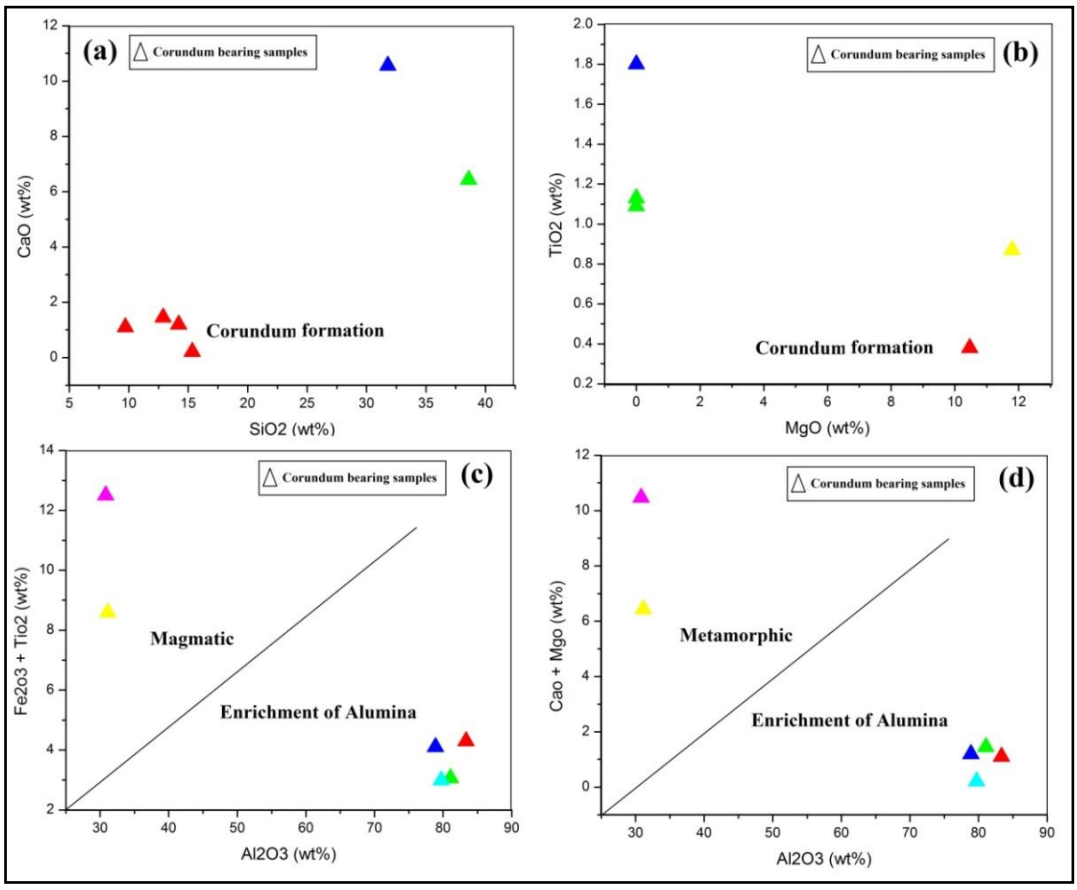

Fig.4.19. (a), (b), (c) and (d) Bulk rock geochemical analysis and binary plots of Ramanagara district samples.

Bulk-rock geochemical data diagrams shows Oxides are in wt. %. (a) CaO vs. SiO_2 showing a significant drop in silica content from the corundum-bearing rocks. (b) TiO2 vs. MgO showing a slight increase in MgO metamorphic deposition during the corundum formation. (c) (Fe_2O_3 + TiO_2) vs Al_2O_3 showing a strong enrichment in alumina for the corundum-bearing rocks in Huthridurga, Varthehalli, Akkur and Hosahalli area. (d) (CaO+MgO) vs Al_2O_3 showing a strong enrichment in Mg for the metamorphic deposits of corundum bearing amphibolite schist in Lakkashettypura and Byranaikanahalli area. (Fig.4.19).

Table: 4.9. Bulk-rock geochemical data of Corundum bearing samples around Ramanagara area.

Major elements are in wt. %											
sl no	**SiO_2**	**Al_2O_3**	**Fe_2O_3**	**CaO**	**MgO**	**K_2O**	**Cr_2O_3**	**TiO_2**	**MnO**	**P_2O_5**	**Total**
65	**9.72**	***83.35***	**2.5**	**1.1**	**0**	**0.23**	**0.27**	**1.8**	**0.085**	**0.75**	**99.80**
66	**12.89**	***81.07***	**1.93**	**1.45**	**0**	**0.23**	**0.41**	**1.13**	**0.02**	**0.72**	**99.85**
67	**14.2**	**78.9**	**2.3**	**1.2**	**0**	**0.24**	**0.24**	**1.8**	**0.072**	**0.65**	**99.60**
68	**15.34**	**79.72**	**1.9**	**0.21**	**0**	**0.21**	**0.26**	**1.09**	**0.082**	**0.68**	**99.49**
69	**31.8**	***30.8***	**12.12**	**10.56**	**10.47**	**0.14**	**2.55**	**0.38**	**0.17**	**0.56**	**99.55**
70	**38.59**	***31.11***	**7.72**	**6.43**	**11.8**	**0.12**	**2.34**	**0.87**	**0.05**	**0.7**	**99.73**
Minor and trace elements in ppm											
sl no	**CuO**	**ZnO**	**Ga_2O_3**	**Rb_2O**	**SrO**	**Y_2O_3**	**ZrO_2**	**NiO**	**Eu_2O_3**	**Yb_2O_3**	**ThO_2**
65	**29.2**	**99.2**	**162**	**0.4**	**41.9**	**20.6**	**341.3**	**27.5**	**237.4**	**7.4**	**13.1**
66	**28.1**	**99.6**	**192**	**1.3**	**42.6**	**19.4**	**331.1**	**27.7**	**244.9**	**7.5**	**13.8**
67	**27.2**	**99.7**	**168**	**4.2**	**42.8**	**20.1**	**329.2**	**27.6**	**245.6**	**7.1**	**12.2**
68	**27.9**	**98.3**	**179**	**1.3**	**41.1**	**21.01**	**321.9**	**27.4**	**243.1**	**6.9**	**12.9**
69	**95.8**	**18**	**27.5**	**15.9**	**243.4**	**12.4**	**11**	**0.16**	**332.1**	**1.2**	**0**
70	**94.4**	**17**	**28.9**	**14.2**	**242.5**	**5.9**	**12**	**0.18**	**329.9**	**0.9**	**0**

4.12. WHOLE ROCK GEOCHEMICAL ANALYSIS OF CORUNDUM BEARING ROCKS AROUND CHAMARAJANAGARA DISTRICT

Chamarajanagara area one corundum bearing samples collected and Geochemical data carried out through laboratory environment (Table.4.10). Chemical compositions of the corundum bearing rocks, deal with ternary diagrams using geochemistry softwares. (CaO+MgO) vs Al_2O_3 vs (Fe_2O_3 + TiO_2) its shows alumina rich Fe and Mg rich minerals. Blue and red color symbols showas alumina rich pelitic rock. Corundum bearing politic rock occurs Budipadaga area, sample no 70 Alumina enriched metamorphic corundum

suit Fe, Mg, Ca and Al rich in mineral assemblages of Chamarajanagara district area (Fig.4.20) (Table.4.10).

Table:4.10. Bulk-rock geochemical analysis data of Corundum bearing samples around Chamarajanagara area.

Major elements are in wt. %											
sl no	SiO_2	Al_2O_3	Fe_2O_3	CaO	MgO	K_2O	Cr_2O_3	TiO_2	MnO	P_2O_5	Total
71	39.1	32.89	11.95	2.624	7.333	3.643	0.076	0.82	0.181	0.881	99.501
Minor and trace elements in ppm											
sl no	CuO	ZnO	Ga_2O_3	Rb_2O	SrO	Y_2O_3	ZrO_2	NiO	Eu_2O_3	IrO_2	V_2O_5
71	87.3	95.6	29.1	124.6	234.7	32.6	132.6	380.4	779.5	2.3	531.8

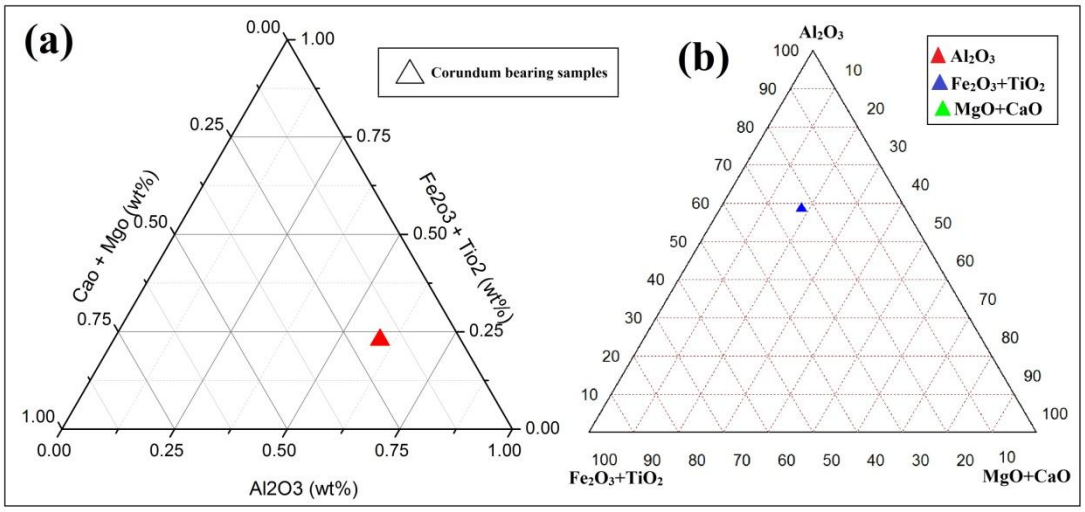

Fig.4.20. (a) and (b) Ternary diagrams showing rock involved in the corundum formation at Chamarajanagara District.

4.13. WHOLE ROCK GEOCHEMICAL ANALYSIS OF CORUNDUM BEARING ROCKS AROUND KOLARA DISTRICT

Bulk-rock major and trace element data for the samples from the Kolara region, corundum and corundum bearing litho units geochemical data carried out lab at Thiruvananthapuram, Kerala (Table. 4.11).

Table:4.11. Bulk-rock geochemical data of Corundum bearing samples from Kolara area.

Major elements are in wt. %											
sl no	**SiO_2**	**Al_2O_3**	**Fe_2O_3**	**CaO**	**MgO**	**K_2O**	**Cr_2O_3**	**TiO_2**	**MnO**	**P_2O_5**	**Total**
72	**17.14**	**78.28**	**1.12**	**1.01**	**0**	**0.214**	**0.232**	**1.381**	**0.05**	**0.22**	**99.656**
73	**19.72**	**73.35**	**1.873**	**1.11**	**0**	**0.236**	**0.37**	**1.9**	**0.07**	**0.641**	**99.272**
Minor and trace elements in ppm											
sl no	**CuO**	**ZnO**	**Ga_2O_3**	**SrO**	**$Y2O_3$**	**ZrO_2**	**NiO**	**Eu_2O_3**	**Yb_2O_3**	**IrO_2**	**V_2O_5**
72	**19.4**	**79.3**	**171**	**40.1**	**17.2**	**323.9**	**22.5**	**209.3**	**7.2**	**3.4**	**905.2**
73	**20.1**	**72.3**	**169**	**41.1**	**19.3**	**331.2**	**24.1**	**213.2**	**7.6**	**3.1**	**904.1**

Whole – rock major element chemical compositions of the corundum bearing rocks, deal with ternary diagrams using softwares. (CaO+MgO) vs Al_2O_3 vs (Fe_2O_3 + TiO_2) its shows alumina rich and Mg rich minerals. Blue and red color symbols showas alumina rich rocks and green color symbol shows Mg and Ca rich metamorphic rocks (Fig.4.21)

Bulk-rock geochemical data diagrams shows Oxides are in wt. %. (a) CaO vs. SiO_2 showing a significant drop in silica content from the corundum-bearing rocks. (b) TiO2 vs. MgO showing a slight increase in MgO metamorphic deposition during the corundum formation. (c) (Fe_2O_3 + TiO_2) vs Al_2O_3 showing a strong enrichment in alumina for the corundum-bearing rocks in Yelasandra area. (d) (CaO+MgO) vs Al_2O_3 showing a strong enrichment in Mg for the metamorphic deposits of corundum bearing amphibolite schist in Kammasandra area. (Fig.4.22).

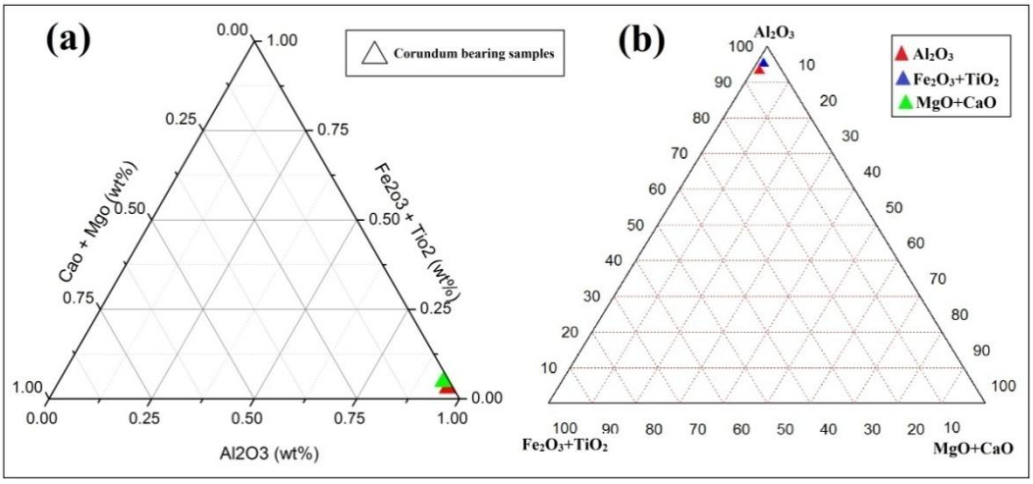

Fig.4.21. (a) and (b) Ternary diagrams showing rock involved in the corundum formation at Kolar District.

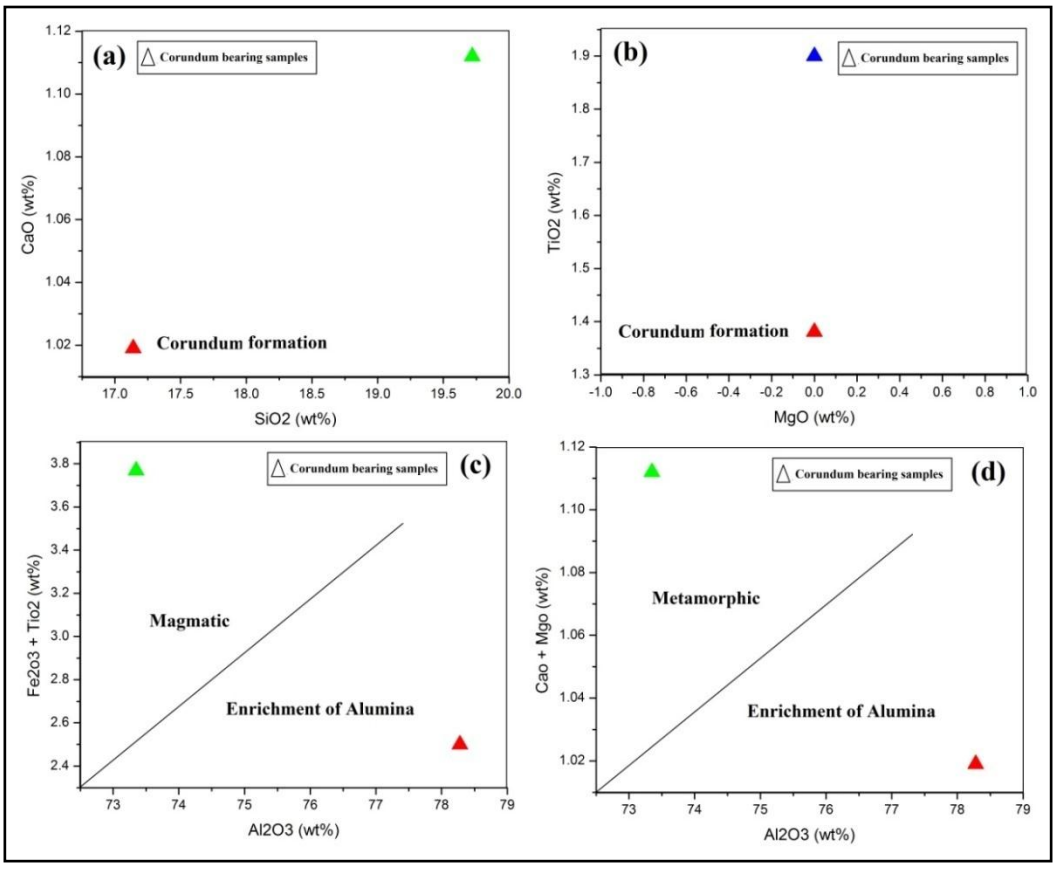

Fig.4.22. (a), (b), (c) and (d) Bulk rock geochemical analysis and binary plots of Kolara district samples.

CHAPTER-V

5.1. HYPERSPECTRAL REMOTESENSING

Hyperspectral remote sensing is one of the advance technology which began in early 1980s is one of the most significant break throughs in Remote Sensing. It emerged as a promising technology in remote sensing for studying earth surface materials by two ways spectrally & spatially (Varshney and Arora., 2004). In this technology imaging and spectroscopy is combined in a single system so this is also known as imaging spectroscopy (Curran Paul., 2001). This technology is developed by breaking a broad band from the visible and infra-red into hundreds of spectral parts to obtain geochemical information from inaccessible planetary surfaces (Goetz et al., 1985). Hyperspectral remote sensing is able to provide a high level of performance in spectral & radiometric calibration accuracy in the data sets. These high performing sensors data can be utilized for extracting information in various quantitative and qualitative applications (Clark et al., 1998). The ample spectral information provided by hyperspectral data is able to identify and distinguish spectrally similar materials which enhance the capability of distinguishing various ground objects in detail (Rechards et al., 1999). Hyperspectral sensorscollect information as a series of narrow and contiguous wavelength bands at 10 to 20 nm intervals (Shippert., 2008). The spectra for a single pixel in hyperspectral data appears similar like a laboratory quality spectra collected by a spectro-radiometer which can be used for understanding the spectral characteristics of the material (Clark., 1998).

5.1.1. PRINCIPLE OF IMAGING SPECTROSCOPY

As Hyperspectral Remote Sensing technology is also known as Imaging Spectroscopy which is considered to be as combination of three following photonic technologies:

1. Conventional Imaging,

2. Spectroscopy, &

3. Radiometry

Above three technologies are used to produce images for which a spectral signature is associated with each pixel (Shih., 2004). The position of imaging spectroscopy and other related technologies is shown in Figure 5.1. The datasets produced by hyperspectral imager is in the form of a three dimensional data cube in which two dimensions represents spatial information and third dimension represents spectral information (Goetz., 1992). The values recorded by Spectral Imager Instrument (SII) can be converted, via proper calibration, to radiometric quantities that are related to the scene phenomenology.

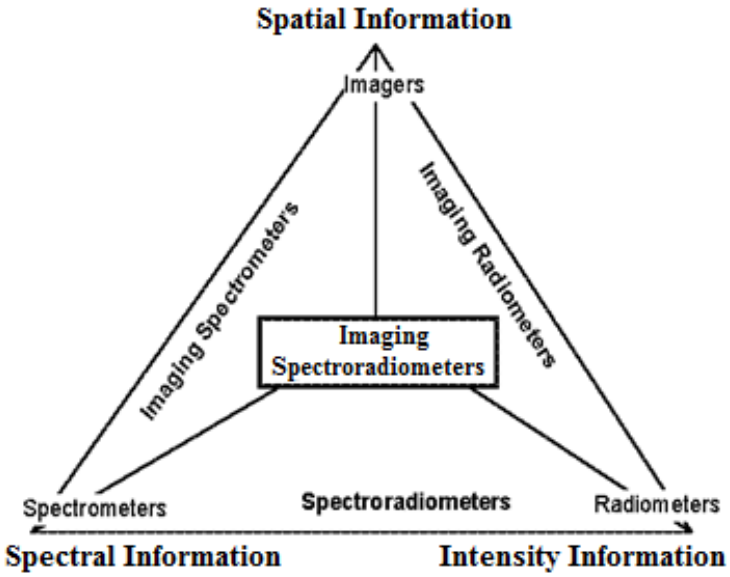

Fig.5.1. Relationship among Radiometric, Spectrometric, and Imaging Techniques (Elachi 1987)

Spectroscopy depends on the pretext that different materials are different because of the difference in their morphology, constituents & structure and because of thae target interact differently with light so they appear different (Goetz., 1992). The aim of Imaging Spectroscopy is to understand the Earth's surface through the detailed analysis of its reflected light, exploiting subtle variations in surface composition and structure in support of real-world requirements. For spectroscopic study, hyperspectral data sets provide ample spectral detail to discern the subtle differences in color distributions from Earth surface materials ((Shippert., 2008). Because Earth's surface is populated with the molecules of the solids and liquids and having characteristic spectral features generally

wider than some tens of nanometers, which establishes a practical definition for the maximum spectral band size for a hyperspectral data set (Dyer Johen., 1994).

The reflectance spectra of most of the Earth's surface materials contain characteristic or diagnostic absorption features in the spectral range of 350 to 2500 nm. Since these diagnostic features are typically of a very narrow spectral appearance, those surface materials can be identified directly, if the spectrum is sampled at sufficiently high spectral resolution which becomes possible using imaging spectrometers. There are three types of main absorption features found generally in the spectral range of 350 to 2500 nm regions which should be understood to realize the requirement of hyperspectral imaging system (Tong et al., 2001).

Charge transfer absorptions: These types of absorptions are caused by light at certain wavelengths causing electrons to be transferred between atoms and generally occur in the visible region of the spectrum, and. For example: Fe3+ and Fe2+. Light at the proper wavelength causes an electron to be transferred from a Fe2+ atom to a Fe3+ atom and due to that rusty objects appear red. Detection of this type of absorption is easy as they are quite broad, so it is possible to detect thoseusing conventional multispectral sensors. As there is overlap among the absorptions caused by different atoms, so Hyperspectral sensors are required to tell them apart (Elachi., 1987) (Varshney and Arora., 2004).

Electron transition absorptions: In atoms with an incomplete electron shell, light at the proper wavelength can bump electrons into different positions in the shell. These absorptions tend to be narrower than the charge transfer absorptions and the type of atom and the position and variety of its neighbors controls the wavelengths of the absorptions. This feature is especially useful in geology, where the arrangement of atoms in a mineral is very well defined. Since subtle variations in the position of the band centre are important, it is necessary to have many narrowly spaced bands to take advantage of this feature (Schowengerdt Robert., 1997).

Vibrational absorptions: When light at the same wavelength as a molecule (or part of a molecule) strikes the molecule, it causes the molecule (or part of the molecule) to vibrate. This leads to light absorption. In general these absorptions are very narrow, although their widths and depths vary. Many of the absorptions seen in the 0.35 to 2.5µm region

actually originate at longer wavelengths, and what we are seeing are combinations and overtones of the original wavelength. Most of these absorptions can be detected with a multispectral sensor (Lillesand and Kiefer., 2002).

5.1.2. MULTISPECTRAL VS. HYPERSPECTRAL

Multispectral datasets are produced by sensors which record reflected electromagnetic energy within some specific sections or broad bands of the electromagnetic spectrum (Barry et al., 2001). These Sensors usually produce 3 to 10 number of spectral bands which ranges from visible to near infrared region. However, the spectral resolution and mineral discrimination power is very low. Example of Multispectral Satellite Sensors (MSS) are Landsat, Spot and IRS satellites ((Pignatti et al., 2009).

Hyperspectral sensors measure energy in narrower and more numerous bands than multispectral sensors. Hyperspectral data contains 100s or more narrow contiguous spectral bands. The numerous narrow bands of hyperspectral sensors provide a continuous spectral measurement across the entire electromagnetic spectrum and therefore, are more sensitive to subtle variations in reflected energy. Images produced from hyperspectral sensors contain much more data than images from multispectral sensors and have a greater potential to detect differences among land and water features (Liew et al., 2002). Hyperspectral sensors are having capability to detect and distinguish individual absorption bands in mineral deposits, vegetation and man-made materials. This discrimination is achieved by spectral sampling at approximately 10 nm intervals across the spectrum. Multispectral images can be used to map forested areas, while hyperspectral images can be used to map tree species within the forest.

Monitoring land cover using satellite sensors such as Landsat and SPOT has been predominant in ecological applications since the 1970s (Pignatti et al., 2009). Considerable advances in Remote Sensing Technology (RST) are driven by environmental issues rapidly arising at regional scales. There is lack of literature on the subject of spaceborne hyperspectral imagery comparison and the assessment of land cover information, specifically in urban areas. By comparing hyperspectral and multispectral imagery, accurate vegetation mapping is possible, especially at dense urban

scales (Liew et al., 2002). The spectral resolution is the main factor that distinguishes hyperspectral imagery from multispectral imagery (Barry et al., 2001). Hyperspectral sensors contain bands with narrow wavelengths while multispectral sensors contain bands with broad wavelengths. The advantage of using hyperspectral data over multispectral data is the ability to define surface features with a higher spectral resolution. A complete list of spaceborne hyperspectral satellites currently in orbit and set to launch is found in Buckingham and Staenz (2008).

Table.5.1. Airborne Hyperspectral Sensors (AHS)

Sensor	Spectral coverage(nm)	No.of Bands	Band width (nm)	Spatial Resolution(m)	Image tech	Country	Launched /developer
GERIS(Geophysical Environment Research Imaging Spectrometer II)	400 - 1000 1400 - 1800 2000 - 2500	24 7 32	25.4 120.0 16.5	1-10	Whisk broom	USA	1987/GRE corp.
AVIRIS(Airborne visible infrared imaging spectrometer)	380-2500	220	10	5-20	Whisk broom	USA	1987/JPL
CASI(Compact Airborne Imaging Spectrometer)	400-800	288	1.8	30	Pushbroom	Canada	1988/ITRES research Ltd
DAIS (Digital Airborne Imaging Spectrometer)	400-1200 1500-1800 2000-2500	72	15-30 45 20	1-10	Pushbroom	Europe	1995/GRE corp.
HYDICE(Hyperspectral Data Image Collection Experiment)	400 - 2500	10.2	210	3	Whisk broom	USA	1996/Naval research lab
HyMAP	400 - 2500	16	125	3-5	Whisk broom	Australia	HyVista Corp
AisaEAGLE	400 - 970	5	200	<1			Spectir Corp

Table.5.2. Spaceborne Hyperspectral Sensors (SHS)

Sensor	Spectral coverage (nm)	No.of Bands	Band width (nm)	Spatial Resolution (m)	Swath (km)	launch Year	Agency
Moderate Resolution Imaging Spectrometer (MODIS)- AQUA	400 - 800	32		250-1000	1500	May 2002	NASA
MODIS- TERA	800 - 1455	36		250-1000	2300	Dec 1999	
MERIS (Medium Resolution Imaging Spectrometer)	410to1050	15	10	Ocean: 1040x 1200, Land & coast: 260 x 300	1150		ESA
Hyperion on EO-1	400-2500	220	10	3	7.5	Nov 2000	NASA
CHRIS (Compact High Resolution Imaging Spectrometer on PROBA-1)	438 -1035	18-64	1.25-11	18-36	14-18	Oct 2001	ESA
HySI(Hyperspectral Imager) on IMS-1	400 - 950	64	<15	550	128	Apr 2008	ISRO
Extraterrestrial hyperspectral sensors							
Chandrayaan-1 HySI	400 - 920	64	15	80	20	2008	ISRO
Chandrayaan-1 M3 (Moon Mineralogy Mapper)	400 - 3000	86	10-40	70-140	40	2008	ISRO
OMEGA(Observatoire pour la Mineralogie, l'Eau, le Glace e l'Activite)	360 to5100		7-20	300-4000	8.8		NASA
CRISM (Compact Reconnaissance Imaging Spectrometer for Mars)	362-3920	545	6.55	15.7 to 19.7	9.4 - 11.9		NASA

Hyperspectral Remote Sensing Sensors: Now-a-days there are many ground-based and airborne hyperspectral sensors but very few spaceborne hyperspectral sensors are

available. Various airborne and spaceborne hyperspectral sensors developed by several space agencies national & international are in Table 5.1 & Table 5. 2

5.1.3. HYPERSPECTRAL DATA PROCESSING

For effective utilization of Hyperspectral sensors data sets, different kind of processing and analyzing techniques are required for various applications. All the Hyperspectral sensors developed have enabled generation of remotely sensed laboratory spectra of various materials such as rocks, soils, plants, snow, ice, water and man-made materials (Varshney and Arora., 2004). These laboratory quality spectra have been used to obtain compositional information of the earth surface as they are able to detect absorption features caused by minerals in visible, Shallow Wave Infrared Range (SWIR) and Thermal Infrared Range (TIR) region of electromagnetic spectrum. AVIRIS sensor by NASA JPL has been used especially for the mapping of cations and anion for identification of various minerals and rocks (Curran Paul., 2001). The large amount of spectral information in hyperspectral data is useful for species level discrimination by identifying components unique to certain species of plants. This hyperspectral technology also provides a means for optical oceanographers to classify and quantify complex oceanic environments (Clark et al., 1998).

5.2. SPECTROSCOPY

Spectroscopy is the study of light interaction as a function of wavelength, interactions contain light emitting, reflection or scattering from any of the material or a target. These principles are applied to get spectroscopy of the mineral and rocks with the help of spectroradiometry is used to measure the radiometric quantities like radiance and irradiance in a continuous bands of spectral ranges 0.35 to 2.5μ in the EMS. Imaging spectroscopy may also called as imaging spectrometry, or hyperspectral by Remote Sensing community, Imaging includes study of rock in the laboratory, a field study site from an aircraft or a planet observation through spacecraft/ Earth based Telescope. Hence, the name Hyperspectral Remote Sensing has taken for this chapter heading, hyperspectral sensitiveness of different rocks and minerals from the Precambrian terrains of southern part of Southern Karnataka has dealt and details are given with reference to

many earlier researchers (Goetz et al., 1985); (Green *et a*l., 1988); (Roger Clark 1999) (Clark et al., 1993) (Vane et al., 1993); (Kruse 1997) (Mustard and Sunshine., 1999) and (Basavarajappa et al., 2019). The Imaging spectroscopy in this context is of purely the spectroscopic studies of rock in the laboratory environment. Spectro-radiometer instrument (Spectral Evolution SR-3500) is extensively used to measure the radiometric quantities (reflection and absorption of radiance spectra) by extracting different diagnostic spectral signature of the rock and minerals, the spectral signature studies and interpretation techniques are utilized to differentiate the minerals and mineral assemblage in the mixture Hunt and Salisbury (1970), Hunt et al., (1971), (Graham Hunt 1977), Hunt and Ashley (1979) and (Kruse et al., 2003).

5.2.1. SPECTRAL REFLECTANCE

All the surficial features, naturally formed and manmade structures occurred on the earth's surface or near surface reflects and emits the Electro Magnetic radiation with respect to characteristics of their chemical composition and physical state, within the range of Electro Magnetic 0.35 to 2.55 μm for the spectral signature (reflectance) studies. Spectral reflectance of a material is described by the interaction of light in continuous EM radiation due its physical phenomena and its inheritance optical property. The measureable reflected light at a particular region of wavelength is a functional nature of the elemental composition of the material and the wavelength covers from visible to near infrared region (Hoover et al., 1993). The two process involved in this measurements are electronic process and vibration process, like crystal field effect, charge transfer and conduction band transitions can detected by electronic process with an example of Fe, Mn, Cr absorption characteristics feature and with molecular vibrational process the parameters of hydroxyl and carbonate is well studied by Rowan et al., 2004; Ali et al., 2008 and Hunt 1977. Gaffey in 1986 said and enlightened the spectral reflectance studies in the visible-near infrared portion of EMS as a rapid, non-destructive and inexpensive technique in the field of mineralogical studies.

Spectral signatures are the representation of the spectral response of certain features in a graphical manner as a function of wavelength and reflectance. According to the elemental and mineralogical composition of a material the spectral curve gives the

different variation in the absorption and reflectance position and it serves to identify the minerals and rock types and other useful information (Hunt, 1977). The present day advanced remote sensing sensors like ASTER and Hyperion and Airborne Sensors taking out the extensive application in the mapping of oxides, sulfides and hydrothermally altered rock (Ferrier and Wadge, 1996). Many of this alterations host the presence of OH and other hydroxyl bonds like Al-OH and Mg-OH will produce the distinctive absorption feature near the SWIR (2-2.4μm) region of the spectrum (Borengasser et al., 2008). The oxides mineral abundance shows the OH and other hydroxyl bond absorption (AL-OH) in the SWIR region and Corundum shows in the region of visible and SWIR (0.65, 2.10, 2.20 and 2.30 μm) as a combination of internal vibration of the corundum mineral (Hunt et al., 1971) (Hunt, 1977; Ferrier and Wadge, 1996) (Ali et al., 2008) (Manjunatha., 2017) and (Jeevan., 2018).

Spectroscopy is the techniques firstly used by the astronomers for the planetary studies further with advancement in the space research and increased awareness brings the usage of spectroscopy, the first spectrometer utilized for imaging spectroscopy is done by Goetz et al., 1982 and Vane et al., 1993. For an Earth Observation Studies Airborne Imaging Spectrometer and Spaceborne Spectrometer activities have taken the huge part and wide basis availabilities in the field of remote sensing and this can be seen from last three decade early from 1990s (Goetz 1983; Kruse et al., 1990 and Green et al.,1998). Reflectance, absorption and emittance of spectral curves are the three properties of all surficial mineral gives the distribution of the key minerals and some indication of the hidden treasures and emittance display the compositional variation in the silicates of the main lithology (Rowan et al., 2005; Moghtaderi, et al., 2007). Reflectance spectroscopy has proven to be most powerful and versatile Remote Sensing technique for determining surface mineralogy, chemical compositions and lithologies of planetary objects, as well as constituents of their atmosphere (Hunt 1980). Spectral reflectance studies is the recent advanced technique used in mapping corundum original zones, lithotypes, mineralization and vegetation. Spectroscopy gives a rich of information about mineralogical content because of its great potentiality in a diagnostic tool which is very sensitive to subtle changes in crystal structure or chemistry of the rock (Clark, 1999).

On the time of data acquisition the remotely sensed data and so called reflectance values will get affected from the many factors includes the physical state of the surface and it also depends on the orientation of the sensors towards the sun position (Ferrier et al., 2002). In the spectral studies of minerals and rocks, the common variation is represented by new or increases spectral structures due to hydroxyl group, ferric and ferrous ion, carbonates and water. Vegetation, organic matters and manmade structures will affect the accuracy and effectiveness of the spectral signature while studying the rocks and their mineral composites. Discrimination of different rock types is simple if these noise factors will not overcome the signal. The signal to noise ratio will permit the further studies in the spectral analysis. Scattering, atmospheric absorption and noise also contribute to the errors in spectral signature. Longshaw in 1974 studied the difference between lab based spectral reflectance and field based reflectance studies for the same rocks and he noticed the main features in both spectral curves and minor difference, and later he said that these are not identical to each other in full region but exerts the main parameters. The researchers like Hunt and Salisbury (1970); Hunt et al. (1971); Hunt et al. (1973); Farmer (1974); Hunt and Ashley (1979); Hunt (1980); Clark (1999); Rowan et al (2004); Rowan et al.(2005); Ali M Qaid and Basavarajappa., (2008); Ali et al., (2009); Rajendran et al., (2011); Magendran and Sanjeevi., (2011); (Ali et al., 2008) (Manjunatha., 2017) and (Jeevan., 2018) (Basavarajappa et al., 2018) amd (Maruthi and Basavarajappa., 2018). basically started and given foremost contribution in the fundamental investigations about the spectral feature of minerals and rocks from the last three decades.

5.2.2. SPECTRAL REFLECTANCE OF ROCKS

The internal molecular structure, cation and anions of the rock mixture are variation factors will always give different spectral characteristics while studying the spectral signatures of the rock. With the advent technology the spectrometry (spectral measurements) made in both laboratory and field environment for different minerals indicated the spectral variations in the both VNIR and SWIR. Visible and Near Infrared regions, where 0.35 to 1.0 µm shows more variation due to the transition metals, such as Fe, Mn, Cu, Ni, Cr etc., and in short wavelength infrared region it is quite dominated by the hydroxyl ions, carbonates and water molecules. Oxides and Hydroxides mineral

zones are associated with corundum, Margaret, clays and hydrated silicates which shows the main combination of hydroxyl ions with magnesium (Mg-OH) and aluminum (AL-OH) diagnostically shows a vibrational absorption bands 2.3 and 2.2 µm respectively. The kaolinite a clay mineral is going to have the combination of Mg-OH and AL-OH which shows doublet variation with absorption dip at 2.3 µm and weaker one at 2.2 µm (Shanks III W.C. Pat., 2010). Montmorillonite and muscovite contains the Mg-OH ion combination gives the absorption band at 2.3 µm. The clay mineral occurrences in a composite gives the peak of reflectance near 1.6 µm and beyond this it decreases due to absorption bands, absorption bands due to water molecule presence gives at 1.4 µm and 1.9 µm. Calcite, dolomite, magnesite, siderite shows absorption variation in spectral analyst at 1.9 µm, 2.35 µm, and 2.55 of SWIR region (Gupta 2003, Ravi and Gupta 2018).

The abundantly occurred silicates, oxides, nitrate and phosphates on the earth surface do not have much diagnostic spectral features in the reflected regions (0.4 to 2.5 µm) of the EMS. For these mineral studies the thermal infrared region is more utilized to characterize the spectral variation in EMS (Hunt, 1977, 1979, 1980; Salisbury and Wald, 1992; Gupta, 2003). The diagnostic spectral characteristics in terms of wavelength and by absorption peak occurrences, the various cations and anions of different mineral and metals absorption peaks occurrences in the EMS are summarized in the table 5.4 listed by Gupta, 2003. However many minerals have their characteristic absorption features that permit to direct identification of the specific mineral. The pioneering work of Graham Hunt of the U.S. Geological survey documented the reflectance spectra of a wide range minerals and ultimately led to the development if hyperspectral sensors(Goetz et al., 1985). Spectral libraries are now available for a large variety of minerals and rocks through the USGS (Clark et al., 2002 and NASA1999) spectral libraries. The spectra of rocks depend on the spectra of the constituent minerals and their textural properties such as grain size, packing, and mixing (Gupta, 2003). In semi-arid and arid areas the spectral reflectance curves of rocks and minerals may be used directly to infer lithology and corundum bearing litho units of the study area (Hunt et al., 1971) (Mather, 2004).

The range between 1.1 and 2.5µm called as Shortwave Infrared (SWIR) region of the spectrum can provide more information about the mineralogical composition more than the spectral features observed in the Visible and Near Infrared (VNIR) regions. Opaque minerals have very distinct effect on the spectra of rocks, because it decreases the total reflectance from the rocks and also quenches the reflectance spectra of the rocks. Basic, mafic and intermediate igneous rocks show low reflectance compared with the acidic igneous rocks (Al-Daghastani, 2003).

Igneous graphic granite displays the H_2O and O-H bonds spectral absorption at 1.4µm, 1.9µm and 2.2µm, but biotite granites and granites have less water, and therefore the OH absorption bands are weaker. Mafic rocks contain iron, pyroxenes, amphiboles and magnetite, and therefore absorption band s corresponding to ferrous and ferric ion appear at 0.7µm and 1.0µm, respectively (Gupta, 2003). The spectral features of ultramafic rocks are dominated by the absorption of Fe, Mg-OH at 2.32µm and 2.38µm, which is due to the phlogopite, biotite and hornblende. Ferrous – iron absorption in olivine and pyroxene causes a broad absorption feature in the 1.00µm region of EMS (Rowan et al., 2006). Sedimentary rocks normally take water absorption bands at 1.4µm and 1.9µm, clay – shale have additional absorption features at 1.2-2.3µm regions, carbonaceous shale and pure siliceous sand do not show any spectral features. Sandstone containing iron oxide exhibits absorption feature at 0.87µm region which is related to Fe^{3+}**.** Carbonate rocks (limestone and Dolomite) exhibit absorption range at 1.9µm and 2.35µm respectively with a shift on absorption according to CaCO3 and MgCaCO3 variation in the mineral chemistry, ferrous ions exhibits spectral feature at 1.0µm, which is more common in dolomites due to the substitution of Mg^{2+} by Fe^{2+} (Rajesh, 2004).

Metamorphic of the deformed rock i.e. in low grade to medium grade metamorphic rocks such as schistose, marbles and quartzite's, the spectral reflectance curves exhibit absorption features at 1.4µm and 1.9µm, which are the ranges for water and hydroxyls. Spectral reflectance curves of all metamorphic rocks reflect feature of water or hydroxyl-like that of igneous rocks. Schistose rocks shows feature of ferric and ferrous, which indicate the existence of chlorite and hornblende The different spectral signatures of various rock types is listed in the table 5.3 (Al – Daghastani, 2003 and Ali M Qaid and Basavarajappa., 2008).

Table.5.3. Spectral features of different Rock types with characteristic absorption signature.

Sl. No	Rock Name	Signature details and cause of signature	ROCK TYPE
1.	Granite	a) Absorption bands in 1.4, 1.9, 2.2 μm corresponding to absorption bands in OH and H_2O absorption b) Absorption in 0.7 and 1 μm corresponding to absorption for crystal field effect/ charge transfer in ferrous (Fe^{+2}) and Fe^{+3}	IGNEOUS ROCK
	Mafic rocks	a) 0.7 and 1.0 μm for absorption bands for ferrous Fe^{+2} and Fe^{+3} ion occurs mineral like pyroxene, amphibolite, olive	
	Ultramafic rocks	a) Absorption band at 1.0 and 2 μm specially for Fe^{+2} as observed in rock like Dunite	
2.	Sandstone	a) Absorption for Ferrous and Ferric ions. Fe rich sandstone produces absorption in 0.87 μm. Greywacke produce absorption due to fundamental/ overcome vibration of clay minerals in 2.1 – 2.4 μm	SEDIMENTARY ROCK
	Shale	a) Mostly due to vibrational overtone combination in OH and H_2O and also due to vibrational absorption for Al-OH and Mg-OH in 2.1 and 2.4 μm respectively	
	Limestone & Dolomite	a) Absorption in 1.9 – 2.35 μm, latter being more increase for combination overtone to the substitution of Mg^{2+} by Fe^{2+}	
3.	Schist	a) Absorption signature in 0.7, 1, 2 μm general due to ferrous and ferric iron and 2.1, 2.3, 2.4 for vibrational absorption for Al-OH, Mg-OH bond in clay mineral	METAMORPHIC ROCK
	Marble	a) 1.9 – 2.5 μm latter being more intense for combination overtone of vibration CO_3 molecule.	

Table. 5.4. Absorption peaks of various cat ions and anions in different regions of EMS

Sl. No	Cations/ Anions	Absorption peaks (µm)
Normal -Visible and Near Infrared (VNIR) Region		
1.	**Ferric ion**	**0.40, 0.50, 0.70 and 0.87nm**
2.	**Ferrous ion**	**0.43, 0.45, 0.57, 0.55, 1.00 and 1.80 – 2.00nm**
3.	**Manganese**	**0.34, 0.37, 0.41, 0.45 and 0.55nm**
4.	**Copper**	**0.80nm**
5.	**Nickel**	**0.40, 0.74 and 1.25nm**
6.	**Chromium**	**0.35, 0.45 and 0.55nm**
Normal -Short Wavelength Infrared (SWIR) Region		
7.	**Hydroxyl ions**	**1.44 and 2.74- 2.77nm**
8.	**Al-OH**	**2.20nm**
9.	**Mg-OH**	**2.30nm**
10.	**Water molecules**	**1.40 and 1.90nm**
11.	**Carbonates**	**1.90, 2.00, 2.16, 2.35 and 2.55nm**
Thermal Infrared (TIR) Region		
12.	**Silicates**	**9.00 – 11.50 (depending upon the crystal structure)**
13.	**Carbonates**	**7 (not used in Remote Sensing) and 11.30nm**
14.	**Sulphates**	**9 and 16nm**
15.	**Phosphates**	**9.25 and 10.30nm**
16.	**Nitrates**	**7.20nm**
17.	**Nitrites**	**8 and 11.8nm**
18.	**Hydroxides**	**11nm**

5.3. SPECTRORADIOMETER

Spectroradiometer is an optical instrument for measuring the radiant energy (radiance or irradiance) from a source at each wavelength throughout spectrum of EMS. A spectroradiometer is also a special kind of spectrometer. Spectrometer are commonly used earlier and the same instrument with calibrated cable are called as spectroradiometer. In 1970s Goetz first described the first portable field spectroradiometer. Alex Goetz subsequently started the company called as ASD Inc (Analytical Spectral device). ASD spectroradimeter is firstly utilized in the measurement of physical quantity called as 'Reflectance factor' a term coined by Nicodemus et al in1977. Spectral reflectance studies for the study area samples are done using the instrument Spectral evolution SR-3500 (Model: SR-3500 serial: 169-80 F7) field portable spectroradiometer in well buildup laboratory environment. (Guha and Kumar., 2016).

RS-3500 compact, portable spectroradiometer Fast, full spectrum UV/VIS/NIR measurements (350-2500nm) with a single scan, Autoshutter, autoexposure, and autodark correction before each new scan, with no optimization step, for one-touch operation Superior reliability no moving optical parts to break down. This instrument measured three types 1. Direct Energy measurement (Spectroradiometry). 2. Reflectance spectroscopy. and 3. Absorbance spectroscopy. Ergonomically designed pistol grip with industry-standard Picatinny rail for mounting accessories, for example, a laser sight its need AC universal power supply , this instrument used DARWin SP.V.1.3.0 Data Acquisition software, Pelican protective case TENBA Shootout padded backpack 5x5 inch reflectance standard (99%) with aluminum case, cover and tripod mount, 1.2 meter metal clad fiber optic with SMA-905 input connector (includes thumb-screw release mount) NIST-traceable radiance cali-bration of 25 degree FOV fi-ber optic cable, Rechargeable battery and universal AC charger (2 of each) Battery power cable, Lightweight and compact the spectroradiometer weighs only 3.3kg/7.3lbs—small enough to carry on-board a plane and around a field or forest. Rugged, handheld micro-computer GETAC PS336 PDA with auto-focus digital camera, e-compass, altimeter, voice note capability, GPS tagging, and sunlight readable VGA display DARWin SP Data Acquisition software for one-touch scanning , automatically saves data as ASCII files for use with 3rd party software (no post-processing), displays reflectance/transmittance data

(percentage) or absorbance (logarithmic) versus wavelength, and produces single and multiple spectral plots . SR-3500— high resolution budget-friendly portable spectroradiometer for a range of laboratory and field appli-cations including ground truthing satellite and flyover data, solar radiance/irradiance measurements, albedo measurements, vegetation studies and environmental research.

Spectral Evolution RS-3500 Spectroradiometer analysis carried out Department studies in Earth Science, Centre for advanced studies in Precambrian geology, University of Mysore and the instrument sponsored by UGC New Delhi. Spectralradiometer is used in the field for a wide range of remote sensing applications, Including :Ground truthing confirming, disputing, or interpreting hyperspectral or multi-spectral data, Environmental research, Agricultural analysis, Ecosystem change, Forestry research, including canopy studies, Glacial change and climate studies, Atmospheric research, Calibration transfer and satellite sensor validation, Water body studies, Plant species identification, Urban development , Crop health, including photosynthesis efficiency, Irrigation assessment, Soil analysis, including topsoil fertility and erosion risks, Soil degradation, mapping, and monitoring, Geological remote sensing, including surveying, mineral identification, and geomorphology.

5.3.1. EZ – ID MINERAL IDENTIFICATION SOFTWARE

EZ-ID provides geologists, geoscientists, and geometallurgists with the tools to identify minerals, create more accurate mineral maps and vector alteration to mineralization, Sample identification has never been faster, easier, or more accurate than with EZ-ID software from Spectral Evolution. EZ-ID provides sample identification capabilities built into SPECTRAL EVOLUTION'S field portable spectrometers and spectroradiometers for applications ranging from vegetation studies, to soil research, crop health, raw materials and plastics ID, minerals, and more. EZ-ID allows you to compare your target scans with the USGS spectral library, other commer-cially available libraries, or your in-house custom library. EZ-ID software can be used on unknown samples in the field or in a lab. EZ-ID features Include: Fast and accurate identification of unknown target sample to known library sample, Easy-to-use—just collect your scan using a SPECTRAL EVOLUTION spectrometer or spectroradiometer and see results in real time, Simple,

consistent user-interface, Software provides a weighted score for best matches, Include or exclude spectral regions of interest for optimal results, EZ-ID works through the DARWin SP Data Acquisition software interface for all our spectrometers and spectroradiometers.

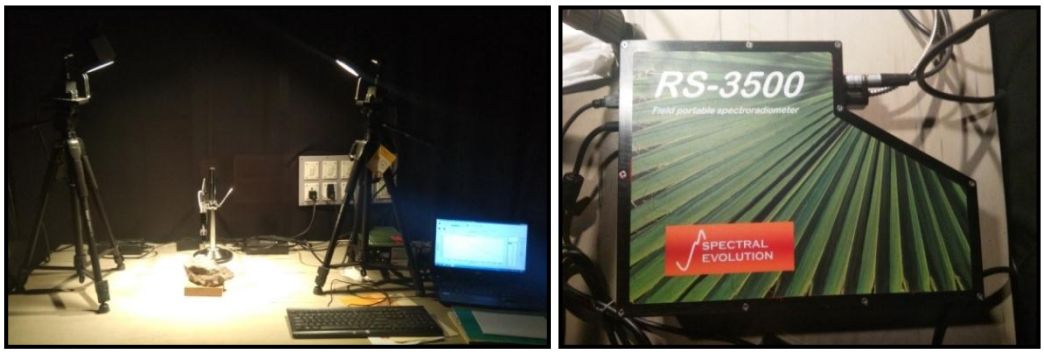

Fig.5.2. Hyperspectral instrument laboratory setup, Department of Earth Science, Centre for Advanced Studies in Precambrian Geology University of Mysore.

5.3.2. HYPERSPECTRAL SIGNATURS

Spectral signature measures all types of wavelengths that reflect, absorb, transmit and emit electromagnetic energy from the objects of the earth surface (Ali M. Qaid et al., 2009). Specral Evolution (SR-3500) Spectro-radiometer instrument has the ability to measure the spectral signatures of different rocks/ minerals. The SR-3500 operate in the wavelength range of 350–2500 nm with three detector elements: The first is a (512-element) Si PDA (Photo Diode Array) element silicon array covering the spectral range from 350 to 1000 nm (280–1000nm) (Maruthi et al., 2018). Two thermoelectrically cooled InGaAs (Indium Gallium Arsenide) arrays of 256 elements each extend the spectral range up to 1900nm and 2500nm respectively. The spectral signatures of the representative samples were compared with mineral spectra of International standards for minerals such as USGS spectral library in DARWin SP.V.1.3.0 (Hunt et al., 1971). Absorption spectral values obtained from the DARWin software lab Spectra is the one character helps in the study of major and minor mineral constituents (Hunt et al., 1971) (basavarajappa et al., 2018). Ten spot observation per sample are recorded to the selected samples from the study area, maximum of 3 to 4 best matched curves of a sample is given in the spectral signature profiles.

Table.5.5. Specifications of Spectral Evolution RS-3500, DoS in Earth science, Centre for advanced studies in Precambrian Geology University of Mysore.

Spectral Range	**350-2500 nm**
Spectral Resolution	**3 nm @ 700 nm** **8 nm @ 1500nm** **6 nm @ 2100 nm**
Sampling Interval	**1.4 nm @ 350-1050 nm** **2 nm @ 1000 – 2500 nm**
Scanning time	**100 millisecond**
Wavelength Reproducibility	**0.1nm**
Wavelength Accuracy	**±0.5 bandwidth**
Spectral Sampling Bandwidth	**Data output** **Spectral Sampling Bandwidth in 1nm increments** **2151 channels reported**
Si Detectors	**512 element Si photodiode array (350–1000nm)**
InGaAs Detectors (thermoelectrically cooled)	**256 element extended wavelength photodiode array (970–1910nm)** **256 element extended wavelength photodiode array (1900-2500nm)**
FOV Options	**SMA-905 fiber end mount lenses: 1, 2, 3, 4, 5, 8 and 10° field of view, irradiance diffuser**
Noise Equivalence Radiance **(1.2 meter fiber optic)**	**$0.8x10^{-9}$ W/cm2/nm/sr @700nm** **$1.2x10^{-9}$ W/cm2/nm/sr @1400nm** **$1.8x10^{-9}$ W/cm2/nm/sr @2100nm**
Input	**1.5m fiber optic** **25^0 field of view**
Calibration Accuracy **(NIST Traceable)**	**±5% @ 400nm** **±4% @ 700nm** **±7% @ 2200nm**
Communications interface	**USB or Class I Bluetooth– laptop or PDA compatible**
Size	**8.5" x 12" x 3.5"**
Weight	**7.3 lbs (spectroradiometer only)**
Calibration	**Wavelength, reflectance, radiance and irradiance** **All calibration are NIST (National Institute of Standard and Technology) traceable**

The samples cut part given the best spectral curve respect to exposure surface of the sample (Ali M. Qaid and Basavarajappa 2008) Basavarajappa et al., 2018; Basavarajappa et al 2019.

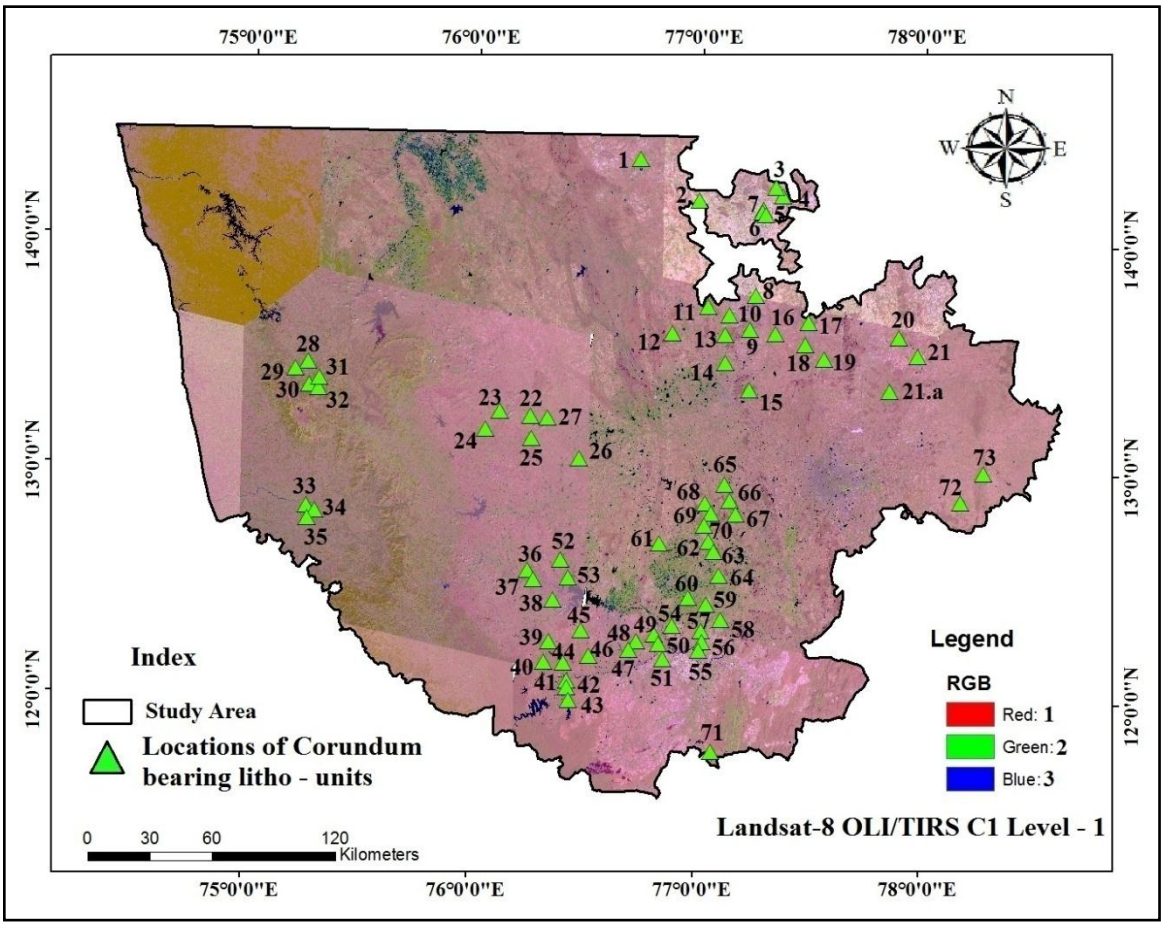

Fig.5.3. Landsat-8, Satellite image showing sample locations of the Study area.

LOCATIONS:

Chitradurga District: 1. Ullarti kaval, 2. Kyadigunte and 2.a. Kyadigunte

Tumkur District: 3. Bettadakelaginahalli, 4. Kyathaganakere, 5. Thimmapura, 6. Veerammanahalli, 7. Kanikalabande, 8. Channamallanahalli, 9. ChinakaVajra, 10. Bittanakurke, 11. Basmangikaval, 12. Molanahalli, 13. Chickthimmanahalli, 14. Devalapura and 15. Devarayanadurga.

Chikballapura District: 16. Hunasavadi, 17. Malenahalli, 18. Kachamachanahalli 19. Kadiridevarahalli, 20. Neralemaradalli, 21. Poolakuntahalli and 21.a. Sidlaghatta.

Hassan District: 22. Makanahalli, 23. Undiganalu, 24. Dasagodanahalli, 25. Nandihalli, 26. Dyavalapura and 27. Belagumba.

Chikmagalur District: 28. Melukoppa, 29. Kogodu, 30. Malanadu, 31. Kunchebylu, and 32. Heggaru.

Dakshina Kannada District: 33. Uppinangadi, 34. Koila and 35. Shanthigodu.

Mysuru District: 36. Honnenahalli, 37. Bylapura, 38. Krishnarajanagara. 39. Uddukaval, 40. Padukotekaval, 41. Adahalli, 42. Katur, 43. Halasur, 44. Hanumanthapura, 45. Handanahalli, 46. Mavinahalli, 47. Someshwarapura, 48. Varuna, 49. Kuppya, 50. Bommanayakanahalli and 51. Eswaragowdanahalli.

Mandya District: 52. Machaholalu, 53. Adaguru, 54. Bannur, 55. Hemmige, 56. Ballegere, 57. Doddaboovalli, 58. Malavalli, 59. Nelamakanahalli, 60. Ahasale, 61. Tharanagere, 62. Kesthur, 63. Hanumanthapura and 64. Maddur.

Ramanagara District: 65. Huthridurga, 66. Varthehalli, 67. Akkur 68. Hosahalli, 69. Lakkashettypura and 70. Byranaikanahalli.

Chamarajanagara Districts: 71. Budipadaga and 71.a. B.R.Hills.

Kolara Districts: 72. Yelesandra, 73. Kammasandra and 73.a. Near Kammasandra.

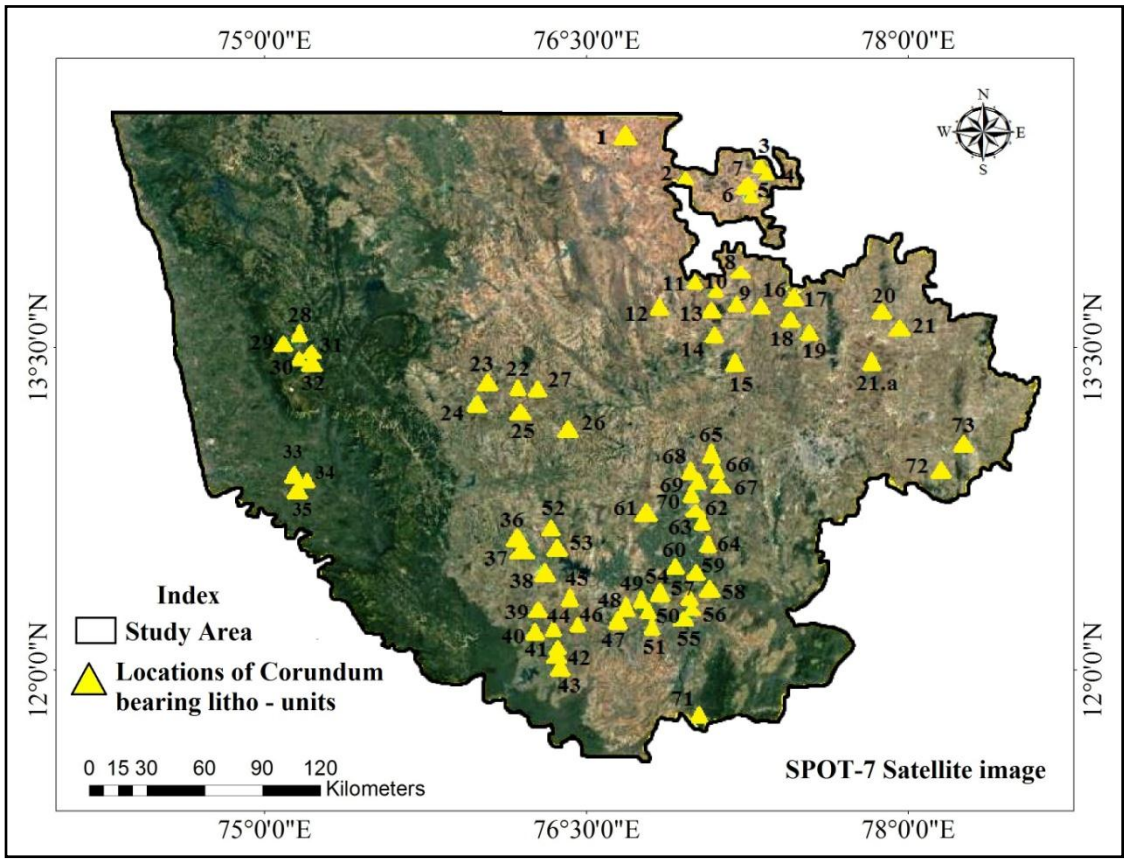

Fig.5.4. SPOT-7 Satellite image shows sample locations of the Study area.

Landsat 8 is an American Earth observation satellite launched on February 11, 2013. It is the eighth satellite in the Landsat program. The satellite was built by Orbital Sciences Corporation, who served as prime contractor for the mission, LANDSAT 8 satellite has two main sensors: the Operational Land Imager (OLI) and the Thermal Infrared Sensor (TIRS) OLI will collect images using nine spectral bands in different wavelengths of visible, near-infrared, and shortwave light to observe a 185 kilometer (115 mile) wide swath of the Earth in 15-30 meter resolution covering wide areas of the Earth's landscape while providing sufficient resolution to distinguish features like urban centers, farms, forests and other land uses, this satellite image shows corundum bearing litho units locations after final remote sensing processing (fig.5.3).

SPOT is a commercial high-resolution Optical Imaging Earth Observation Satellite System (OIEOSS) operating from space. The SPOT system includes a series of satellites and ground control resources for satellite control and programming, image production, and distribution. Earlier satellites were launched using the European Space Agency's Ariane 2, 3, and 4 rockets, while SPOT 6 and SPOT 7 were launched by the Indian PSLV this satellite image shows corundum bearing litho units locations after final Remote Sensing processing (Fig.5.4).

5.4. HYPERSPECTRAL SIGNATURE STUDY ON ROCK SAMPLES AROUND CHITRADURGA DISTRICT.

Corundum bearing rocks were determined at the using spectral signatures. The spectrometer component is a crossed Czerny-Turner configuration using ruled gratings as the dispersive elements. Energy enters the spectrometer and is collimated before being reflected off the gratings and refocused onto the PDA (Photodiode Array) detectors. The spectroradiometer and controlling electronics are contained in the housing. International standards for minerals such as USGS were compared along with the major elements for the field samples to check precision and accuracy of measurement. The certified and analyzed values of USGS are given in the fig.5 along with major element abundances of samples to check the error limits of measurement (Hunt et al., 1971).

Hyperspectral remote sensing for mineral targeting carried out spectral radiometer instrument with help of DARwin software measured single and multiple plots. here we

taken multiple measurement plot of spectral analysis were carried out of samples of Chitradurga District (fig.5.5).

EZ-ID mineral identification tool works to taken USGS standard signatures and match the unknown raw mineral data based on mineral structure and composition give the result based on percentage of mineral composition. Hyperspectral signatures determined the graph showing alumina oxide, Fe and H_2O presence in the sample. Corundum Al_2O_3 mineral type - Oxide this sample prepared from crystals that were brownish near the surface and bluish – green near in the interior. Very sharp corundum reflections suggest excellent crystallinity and compostional homogeneity (Absorption anomalies at wavelength regions of 0.55 µm and 0.9 µm of Fe3+ and Fe2+ ions are observed respectively with low reflectance in the VNIR region (Ali M. Qaid et al., 2009) (Fig.5.6). Major element content as Al_2O_3 content shows high range imparts a corundum character with that of high aluminum content. Library spectrum corundum correlation score 0.854 percent match the curve (Fig-5.6). composition discussion analysis showed the sample to contain 0.27 and 1.54% Cr. 4.56% Fe and 25.65% Si with traces of Ti, V, Mn, Mg, Ca and Cu the iron appears to be present on both ferrous (0.55. 0.45 and 1.1um absorption features) and ferric (0.7. 0.45 and near 0.4um) from the Cr^{3+} ion contributes to the 0.4. 0.55 and 0.7um (emission) features. Spectral discussion Sample plots are correlated with standard USGS Spectral Library using absolute reflectance v/s wavelength which provide strong absorption range in 2.20 µm and 0.65 µm representing the mineral corundum shows intense absorption feature in 2.40 µm of the electromagnetic spectrum (Hunt et al., 1971) (Fig.5.6). Absorption anomalies at wavelength regions of 0.55 µm and 0.9 µm of Fe3+ and Fe2+ ions are observed respectively with low reflectance in the VNIR region (Ali M. Qaid et al., 2009). Major element content as Al_2O_3 content shows high range imparts a corundum character with that of high aluminum content. Library spectrum corundum correlation score 0.854 percent match the curve (Fig-5.6).

Amphiboles are found principally in metamorphic and igneous rocks. They occur in many metamorphic rocks, especially those derived from mafic igneous rocks (those containing dark-coloured ferromagnesian minerals) and siliceous dolomites. Major and minor element content of amphibolite schist shows SiO_2 ranging 40.21% , MgO content

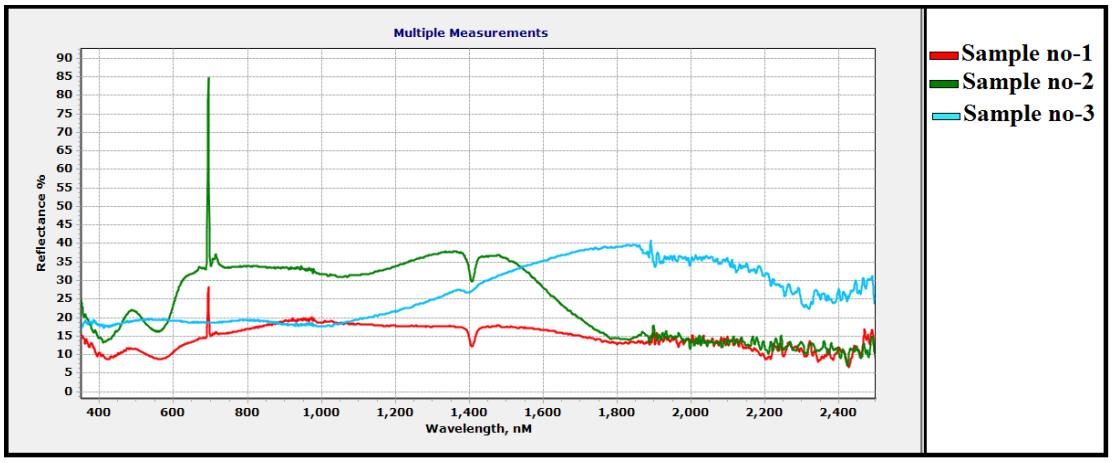

Fig.5.5.Lab Spectral signatures of Corundum bearing rocks.

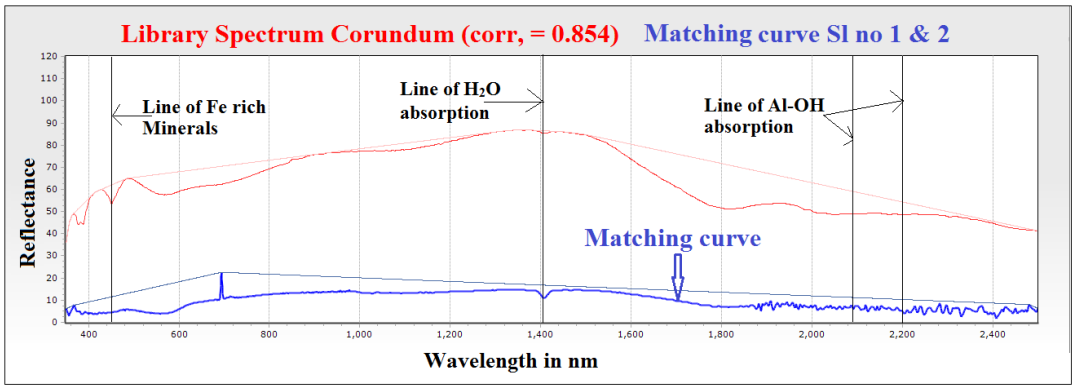

Fig.5.6. EZ-ID Match analysis of Corundum.

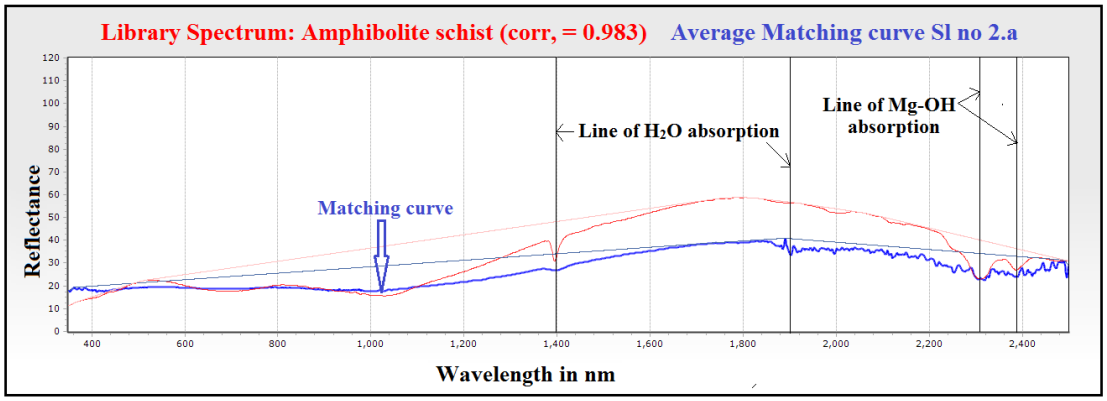

Fig.5.7. EZ-ID Match analysis of Amphibolite schist.

is fairly low and ranges from 10.42%, Al_2O_3 content high ranges 32.86%, CaO content is 8.43%, K_2O content of ranges 0.426%; TiO_2 content is fairly low 0.67% and P_2O_5 ranges 0.5957% (M. Qasim Jan 1988). Spectal discussion Sample plots provide strong absorption range from 2.0 – 2.25 µm representing the mineral corundum whereas

amphibole shows intense absorption feature in 2.35 µm of the electromagnetic spectrum (Hunt et al., 1971). Absorption anomalies at wavelength regions 0.55 µm and 0.9 µm of Fe^{3+} and Fe^{2+} ions are observed respectively (Fig.5.7). Absorption range 1.4µm are noticed due to the presence of water and hydroxyl molecules in the present sample (Ali M.Qaid et al., 2009). Library spectrum Amphibolite Schist correlation score 0.983 percent match the curve (Fig-5.7). Lab spectra of corundum strong absorption range identified in the wavelength of 2.10 µm and 2.20 µm and 0.65 µm representing the mineral corundum shows intense absorption feature in 2.40 µm of the electromagnetic spectrum (Hunt et al., 1971) (Fig-5.7).

5.5. HYPERSPECTRAL SIGNATURE STUDY ON ROCK SAMPLES AROUND TUMKUR DISTRICT

Around 13 samples were carried out for spectra analysis each sample taken 4 targeting and Darwin software give the multiple measurement plots (fig.5.8). in this plot taken EZ-ID analysis tool took a average spectral signatures and give the results. Corundum Al_2O_3 mineral type - Oxide (Hematite group) this sample prepared from crystals that were brownish near the surface. very sharp corundum reflections suggest excellent crystallinity and compostional homogenety. Spectral discussion Sample plots are correlated with standard USGS Spectral Library using absolute reflectance v/s wavelength which provide strong absorption range in 2.20 µm and 0.65 µm representing the mineral corundum shows intense absorption feature in 2.40 µm of the electromagnetic spectrum (Hunt et al., 1971). Absorption anomalies at wavelength regions of 0.55 µm and 0.9 µm of Fe3+ and Fe2+ ions are observed respectively with low reflectance in the VNIR region (Ali M. Qaid et al., 2009) (Fig.5.9). Major element content as Al_2O_3 content shows high range imparts a corundum character with that of high aluminum content. library spectrum corundum correlation score 0.933 percent match the curve (Fig.5.9) .

Hyperspectral signatures determined the graph showing mainly the microcline spectra shows fairly weak H_2O features near 1.4 and 1.9µ, and a very weak feature near 2.2µ due to the OH stretch-Al-OH bend combinatiion. It also displays a quite sharp drop off at approximately 0.55µ which is typical of the ferric oxides. Sample is pinkish in color, which is not due to an alteration coating of ferric oxide. Fe3+ may substitute for Al in

limited amount in normal alkali feldspars, but excess Fe3+ will exsolved either as discrete particles of iron-bearing mineral, or as an iron staining on grain boundaries and cleavage planes. The latter appears to be the case for this microcline, which explains the ferric oxide type of visible spectrum. There is, however, insufficient ferric oxide present to yield a discernible near-infrared feature (Hunt et al., 1973). Library spectrum Closepet Granite correlation score 0.883 percent match the curve (Fig5.10)

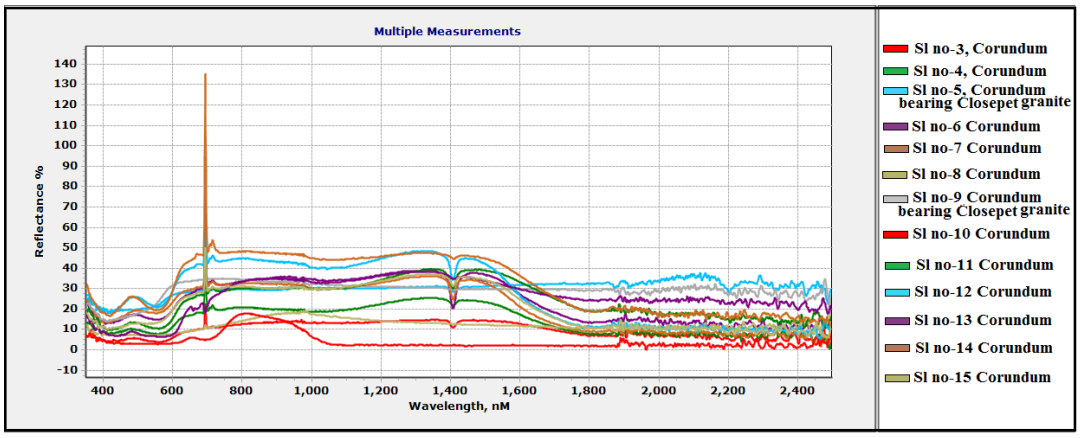

Fig.5.8. Lab Spectral signatures of Corundum bearing rocks.

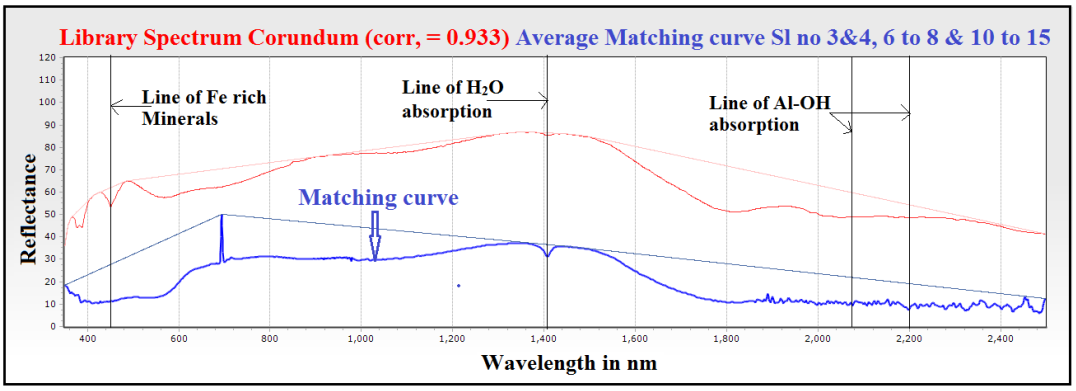

Fig.5.9. Fig.5.6. EZ-ID Match analysis of Corundum.

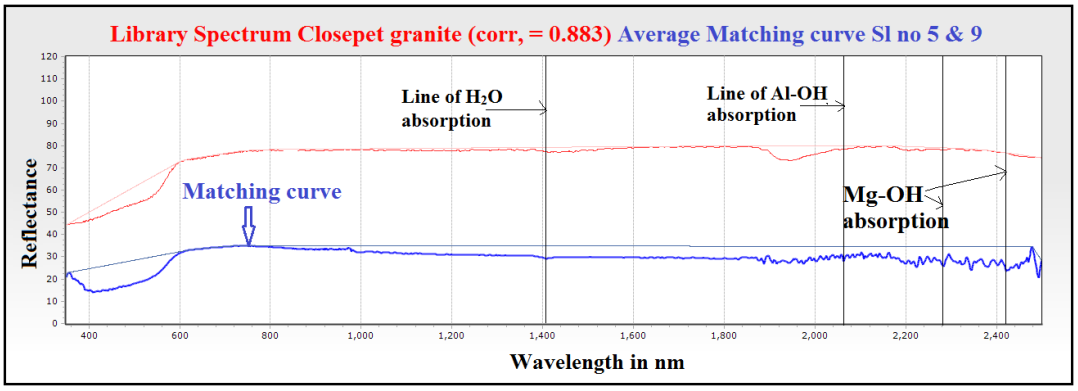

Fig.5.10. EZ-ID Match analysis of Closepet granite.

5.6. HYPERSPECTRAL SIGNATURE STUDY ON ROCK SAMPLES AROUND CHIKBALLAPURA DISTRICT

Chikballapura district cover 7 corundum bearing litho units. Hyperspectral remote sensing for mineral targeting carried out spectral radiometer instrument with help of DARwin software measured single and multiple plots. here we taken multiple measurement plot of Chikballapur area samples (fig.5.11).

Hyperspectral signatures determined the graph showing alumina oxide, Fe and H_2O presence in the sample. Corundum Al_2O_3 mineral type - Oxide this sample prepared from crystals that were brownish near the surface and bluish – green near in the interior. Very sharp corundum reflections suggest excellent crystallinity and compostional homogeneity. composition discussion EZ-ID match analysis showed the sample to contain Cr, Fe, Al, Si with traces of Ti, V, Mn, Mg, Ca and Cu the iron appears to be present on both ferrous (0.55. 0.45 and 1.1um absorption features) and ferric (0.7. 0.45 and near 0.4um) from the Cr^{3+} ion contributes to the 0.4. 0.55 and 0.7um (emission) features. Spectral discussion Sample plots are correlated with standard USGS Spectral Library using absolute reflectance v/s wavelength which provide strong absorption range in 2.20 µm and 0.65 µm representing the mineral corundum shows intense absorption feature in 2.40 µm of the electromagnetic spectrum (Hunt et al., 1971). Absorption anomalies at wavelength regions of 0.55 µm and 0.9 µm of Fe3+ and Fe2+ ions are observed respectively with low reflectance in the VNIR region (Ali M. Qaid et al., 2009) (Fig.5.12). Major element content as Al_2O_3 content shows high range imparts a corundum character with that of high aluminum content. Library spectrum corundum correlation score 0.902 percent match the curve (Fig5.12)

Hyperspectral signatures determined the graph showing mainly the microcline spectra shows fairly weak H_2O features near 1.4 and 1.9µ, and a very weak feature near 2.2µ due to the OH stretch-AlOH bend combinatiion. It also displays a quite sharp drop off at approximately 0.55µ which is typical of the ferric oxides. Sample is pinkish in color, which is not due to an alteration coating of ferric oxide. Fe3+ may substitute for Al in limited amount in normal alkali feldspars, but excess Fe3+ will exsolved either as discrete particles of iron-bearing mineral, or as an iron staining on grain boundaries and cleavage planes. The latter appears to be the case for this microcline, which explains the

ferric oxide type of visible spectrum. There is insufficient ferric oxide present to yield a discernible near-infrared feature. Library spectrum Closepet Granite correlation score 0.821 percent match the curve (Fig5.13)

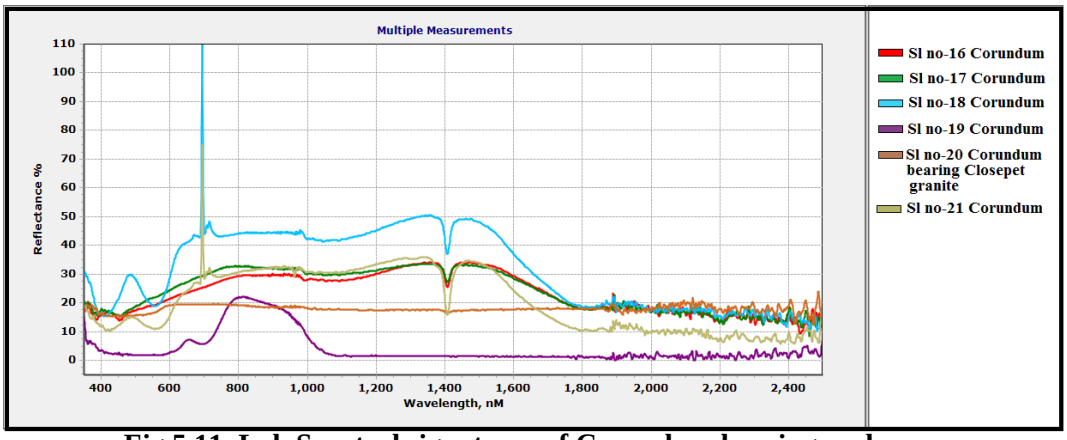

Fig.5.11. Lab Spectral signatures of Corundum bearing rocks.

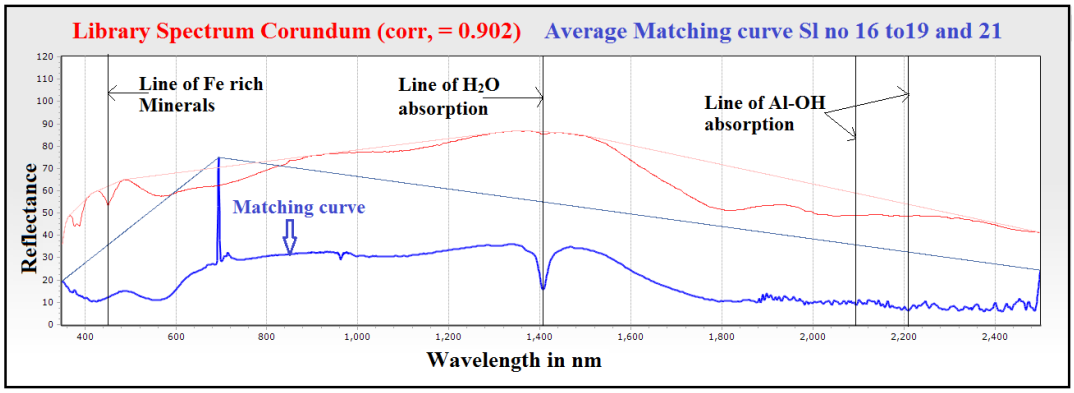

Fig.5.12. Fig.5.6. EZ-ID Match analysis of Corundum.

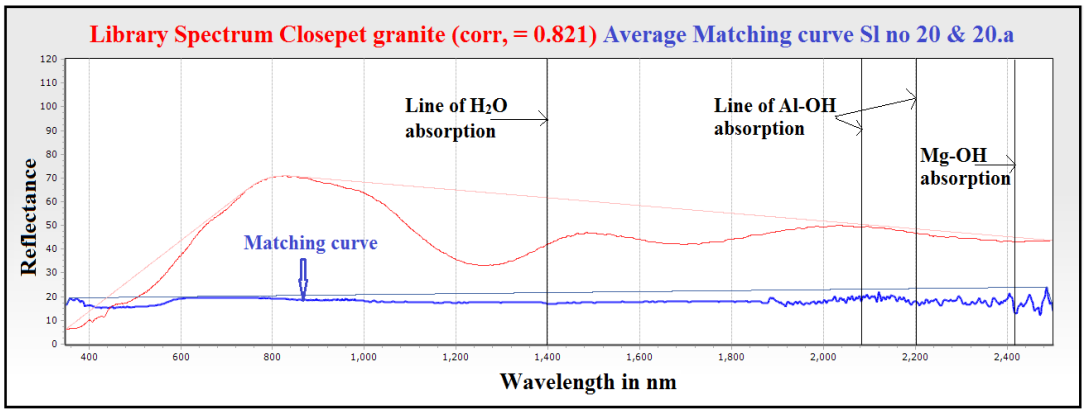

Fig.5.13. EZ-ID Match analysis of Closepet granite.

5.7. HYPERSPECTRAL SIGNATURE STUDY ON ROCK SAMPLES AROUND HASSAN DISTRICT

Hyperspectral remote sensing for mineral targeting carried out spectral radiometer instrument with help of DARwin software measured single and multiple plots. here we taken multiple measurement plot of Hassan area samples (fig.5.14).

In this plot took spectral signatures of DARWin software, EZ-ID analysis tool took a average spectral curves and give the results. Corundum Al_2O_3 mineral type - Oxide (Hematite group) this sample prepared from crystals that were brownish near the surface. very sharp corundum reflections suggest excellent crystallinity and compostional homogenety. spectral discussion Sample plots are correlated with standard USGS Spectral Library using absolute reflectance v/s wavelength which provide strong absorption range in 2.20 µm and 0.65 µm representing the mineral corundum shows intense absorption feature in 2.40 µm of the electromagnetic spectrum. Absorption anomalies at wavelength regions of 0.55 µm and 0.9 µm of Fe3+ and Fe2+ ions are observed respectively with low reflectance in the VNIR region (Fig.5.15). Major element content as Al_2O_3 content shows high range imparts a corundum character with that of high aluminum content. library spectrum corundum correlation score 0.941 percent match the curve (Fig.5.15)

Spectral signatures find the graph showing H2O content Al_2O_3 and Fe, Mg, OH minerals presence in the Sample. Amphiboles are found principally in metamorphic and igneous rocks. They occur in many metamorphic rocks, especially those derived from mafic igneous rocks and siliceous dolomites. Spectal discussion Sample plots provide strong absorption range from 2.0 – 2.25 µm representing the mineral corundum whereas amphibole shows intense absorption feature in 2.35 µm of the electromagnetic spectrum (Hunt et al., 1971). Absorption anomalies at wavelength regions 0.55 µm and 0.9 µm of Fe^{3+} and Fe^{2+} ions are observed respectively (Fig.5.10). Absorption range 1.4µm is noticed due to the presence of water and hydroxyl molecules in the present sample (Ali M.Qaid et al., 2009). Library spectrums Corundum bearing Amphibolite Schist correlation score 0.883 percent match the curve (Fig.5.10). Lab spectra of corundum bearing amphibolites schist strong absorption range identified in the wavelength of 2.10

μm and 2.20 μm and 0.65 μm representing the mineral corundum shows intense absorption feature in 2.40 μm of the electromagnetic spectrum (Hunt et al., 1971) (Fig.5.10).

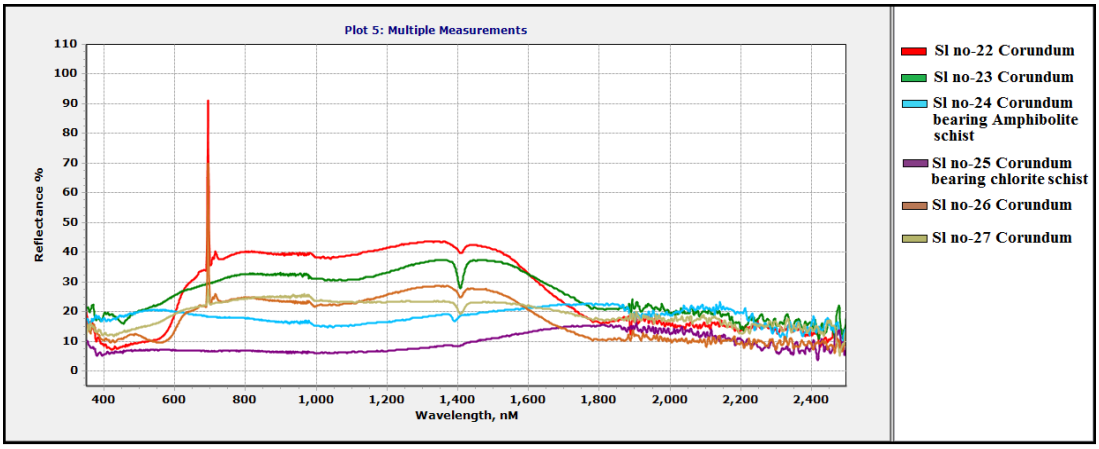

Fig.5.14. Lab Spectral signatures of Corundum bearing rocks.

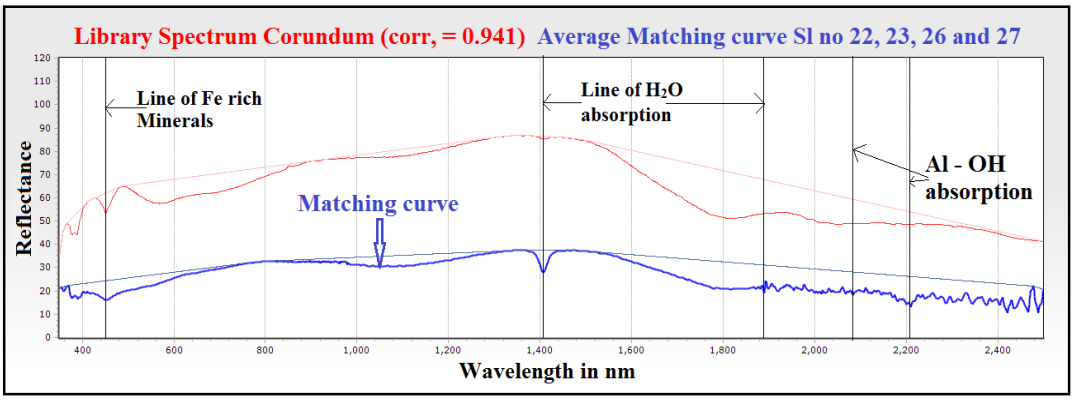

Fig.5.15. Fig.5.6. EZ-ID Match analysis of Corundum.

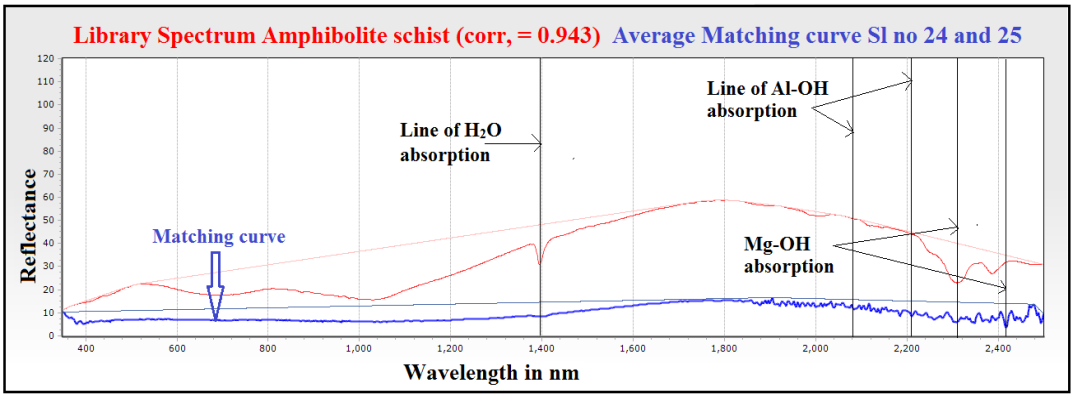

Fig.5.16. EZ-ID Match analysis of Amphibolite schist.

5.8. HYPERSPECTRAL SIGNATURE STUDY ON ROCK SAMPLES AROUND CHIKMAGALUR DISTRICT

Chikmagalur district cover 5 corundum bearing litho units . Hyperspectral Remote Sensing for mineral targeting carried out spectral radiometer instrument with help of DARwin software measured single and multiple plots. here we taken multiple measurement curves plot of Chikmagalur area (Fig.5.17).

Hyperspectral signatures determined the graph showing alumina oxide, Fe and H_2O presence in the sample. Corundum Al_2O_3 mineral type - Oxide this sample prepared from crystals that were brownish near the surface and bluish – green near in the interior. Very sharp corundum reflections suggest excellent crystallinity and compostional homogeneity. composition discussion EZ-ID match analysis showed the sample to contain Cr, Fe, Al, Si with traces of Ti, V, Mn, Mg, Ca and Cu the iron appears to be present on both ferrous (0.55. 0.45 and 1.1um absorption features) and ferric (0.7. 0.45 and near 0.4um) from the Cr^{3+} ion contributes to the 0.4. 0.55 and 0.7um (emission) features. Spectral discussion Sample plots are correlated with standard USGS Spectral Library using absolute reflectance v/s wavelength which provide strong absorption range in 2.20 µm and 0.65 µm representing the mineral corundum shows intense absorption feature in 2.40 µm of the electromagnetic spectrum (Hunt et al., 1971). Absorption anomalies at wavelength regions of 0.55 µm and 0.9 µm of Fe3+ and Fe2+ ions are observed respectively with low reflectance in the VNIR region (Ali M. Qaid et al., 2009) (Fig.5.18). Major element content as Al_2O_3 content shows high range imparts a corundum character with that of high aluminum content. Library spectrum corundum correlation score 0.877 percent match the curve (Fig5.18)

Amphiboles occur in many metamorphic rocks, especially those derived from mafic igneous rocks (those containing dark-coloured ferromagnesian minerals) and siliceous dolomites. Major and minor element content of amphibolite schist shows SiO_2, MgO moderate ranging content is fairly low and ranges Al_2O_3 content high ranges CaO, K_2O, TiO_2, and P_2O_5 (M. Qasim Jan 1988). Spectal discussion Sample plots provide strong absorption range from 2.0 – 2.25 µm representing the mineral corundum whereas

amphibole shows intense absorption feature in 2.35 µm of the electromagnetic spectrum (Hunt et al., 1971). Absorption anomalies at wavelength regions 0.55 µm and 0.9 µm of

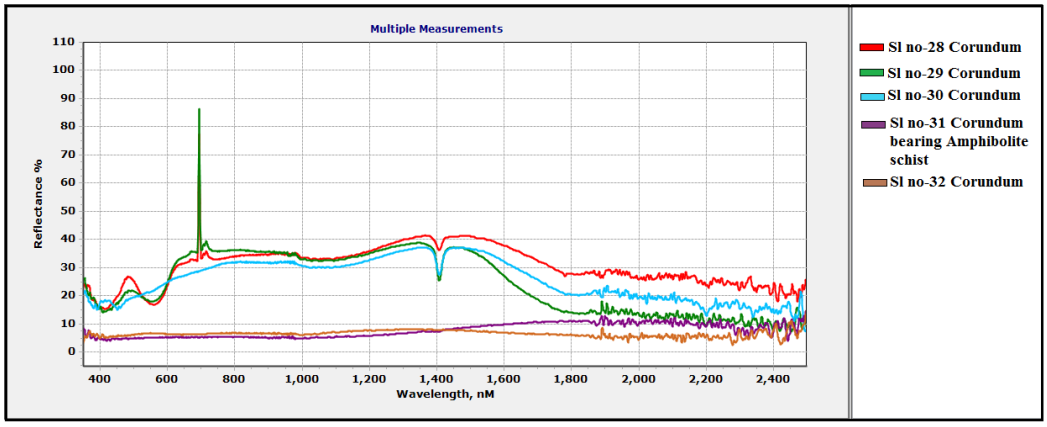

Fig.5.17. Lab Spectral signatures of Corundum bearing rocks.

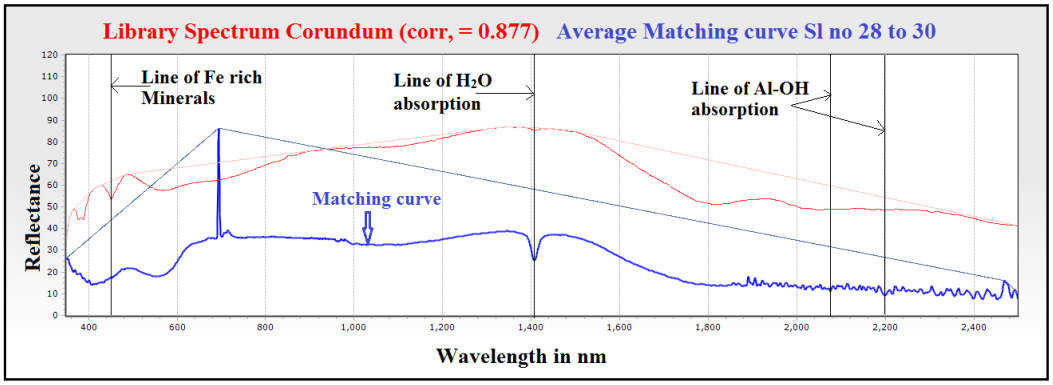

Fig.5.18. Fig.5.6. EZ-ID Match analysis of Corundum.

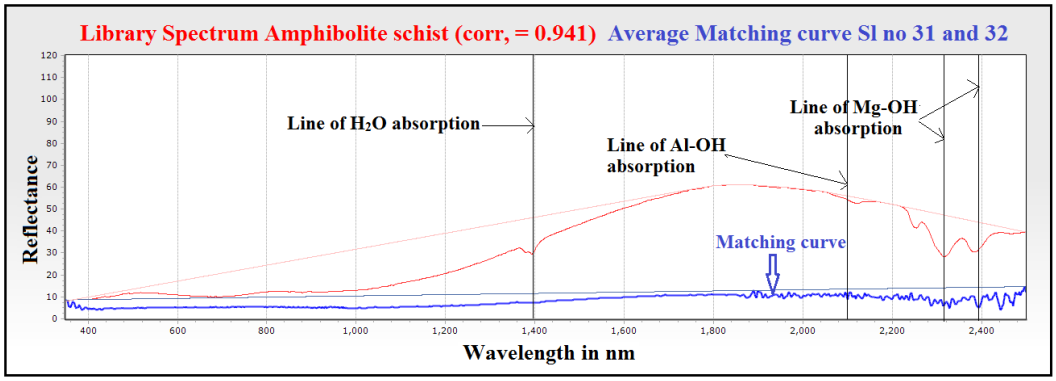

Fig.5.19. EZ-ID Match analysis of Amphibolite schist.

Fe^{3+} and Fe^{2+} ions are observed respectively (Fig.5.19). Absorption range 1.4µm are noticed due to the presence of water and hydroxyl molecules in the present sample (Ali M.Qaid et al., 2009). library spectrum Amphibolite Schist correlation score 0.941 percent match the curve (Fig-5.19). Lab spectra of corundum strong absorption range identified

in the wavelength of 2.10 µm and 2.20 µm and 0.65 µm representing the mineral corundum shows intense absorption feature in 2.40 µm of the electromagnetic spectrum (Fig-5.19).

5.9. HYPERSPECTRAL SIGNATURE STUDY ON ROCK SAMPLES AROUND DAKSHINA KANNADA DISTRICT

In Dakshina Kannada district about 3 samples were carried out spectral analysis each sample taken 4 targeting and Darwin software give the multiple measurement plots (fig.5.20). in this plot taken EZ-ID analysis tool took a average spectral signatures and give the results. Corundum Al_2O_3 this sample prepared from crystals that were brownish near the surface. very sharp corundum reflections suggest excellent crystallinity and compostional homogenety. spectral discussion Sample plots are correlated with standard USGS Spectral Library using absolute reflectance v/s wavelength which provide strong absorption range in 2.20 µm and 0.65 µm representing the mineral corundum shows intense absorption feature in 2.40 µm of the electromagnetic spectrum (Hunt et al., 1971). Absorption anomalies at wavelength regions of 0.55 µm and 0.9 µm of Fe3+ and Fe2+ ions are observed respectively with low reflectance in the VNIR region (Ali M. Qaid et al., 2009) (Fig.5.21). Major element content as Al_2O_3 content shows high range imparts a corundum character with that of high aluminum content. library spectrum corundum correlation score 0.908 percent match the curve (Fig.5.21)

Amphiboles occur in many metamorphic rocks, especially those derived from mafic igneous rocks (those containing dark-coloured ferromagnesian minerals) and siliceous dolomites. Major and minor element content of amphibolite schist shows SiO_2, MgO moderate ranging content is fairly low and ranges Al_2O_3 content high ranges CaO, K_2O, TiO_2, and P_2O_5 (M. Qasim Jan 1988). Spectal discussion Sample plots provide strong absorption range from 2.0 – 2.25 µm representing the mineral corundum whereas amphibole shows intense absorption feature in 2.35 µm of the electromagnetic spectrum (Hunt et al., 1971). Absorption anomalies at wavelength regions 0.55 µm and 0.9 µm of Fe^{3+} and Fe^{2+} ions are observed respectively (Fig.5.22). Absorption range 1.4µm are noticed due to the presence of water and hydroxyl molecules in the present sample (Ali M.Qaid et al., 2009). library spectrum Amphibolite Schist correlation score 0.878 percent

match the curve (Fig-5.22). Lab spectra of corundum strong absorption range identified in the wavelength of 2.10 µm and 2.20 µm and 0.65 µm representing the mineral corundum shows intense absorption feature in 2.40 µm of the electromagnetic spectrum Maruthi et al., 2018 (Fig-5.22).

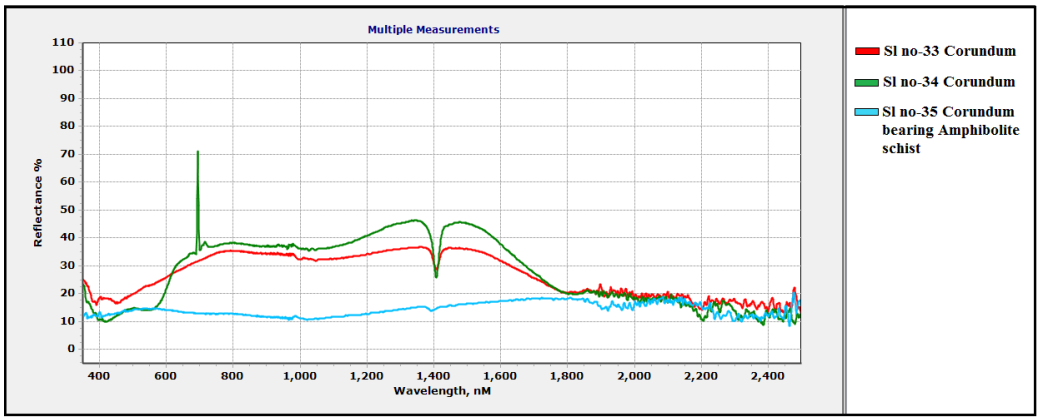

Fig.5.20. Lab Spectral signatures of Corundum bearing rocks.

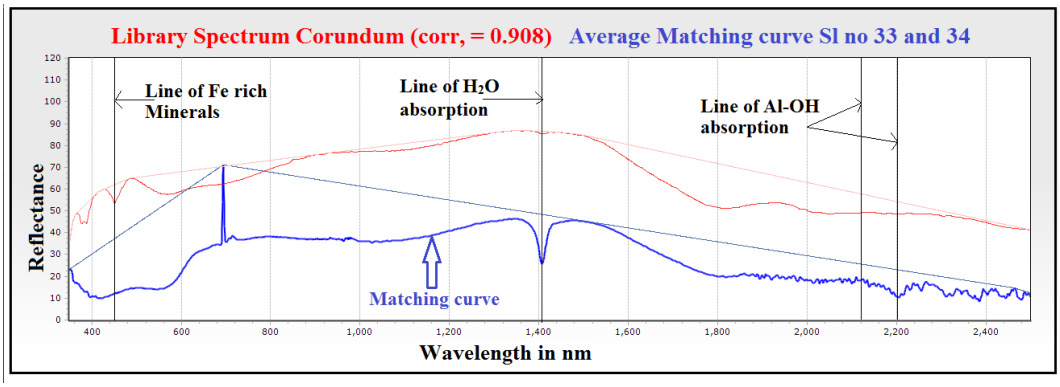

Fig.5.21. Fig.5.6. EZ-ID Match analysis of Corundum.

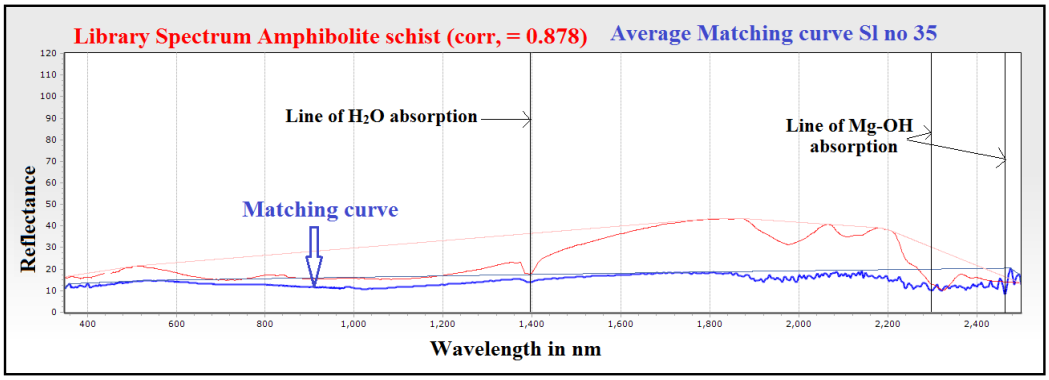

Fig.5.22. EZ-ID Match analysis of Amphibolite schist.

5.10. HYPERSPECTRAL SIGNATURE STUDY ON ROCK SAMPLES AROUND MYSURU DISTRICT.

Hyperspectral remote sensing for mineral targeting carried out spectral radiometer instrument with help of DARwin software measured single and multiple plots. Mysuru area collected around 16 samples carried out spectra each sample taken 4 targeting and Darwin software give the multiple measurement plots (fig.5.23).

EZ-ID mineral identification tool works to taken USGS standard signatures and match the unknown raw mineral data based on mineral structure and composition give the result based on percentage of mineral composition. Hyperspectral signatures determined the graph showing alumina oxide, Fe and H_2O presence in the sample. Corundum Al_2O_3 mineral type - Oxide this sample prepared from crystals that were brownish near the surface and bluish – green near in the interior. Very sharp corundum reflections suggest excellent crystallinity and compostional homogeneity (Absorption anomalies at wavelength regions of 0.55 µm and 0.9 µm of Fe3+ and Fe2+ ions are observed respectively with low reflectance in the VNIR region (Ali M. Qaid et al., 2009) (Fig.5.24). Major element content as Al_2O_3 content shows high range imparts a corundum character with that of high aluminum content. Library spectrum corundum correlation score 0.936 percent match the curve (Fig5.24). composition discussion analysis showed the sample to contain 41.2% to 95.27%Al. 0.34 and 2.55% Cr. 2.61% Fe and 4.26% Si with traces of Ti, V, Mn, Mg, Ca and Cu the iron appears to be present on both ferrous (0.55. 0.45 and 1.1um absorption features) and ferric (0.7. 0.45 and near 0.4um) from the Cr^{3+} ion contributes to the 0.4. 0.55 and 0.7um (emission) features. Spectral discussion Sample plots are correlated with standard USGS Spectral Library using absolute reflectance v/s wavelength which provide strong absorption range in 2.20 µm and 0.65 µm representing the mineral corundum shows intense absorption feature in 2.40 µm of the electromagnetic spectrum (Hunt et al., 1971) (Ali M. Qaid et al., 2009). Major element content as Al_2O_3 content shows high range imparts a corundum character with that of high aluminum content. Library spectrum corundum correlation score 0.936 percent match the curve (Fig.5.24) .

Major and minor element content of amphibolite schist shows SiO_2 ranging 25.12% , MgO content is fairly low and ranges from 10.48%, Al_2O_3 content high ranges 41.21%,

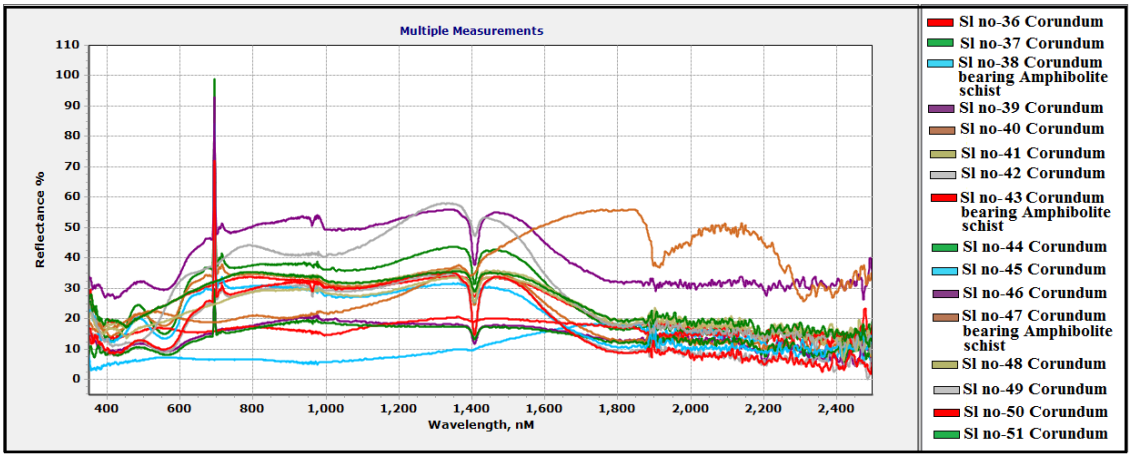

Fig.5.23. Lab Spectral signatures of Corundum bearing rocks.

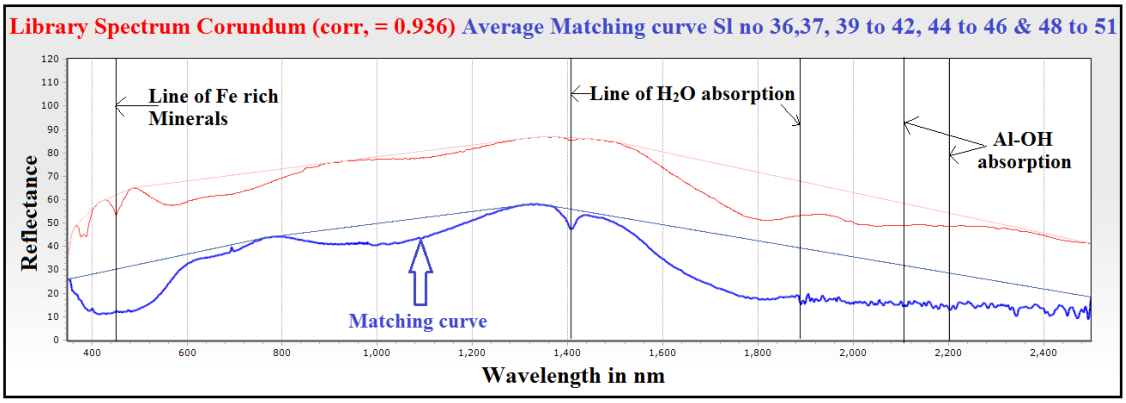

Fig.5.24. Fig.5.6. EZ-ID Match analysis of Corundum.

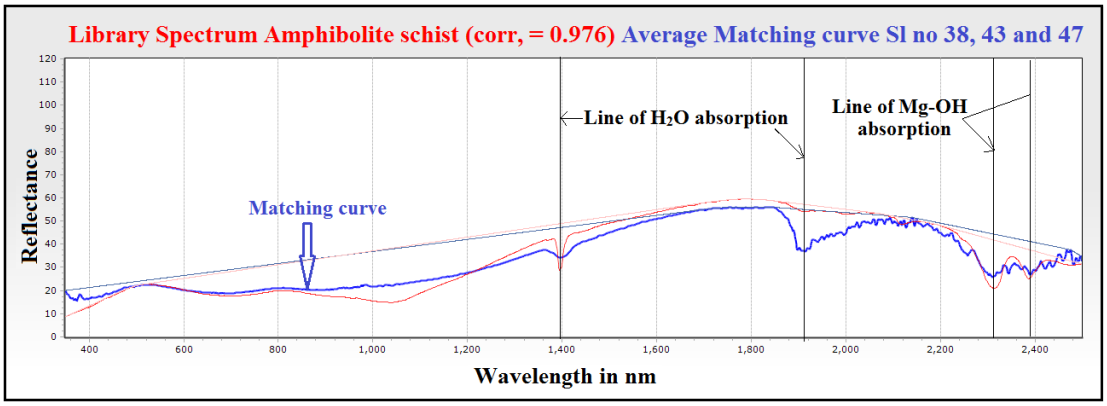

Fig.5.25. EZ-ID Match analysis of Amphibolite schist.

CaO content is 10.43%, K_2O content of ranges 0.137%; TiO_2 content is fairly low 0.484% and P_2O_5 ranges 0.572% (M. Qasim Jan 1988). Spectal discussion Sample plots

provide strong absorption range from 2.0 – 2.25 µm representing the mineral corundum whereas amphibole shows intense absorption feature in 2.35 µm of the electromagnetic spectrum (Hunt et al., 1971). Absorption anomalies at wavelength regions 0.55 µm and 0.9 µm of Fe^{3+} and Fe^{2+} ions are observed respectively (Fig.5.25). Absorption range 1.4µm are noticed due to the presence of water and hydroxyl molecules in the present sample (Ali M.Qaid et al., 2009). library spectrum Amphibolite Schist correlation score 0.976 percent match the curve (Fig-5.25). Lab spectra of corundum strong absorption range identified in the wavelength of 2.10 µm and 2.20 µm and 0.65 µm representing the mineral corundum shows intense absorption feature in 2.40 µm of the electromagnetic spectrum (Hunt et al., 1971) (Fig-5.25).

5.11. HYPERSPECTRAL SIGNATURE STUDY ON ROCK SAMPLES AROUND MANDYA DISTRICT.

Mandya district covers 13 corundum bearing litho units locations. Spectral radiometer instrument with help of DARwin software measured single and multiple plots. Here we took multiple measurement curves of Mandya area samples (fig.5.26).

Hyperspectral signatures determined the graph showing alumina oxide, presence in the sample. Corundum Al_2O_3 mineral type - Oxide this sample prepared from crystals that were brownish near the surface and bluish – green near in the interior and compostional homogeneity. composition discussion EZ-ID match analysis showed the sample to contain Cr, Fe, Al, Si with traces of Ti, V, Mn, Mg, Ca and Cu the iron appears to be present on both ferrous (0.55. 0.45 and 1.1um absorption features) and ferric (0.7. 0.45 and near 0.4um) from the Cr^{3+} ion contributes to the 0.4. 0.55 and 0.7um (emission) features. Spectral discussion Sample plots are correlated with standard USGS Spectral Library using absolute reflectance v/s wavelength which provide strong absorption range in 2.20 µm and 0.65 µm representing the mineral corundum shows intense absorption feature in 2.40 µm of the electromagnetic spectrum (Hunt et al., 1971). Major element content as Al_2O_3 content shows high range imparts a corundum character with that of high aluminum content. Library spectrum corundum correlation score 0.949 percent match the curve (Fig5.27) Amphiboles occur in many metamorphic rocks, especially those derived from mafic igneous rocks (those containing dark-coloured ferromagnesian

minerals) and siliceous dolomites. Major and minor element content of amphibolite schist shows SiO_2, MgO moderate ranging content is fairly low and ranges Al_2O_3 content high ranges CaO, K_2O, TiO_2, and P_2O_5 (M. Qasim Jan 1988). Spectal discussion Sample plots provide strong

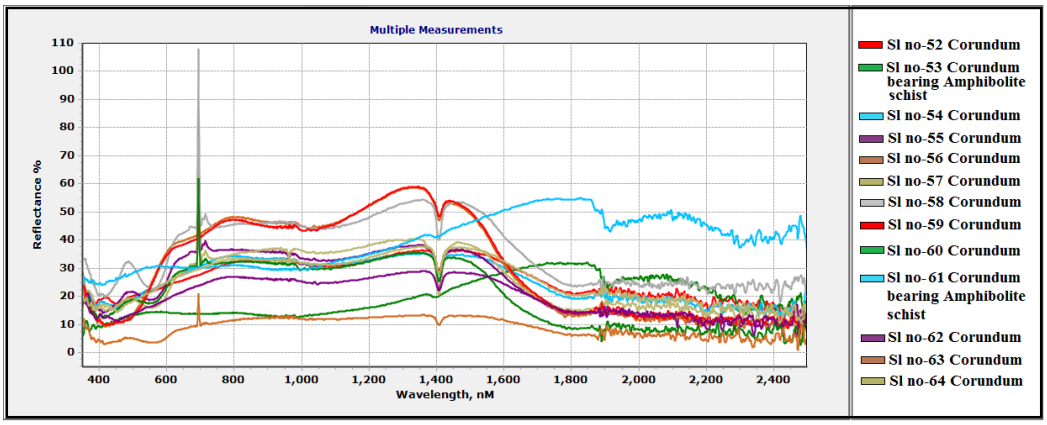

Fig.5.26. Lab Spectral signatures of Corundum bearing rocks.

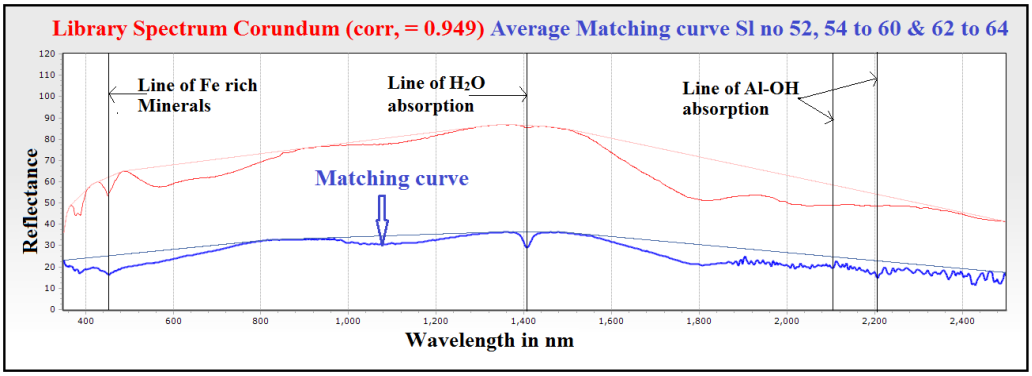

Fig.5.27. Fig.5.6. EZ-ID Match analysis of Corundum.

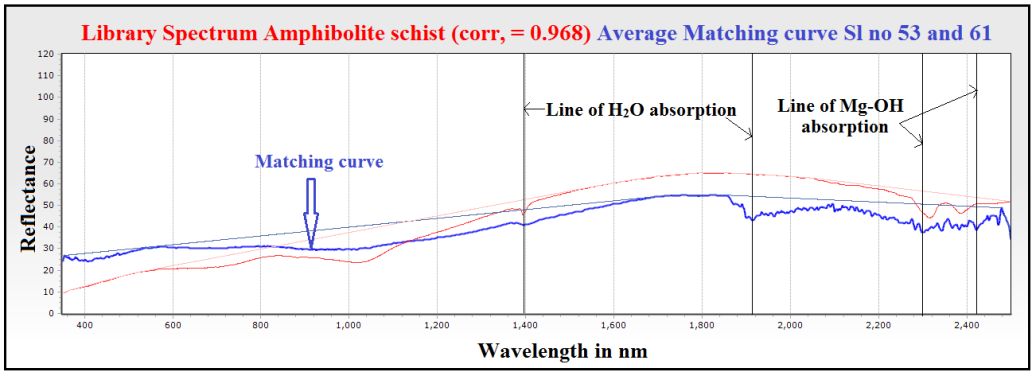

Fig.5.28. EZ-ID Match analysis of Amphibolite schist.

absorption range from 2.0 – 2.25 µm representing the mineral corundum whereas amphibole shows intense absorption feature in 2.35 µm of the electromagnetic spectrum

(Hunt et al., 1971). Absorption range 1.4µm are noticed due to the presence of water and hydroxyl molecules in the present sample (Ali M.Qaid et al., 2009). library spectrum Amphibolite Schist correlation score 0.968 percent match the curve (Fig-5.28). Lab spectra of corundum strong absorption range identified in the wavelength of 2.10 µm and 2.20 µm and 0.65 µm representing the mineral corundum shows intense absorption feature in 2.40 µm of the electromagnetic spectrum (Hunt et al., 1971) (Fig-5.28).

5.12. HYPERSPECTRAL SIGNATURE STUDY ON ROCK SAMPLES AROUND RAMANAGARA DISTRICT.

Ramanagara district covers 7 corundum bearing litho units locations it's a contact zone of closepet granite. Spectral radiometer instrument with help of DARwin software measured single and multiple plots. Here we took multiple measurement curves of Ramanagara area samples (fig.5.29).

Hyperspectral signatures determined the graph showing alumina oxide, presence in the sample. Corundum Al_2O_3 mineral type – Oxide, this sample composition discussion EZ-ID match analysis showed the sample to contain Cr, Fe, Al, Si with traces of Ti, V, Mn, Mg, Ca and Cu the iron appears to be present on both ferrous (0.55. 0.45 and 1.1um absorption features) and ferric (0.7. 0.45 and near 0.4um) from the Cr^{3+} ion contributes to the 0.4. 0.55 and 0.7um (emission) features. Spectral discussion Sample plots are correlated with standard USGS Spectral Library using absolute reflectance v/s wavelength which provide strong absorption range in 2.20 µm and 0.65 µm representing the mineral corundum shows intense absorption feature in 2.40 µm of the electromagnetic spectrum (Hunt et al., 1971). Major element content as Al_2O_3 content shows high range imparts a corundum character with that of high aluminum content. Library spectrum corundum correlation score 0.895 percent match the curve (Fig5.30)

Major and minor element content of amphibolite schist shows SiO_2, MgO moderate ranging content is fairly low and ranges Al_2O_3 content high ranges CaO, K_2O, TiO_2, and P_2O_5 (M. Qasim Jan 1988). Spectal discussion Sample plots provide strong absorption range from 2.0 – 2.25 µm representing the mineral corundum whereas amphibole shows intense absorption feature in 2.35 µm of the electromagnetic spectrum (Hunt et al., 1971).

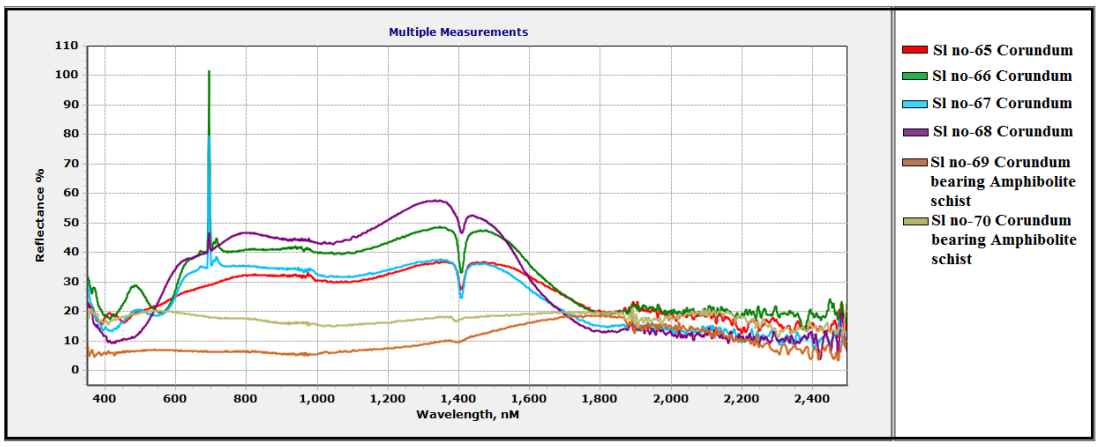

Fig.5.29. Lab Spectral signatures of Corundum bearing rocks.

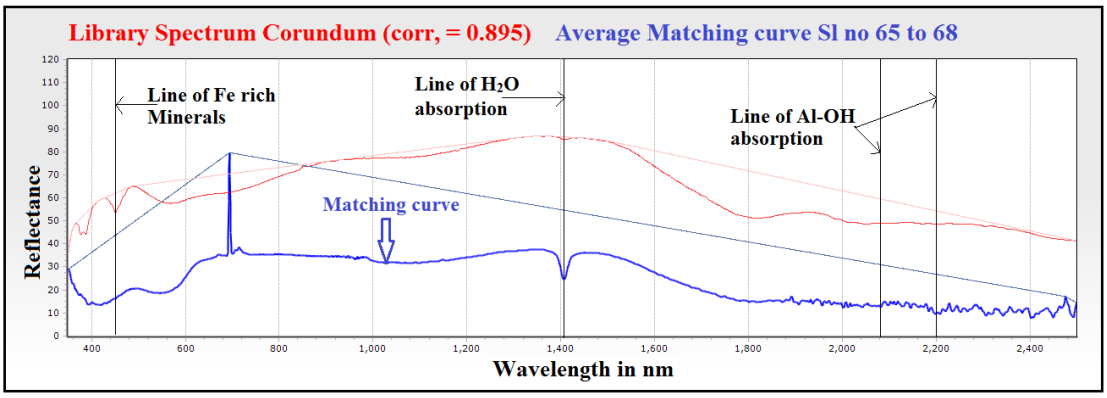

Fig.5.30. Fig.5.6. EZ-ID Match analysis of Corundum.

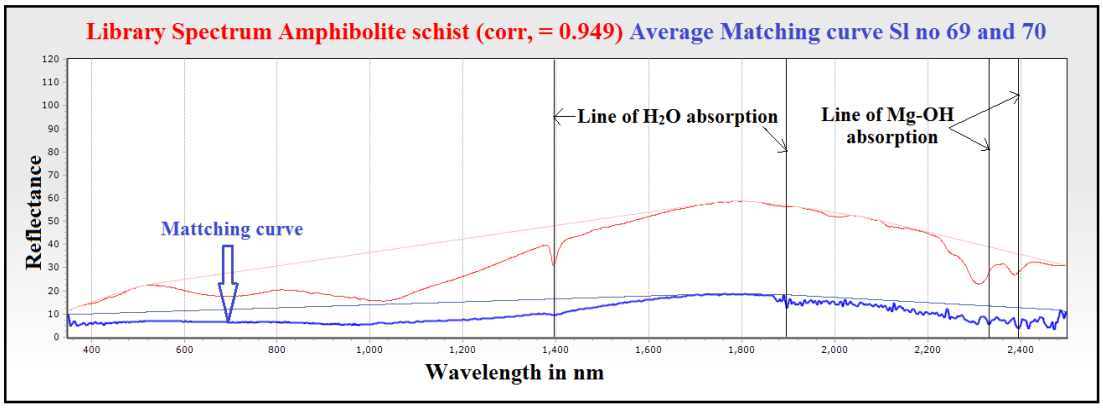

Fig.5.31. EZ-ID Match analysis of Amphibolite schist.

Absorption range 1.4µm are noticed due to the presence of water and hydroxyl molecules in the present sample (Ali M.Qaid et al., 2009). Library spectrum Amphibolite Schist correlation score 0.949 percent match the curve (Fig-5.31). Lab spectra of corundum

strong absorption range identified in the wavelength of 2.10 µm and 2.20 µm and 0.65 µm representing the mineral corundum shows intense absorption feature in 2.40 µm of the electromagnetic spectrum (Hunt et al., 1971) (Fig-5.31).

5.13. HYPERSPECTRAL SIGNATURE STUDY ON ROCK SAMPLES AROUND CHAMARAJANAGARA DISTRICT.

Chamarajanagara area collected 2 corundum bearing litho unit locations. Fe garnet rich Corundum rock occurs Biligirirangan hill ranges and Corundum bearing politic rock occurs Budipadaga area. Spectral radiometer instrument measured single and multiple plots. Here we took multiple measurement curves of Chamarajanagara area samples (fig.5.32).

Pelites is a metamorphosed fine grained sedimentary rocks, its composition of is simple and mostly contains hornblende, plagioclase quartz anthophyllite, garnet and epidote plagioclase and typically include green pyroxene. Corundum bearing politic rock composition discussion EZ-ID match analysis showed the sample to contain Cr, Fe, Al, Si with traces of Ti, V, Mn, Mg, Ca and Cu the iron appears to be present on both ferrous (0.55. 0.45 and 1.1um absorption features) and ferric (0.7. 0.45 and near 0.4um) from the Cr^{3+} ion contributes to the 0.4. 0.55 and 0.7um (emission) features. Spectral discussion Sample plots are correlated with standard USGS Spectral Library using absolute reflectance v/s wavelength which provide strong absorption range in 2.20 µm and 0.65 µm representing the mineral corundum shows intense absorption feature in 2.40 µm of the electromagnetic spectrum (Hunt et al., 1971). Major element content as Al_2O_3 content shows high range imparts a corundum character with that of high aluminum content. Library spectrum corundum bearing politic rock correlation score 0.893 percent match the curve (Fig.5.33)

Fe Garnet rich Corundum rock associated with granulite zones. This sample is slightly contaminated with (spectrally neutral) quartz (Wilbur et al., 1990). It displays typically opaque behavior, decreasing in reflectivity with decreasing particle size. It is unusual in that it also exhibits a very weak band near 1.0µm due to the ferrous ion (Friedman et al,. 1989). This sample shows SiO_2, MgO moderate ranging content is fairly low and ranges Al_2O_3 content high ranges CaO, K_2O, TiO_2, and P_2O_5 (M. Qasim Jan 1988). Spectal discussion Sample plots provide strong absorption range from 2.0 – 2.25 µm representing

the mineral corundum whereas amphibole shows intense absorption feature in 2.35 µm of the electromagnetic spectrum (Hunt et al., 1971). Library spectrum Fe Garnet rich Corundum rock correlation score 0.911 percent match the curve (Fig-5.34).

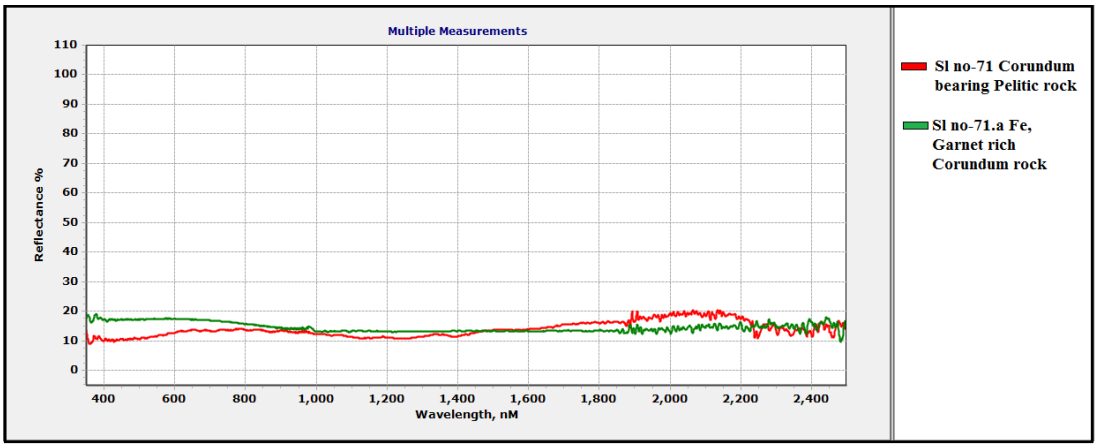

Fig.5.32. Lab Spectral signatures of Corundum bearing rocks.

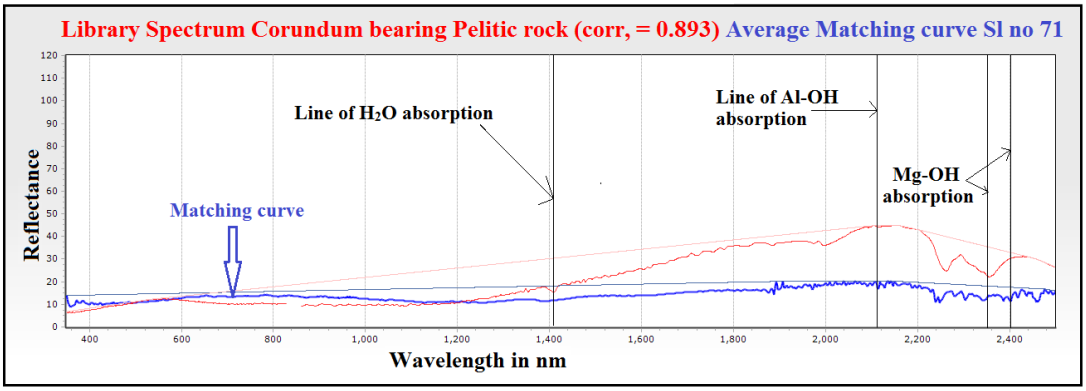

Fig.5.33. Fig.5.6. EZ-ID Match analysis of Corundum bearing pelitic rock.

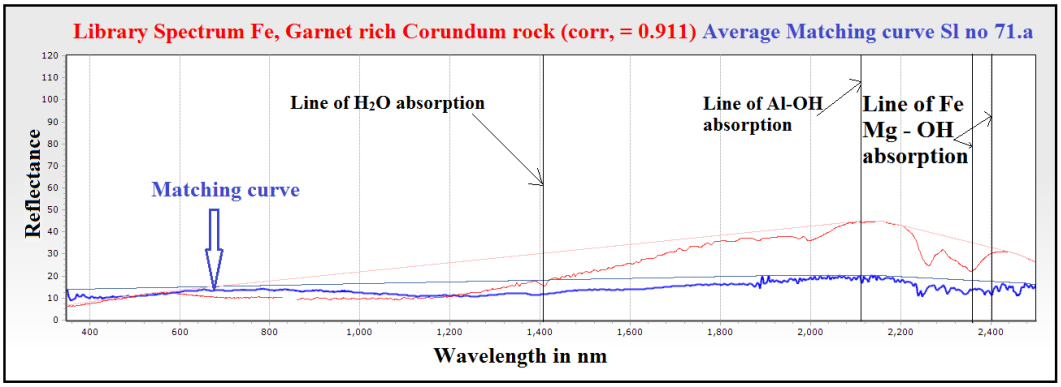

Fig.5.34. EZ-ID Match analysis of Fe garnet rich corundum.

5.14. HYPERSPECTRAL SIGNATURE STUDY ON ROCK SAMPLES AROUND KOLARA DISTRICT.

Kolara area collected 3 corundum bearing litho unit locations. Corundum rock occurs Yelesandra and Kammasandra area, Corundum bearing mica schist occurs near Kammasandra area. Spectral radiometer instrument measured single and multiple plots. Here we took multiple measurement curves of Kolara area samples (fig.5.35).

Hyperspectral signatures determined the graph showing alumina oxide, presence in the sample. Corundum Al_2O_3 mineral type – Oxide, this sample composition discussion EZ-ID match analysis showed the sample to contain Cr, Fe, Al, Si with traces of Ti, V, Mn, Mg, Ca and Cu the iron appears to be present on both ferrous (0.55. 0.45 and 1.1um absorption features) and ferric (0.7. 0.45 and near 0.4um) from the Cr^{3+} ion contributes to the 0.4. 0.55 and 0.7um (emission) features. Spectral discussion Sample plots are correlated with standard USGS Spectral Library using absolute reflectance v/s wavelength which provide strong absorption range in 2.20 µm and 0.65 µm representing the mineral corundum shows intense absorption feature in 2.40 µm of the electromagnetic spectrum (Hunt et al., 1971). Major element content as Al_2O_3 content shows high range imparts a corundum character with that of high aluminum content. Library spectrum corundum correlation score 0.941 percent match the curve (Fig.5.36)

Major and minor element content of Corundum bearing Amphibolite schist shows MgO, SiO_2 moderate ranging content is fairly low and ranges Al_2O_3 content high ranges K_2O, CaO, TiO_2, and P_2O_5 (M. Qasim Jan 1988). Spectal discussion Sample plots provide strong absorption range from 2.0 – 2.25 µm representing the mineral corundum whereas amphibole shows intense absorption feature in 2.35 µm of the electromagnetic spectrum (Hunt et al., 1971). Absorption range 1.4µm are noticed due to the presence of water and hydroxyl molecules in the present sample (Ali M.Qaid et al., 2009). Library spectrum Amphibolite Schist correlation score 0.853 percent match the curve (Fig-5.37). Lab spectra of corundum strong absorption range identified in the wavelength of 2.10 µm and 2.20 µm and 0.65 µm representing the mineral corundum shows intense absorption feature in 2.40 µm of the electromagnetic spectrum (Hunt et al., 1971) (Fig-5.37).

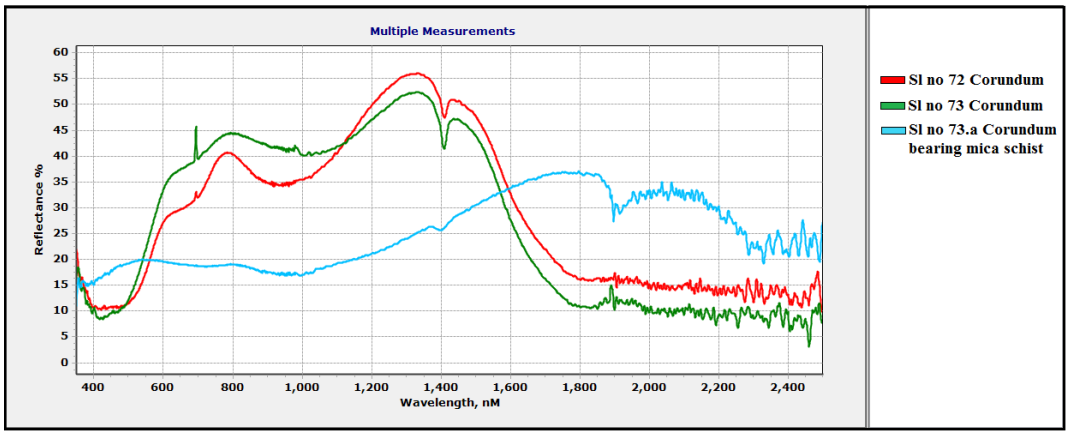

Fig.5.35. Lab Spectral signatures of Corundum bearing rocks.

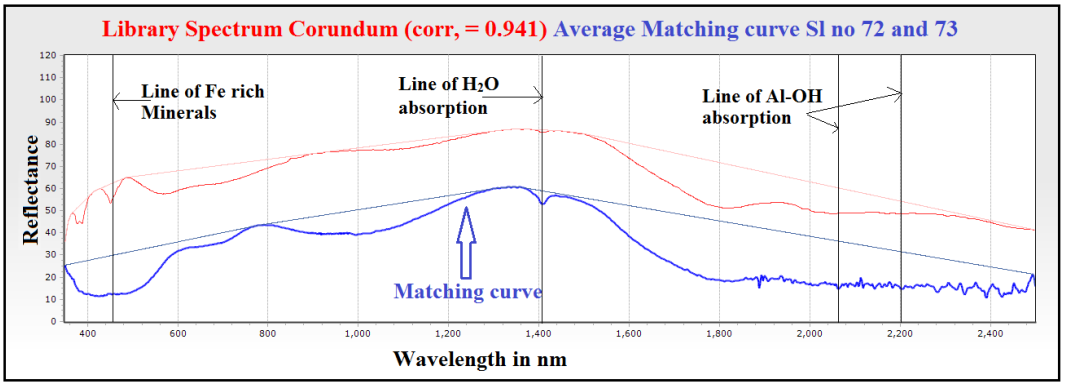

Fig.5.36. Fig.5.6. EZ-ID Match analysis of Corundum.

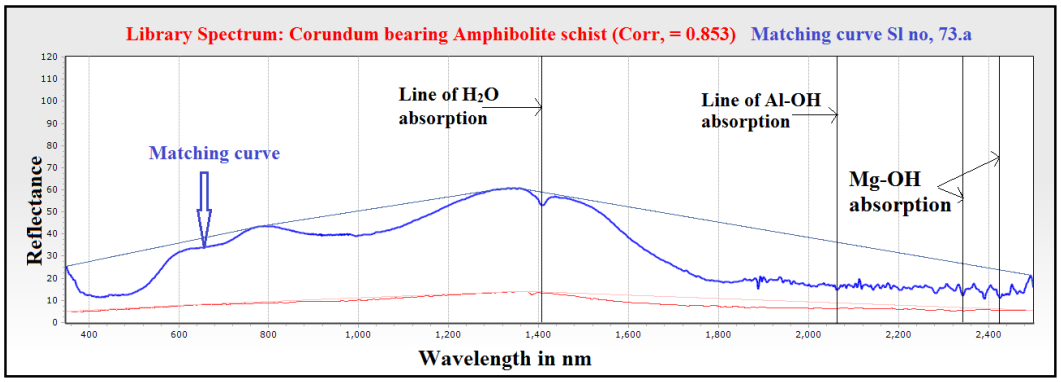

Fig.5.37. EZ-ID Match analysis of Amphibolite schist.

CHAPTER-VI

6.1. RESULT AND DISCUSSION

Corundum bearing litho units are located in the state of Karnataka. its consist major schist belts, migmatite zones, younger closepet granite zone and granulate terrains. Study area comes to southern Karnataka region and its covers 20 districts. The purpose of the present study is infer the petrology, geochemistry and spectral behavior of corundum bearing rocks collected from the Study area Karnataka. Corundum is formed upper mantle with high presser and temperature condition with help of magma and magma flumes corundum reaches to surface. Corundum is a rock forming mineral that is found in Igneous, Sedimentary and Metamorphic rocks and it has hexagonal crystal structure, it is second hardest mineral after diamond (Basavarajappa et al., 2018). The corundum shows similar color appearance in both plane and crossed polarized lights. Corundum is depicted by pink to blood-red colored and can vary within each gem variety of the mineral Corundum. The red color is caused by the mineral chromium and shows brownish tone due to the presence of iron. Optical properties shows uniaxial, birefringence & pleochroism is very strong in ordinary light and shows deep red color when viewed in the direction of vertical axis and a much lighter color to nearly colorless in view at right angles to this axis. In all 73 locations we have traced out the corundum in the form of 99% of Al with impurities of variety of Corundum minerals in the Study area. Results of demarcating the Corundum horizons in the map using Field petrography, Geochemical signatures (XRF), EDS study and Hyperspectral study, Remote Sensing technology with GIS tools Correlate and composition to analyze and integrate the Study involved in the research to achieve the final results in the Proposed Research problem.

Karnataka before 2005 corundum deposits found only 15890 tonne, after 2010 these kind of research work and ground truth checking finally corundum deposits found 646860 tonnes. This estimation shows we need more research on precious minerals, gemstones and metals.

6.2. INTIGRATION OF GEOCHEMISTRY AND REFLECTANCE SPECTRA

X-Ray Fluorescence (XRF) analysis was carried out to estimate the major oxides in the Corundum bearing rocks. The chemical composition of major and minor oxides of southern Karnataka region corundum, corundum bearing amphibolites schist, corundum bearing chlorite schist and corundum bearing pelitic rocks and contact of Closepet granites and other litho units of the study area are presented in Table.6.1 and 6.2. Aluminum, silicates, Fe and chromium oxides are the four major oxides normally dominated in corundum composition. The percentages of these four oxides are aluminum high is considered as a perfect analog composition for corundum bearing rocks. Slightly observed southern Karnataka corundum composed and associated with metamorphic rock geochemical data proves genesis of corundum deposits under deep seated that time mafic magma along with corundum tacked out and cooled in subsurface then tectonic activity of uplifment may happen Corundum bearing rocks seen in surface in the form of outcrops of the study area.

Spectral reflectance measurements were being conducted as an additional tool to determine surface mineralogical composition of corundum bearing litho units and oxides through Remote Sensing Technique. The absorption features of specific rock forming minerals in the spectral range of 0.35 to 2.5 μm were studied in detail by several workers Adams and McCord, 1973; Adams 1974, 1975; Hunt and Salisbury 1977, Adams, 1977; Charette., 1982; Pieters, 1986; Ali et al., 2008; Manjunatha and Basavarajappa., 2017; Ranjendran et al., 2018; Jeeven and Basavarajappa., 2018; Maruthi and Basavarajappa., 2018; Maruthi et al., 2018; Basavarajappa et al., 2018; Basavarajappa et al., 2019. Such reflectance measurements were made for the corundum surface using laboratory spectrometers. Spectral curves measures corundum wavelength/ reflectance of 2.10, 2.20, 2.40 0.65, 1.4, 1.9nm and corundum bearing amphibolie schist reflectance curve observation 2.10, 2.20, 2.40, 0.65, 0.88, 1.4, 1.9, 2.25, 2.35nm.

The present study understanding the corundum bearing litho units of petrology, geochemistry, mineralogy, Remote Sensing and spectral reflectance, integration of spectral and geochemical data given table 6.1 and 6.2 district wise calculating and average of all major elements and correlate the spectral data. Corundum at Chitradurga,

Tumakur, Chikballapura, Hassan, Chikmagalur, Dakshina Kannada, Mysuru, Mandya Ramanagara, Chamarajanagara and Kolar of southern Karnataka area Samples plots are correlated with standard USGS Spectral Library using absolute reflectance v/s wavelength which provide strong absorption range in 0.65 µm and 2.20 µm representing the mineral Corundum shows intense absorption feature in 2.40 µm of the electromagnetic spectrum (Hunt et al., 1971).

Absorption anomalies at wavelength regions of 0.55 µm and 0.9 µm of Fe^{3+} and Fe^{2+} ions are observed respectively with low reflectance in the VNIR region (Ali M. Qaid et al., 2009). The chemical analysis of corundum shows the distribution of major element content as Al_2O_3 content shows high range from 75.81% to 87.69%; and minor content as SiO_2 ranging between 1.31% and 3.53%; MgO content is fairly low, CaO content ranges from 0.99% to 4.82%; K_2O content ranges from 0.09% to 0.58%; TiO_2 content is fairly low and varies from 0.3% to 1.96%; P_2O_5 ranges from 0.35% to 0.86%. High Al_2O_3 (>80%), SiO_2 (>3%) and low TiO_2 (0.86%) content imparts a corundum character with that of high aluminum content (Table.6.1).

Corundum bearing amphibolites schist at Chitradurga, Tumakur, Chikballapura, Hassan, Chikmagalur, Dakshina Kannada, Mysuru, Mandya Ramanagara, Chamarajanagara and Kolar area Sample plots provide strong absorption range from 2.0 – 2.25 µm representing the mineral corundum whereas amphibole shows intense absorption feature in 2.35 µm of the electromagnetic spectrum (Hunt et al., 1971). Absorption anomalies at wavelength regions 0.55 µm and 0.9 µm of Fe^{3+} and Fe^{2+} ions are observed respectively . Absorption range from 1.4 – 1.9 µm are noticed due to the presence of water and hydroxyl molecules in the present sample (Ali M.Qaid et al., 2009). Major and minor element content of amphibolite schist shows SiO_2 ranging between 18.12% and 62.6%; MgO content is fairly low and ranges from 0.25% to 16.64%; Al_2O_3 content high ranges from 23.65% to 38.21%; CaO content is 0.35% to 10.11%; K_2O content of ranges from 0.1% to 7.44%; TiO_2 content is fairly low and varies from 0.25% to 1.01% and P_2O_5 ranges from 0.032% to 0.88% (Table.6.2).

This integration study compare the geochemical data and hyperspectral data, it's give the result outstanding performance of software work and ground truth checking is 95%

correlated geochemical data and hyperspectral laboratory data. Further studies hyperspectral instrument helps to identifying unknown minerals need not to geochemical data EZ-ID tool explain everything including percentage of composition also, table 6.1 and 6.2.

In future hyperspectral satellite data (hiperion and ali) using spectral signatures known area to unknown area it's given 99% result after band combination color enhancing particular minerals using ENVI software find the results.

Table.6.1. Integration of Geochemical data and Spectral Analysis of Corundum samples of the Study area

Chemical Elements Sample numbers		Corundum Samples									
		Chitradurga 1 -2	Tumakur 3-4,6-8,10-15	Chikballapura 16-19 and 21	Hassan 22,23,26&27	Chikmagalur 28 - 30	Dakshina Kannada 33 &34	Mysuru 36 - 51	Mandya 52 - 64	Ramanagara 65 - 68	Kolara 72 - 73
Average Elements wt%	SiO_2	17.68	11.42	10.98	15.62	14.09	16.75	7.3	11.77	13.03	19.43
	Al_2O_3	*72.84*	*81.37*	*81.64*	77.34	79.83	75.82	87.69	82.66	80.76	75.81
	Fe_2O_3	3.53	2.72	3.04	1.31	1.43	1.03	1.12	1.53	2.15	1.49
	CaO	1.16	1.2	1.06	4.26	1.43	4.82	0.98	1.07	0.99	1.06
	MgO	0	0	0	0	0	0	0	0	0	0
	K_2O	0.58	0.26	0.23	0.09	0.18	0.3	0.18	0.21	0.22	0.22
	Cr_2O_3	0.91	0.29	0.25	0.17	0.56	0.16	1	0.24	0.29	0.3
	TiO_2	1.96	1.65	1.7	0.47	1.34	0.3	0.81	1.29	1.45	1.64
	MnO	0.11	0.04	0.04	0.01	0.04	0.34	0.08	0.05	0.06	0.06
	P_2O_5	0.86	0.59	0.59	0.35	0.63	0.22	0.32	0.67	0.7	0.43
	Total	99.79	99.54	99.53	99.62	99.53	99.74	99.48	99.49	99.65	100.44
Rock type		Corundum	Corundum	Corundum	Corundum	Corundum	Corundum	Corundum	Corundum	Corundum	Corundum
Spectral Analysis											
Correlation score	EZ-ID	0.854	0.933	0.902	0.941	0.877	0.908	0.936	0.949	0.895	0.941
Absorption spectra (µm)	Lab spectral signature	2.10, 2.20, 2.40 0.65, 1.4, 1.9	2.10, 2.20, 2.40 0.65, 1.4, 1.10	2.10, 2.20, 2.40 0.65, 1.4, 1.11	2.10, 2.20, 2.40 0.65, 1.4, 1.12	2.10, 2.20, 2.40 0.65, 1.4, 1.13	2.10, 2.20, 2.40 0.65, 1.4, 1.14	2.10, 2.20, 2.40 0.65, 1.4, 1.15	2.10, 2.20, 2.40 0.65, 1.4, 1.16	2.10, 2.20, 2.40 0.65, 1.4, 1.17	2.10, 2.20, 2.40 0.65, 1.4, 1.18
Best matches to	USGS	Corundum	Corundum	corundum	corundum	corundum	corundum	corundum	corundum	corundum	corundum

Table.6.2. Integration of Geochemical data and spectral analysis of corundum bearing litho units of the Study area

Chemical Elements Sample numbers		Corundum bearing Amphibolite schist and other Samples									
		Chitradurga 2.a	Tumakur 5 and 9	Chikballapura 20 and 22	Hassan 24 and 25	Chikmagalur 31 and 32	Dakshina Kannada 35	Mysuru 38, 43& 47	Mandya 53 & 61	Ramanagara 69 & 70	Chamarajanagara 71 & 71.a
Avarage Elements wt%	SiO_2	40.21	62.6	62.38	31.56	22	18.12	24.84	36.71	35.19	39.1
	Al_2O_3	*32.86*	*23.65*	23.78	29.16	29.85	38.21	37.45	37.36	30.95	32.89
	Fe_2O_3	5.98	1.88	3.343	10.58	9.59	12.121	16.58	5.51	9.92	11.953
	CaO	8.43	0.35	1.281	10.11	8.77	10.566	7.88	7.94	8.49	2.624
	MgO	10.12	6.47	0.255	16.64	10.17	10.476	9.8	10.17	11.13	7.333
	K_2O	0.42	0.21	7.419	0.25	0.13	0.147	0.1	0.41	0.13	3.643
	Cr_2O_3	0.002	0	0	0.1	6.68	8.559	1.42	0.002	2.44	0.076
	TiO_2	1.01	0.29	0.256	0.08	0.53	0.384	0.28	0.68	0.62	0.82
	MnO	0.67	0.18	0.029	0.16	0.16	0.17	0.33	0.03	0.11	0.181
	P_2O_5	0.032	0.84	0.723	0.68	0.44	0.562	0.59	0.5	0.63	0.881
	Total	99.32	96.47	99.46	99.32	88.32	99.31	99.27	99.31	99.61	99.5
Rock type		Corundum bearing Amphibolite schist	Corundum bearing Closepet granite	Corundum bearing Closepet granite	Corundum bearing Amphibolite schist	Corundum bearing Amphibolite schist	Corundum bearing Amphibolite schist	Corundum bearing Amphibolite schist	Corundum bearing Amphibolite schist	Corundum bearing Amphibolite schist	Corundum bearing Pelitic rock
Spectral Analysis											
Absorption spectra (µm)	Lab spectral signature	2.10, 2.20, 2.40, 0.65, 0.88, 1.4, 1.9, 2.25, 2.35,	2.10, 2.20, 2.40, 0.65, 0.88, 1.4, 1.9, 2.25, 2.35,	2.10, 2.20, 2.40, 0.65, 0.88, 1.4, 1.9, 2.25, 2.35,	2.10, 2.20, 2.40, 0.65, 0.88, 1.4, 1.9, 2.25, 2.35,	2.10, 2.20, 2.40, 0.65, 0.88, 1.4, 1.9, 2.25, 2.35,	2.10, 2.20, 2.40, 0.65, 0.88, 1.4, 1.9, 2.25, 2.35,	2.10, 2.20, 2.40, 0.65, 0.88, 1.4, 1.9, 2.25, 2.35,	2.10, 2.20, 2.40, 0.65, 0.88, 1.4, 1.9, 2.25, 2.35,	2.10, 2.20, 2.40, 0.65, 0.88, 1.4, 1.9, 2.25, 2.35,	2.10, 2.20, 2.40, 0.65, 0.88, 1.4, 1.9, 2.25, 2.35,
Correlation score	EZ-ID	0.983	0.883	0.821	0.943	0.941	0.878	0.976	0.968	0.949	0.893
Best matches to	USGS	Amphibole, Corundum	Amphibole, Corundum	Amphibole, Corundum	Amphibole, Corundum	Amphibole, Corundum	Amphibole, Corundum	Amphibole, Corundum	Amphibole, Corundum	Amphibole, Corundum	Amphibole, Corundum

6.3. Energy – Dispersive X-ray Specctroscopy (EDS)

Fig.6.1. EDS instrument UOM

Energy dispersive X-ray spectroscopy (EDS, EDX, EDXS OR XEDS). sometimes called energy dispersive X ray analysis (EDXA) or energy dispersive X-ray microanalysis (EDXMA), is an analytical technique used for the elemental analysis or chemical characterization of a sample (Severin Kenneth., 2004). it relies on an interaction of some source of X-ray excitation and a sample. its characterization capabilities are due in large part to the fundamental principle that each element has a unique atomic structure allowing a unique set of peaks on its electromagnetic emission spectrum (PinakiSengupta et al., 2008).

Interaction of an electron beam with a sample target produces a variety of emissions, including x-rays (Severin Kenneth., 2004). An energy-dispersive (EDS) detector is used to separate the characteristic x-rays of different elements into an energy spectrum, and EDS system software is used to analyze the energy spectrum in order to determine the abundance of specific elements (Goldstein., 2003). EDS can be used to find the chemical composition of materials down to a spot size of a few microns, and to create element composition maps over a much broader raster area (Reimer., 1998). Together, these capabilities provide fundamental compositional information for a wide variety of materials (Egerton., 2005).

An element map is an image showing the spatial distribution of elements in a sample. because it is acquired from a polished section, it is a 2D section through the unknown sample. Element maps are extremely useful for displaying element distributions in textural context, particularly for showing compositional zonation (Santos and Brandno, 2005). one can use either an EDS or WDS system to produce an element map either way, the image is produced by progressively rastering the electron beam point by point over an area of interest (Clarke., 2002). Think of element map as a pixel by pixel (bitmap) image based on chemical elements. Resolution is determined by how long the beam dwells on

each point (and of course the actual concentration). Greater distinction can be made by longer analysis, but at the cost of time. In many cases, adequate element maps can be acquired by EDS system (Clarke., 2002). This is typically a faster approach, but sacrifices resolution and detection limits. the best element maps are acquired using a WDS system on an electron microscope, but the trade-off in using the spectrometers is longer acquisition time (PinakiSengupta et al., 2008).

6.4. EDS ANALYSIS AND ELEMENTAL MAP OF CORUNDUM BEARING ROCK AROUND CHITRADURGA DISTRICT

Corundum bearing rock has high aluminum content and other elements also the present study helps to better understanding chemical composition of rock with help of EDS instrument (Hitachi S-3400N 5.00 kV model EVO LS15). EDS Analysis is a great method for determining particle sizes and elemental composition. It is also a go-to analytical technique for performing Nano characterization. Not only that, used in conjunction with EDS it is possible to compare different chemical compositions between each layer. The topography of films can at times mask the number of film layers in a sample (Santos and Brandno, 2005). Energy Dispersive X-ray Spectroscopy (EDS) as an analysis method, corundum shows EDS lines at similar energies detect the chemical composition of Al, Si, Ca, Cr, Cl, C and O, percentage of aluminum presence in 20.70% and atom 12.78% (Fig.6.1)(Table.6.3). The EDS technique detects x-rays emitted from the sample during bombardment by an electron beam to characterize the elemental composition of the analyzed volume. Features or phases as small as 0.01 μm or less can be analyzed. keep the electron beam stationary on a spot or series of spots and generate spectra that will provide more localized elemental information, have the electron beam follow a line drawn on the Corundum sample image and generate a plot of the relative proportions of previously identified elements along that spatial gradient, defined elements over the scanned area identify the elements of Al, Si, Ca, Cr, C and O (Fig.6.1) (Table.6.3).

Elemental map its easily understanding the percentage of chemical composition and which part is more aluminum content of particular sample, in this chitradurga region sample EDS can be used in semi-quantitative mode to determine chemical composition

by peak-height ratio relative to a standard. This sample more in Al and O content and other elements of Si, Ca, Cr, Cl and C, aluminum atomic number 13 and its atomic mass 26.982 is x-ray counts 1639 times its high energy observed in this map (Fig.6.2).

Table.6.3. Phase fractions (wt %) Corundum composition measured by EDS

Element Line	Weight %	Weight % Error	Atom %
C- K	16.44	± 0.57	22.80
O- K	61.19	± 0.47	63.71
Al -K	20.70	± 0.19	12.78
Si -K	0.38	± 0.06	0.23
Cl- K	0.27	± 0.04	0.13
Ca- K	0.28	± 0.04	0.12
Ca- L	---	---	---
Cr -K	0.73	± 0.09	0.23
Total	100.00		100.00

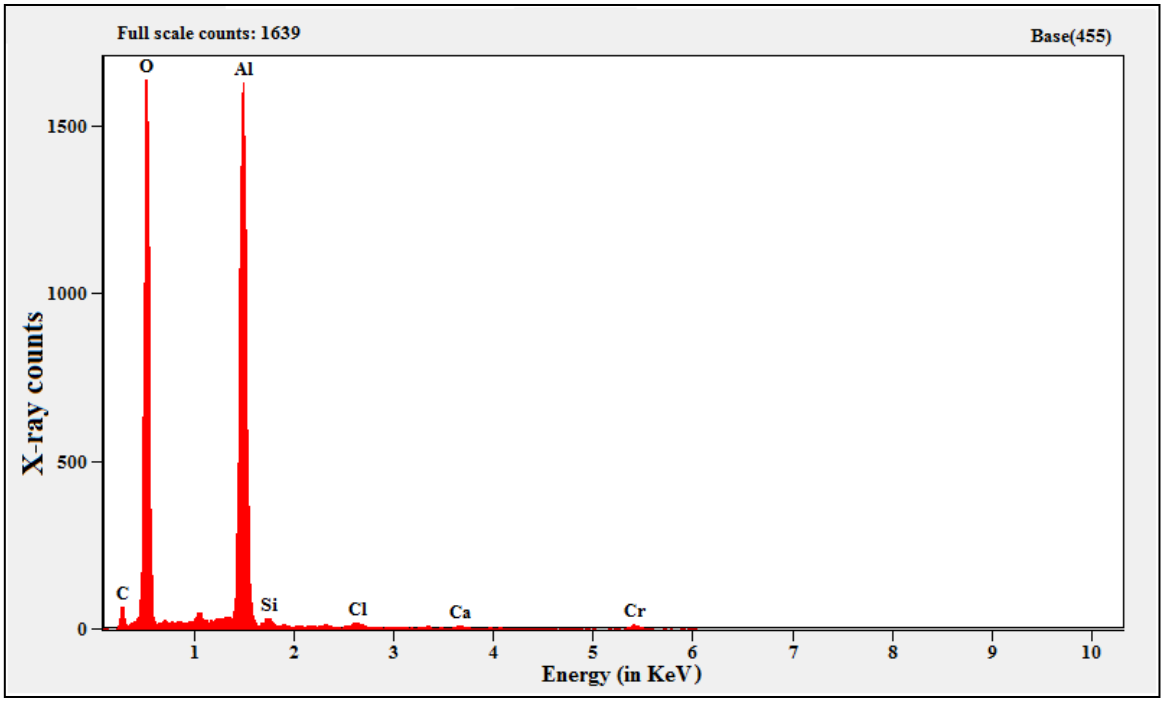

Fig.6.2. EDS spectrum Corundum rock of Chitradurga region.

Typical EDS spectrum: y-axis depicts the number of counts and x-axis the energy (in KeV) of the X-rays. The position of the peaks leads to the identification of the elements and the peak height helps in the quantification of each element's concentration in the Corundum sample (Fig.6.2).

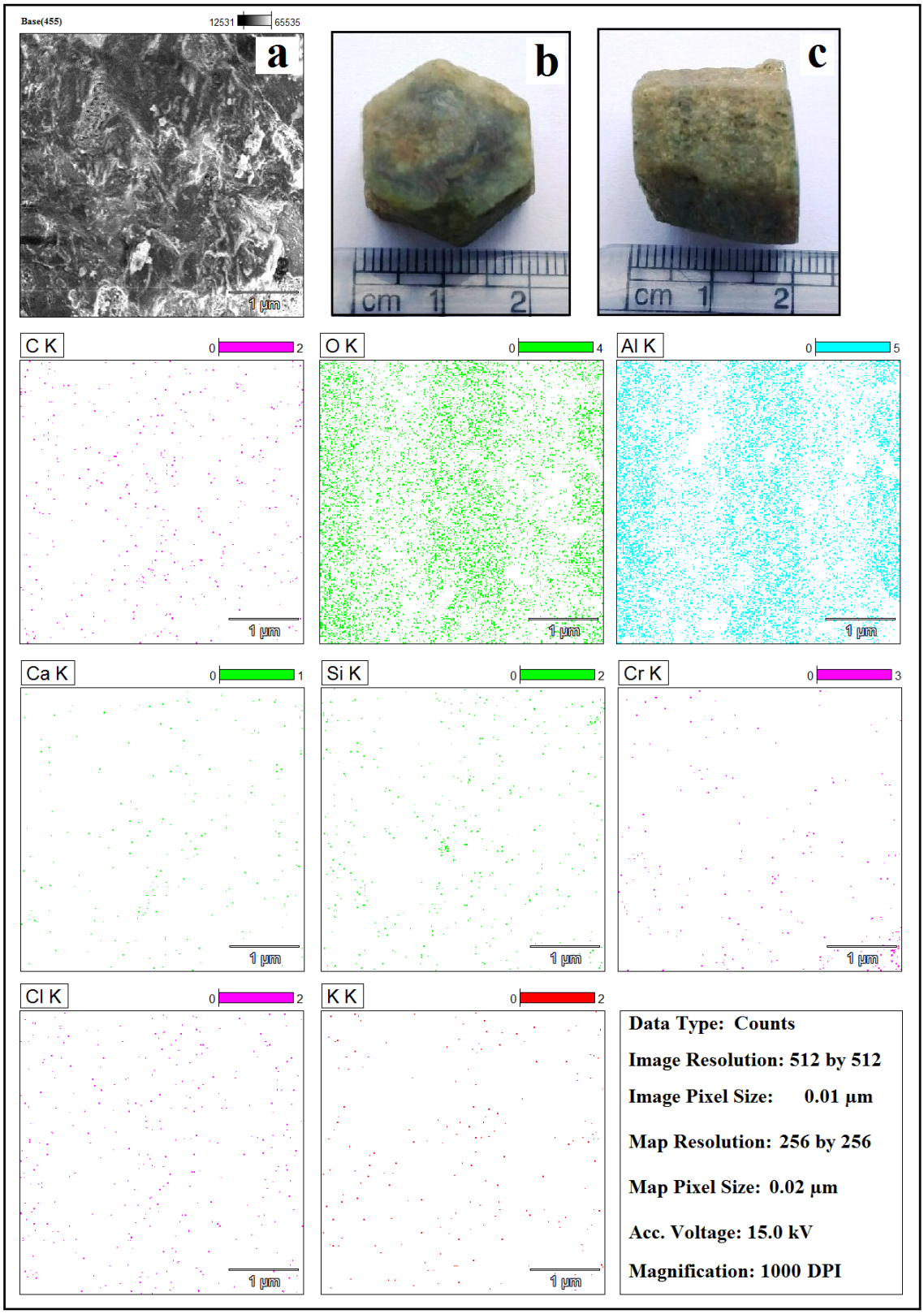

Fig.6.3. Elemental map of Corundum sample, (a) polished surface EDS image, (b) polished sample (c) field sample of corundum.

6.5. EDS ANALYSIS AND ELEMENTAL MAP OF CORUNDUM BEARING ROCK AROUND TUMKUR DISTRICT

EDS analysis take over the Tumkur region corundum sample its Phase fractions Corundum composition measured we seen (Table.6.4). Its shows elements and their weight percentage and atom percentage, here O, Al and C is more composition in this sample (Table.6.4). The graph shows x and y axis is measured x-ray counts and energy, Al, 2006 X-ray counts observed, results shows high energy alumina content presence in Tumkur region corundum sample (fig.6.4).

Table.6.4. Phase fractions (wt%) Corundum composition measured by EDS

Element Line	Weight %	Weight % Error	Atom %
C- K	19.82	± 0.52	26.62
O -K	61.89	± 0.43	62.40
Na- K	0.83	± 0.10	0.58
Al- K	16.83	± 0.16	10.06
Si -K	0.40	± 0.05	0.23
Cl -K	0.24	± 0.03	0.11
Total	100.00		100.00

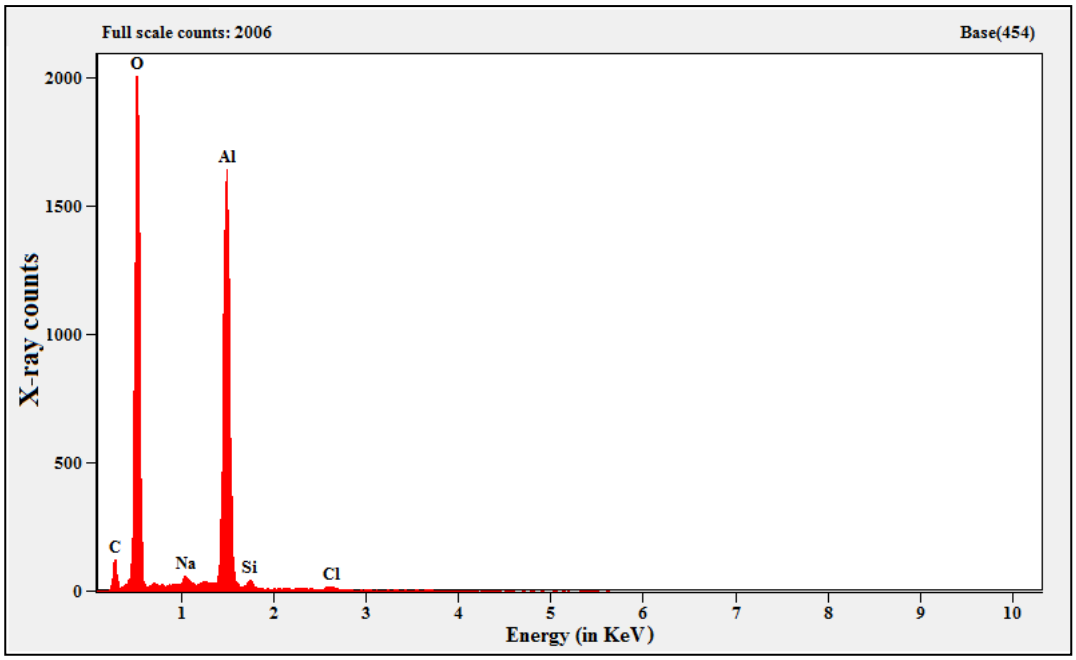

Fig.6.4. EDS spectrum Corundum rock of Tumkur region.

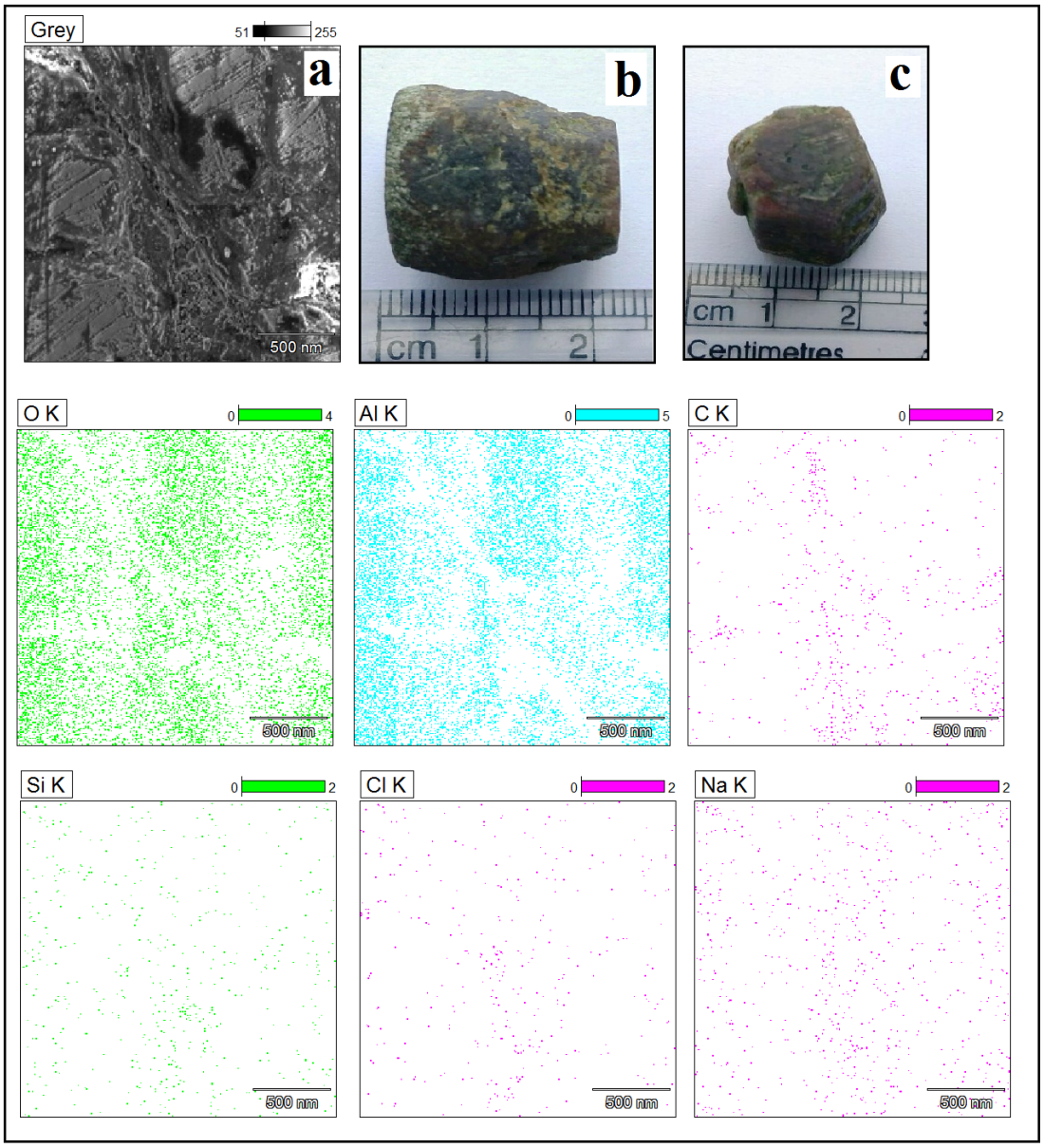

Fig.6.5. Elemental map of Corundum sample, (a) polished surface EDS image, (b) field sample of corundum (c) polished sample.

Elemental map its easily understanding the percentage of chemical composition and which part is more aluminum content of particular sample, in this Tumkur region sample EDS can be used in semi-quantitative mode to determine chemical composition by peak-height ratio relative to a standard. This sample more in Al, O and C content and other elements of Si, Ca, Na and Cl aluminum atomic number 13 and its atomic mass 26.982 is x-ray counts 1639 times its high energy observed in this map (Fig.6.5).

6.6. EDS ANALYSIS AND ELEMENTAL MAP OF CORUNDUM BEARING ROCK AROUND MYSURU DISTRICT

EDS analysis result take over the Mysuru district corundum sample its Phase fractions Corundum composition measured we seen (Table.6.5). Its shows elements and their weight percentage and atom percentage, here Al & O, is more composition observed in this sample and minor elements observed C, Na, Si and Cl (Table.6.5).

The graph shows x and y axis is measured x-ray counts and energy, Al, 1459 X-ray counts observed, results shows high energy alumina content presence in Mysuru District corundum bearing rock (fig.6.6).

Table.6.5. Phase fractions (wt%) Corundum composition measured by EDS

Element Line	Weight %	Weight % Error	Atom %
C -K	7.93	± 0.90	11.82
O- K	59.34	± 0.62	66.41
Na- K	1.08	± 0.15	0.84
Al -K	30.34	± 0.28	20.13
Si- K	0.97	± 0.10	0.62
Cl- K	0.34	± 0.06	0.17
Total	100.00		100.00

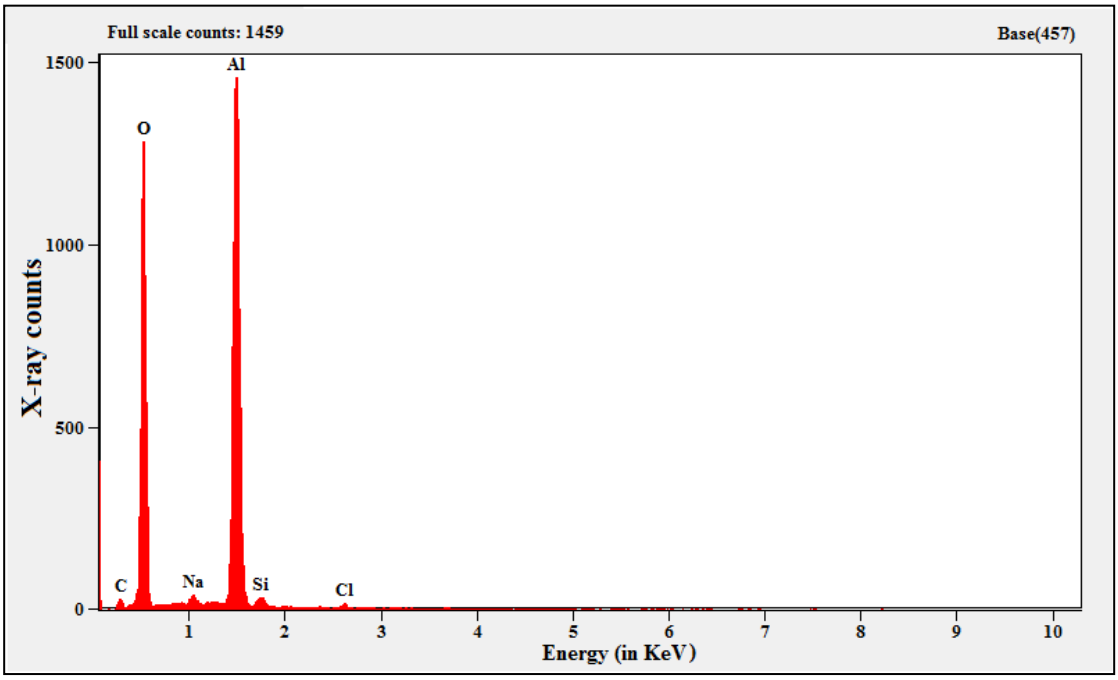

Fig.6.6. EDS spectrum Corundum rock of Mysuru region.

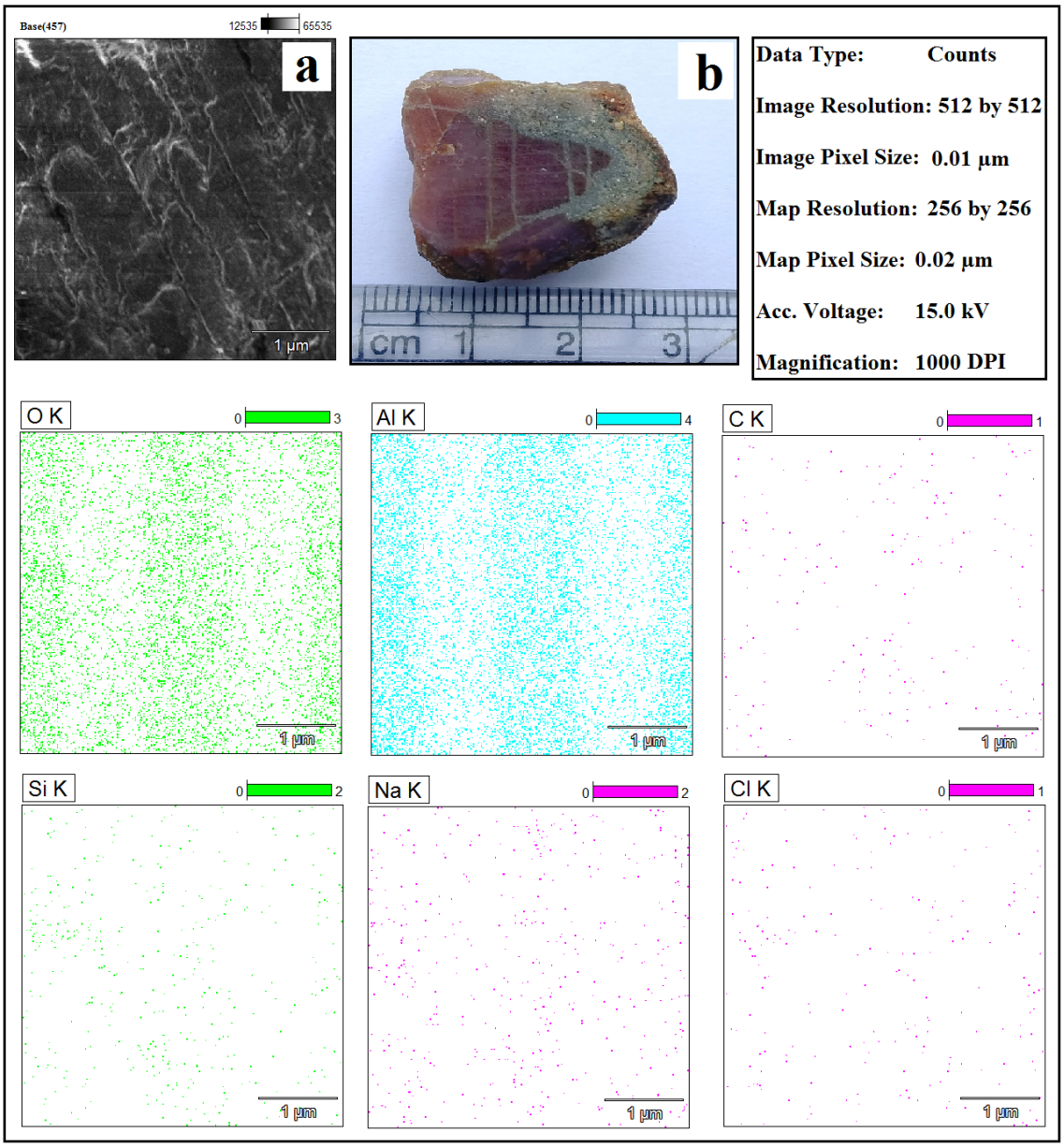

Fig.6.7. Elemental map of Corundum sample, (a) polished surface EDS image, (b) Polished sample of corundum

Elemental map it easily understands the result of chemical composition and which part is more aluminum content of particular sample, in this Mysuru region sample EDS can be used in elemental zoning and mapping of corundum rock. This rock more in Al, O and Na content and other elements of Si, Ca, and Cl, aluminum atomic number 13 and its atomic mass 26.982 is x-ray counts 1459 times its high energy alumina content observed in this map (Fig.6.7).

6.7. EDS ANALYSIS AND ELEMENTAL MAP OF CORUNDUM BEARING ROCK AROUND DAKSHINA KANNADA DISTRICT

EDS analysis result take over the Dakshina Kannada district corundum sample its Phase fractions corundum composition measured we seen (Table.6.6). Its shows elements and their weight percentage and atom percentage, here Al, Cr & O, is more composition observed in this sample and minor elements observed C, Na, Si and Cl (Table.6.6).

The graph shows x and y axis is measured x-ray counts and energy, Al, 4410 X-ray counts observed, results shows high energy alumina content presence in Dakshina Kannada district corundum bearing rock (fig.6.8).

Table.6.6. Phase fractions (wt %) Corundum composition measured by EDS

Element Line	Weight %	Weight % Error	Atom %
C- K	0.00	---	0.00
O- K	58.32	± 0.35	70.52
Na -K	1.36	± 0.10	1.14
Al -K	37.89	± 0.21	27.17
Si- K	0.44	± 0.07	0.30
Cl -K	0.53	± 0.09	0.29
Ca- K	0.25	± 0.05	0.12
Cr- K	1.21	± 0.09	0.45
Total	100.00		100.00

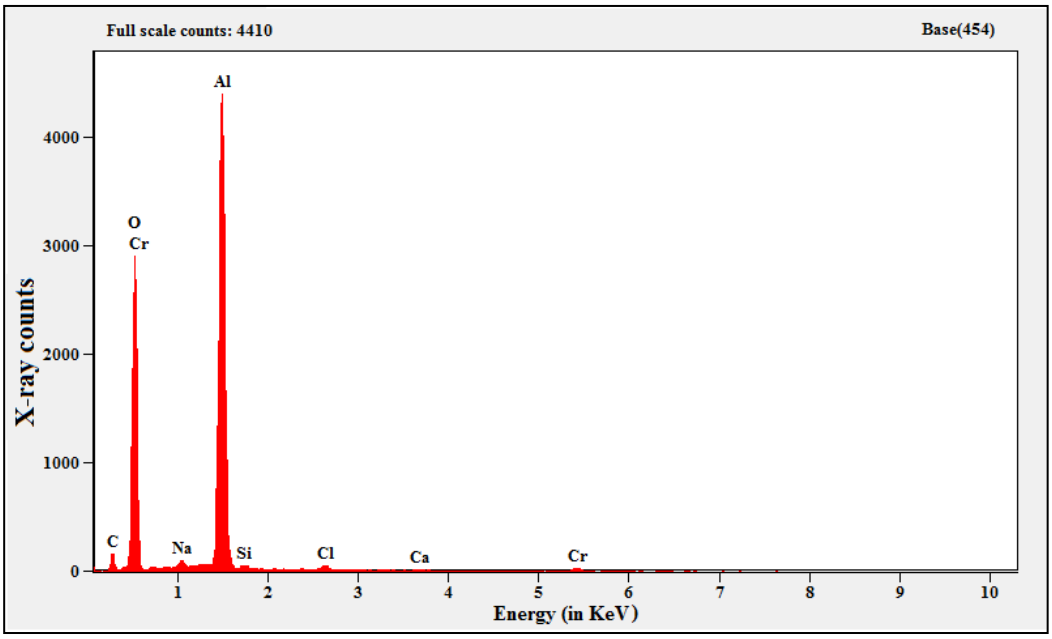

Fig.6.8. EDS spectrum Corundum rock of Dakshina Kannada region.

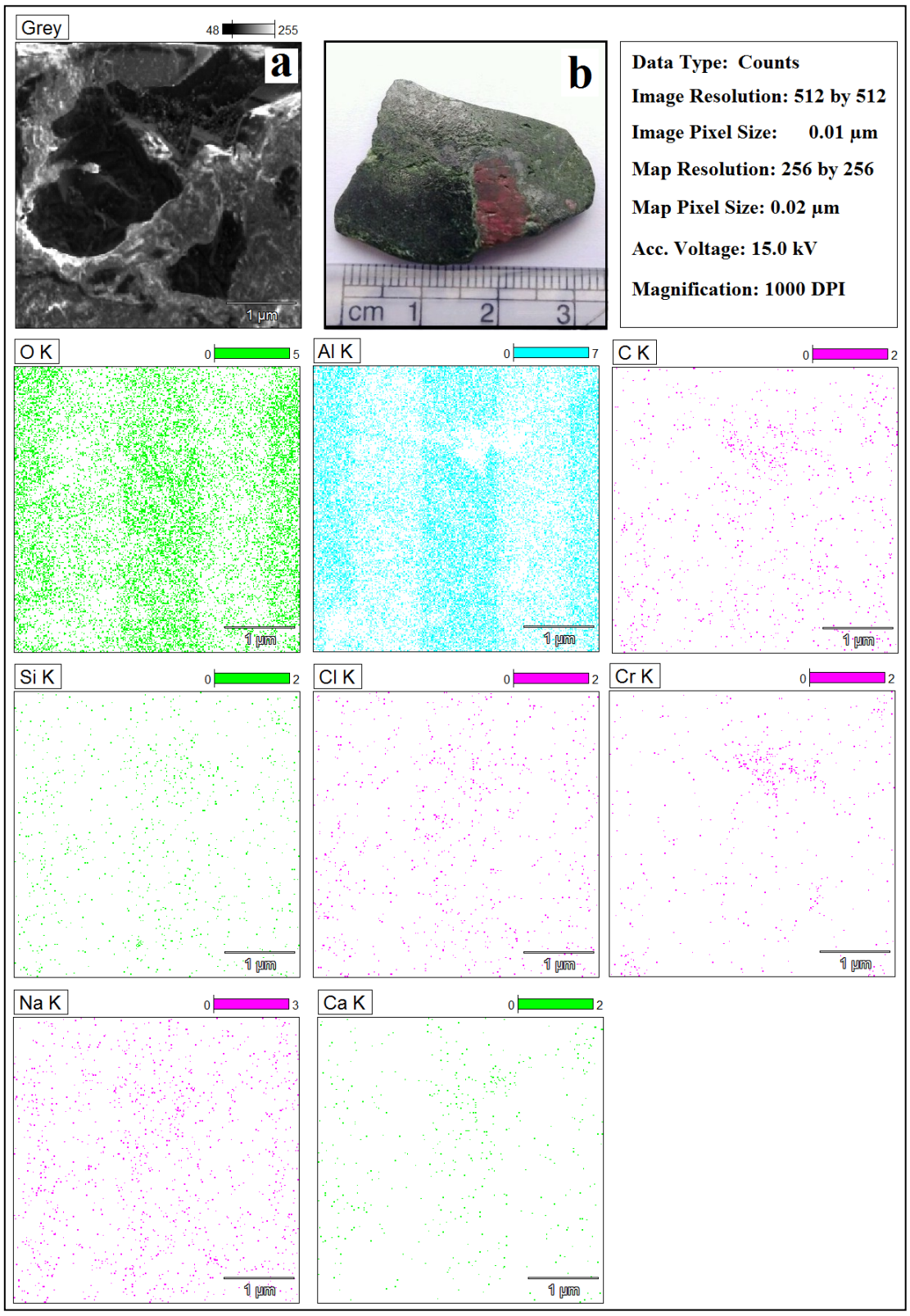

Fig.6.9. Elemental map of Corundum sample, (a) polished surface EDS image, (b) Polished sample of corundum bearing rock.

Elemental map it easily understands the result of chemical composition and which part is more aluminum content of particular sample, in this Dakshina Karnataka sample EDS can be used in elemental zoning and mapping of corundum sample. This sample more in Al, O and Cr content and other elements of Si, Ca, Na, C and Cl, aluminum atomic number 13 and its atomic mass 26.982 is x-ray counts 4410 times its high energy alumina content observed in this map (Fig.6.9).

EDS study on corundum bearing samples majorly Sothern Karnataka high granulate terrain and composition of highly sheared schist belts, here I am divided four region of my study area a. Chitradurga b. Tumkur c. Mysuru and d. Dakshina kannada districts these parts having more alumina content is observed particularly Dakshina Kannada district having more alumina and chromium content because of this impurities corundum shows more red color. Chitradurga al so field sample shows white color because less impurities observed and it has high alumina content of magmatic deposition, Tumkur and Mysuru region corundum samples occurs associated with metamorphic rocks, through EDS observed these samples has a high alumina content observed.

Present research study better understanding crystal structure, optical properties, chemical composition and spectral signature study on corundum bearing samples of southern Karnataka region.

CHAPTER-VII

7.1. SUMMARY AND CONCLUSION

Southern Karnataka is located in the wedge shaped Indian peninsular and it comes to Western Dharwar Craton part, the geological history of Karnataka is mainly confined to the two major oldest eras namely the Archaean and Proterozoic. The study area geological succession covers oldest Sargur group 3300my, Peninsular Gneissic Complex and Dharwar super group covers the Bababudan group and Chitradurga group.

Southern Karnataka mainly consist of major schist belts like Chitradurga schist belt, Holenarasipura schist belt, Nuggehalli schist belt, Sargur schist belt, Bababudan schist belt, Kudremukh schist belt, Shimoga schist belt, Javanahalli schist belt, Kunigal schist belt, Kolara schist belt, Kadiri and Ramgiri schist belt.

Corundum is a crystalline form of the Aluminium oxide, which can be found in three main geological environments of Magmatic, Metamorphic and Sedimentary Deposits. In the Study area almost corundum occurs magmatic and metamorphic deposits only, in contact zone of Closepet Granite mafic magma carried out the corundum deposits to the surface, in chapter 2 using ground truth checking data with help of Remote Sensing and GIS techniques demarcated the Corundum locations in the study area.

Field geology and petrographic study understanding the surface features, underground structure of lithosphere, composition and characterization of corundum bearing litho units and geological aspects, in this area 11districts are demarcated the corundum horizons.

Chitradurga area, magmatic deposits found loose barrel shaped crystals of pink corundum and metamorphic deposits of corundum bearing amphibolites schist occur in Kyadigunte area.

Tumkur district demarcated 13 locations of corundum bearing rocks mainly occur in contact zone of closepet granite.

In Chikballapura district also found corundum bearing closepet granite and corundum occurs in 6 locations.

In Hassan district mainly in Arsikere region corundum found in magmatic deposits and Belagumba area found corundum bearing amphibolites.

In Chikmagalur area found 5 locations of corundum bearing rocks.

In Dakshina Kannada district also mainly corundum occurs Uppinangadi and Koila area, corundum bearing amphibolites schist occurs Shanthigodu and Sullia area.

In Mysuru district covers 16 locations have been identified corundum bearing horizons.

In Mandya also 13 locations are demarcated in corundum bearing rocks. Ramnagara 6 locations have been identified corundum deposits.

In Chamarajanagara district found corundum bearing pelitic rock in Budipadaga area and Fe garnet rich corundum found in Biligirirangan hills.

Kolara occurs corundum deposits of Yelesandra and Kammasandra area.

Field observing ground truth check, physical and optical properties have been identified as Corundum presence in the Study area.

After through examination and study of Geochemical, Spectral Signatures with correlation of the optical Physical and petrological characteristic features of corundum in pure and nearly very important deposits in all the locations of the Study area.

Geochemical data shows percentage of chemical composition that result carried out with help of Orogin pro 8.5 and Tridraw softwares, geochemical study shows corundum has a high alumina content and less Si, Cr, Fe, Ti, Ca, and Mg conents, in all the locations of the Study area.

Hyperspectral remote sensing is one of the advance technology Spectroscopy is the study of light interaction as a function of wavelength, interactions contain light emitting, reflection or scattering from any of the material. Spectroradiometer Spectral Evolution RS-3500 (DARWin SP.V.1.3.0 Data Acquisition software) is used to measure the radiometric quantities like radiance and irradiance in continuous bands of spectral ranges 0.35 to 2.5µ in the EMS. EZ-ID provides geologists, geoscientists, and geometallurgists

with the tools to identify minerals, create more accurate mineral maps and vector alteration to mineralization, Sample identification has never been faster, easier, or more accurate than with EZ-ID software from Spectral Evolution.

Based on these spectral studies and relating them with the USGS spectral library, it was observed that corundum, actinolite, hornblende, sericite, iron oxide and chromium are more abundant corundum bearing rocks found in the study area.

Spectral analysis corundum absorption spectra (μm) 2.10, 2.20, 2.40 0.65, 1.4 and 1.9 nm observed. Corundum bearing amphibolites schist spectral signatures observed 2.10, 2.20, 2.40, 0.65, 0.88, 1.4, 1.9, 2.25 and 2.35nm.

The integration study compare the geochemical data and hyperspectral data, it's give the result outstanding performance of software work and ground truth checking is 95% correlated geochemical data and hyperspectral laboratory data. Chitrdurga 72.84%, Tumkur 81.64%, Chikballapura 81.64%, Hassan 77.34%, Chikmagalur 79.83, Dakshina Kannada 87.69%, Mysuru 87.69%, Mandya 82.66, Ramanagara 80.76%, Chamarajanagara 32.89% and Kolara 75.81% of districts has alumina content observed in the study area. Finaly Geochemical results shows purity of the Corundum mineral present in the Precambrian basement rocks of the Southern Karnataka.

Hyperspectral data has been used to identify and distinguish spectrally similar materials having characteristic reflectance spectra. Due to the capability of distinguishing various ground objects in detail, hyperspectral datasets are able to detect and map a wide variety of materials in the study area. Spectral reflectance in visible and near-infrared offers a rapid and inexpensive technique for determining the mineralogy of samples and obtaining information on chemical composition.

The Research Study Aims to carry out on corundum bearing horizons and their detail Mapping through hyperspectral and with the mineralization, its characterization is particular the types of corundum is precious and semi-precious to utilization in Gem Industry, which is having gemology and Gemstone in Industrial Applications of the state and Indian region.

Purity of Corundum is all the demarcated areas percentage of AL content high and oxygen is more than 60% based on the Al and oxygen present in the Corundum, at present recent trends on this particular mineral not only used as a abrasive, precious and gems industry . now Medical field, Electrical field, Watch industry, in Ayurveda bone, mucels and body pain healing purpas used and add nano technology implementing the paints al so this mineral is using.

Based on above Research problem we can store the Hyperspectral curves and further all these curves may Indian Standerds of Hyperspectral library of Precambrian terrains for further and futures researchers in the Department. All Geoscientist, throughout the world feature works can use them as standards of ISI.

7.2. Recommendations for future Research

1. Apply the same study of other gemstone deposits in the study area.

2. Correlation work on between the Precambrian basement rocks of similar geological Terrains and comparison studies for the corundum bearing litho units of the Indian Continent.
3. Utilization of Hyperion, ALI and AVIRIS which provides 242 bands (350 to 2500nm)

Of high resolution satellite images and Airborne images are the advanced techniques

as to utilize for studying the Corundum bearing horizons.

4. Generate the Indian Spectral Library for major & minor minerals of recent dated rock

types to Precambrian rocks of the Indian terrain.

BIBLOGRAPHY

A. A. Green, M. Berman, P. Switzer and M. D. Craig (1988) "A Transformation for Ordering Multispectral Data in Terms of Image Quality with Implications for Noise Removal," IEEE Transactions on Geoscience and Remote Sensing, Vol. 26, No. 1, 1988, Pp. 65-74.

Albarede, Francis (2007). Geochemistry : an introduction. Translated from the French. (5th ed.). Cambridge: Cambridge Univ. Press. ISBN 9780521891486. Cambridge University Press 978-0-521-88079-4 - Geochemisry: An Introduction: Second Edition Francis Albarède Frontmatte.

AL-Daghastani, N. S. (2003) "Remote sensing: principle and application", Dar Al-Manaheeg for publication and deliveries, Amman, Jordanian, pp 473.

Ali M Qaid and Basavarajappa H.T., (2008). Application of Optimum Index Factor Technique to LANDSAT-7 ETM+ data for geological mapping of North-East of Hajja, Yemen, American Euratian Journal of Scientific Research, IDOSI Publication., Vol.3, No.1, Pp: 84-91.

Ali M. Qaid, Basavarajappa H.T. and Rajendran S. (2009). Integration of VNIR and SWIR Spectral Reflectance for Mapping Mineral Resources; A case study, North East of Hajjah, Yemen, *J. Indian. Soc. Remote Sens,* Vol.37, Pp: 305-315.

Ali M. Qaid., Basavarajappa, H.T and Rajendran S. (2009). Application of Principal Component Analysis to ASTER and ETM+ Data for Mapping the Alteration Zones in North East of Hajjah, Yemen. Asian Journal of Geoinformatics, Vol.9, No.2, Pp: 15-21.

Alvaro P. Crosta, Charles Sabine and James V. Taranik. Hydrothermal alteration mapping at Bodie California. Using AVIRIS Hyperspectral data.Elsevier science Inc. Remote sensing environ, 65-309-319 (1998).

Analytical Spectral Devices Inc., (2002). Field Spec ® Pro: User Guide. Boulder Co., USA.

Aspen, P., Upton, B.G.J., Dicken, A.P., 1990. Anorthoclase, sanidine and associated megacryts in Scottish alkali basalts: high pressure syenitic debris from upper mantle sources European Journal of Mineralogy 2, 503–517

Awasthi SK, Krishnamurthy KV (1979). Geology of parts of Puttur and Sullia talucks, South Kanara district, Karnataka. Progress report for the field season 1978-1979, Geological Survey of India, Karnataka (South) Circle, 1-11.

Aydogan, S.M. and Moazzen, M., (2012): Origin and metamorphism of corundum-rich metabauxites at Mt Ismail in the southern Menderes Massif, SW Turkey. Resource Geology Journal, V.62, p.243-262.

B. M. Ravindra and A. S. Janardhan, (1981) Preliminary report on aegerine augite bearing syenite near SuBia Town, Dakshina Kannada District Karnataka. Journal Geological Society of India, Vol. 22, Aug. pp. 399 to 402.

Babaie Hassan A (2001) The Brunton compass and Geological objects. Georgia Geological Society Guidebooks V,21. No1. October, P55-60.

Barry, P. Seqal, C., and Carman, S. 2001. EO-1 Hyperion science Data User's Guide. TRW Space, Defense and Information Systems. Vol. 01, No. 077 pp: 1-65.

Basavarajappa H.T and Dinakar S, (2005). Land use and Land cover studies around Kollegal taluk, Chamarajanagar district using Remote Sensing and GIS techniques., The Indian Mineralogist, MSI, Special Vol.1, No.1, Pp: 89-94.

Basavarajappa H.T and Manjunatha M.C (2014). Geoinformatics Technique on Mapping and Reclamation of Wastelands in Chitradurga district, Karnataka, India, International Journal of Computer Engineering & Technology, Vol.5, Issue.7, Pp. 99-110.

Basavarajappa H.T and Manjunatha M.C (2015). "Groundwater Quality Analysis in Precambrian rocks of Chitradurga district, Karnataka, India using Geo-informatics Technique", International Conference of Water Resources, Coastal and Ocean Engineering (ICWRCOE-2015), Elsevier Aquatic Procedia, Vol.4, Pp: 1354-1365.

Basavarajappa H.T and Maruthi N.E (2018). Hyperspectral And Petro - Chemical Signatures Study On Shear Zone Controlled Corundum Bearing Pelitic Rocks Of Budipadaga Area, Chamarajanagara District, Karnataka, India. International Journal of Research and analytical Reviews (IJRAR) Volume 5, Issue 3, pp. 906-913.

Basavarajappa H.T and Maruthi N.E (2018). Hyperspectral and Petro - Chemical Signatures study on Corundum Bearing Litho-Units around Sringeri Area, Chikmagalur District, Karnataka, India. RESEARCH REVIEW International Journal of Multidisciplinary Volume 3, Issue10, pp. 899-904.

Basavarajappa H.T and Maruthi N.E (2018). Petro – Chemical And Spectral Signatures On Corundum Bearing Precambrian Amphibolites In Sullia Area, Dakshina Kannada District, Karnataka, India. Journal of Emerging Technologies and Innovative Research (JETIR) Volume 5, Issue 7, pp. 75-83.

Basavarajappa H.T and Maruthi N.E (2018). Petrochemical characteristics and Hyperspectral signatures on Corundum bearing Precambrian litho-units of Varuna area, Mysuru district, Karnataka, India. International Journal of Creative Research Thoughts, Volume6, Issue1, Pp.998-109.

Basavarajappa H.T, and Maruthi N.E (2018). Hyperspectral Signature Study Finds Corundum Alters To Diaspore Influeance Of Climate Change Of Dharwar Craton Arsikere Band Of Haranahalli, Hassan District, Karnataka, India. Journal of Environmental Science, Computer Science and Engineering and Technology (JECET) Volume 7, Issue 2, Pp.238-246.

Basavarajappa H.T, Dinakar S and Manjunatha M.C (2014 c). Analysis of Land use/ land cover classification around Mysuru and Chamarajanagara district, Karnataka, India using IRS-1D, PAN+LISSIII Satellite data, International Journal of Civil Engineering and Technology (IJCIET), Vol.5, Issue.11, Pp: 79- 96.

Basavarajappa H.T, Dinakar S, Satish M.V and Honne Gowda H (2008). Morphometric analysis of subwatersheds of river Suvarnavathi Catchment, using GIS, Chamarajanagara District, Karnataka, Remote Sensing and GIS Applications, Edited Volume, University of Mysore, Vol.1, No.1, Pp.45-53.

Basavarajappa H.T, Dinakar S, Satish M.V, Nagesh D, Balasubramanian A and Manjunatha M.C (2013). Delineation of Groundwater Potential Zones in Hard Rock Terrain of Kollegal Shear Zone (KSZ), South India, using Remote Sensing and GIS, International Journal of Earth Sciences and Engineering (IJEE), Cafet-Innova, Hydrology & Water Resource Management- special issue, Vol.6, No.5, Pp: 1185-1194.

Basavarajappa H.T, Jeevan L, Rajendran S and Manjunatha M.C. (2015). Discrimination of Banded Magnetite Quartzite (BMQ) deposits and associated Lithology of parts of Chikkanayakanahalli Schist Belt of Dharwar Craton, Karnataka, India using Remote Sensing technique, International Journal of Advanced Remote Sensing and GIS, Cloud Publications, Vol.4, Issue.1, Pp: 1033-1044.

Basavarajappa H.T, Jeevan L, Rajendran S and Manjunatha M.C., (2015 c). Discrimination of Banded Magnetite Quartzite (BMQ) deposits and associated Lithology of parts of Chikkanayakanahalli Schist Belt of Dharwar Craton, Karnataka, India using Remote Sensing technique, International Journal of Advanced Remote Sensing and GIS, Cloud Publications, Vol.4, Issue.1, Pp: 1033-1044.

Basavarajappa H.T, Manjunatha M.C and Jeevan L (2014 a). Application of Geoinformatics in Delineation of Groundwater Potential Zones of Chitradurga District, Karnataka, India, International Journal of Computer Engineering & Technology, Vol.5, Issue.5, Pp. 94-108.

Basavarajappa H.T, Manjunatha M.C and Maruthi N.E (2016). Land Use/Land Cover change detection analysis in Hosadurga taluk of Chitradurga district, Karnataka, India using Geo-informatics technique, Journal of International Academic Research for Multidisciplinary (IJARM), Vol.4, Issue.2, Pp: 304-314.

Basavarajappa H.T, Manjunatha M.C and Rajendran S (2015 a). Integration of Hyperspectral Signatures and major elements of Iron Ore Deposits around Holalkere range of Megalahalli, Chitradurga Schist Belt, Karnataka, India, Journal of The Indian Mineralogist, MSI, Vol.49, No.1, Pp: 85-93.

Basavarajappa H.T, Manjunatha M.C and Rajendran S (2015). Integration of Hyperspectral Signatures and major elements of Iron Ore Deposits around Holalkere

range of Megalahalli, Chitradurga Schist Belt, Karnataka, India, Journal of The Indian Mineralogist, MSI, Vol.49, No.1, Pp: 85-93.

Basavarajappa H.T, Manjunatha M.C, Rajendran S and Jeevan L (2017) Determination of Spectral Characteristics on Archaean Komatiites in Ghattihosahalli Schist Belt (GSB) of Kumminagatta, Chitradurga District, Karnataka, India. International Journal of Advanced Remote Sensing and GIS 2017, Volume 6, Issue 1, pp. 2416-2423.

Basavarajappa H.T, Maruthi N.E and Manjunatha M.C (2017). Hyperspectral Signatures and Field Petrography of Corundum bearing litho-units in Arsikere band of Haranahalli, Hassan District, Karnataka, India. International Journal of Creative Research Thoughts, Volume5, Issue4, Pp.3791-3798.

Basavarajappa H.T, Maruthi N.E, Jeevan L and Manjunatha M.C (2018). Physico-chemical charectristics and hyperspectral signature study using geomatics on gem verity of corundum bearing precambrian litho-units of Mavinahalli area, Mysuru district, Karnataka, India. International Journal of Computer Engineering and Technology(IJCET) Volume 9, Issue 1, pp. 102-112.

Basavarajappa H.T, Maruthi N.E, Jeevan L and Manjunatha M.C.(2018). Physico-chemical charectristics and hyperspectral signature study using geomatics on gem verity of corundum bearing precambrian litho-units of Mavinahalli area, Mysuru district, Karnataka, India. International Journal of Computer Engineering & Technology (IJCET) ISSN: 0976–6375 Volume 9, Issue 1, Jan-Feb 2018, pp. 102–112.

Basavarajappa H.T, Pushpavathi K.N and Balasubramanian A (2009). Mapping of Geological and geomorphological landforms of Chamarajanagar taluk, Karnataka, India, by Remote Sensing and GIS techniques, Journal of Indian Academy of Geosciences, Vol.52, No.1, Pp: 1-10.

Basavarajappa H.T, Pushpavathi K.N. Balasubramanian A and Manjunatha M.C, (2012). Mapping and Integration of Geology and Geomorphological Landforms of Mysore district, Karnataka, India using Remote Sensing and GIS Techniques, Frontiers of Earth Science Research, Proceeding/Edited Vol.1, No.1, Pp.164-175.

Basavarajappa H.T., (1992). Petrology, Geochemistry and Fluid inclusions studies of Charnockites and associated rocks around Biligiri-Rangan hills, Karnataka, India, Unpub PhD Thesis, University of Mysore, Pp: 1-96.

Basavarajappa H.T., Pushpavathi K.N. and Manjunatha M.C., (2015 d). Climate Change and its impact on Groundwater Table Fluctuation in Precambrian rocks of Chamarajanagar district, Karnataka, India using Geomatics Technique, International Journal of Geomatics and Geosciences (IJGG), Vol.5, No.3, Pp: 285-299.

Boardman JW, Kruse FA, Green RO (1995). Mapping target signatures via partial unmixing of AVIRIS data, Summaries, Proceedings of the Fifth JPL Airborne Earth Science Workshop, 23–26 January, Pasadena, California, JPL Publ., 95-1, 1: Pp. 23–26.

Borengasser, M., William, S., Hungate, W. S. and Watkins, R. (2008). Hyperspectral Remote Sensing: Principles and Applications. Taylor and Francis Group Boca Raton London New York, Pp 119.

BOTRILL, R.S. (1998): A corundum-quartz assemblage in altered volcanic rocks, Bond Range, Tasmania. Mineral. Mag. 62, 325—332.

Brousse, R. and Varet, J., (1966): Les trachytes du Mont-Dore et du Cantal septentrional etleurs enclaves. Bulletin of the Geological Society of France, V.7, p. 246–262.

BROWNLOW, A.H. & KOMOROWSKI, J.C. (1988): Geology and origin of the Yogo sapphire deposit, Montana. Econ. Geol. 83, 875—880.

Bruce Foote R., (1882). Notes on a traverse across the Gold Fields of Mysore. Rec. Geol., Survey of India. Vol.15, No.4, Pp: 191-201.

Bruce Foote, R. (1886). Notes on the geology of parts of Bellary and Anantapur districts. Rec. Geological survey of India. 19(2): Pp: 97-111.

Bruce Foote, R. (1900). Geological notes on traverses through the Mysore State. Mem. Mysore Geol. Dept., 1; Pp. 103.

Bruce Foote. R, (1888) "The Dharwar System" the chief auriferous rocks in south India. Rec. Geol. Surv. India, 21 (2): Pp 1-40.

Buckingham, R., and Staenz, K. 2008. Review of current and planned civilian space hyperspectral sensors for EO. Canadian Journal of Remote Sensing. Vol. 34, pp: 187-197.

Burrough P.A and McDonnell R.A (1998). Principles of Geographic Information Systems, 2nd Edition, New York, NY: Oxford University Press, Pp: 333.

CESBRON, F., LEBRUN, P., LE CLÉAC.'H, J.M., NOTARI, F., GROBON, C. & DEVILLE, J. (2002): Corindons et spinelles. Minéraux et Fossiles 15, Paris, France.

Chadwick B and Ramakrishnan M., (1891). The stratigraphy and structure of the Chitradurga region: an illustration of cover-basement interaction in the late Archaean evolution of the Karnataka Craton, Southern India., Precambrian Res.

Chadwick B, Ramakrishanan M., Vishwanatha M.N and Srinivasa Murthy V., (1978). Structural studies in the Archaean Sargur and Dharwar Supracrustal rocks of the Karnataka Craton., J. Geol. Soc. India., Vol.19, Pp: 531-549.

Chakrapani Naidu M.G. (1982). Optical Mineralogy Laboratory Manual, Pp: 41-48.

Chandrashekhar, H. and Nazeer Ahmed (1994). Ruby Corundum and garnet occurrence in Karnataka. In: Geokarnataka, MGD Centenary volume, Karnataka Asst. Geologist Association, Bangalore., pp.193-204.

Chris Yakymchuk , Kristoffer Szilas (2018) Corundum formation by metasomatic reactions in Archean metapelite, SW Greenland: Exploration vectors for ruby deposits within high-grade greenstone belts. Journal of ELSEVIER Geoscience Frontiers 9 (2018) 727-749.

Chris Yakymchuk, Kristoffer Szilas (2018). Corundum formation by metasomatic reactions in Archean metapelite, SW Greenland: Exploration vectors for ruby deposits within high-grade greenstone belts. ELSEVIER Geoscience Frontiers 9 (2018) 727e749.

Clark M.D, (1987). Geologic map of the Al Bad quadrangle, Sheet 28A, Kingdom of Saudi Arabia, Saudi Arabian Deputy Ministry for mineral resources geoscience map, GM-81C, Scale 1:250,000, Pp: 46.

Clark R.N & Roush T.L, (1984). Reflectance Spectroscopy: Quantitative Analysis Techniques for Remote Sensing Applications, Journal of Geophysical Research, Vol.89, Pp: 6329-6340.

Clark R.N, (1999). Spectroscopy of Rocks and Minerals and Principles of Spectroscopy, in Manual of Remote Sensing, Vol.3, Remote Sensing for the Earth Sciences, (A.N. Rencz, ed) John Wiley and Sons, New York, Pp: 3-58.

Clark R.N, Swayze G.A, Gallagher A, King T.V.V and Calvin W.M (1993). Digital Spectral Library: Version 1: 0.2 to 3.0, U.S. Geological Survey, Open File Report, 93-592, Pp: 1326.

Clark R.N, Swayze G.A, Livo K.E, Kokaly R.F, King T.V.V, Dalton J.B, Vance J.S, Rockwell B.W, Hoefen T and McDougal R.R (2002). Surface Reflectance Calibration of Terrestrial Imaging Spectroscopy Data: a Tutorial using AVIRIS, In proceedings of the 10th Airborn Earth Science workshop, R.O. Green (Ed), JPL publication, Vol.2, No.1.

Clark, R. N., S. Vance, K.E. Livo, and R. Green, Mineral Mapping with Imaging Spectroscopy: the Ray Mine, AZ, Summaries of the 7th Annual JPL Airborne Earth Science Workshop, R.O. Green, Ed., JPL Publication 97-21. pp 67-76, Jan 12-14, 1998.

Clark, R. N., S. Vance, K.E. Livo, and R. Green, Mineral Mapping with Imaging Spectroscopy: the Ray Mine, AZ, Summaries of the 7th Annual JPL Airborne Earth Science Workshop, R.O. Green, Ed., JPL Publication 97-21. pp 67-76, Jan 12-14, 1998.

Clark, R. N., Swayze, G. A., Gallagher, A, King, T. V. V. and Calvin, W. M. (1993). Digital Spectral Library: Version 1: 0.2 to 3.0 μm, U.S. Geological Survey, Open File Report 93-592, Pp. 1326.

Clarke, A. R. (2002) Microscopy techniques for materials science. CRC Press (electronic resource).

Classification des gisements de corindon. Le Règne Mineral. V.55, p.4–47.

Coenraads, R.R., (1992): Sapphires and rubies associated with volcanic provinces: inclusions and surface features shed light on their origin. Australian Gemmologist Journal, V.18, p.70-78.

Coenraads, R.R., 1992. Sapphires and rubies associated with volcanic provinces: inclusions and surface features shed new light on their origin. Australian Gemmologist 18 (3), 70–78.

Coenraads, R.R., Sutherland, F.L., Kinny, P.D., 1990. The origin of sapphires: U–Pb dating of zircon inclusions sheds new light. Mineralogical Magazine 54, 113-122.

continental margins intraplate basaltic fields. Journal of ELSEVIER Ore Geology Reviews 34 (2008) 200–215.

Crawford A. R., (1969). Reconnaissance Rb-Sr dating of the Precambrian rocks in Southern Peninsular India., J.Geol.Soc. India., Vol.10, Pp: 117-166.

Curran, Paul. J. (2001). Imaging spectrometry for ecological application, JAG,Vol.3-Issue 305-312.

Drury S A., (1987). Image Interpretation in Geology (London: Allen &Unwin), Pp: 1-243.

Drury, S., (2001). Image Interpretation in Geology. Third Edition. Blackwell Science Inc. Pp: 122-157.

Dyer, Johen.R., 1994: Application of absorption Spectroscopy of Organic Compounds, Prentice Hall of India.

Egerton, R. F. (2005) Physical principles of electron microscopy : an introduction to TEM, SEM, and AEM. Springer, 202.

Elachi, C. Introduction to the Physics and Techniques of Remote Sensing, Wiley Interscience, 1987.

Fact Sheet - LDCM Earth Image Collection Satellite. Orbital Sciences Corporation. Retrieved 12 February 2013.

Farmer, V. C. (1974). The Infrared Spectra of Minerals, Mineralogical Society Monograph 4. Mineralogical Society, London, UK, Pp. 539.

Fermor, L, L., (1936). An attempt at the correlation of ancient schistose formations of Peninsular India. Mem. Geol. Surv, India, V.70 (1): 1-52; V.70 (2): Pp 53 - 218.

Fernando, G.W.A.R, Attanayake, A.N.B and Hofmeister, Wolfgang. Corundum-Spinel-Taafeite-Scheelite bearing Metasomatites in Bakamuna, Sri Lanka Modeling of its Formation, Proceedings of the International Symposium, Hanoi, September 26-October 2, 2005 .

Ferrier, G. and Wadge, G. (1996). The application of imaging spectrometry data to mapping alteration zones associated with gold mineralization in southern Spain. International Journal of Remote Sensing, 17, Pp. 331-350.

Ferrier, G., White, K., Griffiths, G., Bryant, R. and Stefouli, M. (2002). 'The mapping

Frederic H. Lahee, (1941). Field Geology McGRAW – hill book company INC, printed in the united states of America, Fourth edition P 3 – 263.

Friedman, J.D., F.E. Mutschler, R.E. Zaartman, P.H. Briggs, G.A. Swayze, and A.F. Theisen, 1989, Shawangunk ore district, New York: Geochemical and spectral data. USGS Open-File Report 89-193, p. 92.

Gaffey, S.J., (1986). Spectral reflectance of carbonate minerals in the visible and near infrared (0.35–2.55 microns): calcite, aragonite, and dolomite. Am. Mineral. 71, Pp. 151–162.

GARNIER, V., GIULIANI, G., MALUSKI, H., OHNENSTETTER, D., PHAN, T.T., HOÀNG, Q.V., PHAM, V.L., VU, V.T. & SCHWARZ, D. (2002b): Ar.–Ar ages in phlogopites from marble-hosted ruby deposits in northern Vietnam: evidence for Cenozoic ruby formation. Chem. Geol. 188, 33.– 49.

GARNIER, V., GIULIANI, G., OHNENSTETTER, D. & SCHWARZ, D. (2004a): Saphirs et rubis. Classification des gisements de corindon. Le Règne Minéral 55, 4.–47.

Garnier, V., Giuliani, G., Ohnenstetter, D. and Schwarz, D., (2004a): Saphirs et rubis.

GARNIER, V., OHNENSTETTER, D., GIULIANI, G. & SCHWARZ, D. (2002a): Rubis trapiches de Mong Hsu, Myanmar. Rev. Ass. Fr. Gemmol. AFG 144,5.–12.

GARNIER, V., OHNENSTETTER, D., GIULIANI, G., MALUSKI, H., DELOULE, E., PHAN, T.T., PHAM, V.L. & HOANG, Q.V. (2004b): Age and significance of ruby-bearing marbles from the Red River shear zone, northern Vietnam. Can. Mineral. 43, 1315.–1329.

Gaston Giuliani, Daniel Ohnenstetter, Anthony E Fallic, Lee Groat, Andrew J, Fagan (2014). The Geology and Genesis of Gem Corundum Deposits, Mineralogical Association of Canada, short course 44, Tucson AZ February 2014, p, 29 – 112.

Geo Karnataka: Geology of Karnataka. Geokarnataka.blogspot.com (2007-03-18). Retrieved on 2011-03-21.

Goetz A.F.H.(1992) Imaging spectrometry for earth remote sensing, Imaging spectroscopy: Fundamentals and prospective applications:1-19.

Goetz, A. F., G. Vane, J. E. Soloman, and B. N. (1985). Rock, Imaging Spectrometry for Earth Remote Sensing. Science, 228, 1147.

Goetz, A.F.H. (1992b) Principles of Narrow Band Spectrometry, in The Visible and IR: Instruments and Data Analysis in Imaging Spectroscopy: Fundamentals and Prospective Applications, F. Toselli and J. Bodechtel, Eds., pp. 21-32, Brussels and Luxembourg.

Goetz, A.F.H., Rock, B.N. and Rowan, L. C (1983). "Remote sensing for exploration: An overview'. Economic Geology, Vol. 78, No. 4, Pp. 573–590.

Goetz, AFFH, Rowan, LC and Kigston, MJ (1982). 'Mineral Identification from orbit initial results from the shuttle multispectral infrared radiometer, Science, Vol 218, Pp. 1020-1024.

Golani, P.R. (1989) Sillimanite Corundum deposits of Sonapahar, Meghalaya, India: A metamorphosed Precambrian Palaeosol. Precambrian Res., Vol.43, Pp: 175–189.

Goldstein, J. (2003) Scanning electron microscopy and x-ray microanalysis. Kluwer Adacemic/Plenum Pulbishers, 689 p.

Graham R. Hunt (1977). Spectral Signatures of particulate minerals in the visible and near infrared. Geophysics, Vol. 42. No.3, Pp: 501-513.

Graham, I., Sutherland, L., Khin, Zaw, Nechaev, V., Khanchuk, A., 2006a. Advances in our understanding of the basalt-derived gem sapphire-ruby deposits of theWest Pacific margins. 12th Quadrennial IAGOD Symposium 2006, Moscow, Russia, Extended Abstract CDROM.

Graham, I.T., Sutherland, F.L., Webb, G.B., Fanning, C.M., 2004. Polygenetic corundums from New South Wales gemfields. In: Khanchuk, A.I., Gonevchuk, G.A., Mitrokhin, A.N., Simanenko, I.F., Cook, N.J., Seltmann, R. (Eds.), Metallogeny of the Pacific Northwest: Tectonics, magmatism and metallogeny of active continental margins. Dalnauka, Vladivostok, pp. 336–339.

GSI (1981). Geological and Mineral map of Karnataka, Geological Survey of India.

GSI, Memoir (1981). "Early Precambrian Supracrustals of Southern Karnataka., Swaminath J and Ramakrishnan M, A Geological Survey of India, Govt. of India, Vol-112, Pp: 163-198.

GSI., (2006). Geology and Mineral Resources of the States of India, Geological Survey of India, Misc Publ.30, Part-VII, Bengaluru, Pp: 1-65.

Guha, A.; Kumar, K.V. (2016). New ASTER derived thermal indices to delineate mineralogy of different granitoids of an Archaean Craton and analysis of their potentials with reference to Ninomiya's indices for delineating quartz and mafic minerals of granitoids—An analysis in Dharwar Craton. Ore Geol. Rev, 74, Pp 76–87.

Gupta S, Rai S.S, Prakasam K.S, Srinagesh D, Chadha R.K, Priestley K and Gaur V.K (2003). First evidence for anomalous thick crust beneath mid-Archaean Western Dharwar Craton, Current Science, Vol.84, Pp: 1219-1226.

Harlow, G.E. and Bender, W., (2013): A study of ruby (corundum) compositions from the Mogok Belt. American Mineralogy, V.98, p.1120–1132.

Harris D.C and Bertolucci M.D, (1989). Symmetry and Spectroscopy, an introduction to vibrational and electronic spectroscopy, Dover publications, Inc. New York, Pp: 206.

Harris, J., Wilkimson L. and Heather K. (2001). Application of GIS processing techniques for producing mineral productivity maps, A case study: mesothermal Au in Swayze greenstone belt, Ontario, Canada. Natural Resources, 10, Pp 91- 124.

Holland, T.H., (1900). The charnockite series, a group of Archaean hypersthene rocks in Peninsular India. Mem. Geol. Surv. India, 28 (2): Pp. 117 – 249.

Hoover, D. B., Heran, W. D. and Hill, P. L. (1993). The Geophysical Expression of Selected Mineral Deposit Models, United States, Department of the Interior Geological Survey, Pp. 58-60.

Horler D.N.H, Dockray M and Barber J, (1983). The red edge of plant leaf reflectance, International Journal of Remote Sensing, Vol.4, Pp: 273-288.

Hughes R.W., Corundum: ruby and sapphire, White Lotus, 1991.

Hughes, R. W. 1990. **Corundum**, Courier International Ltd., England, 314 p.

Hughes, R.W., (1997): Ruby and sapphire. Boulder, U.S.A, V.75, p.420.

Hughes, R.W., (1997): Ruby and sapphire. Boulder, U.S.A, V.75, p.420.

Hunt and Ashley (1979) Spectra of Altered Rocks in the Visible and Near infrared. Journal of Economic Geology, Volume 74 number 7, Pp1613-1629.

Hunt G.R (1977). Spectral signatures of particular minerals in the visible and near infrared, Geophysics, Vol.42, Pp: 501-513.

Hunt G.R (1980). Electromagnetic radiation: The communication link in remote sensing. In: B.S. Siegal and A.R. Gillespie, (Editors), Remote Sensing geology, John Wiley and Sons, New York, Pp: 5-46.

Hunt G.R and Ashley R.P (1979). Spectra of altered rocks in the visible and near infrared, Economic Geology, Vol.74, Pp: 1613-1629.

Hunt G.R and Salisbury J.W, (1970). Visible and near-infrared spectra of minerals and rocks, Modern Geology, Vol.1, Pp: 283-300.

Hunt G.R and Vincent R.K (1968). The behavior of spectral features in the infrared emission from particulate surfaces of various grain sizes, Journal of Geophysical Research Vol.73, No.18, Pp: 6039-6046.

Hunt G.R, JW. Salisbury, C.J, Lenhoff (1971). Visible and Near Infrared Spectra of minerals and Rocks III oxides and Hydroxides,mod, Geo, 2 pp 195-205.

Hunt G.R, Salisbury J.W and Lehnoff C.J (1971). Visible and Near Infrared Spectra of Minerals and Rocks: III. Oxides and Oxy-hydroxides, Modern Geology No.2, Pp: 195-205.

Hunt, G.R., J.W. Salisbury, and C.J. Lenhoff, 1971, Visible and near-infraredd spectra of minerals and rocks: III. Oxides and hydroxides. Modern Geology, v. 2, p. 195-205.

Hunt, G.R., J.W. Salisbury, and C.J. Lenhoff, 1973, Visible and near-infrared spectra of minerals and rocks: VI. Additional silicates. Modern Geology, v. 4, p. 85-106.
Hunt, G.R., J.W. Salisbury, and C.J. Lenhoff, 1973, Visible and near-infrared spectra of minerals and rocks: VI. Additional silicates. Modern Geology, v. 4, p. 85-106.

Hunt, G.R., Salisbury, J.W. and Lehnoff, C.J. (1971) Visible and near infrared spectra of minerals and rocks: 111 Oxides and Oxyhydroxides. Modern Geology 2: Pp. 195-205.

Ian Graham, Lin Sutherland, Khin Zaw, Victor Nechaev and Alexander Khanchuk (2008). Advances in our understanding of the gem corundum deposits of the West Pacific

ISRO prepares for historic 100th mission. Times of India. Retrieved 2014-09-21.

Isro's PSLV-C23 lifts off with five foreign satellites. Times of India. Retrieved 2014-09-21.

Jayananda M, Janardhan A.S, Sivasubramanian P and Peucat J.J (1995). Geochronological and isotopic constrains on granulite formation in the Kodikanal area, South India, In: Sontosh M and Yoshida M. (Eds). India and Antartica during the Precambrian Mem. Geol. Soc. India, Vol.34, Pp: 373-390.

Jayaram B.N., (1965). Systematic geological mapping of South western parts of the Chitaldurg Schist Belt, Mysore State. Geol.Surv.India, Unpublished Report.

Jayaram, B.(1917) Report on the Corundum Bearing rocks of the Arsikere Taluk with note on other localities., Rec. Mysore Geol. Dept., Vol.15, No.2, Pp: 63-91.

Jayaram, B., (1920). Report on the limestones and associated rocks of the Voblapura area with notes on traverse and revision work done during the field season 1916 -17.Rec. Mysore Geol. Dept., 18: Pp. 33-92.

Jayashree Panjikar, Chandrashekar, H., Muniswamaiah, M. and Nazeer Ahmed (1984). Study of gem variety of Corundum from Parts of Tumkur and Mysore districts. Jour. Geol. Soc. India., v.43, pp. 311-313.

Jeevan L and Basavarajappa H.T (2018) Application Of Hyperspectral Remote Sensing And Gis Techniques For Mapping Of Hydrothermal Alteration Zones Of Precambrian Rocks In Parts Of Chitradurga Schsit Belt, Dharwar Craton, India (un published thesis).

Joseph Hyde Pratt (1906). Corundum and its occurrence and distribution in the united states, a revised and enlarged edition of bulletin no 180 and 269, series A, Economic Geology 61, Washington p 9-168.

Kane R.E. et al, Ruby and Fancy sapphire from Gem & Gemology, 27 / 136,1991.

Karanth R.V., Gems and Gem Industry in India, Geological society of India Banglore,

Kepezhinskas, P., (2011): Indicator minerals in diamond exploration: A case study from eastern Finnmark, Finland. Vuorimiesyhdistys, V.92, p.72.

Khin Zaw, Sutherland, F.L., Dellapasqua, F., Ryan, G.C., Tzen-Fu, Y., Mernagh, P.T. and Duncan, D., (2006): Constrats in gem corundum characteristics, eastern Australian basaltic fields: trace elements, fluid/melt inclusions and oxygen isotopes. Mineralogical Magazine, V.70, p.669-687.

Khin Zaw, Sutherland, L., Fu Yui, T., Meffre, S. and Thu, K., (2014): Vanadium-rich ruby and sapphire within Mogok Gemfield, Myanmar: implications for gem color and genesis. Mineral Deposita, V.50, p.200.

Kissin, A., (1994): Ruby and sapphire from the southern Ural Mountains, Russia. Gems and Gemology, V.30, p. 243–252.

Koltsov, A.B., (2001): Ruby-bearing metasomatites in marbles: conditions and numerical model of the formation. Exploration Geoscience, V. 10, p. 94–95.

Kragh, Helge (2008). "From geochemistry to cosmochemistry: The origin of a scientific discipline, 1915–1955". In Reinhardt, Carsten. Chemical Sciences in the 20th Century: Bridging Boundaries. John Wiley & Sons. pp. 160–192. ISBN 3-527-30271-9.

Kruse F. A., Boardman J. W. and Huntington J. F. (2003) "Comparison of airborne hyperspectral data and EO-1 Hyperion for mineral mapping". IEEE Transactions on Geoscience and Remote Sensing, (Special Issue), Vol. 41, No. 6, pp. 1388-1400.

Kruse, F. A., 1988, Use of Airborne Imaging Spectrometer data to map minerals associated with hydrothermally altered rocks in the northern Grapevine Mountains, Nevada and California: Remote Sensing of Environment, v. 24, no.1, Pp. 31-51.

Lasnier, B., (1977): Persistance d'une série granulitique au coeur du Massif Central Français (Haut Allier). Ph.D. thesis, University of Nantes, France, V.26, p. 345.

Lawson, A., (1903): Plumasite, an oligoclase–corundum rock near Spanish Peak, California. University of California Publications on Geological Sciences collection, V. 3, p. 219–229.

LDCM Spacecraft. NASA. Retrieved 12 February 2013.

Levinson, A.A., Cook, F.A., 1994. Gem corundum in alkali basalts: origin and occurrence. Gems and Gemology 30, 253–262.

Liew, S. C., Change, C. W., and Lim, K.H. 2002. Hyperspectral Land Cover Classification of EO-1 Hyperion Data by Principal Component Analysis And Pixel Unmixing. Centre for Remote Sensing, Imaging and Processing, National University of Sinagpore, pp. 3111-3113.

Lillesand, T.M. and Kiefer. R. W., Remote Sensing and Image Interpretation, Fourth Edition, John Wiley and Sons, 2002, ISBN 9971-51-427-3.

M. Deb (2014). Precambrian Geodynamics and Metallogeny of the Indian shield ore Geology Reviews ELSEVIER, Vol 57, March 2014, p, 1-28.

M. Rajamanickam, S. Balakrishnan and R. Bhutani (2014). Rb-Sr and Sm-Nd istope systematics and Geochemical studies on metavolcanic rocks from peddavora greenstone belt evidence for presence of mesoarchean continental crust in easternmost patts of Dharwar craton, India. Journal of Earth System Science Springer, Vol 123 issue 5, Pp 989 – 1011.

M. Ramakrishnan and R. Vaidyanadhan (2010) Geology of India. Geological society of India Bangalore Vol-I, p 1-519.

Mackenzic W.S and Guilford .C, Atlas of rock – forming minerals in thin section Pp: 84

Magendran and S. Sanjeevi (2011) "Assessing the Grades of Iron Ores of Noamundi, India by Ground Based Hyperspectral Remote Sensing", International Journal of Earth Science and Engineering (IJEE), Vol. 04, No. 08, pp. 7 – 16.

Manjunatha BR, Harry NA (1994). Geology of western coastal Karnataka. Geo Karnataka, Mysore Geological Department, Centenary volume, 109-116.

Manjunatha BR, Harry NA (1994). Geology of western coastal Karnataka. Geo Karnataka, Mysore Geological Department, Centenary volume, 109-116.

Manjunatha M.C and Basavarajappa H.T (2017) Applications Of Hyperspectral Remote Sensing And Gis On Ne-Sw Transects Of Chitradurga District, Karnataka, India (un published thesis).

Maruthi N.E and Basavarajappa H.T (2018). Hyperspectral and Petro - Chemical Signatures study on Corundum Bearing Amphibolite Schist of Magadi Area, Ramanagara District, Karnataka, India. RESEARCH REVIEW International Journal of Multidisciplinary Volume 9, Issue 3, pp. 773-779.

Maruthi N.E and Basavarajappa H.T (2018). Hyperspectral And Petro - Chemical Signatures Study On Corundum Bearing Litho-Units Of Precambrian Basement Rocks Around Closepect Granite Madhugiri Area, Karnataka, India. Journal of Emerging Technologies and Innovative Research (JETIR) Volume 5, Issue 12, pp. 619 - 628.

Maruthi N.E and Basavarajappa H.T (2018). Hyperspectral Signatures and Petro - Chemical Charectistics Study on Corundum Bearing Litho-Units of Sargur Area, Mysuru District, Karnataka, India. International Journal of Research and analytical Reviews (IJRAR) Volume 5, Issue 4, pp. 65-74.

Maruthi N.E, Basavarajappa H.T, Jeevan .L and Siddaraju M.S (2018). Hyperspectral Signatures On Corundum Bearing Litho-Units Of Precambrian Basement Rocks Around Closepet Granite Pavagada Area, Karnataka. International Journal of Computer Engineering and Technology (IJCET) Volume 9, Issue 3, pp. 86-94.

Maruthi N.E, Basavarajappa H.T, Manjunatha M.C, and Harshavardhana A.S. (2019). Hyperspectral Study And Integration Of Petro-Chemical Signatures On Corundum Bearing Litho-Units Around Maddur, Mandya District, Karnataka, India. International Journal of Research and Analytical Reviews (IJRAR), Volume.6, Issue 1, Page No pp.897-903, January -March 2019.

Maslen, E.N., V.A. Streltsov, N.R. Streltsova, N. Ishizawa, and Y. Satow (1993) Synchrotron X-ray study of the electron density in $\alpha - Al_2O_3$. Acta Cryst., 49, 973–980.

Mather, P. M. (2004). Computer Processing of Remotely-Sensed Images: An Introduction, 3rd edition, John Wiley and Sons, Ltd, Chichester, Pp 324.

McSween H.Y, I.O. McGlynn and A.D. Rogers (2010). Determining the Modal mineralogy of martian soils, Journal of Geophysical Research, Vol, 115 E00f 12, p, 1-10.

Mehnert K.R., (1969). Petrology of the Precambrian basement complex, In: P.J.Hart (Editor), "The earth's crust and upper mantle', Geophy.Monograph.13, Am. Geophy.Union, Washinton., Pp: 513-518.

Mehnert K.R., (1973). Migmatites and the origin of granitic rocks. Elsevier, Amsterdem, Third Edition.

Moghtaderi, A., Moore, F. and Mohammadzadeh, A. (2007). The application of advanced space-borne thermal emission and reflection (ASTER) radiometer data in the detection of alteration in the Chadormalu paleo-crater, Bafq region, entral Iran. Journal of Asian Earth Sciences,

MOYD, L. (1949): Petrology of the nepheline and corundum rocks of southeastern Ontario. Amer. Mineral. 34, 736—751.

MURDOCH, J. & WEBB R.W. (1942): Minerals of California, California State. Div. Mines Bull. 136, San Francisco, California, U.S.A.

Mustard, J. F. and Sunshine, J. M. Spectral Analysis for Earth Science (1999) Investigations Using Remote Sensing Data. In: Rencz, A. N. (Ed.), Remote Sensing for the Earth Sciences: Manual of Remote Sensing. 3thed, Vol. 3, John Wiley & Sons, New York, Pp. 251-306.

Naqvi SM, Rogers JJW (1983). Introduction In: Naqvi S M and Rogers JJW (eds). Precambrian of South India. Geological Society Memorandum, 4, 6-16.
Naqvi SM, Rogers JJW (1983). Introduction In: Naqvi S M and Rogers JJW (eds). Precambrian of South India. Geological Society Memorandum, 4, 6-16.

Narayan Sangam and Pavanaguru. Geology of Corundum Occurrances in Parts of Khammam Schist Belt, International Journal of Scientific and Research Publications, Volume 3, Issue 2, February 2013.

Neteler M and Mitasova H, (2007). Open source GIS: A GRASS GIS approach, 3rd Edition. The International Series in Engineering and Computer Science, Springer, New York Inc, Vol.773, Pp: 406.

Newbold, S. T. 1846. Summary of the geology of southern India. Journal. Royal Asiatic. Soc., New Series, 8. Mysore Journal. Geol. Soc. India, 18: Pp. 102- 110.

Nguyen Viet .Y. et al, On the forming origin of sapphire and ruby in Vietnam, Journal
Nutman A.P, Chadwick B, Ramakrishnan M and Vishwanatha M.N, (1992). SHRIMP-U/Pb ages of detrital zircon in Sargur supracrustal rocks in western Karnataka, Southern India, J. Geol. Soc. India, Vol.39, Pp: 364-374.

of Geology, B/23,2004.

of hydrothermal alteration zones on the island of Lesvos, Greece, using an integrated remote sensing data set'. International Journal of Remote Sensing, 23, Pp. 341-356.

Okrusch, M., T.E. Bunch, and H. Bank (1976) Paragenesis and petrogenesis of a corundum-bearing marble at Hunza (Kashmir). Mineralium Deposita, 11, 278–297.

P.F. Carey (2004). Field Geology, Encyclopedia of Life support systems, Geoinformatics, Vol-I.

P.Parikh, D.M.Bhardwaj, R.P.Gupta†, N.L. Saini, S. Fernandes‡, R.K.Singhal, D.C. Jain and K.B. Garg. Comparative Study Of The Electronic Structure Of Natural And Synthetic Rubies Using Xafs And Edax Analyses, december 2002-Indian Academy of Sciences pp. 653–656.

Palache, C., H. Berman, and C. Frondel (1944) Dana's system of mineralogy (7th edition), v. I, 520–527.

Paul I.A, Michael G.F, David M.J and David R.W (2005). Geographic Information Systems and Science, 2nd edition, John Willey and Sons, Pp: 536.

Peretti, A. and Hahn, L., (2013): Record-breaking discovery of ruby and sapphire at the Didy mine in Madagascar: investigating the source. In Color, V.21, p.22–35.

Peretti, A., Mullis J. and Kundig R., (1990): Die Kashmir Saphire and ihr geologisches Errinnerungsmogen. Neuer Zurchur Zeitung, V.187, p.59.

Peter Bajcsy and Peter Groves (2004) Methodology For Hyperspectral Band Selection, Published in Photogrammetric Engineering and Remote Sensing journal, Vol. 70, Number 7, July 2004, Pp. 793-802.

Peter G., Read.,Gemological instruments (2nd edition).Butterworth Scientific London,

Peucat, J. J., Ruffaut, P., Fritsch, E., Bouhnik-Le, E., Simonet, C. and Lasnier, B., (2007): Ga/Mg ratio as new geochemical tool to differentiate magmatic from metamorphic blue sapphire. Lithos, V.98, p.261-271.

Phillips, W.R. and D.T. Griffen (1981) Optical mineralogy, 24–26.

Pichamuthu, C.S., 1946a. Cycles in Dharwar sedimentation. Curr. Sci., 15: Pp 273 - 274.

Pichamuthu, C.S., 1947. Some aspects of Dharwar geology with special reference to Mysore State. Presidential address, 34th Indian Sci. Cong., Delhi .pp.1-16 (Also Rec. Mysore Geol. Dept. 46(2): Pp 1- 34.

Pichamuthu. C.S., 1951. Some observations on the structure and classification of Dharwar of Mysore State. Curro Sci., 20: Pp 117-119.

Pignatti, S., Cavalli, R.M., Cuomo, V., Fusilli, L., Pascucci, S., Poscolieri, M., and Santini, F. 2009. Evaluating Hyperion Capability for Land Cover Mapping in a Fragmented Ecosystem: Pollino National Park, Italy. Remote Sensing of Environment. Vol. 113, pp. 622-634.

PIN, CH., MONCHOUX, P., PAQUETTE, J.-L., AZAMBRE, B., WANG, R.C. & MARTIN, B. (2006): Igneous albitite dikes in orogenic lherzolites, western Pyrénées, France: a possible source for corundum and alkali feldspar xenocrysts in basaltic terranes. II. Geochemical and petrogenetic considerations. Can. Mineral. 44, 837—850.

PinakiSengupata, Pradip C Saikia and Prakash C Borthakur (2008). SEM-EDX characterization of an Iron-rich Kaolinite clay. Journal of scientific and Industrial Research Vol 67. Pp 812-818.

Prakash, P. Chandra Singh And T. Hokada. A New Occurrence of Sapphirine-Spinel-Corundum-bearing Granulite from NE of Jagtiyal, Eastern Dharwar Craton, Andhra Pradesh. Journal Geological Society Of India Vol.82, July 2013, pp.5-8.

Qaid Ali, M., Basavarajappa, H. T. and Rajendran, S. (2009) "Integration of VNIR and SWIR spectral reflectance for mapping mineral resources; A case study, north east of Hajjah, Yemen", Journal of the Indian Society of Remote Sensing Vol. 37, No. 2, pp. 305-315.

Qasim Jan M. (1988) Geochemistry of amphibolites from the southern part of the Kohistan arc, N. Pakistan, Mineralogical Society, J. Mineralogical Magazine, Vol. 52, Pp: 147-159.

Radhakrishna B.P (1967). Reconsideration of some problems in the Archaean complex of Mysore, J.Geol.Soc.India., Vol.18, Pp: 102-110.

Radhakrishna B.P (1974). Peninsular gneissic complex of the Dharwar Craton: a suggested model for its evolution. J.Geol.Soc.India Vol.15, Pp: 339-454.

Radhakrishna B.P and Naqvi S.M, (1986). Precambrian continental crust of India and its evolution.

Radhakrishna B.P. (2003) Mineral Resources of Karnataka, Published by the Geological Society of India, Bengaluru.

Radhakrishna B.P. (2013) Mineral Resources of Karnataka, Published by the Geological Society of India, Bengaluru,Pp: 1 - 214.

Radhakrishna BP (1983). Archean granite-greenstone terrain of the South Indian Shield. In: Naqvi S W and Rogers J J W (eds.), Precambrian of South India. Geological Society of India Memorandum, 4, 1-46.

Radhakrishna BP, Naqvi SM (1986). Precambrian continental crust of India and its evolution. Journal of Geology, 94, 145-166.

Radhakrishna, B.P., Sreenivasaiah, G., (1974). Bedded baryte from the Precambrian of Karnataka. J. Geol. Soc.India, Vo.15, Pp: 314–315.

Radhakrishnan B.P and Vaidyanadhan R., (1997). Geology of Karnataka, Geological Society of India (GSI) Publication, Second Edition, Bangalore.

Radhakrishnan, B.P. (1953) Abrasives in Mysore., Rec. Mysore Geol. Dept., Vol.69, No.2, Pp: 31-43.

Raja.S , Rajendran.S , PoovalingaGanesh.B and Thirunavukkarasu.A. 2010 Study On Hyperspectral Signatures For Magnetite Iron Ore In Thattayengerpet Region Of Trichirappalli District In Tamil Nadu State, India. International Journal of Geomatics and Geosciences volume 1, no 2, 2010.

Rajendran, S., Thirunavukkarasu, A., Balamurugan, G. and Shankar, K. (2011). Discrimination of Iron Ore Deposits of Granulite Terrain of Southern Peninsular India using ASTER Data. Journal of Asian Earth Sciences, Vol.41, Pp: 99-106.

Rajesh, H. M. (2004). Application of Remote Sensing and GIS in Mineral Resource Mapping-An Overview. Journal of Mineralogical and Petrological Sciences, 99, Pp. 83-103.

Ram Rao, B. (1968). Mineral Resources of Hassan, Mandya and Mysore districts, Dept Mines and Geology, Bull No.28.

Rama Rao B, (1945). The charnockitic rocks of Mysore, Mysore Geol. Dept Bull, Vol.18, Pp: 163.

Rama Rao B, (1962). A hand book of the geology of Mysore State, Southern India, Bangalore printing and publishing Co., Bangalore, Pp: 264.

Rama Rao, B., 1940. Archaean Complex of Mysore. Mysore Geol. Dept. Bull, 17: pp. 95.

Ramakrishnan D and Rishikesh Bharti., (2015). Hyperspectral Remote Sensing and geological applications., Special Section: Hyperspectral Remote Sensing, Current Science, Vol.108, No.5, Pp: 879-891.

Ramakrishnan D and Rishikesh Bharti., (2015). Hyperspectral Remote Sensing and Geological applications, Current Science, Vol.108, No.5, Pp: 879-891.

Ramakrishnan M and Vaidyanadhan R., (2008). Geology of India, Vol.1 & 2, Geological Society of India, Bangalore.

Ramakrishnan M and Vaidyanadhan R., (2010). Geology of India, Vol.1 & 2, Geological Society of India, Bangalore.

Ramakrishnan M, Mahabaleswar B and Viswanathan S (2012). The abundances of some Trace-elements in the First-ever Reported Sample of Spinifex-Textured Komatiite from Ghattihosahalli, Karnataka, Jour. Geol.Soc.Ind., Vol.79, Pp: 361-366.

Ramakrishnan M. and R. Vaidyanadhan. (2008). Geology of India, Volume-1, Pp: 108-120.
Ramakrishnan M. and R. Vaidyanadhan. (2008). Geology of India, Volume-1, Pp: 108-120.

Ramakrishnan, m, Vishwanatha, M.N and Swami Nath, J., 1976, Basement Cover relationships of peninsular Gneiss with grade Schists and Greenstone belts of southern Karnataka. Journal Geoloical Society of India. Vol 7 Pp 97-111.

Ravi P. Gupta. 2018. Spectra of Minerals and Rocks. Remote Sensing Geology, Pp 23-35.

Ravindra kumar G.R (1982). Petrological and Structural studies of the Precambrian terrain around Gundlupet, Mysore dist., Karnataka, Unpub. PhD thesis, Univ. of Mysore, Mysuru.

Ravindra kumar G.R (1982). Petrological and Structural studies of the Precambrian terrain around Gundlupet, Mysore dist., Karnataka, Unpub. PhD thesis, Univ. of Mysore, Mysuru.

Rechards, John.R, and Jia, X., 1999:Remote Sensing Digital Image Analysis, Springer.

Reimer, L. (1998) Scanning electron microscopy : physics of image formation and microanalysis. Springer, 527 p.

Robertson, A.D.C. and Sutherland, F.L., (1992): Possible origins and ages for sapphire and diamond from the central Queensland gemfields. Records of the Australian Museum Supplement. V.15, p. 45–54.

Rowan, L. C, Simpson, C. J. and Mars, J. C. (2004). Hyperspectral Analysis of the ultramafic complex and adjacent lithologies at Mordor, NT, Australia, Remote Sensing of Environment, 91, Pp. 419- 431.

Rowan, L. C., Mars, J. C. and Simpson, C. J. (2005). Lithologic mapping of the Mordor, NT, Australia ultramafic complex using the Advanced Spaceborne Thermal Emission and Reflection Radiometer (ASTER). Remote Sensing of Environment, 99, Pp. 105-126.

Rowan, L. C., Schmidt, R. G. and Mars, J. C. (2006). Distribution of Hydrothermally Altered rocks in the Reko Diq, Pakistan. Remote Sensing of Environment, 104, Pp. 74-87.

Sampath Iyengar, P. (1922) Report on the economic mineral deposits in parts of the Hassan district. Rec. Mysore Geol. Dept., Vol.18, No.2, Pp: 103-105.

Santos, L D and Brandno, P R G, 2005. LM, SEM and EDS study of microstructure of Brazilian iron ores, Microscopy and Analysis, 19(1):17-19.

Schowengerdt, Robert.A, 1997: Remote Sensing Modals and Methods for Image Processing, Academic Press.

Seshadri T.S and Mallikarjuna C (1968). Detailed mapping to the south of Kallehadlu, Chitradurga district, Mysore State. Geol. Surv. India, Unpublished Report.

Severin, Kenneth P., 2004, Energy Dispersive Spectrometry of Common Rock Forming Minerals. Kluwer Academic Publishers, 225 p.--Highly recommended reference book of representative EDS spectra of the rock-forming minerals, as well as practical tips for spectral acquisition and interpretation.

Shanks W.C.P. III (2010), Hydrothermal Alteration, Volcanogenic Massive Sulfide Occurrenes Model, Scientific Investigation Report.

Shih, T.-Y., 2004. On The Atmospheric Correction for a Hyperion Scene Taiwan. www.aars.org/acrs/proceedings/ACRS2004/Papers/HDP04.2.htm.

Shippert, P., 2008. Introduction to Hyperspectral Image Analysis. http://satjournal.tcom.ohiou.edu/pdf/shippert.pdf.

Simonet, C., Fritsch, E. and Lasnier, B., (2008): A classification of gem corundum deposits aimed towards gem exploration. Ore Geology Reviews, V.34, p.127-133.

Singer R.B. (1981) Near – Infrared spectral reflectance of mineral mixtures systematic combination of pyroxenes olivine and iron oxides, journal of Geophysics V. 86. Pp 7967-7982.

Smeeth W.F, (1916). Outline of the geological history of Mysore, Mysore Geol. Dept. Bull. Vol.6, Pp: 22.

Smeeth, W.F. and Sampath Iyengar (1916). Mineral Resources of Mysore.,Mysore Geol. Dept., Bull No.7, Pp:123-130.

Srikantappa C and Hensen B.J, (1992). Metamorphic conditions and Precambrian of fluids in the M.M Hills granulites, Karnataka, India, N. Jb. Miner. Mh, Vol.11, Pp: 495-506.

Srinivasan K (1991). Geology of Peddavuru and Jounnagiri schist belts A. P, Rec, Geological survey of India 124 (pt5) 261 – 263.

Subrahmanya KR, Murthy TRS, Jayappa KS, Suresh GC (1991). Some aspects of Quaternary events around Mangalore, Karnataka. Proceedings of seminar on Quaternary land scape of Indian subcontinent, Baroda University, Baroda 186-194.

SUNAGAWA, I., BERNHARDT, H.-J. & SCHMETZER K. (1999): Texture formation and element partitioning in trapiche ruby. J. Cryst. Growth 206, 322.–330.

Sutherland, F.L., 1996. Alkaline rocks and gemstones, Australia: a review and synthesis. Australian Journal of Earth Sciences 43, 323–343.

Sutherland, F.L., Graham, I.T., Pogson, R.E., Schwarz, D., Webb, G.B., Coenraads, R.R., Fanning, C.M., Hollis, J.D., Allen, T.C., 2002a. The Tumbarumba Basaltic Gem Field,

New South Wales: in relation to sapphire–ruby deposits of Eastern Australia. Records of the Australian Museum 54, 215–248.

Sutherland, F.L., Graham, I.T., Webb, G.B., 2004. Sapphire–ruby–zircon deposits from basaltic fields,West Pacific continental margins. In: Khanchuk, A.I., Gonevchuk, G.A., Mitrokhin, A.N., Simanenko, L.F., Cook, N.J., Seltmann, R. (Eds.), Metallogeny of the Pacific Northwest: Tectonics, magmatism and metallogeny of active continental margins. Dal'nauka, Vladivostok, Russia, pp. 385–387.

Sutherland, L.F., Schwarz, D., Jobbins, E.A. and Coenraads, R.R., (1998a): Distinctive gem corundum suites from discrete basalt fields: a comparative study of Barrington, Australia, and West Pailin, Cambodia, gem fields. Journal of Gemmology, V. 26, p.65–85.

Swaminath J, Ramakrishnan M (1981). Present classification and correlations. In: Swaminath J and Ramakrishnan M (eds.), Early Precambrian supracrustals of southern Karnataka. Geological Survey of India Memorandum, 112, 23-38.

Swaminathan J and Ramakrishnan M, (1981). Early Precambrian supracrustals of Southern Karnataka, Mem. Geol.Surv. India, Vol.112, Pp: 350.

Sween M. C, Jr, Harry Y, Huss, and Gary R. (2010). Cosmochemistry. Cambridge University Press. ISBN 9781139489461.

Tangestani, M.H. and M.Hosseinjani, "Discrimination of Alteration zones by using Spectral Angle Mapping and Linear Spectral Unmixing of the ASTER data at Sarduiyeh area", SE Kerman, Iran, 26th Symposium on Geosciences, 17-19 Feb., Tehran, Iran, 2008.

Terekhov, E.N., Kruglov, V.A. and Levitskiy, V.I., (1999): Rare-earth elements in corundum bearing metasomatites and related rocks of the Eastern Pamirs. Geokhimiya, V. 3, p.238–250.

Themelis T., The heat treatment of ruby and sapphire, Gemlab Inc., USA, 1992

Tomoaki Morishita and Shoji Arai (2001). Petrogenesis of corundum bearing mafic rock in the Horoman peridotite complex Japan, Journal of petrology Vol, 42 issue7, pp 1279-1299.

TOMOAKI MORISHITA, SHOJI ARAI and DAVID H. GREEN. Possible Non-melted Remnants of Subducted Lithosphere: Experimental and Geochemical Evidence from Corundum-Bearing Mafic Rocks in the HoromanPeridotite Complex, Japan ,2004, Journal of Petrology, pp.235-252.

Tong,Q.,Tian,Q.,Pu,O., and zhao,C.,2001,Spectrscopic determination of wheat Water status using 1650-1850 nm spectral absorption features, Int.J.Rs, Vol 22,No.12, 2329-2338.

United Launch Alliance Successfully Launches Second NASA Payload in Just 12 Days. United Launch Alliance. 11 February 2013. Retrieved 12 February 2013.

Upton, B., Hinton, R.W., Aspen, P., Finch, A. and Valley, J.W., (1999): Megacrysts and associated xenoliths, evidence for migration of geochemically enriched melts in the upper mantle beneath Scotland. Journal of Petrology, V. 40, p. 935–956.

Vane, G, Green, RO, Chrien, G, Enmark, HT, Hansen, EG & Porter, WM, (1993) 'The Airborne Visible/Infrared Imaging Spectrometer' Remote Sensing of Environment, vol. 44, Pp. 127-14.

Varshney, P.k. and Arora, M.K., 2004. Advanced Image Processing Techniques for Remotely Sensed Hyperspectral data. Springer-Verlag Berlin Heidelberg New York.

Viswanatha, M.N. (1972). Corundum pegmatites and Corundum – Sillimanite pegmatites from Kalyadi area, Hassan district, Indian Minerals, Vol.26, No.3, Pp: 20-23.

White, J.S. (1979) Boehmite exsolution in corundum. Amer. Mineral., 64, 1300–1302.

Wilbur, J.S, F.E. Mutschler, J.D. Friedman, and R.E. Zartman, 1990, New chemical, isotopic, and fluid inclusion data from zinc-lead-copper veins, Shawangunk Mountains, New York. Economic Geology, v.85 no.1, pp. 182-196.

Yui, T.-F., Wu, C.-M., Limtrakun, P., Sricharn, W., Boonsoong, A., 2006. Oxygen isotope studies on placer sapphire and ruby in the Chanthaburi–Trat alkali basaltic gemfield, Thailand. Lithos 86, 197–211.

Zen. Metamorphic mineral assemblages of slightly calcic Pelitic rocks in and around the Taconic Allochthon, southwestern Massachusetts and adjacent Connecticut and New York, E-an, 1981, USGS Publications Warehouse, G.P.O.128 p.

RESEARCH PUBLICATIONS

1. Basavarajappa H.T and Maruthi N.E (2018). Hyperspectral And Petro - Chemical Signatures Study On Shear Zone Controlled Corundum Bearing Pelitic Rocks Of Budipadaga Area, Chamarajanagara District, Karnataka, India. International Journal of Research and analytical Reviews (IJRAR) Volume 5, Issue 3, pp. 906-913.

2. Basavarajappa H.T and Maruthi N.E (2018). Hyperspectral and Petro - Chemical Signatures study on Corundum Bearing Litho-Units around Sringeri Area, Chikmagalur District, Karnataka, India. RESEARCH REVIEW International Journal of Multidisciplinary Volume 3, Issue10, pp. 899-904.
3. Basavarajappa H.T and Maruthi N.E (2018). Petro – Chemical And Spectral Signatures On Corundum Bearing Precambrian Amphibolites In Sullia Area, Dakshina Kannada District, Karnataka, India. Journal of Emerging Technologies and Innovative Research (JETIR) Volume 5, Issue 7, pp. 75-83.
4. Basavarajappa H.T and Maruthi N.E (2018). Petrochemical characteristics and Hyperspectral signatures on Corundum bearing Precambrian litho-units of Varuna area, Mysuru district, Karnataka, India. International Journal of Creative Research Thoughts, Volume6, Issue1, Pp.998-109.
5. Basavarajappa H.T, and Maruthi N.E (2018). Hyperspectral Signature Study Finds Corundum Alters To Diaspore Influeance Of Climate Change Of Dharwar Craton Arsikere Band Of Haranahalli, Hassan District, Karnataka, India. Journal of Environmental Science, Computer Science and Engineering and Technology (JECET) Volume 7, Issue 2, Pp.238-246.
6. Basavarajappa H.T, Maruthi N.E and Manjunatha M.C (2017). Hyperspectral Signatures and Field Petrography of Corundum bearing litho-units in Arsikere band of Haranahalli, Hassan District, Karnataka, India. International Journal of Creative Research Thoughts, Volume5, Issue4, Pp.3791-3798.
7. Basavarajappa H.T, Maruthi N.E, Jeevan L and Manjunatha M.C (2018). Physico-chemical charectristics and hyperspectral signature study using geomatics on gem verity of corundum bearing precambrian litho-units of Mavinahalli area, Mysuru

district, Karnataka, India. International Journal of Computer Engineering and Technology(IJCET) Volume 9, Issue 1, pp. 102-112.

8. Maruthi N.E and Basavarajappa H.T (2018). Hyperspectral and Petro - Chemical Signatures study on Corundum Bearing Amphibolite Schist of Magadi Area, Ramanagara District, Karnataka, India. RESEARCH REVIEW International Journal of Multidisciplinary Volume 9, Issue 3, pp. 773-779.
9. Maruthi N.E and Basavarajappa H.T (2018). Hyperspectral And Petro - Chemical Signatures Study On Corundum Bearing Litho-Units Of Precambrian Basement Rocks Around Closepect Granite Madhugiri Area, Karnataka, India. Journal of Emerging Technologies and Innovative Research (JETIR) Volume 5, Issue 12, pp. 619 - 628.
10. Maruthi N.E and Basavarajappa H.T (2018). Hyperspectral Signatures and Petro - Chemical Charectistics Study on Corundum Bearing Litho-Units of Sargur Area, Mysuru District, Karnataka, India. International Journal of Research and analytical Reviews (IJRAR) Volume 5, Issue 4, pp. 65-74.
11. Maruthi N.E, Basavarajappa H.T, Jeevan .L and Siddaraju M.S (2018). Hyperspectral Signatures On Corundum Bearing Litho-Units Of Precambrian Basement Rocks Around Closepet Granite Pavagada Area, Karnataka. International Journal of Computer Engineering and Technology (IJCET) Volume 9, Issue 3, pp. 86-94.
12. Maruthi N.E, Basavarajappa H.T, Manjunatha M.C, and Harshavardhana A.S. (2019). Hyperspectral Study And Integration Of Petro-Chemical Signatures On Corundum Bearing Litho-Units Around Maddur, Mandya District, Karnataka, India. International Journal of Research and Analytical Reviews (IJRAR), Volume.6, Issue 1, Page No pp.897-903, January -March 2019.